8-1976

Lumped Parameter, State Variable Dynamic Models for U-tube Recirculation Type Nuclear Steam Generators

Mohamed Rabie Ahmed Ali
University of Tennessee - Knoxville

To the Graduate Council:

I am submitting herewith a dissertation written by Mohamed Rabie Ahmed Ali entitled "Lumped Parameter, State Variable Dynamic Models for U-tube Recirculation Type Nuclear Steam Generators." I have examined the final electronic copy of this dissertation for form and content and recommend that it be accepted in partial fulfillment of the requirements for the degree of Doctor of Philosophy, with a major in Nuclear Engineering.

T. W. Kerlin, Major Professor

We have read this dissertation and recommend its acceptance:

P. F. Pasqua, J. C. Robinson, Kike Kiser, Jivan Thakkar

Accepted for the Council:
Dixie L. Thompson

Vice Provost and Dean of the Graduate School

(Original signatures are on file with official student records.)

July 9, 1976

To the Graduate Council:

I am submitting herewith a dissertation written by Mohamed Rabie Ahmed Ali Entitled "Lumped Parameter, State Variable Dynamic Models for U-tube Recirculation Type Nuclear Steam Generators." I recommend that it be accepted in partial fulfillment of the requirements for the degree of Doctor of Philosophy, with a major in Nuclear Engineering.

T. W. Kerlin, Major Professor

We have read this dissertation and recommend its acceptance:

Accepted for the Council:

Vice Chancellor
Graduate Studies and Research

LUMPED PARAMETER, STATE VARIABLE DYNAMIC MODELS FOR U-TUBE RECIRCULATION TYPE NUCLEAR STEAM GENERATORS

A Dissertation

Presented for the

Doctor of Philosophy

Degree

The University of Tennessee, Knoxville

Mohamed Rabie Ahmed Ali

August 1976

ACKNOWLEDGEMENTS

The author would like to thank Dr. T. W. Kerlin, the major professor and the research advisor, for his patience in smoothing the rough spots during the course of this work. His guidance and encouragement together with the valuable suggestions of the other members of the doctoral committee contributed to the successful completion of this dissertation.

He wishes to express his gratitude to Dr. P. F. Pasqua, head of the Nuclear Engineering Department for making the completion of the resident requirements for the Ph. D. program possible through a graduate assistantship.

The assistance of Mssrs. Mike Kiser and Jivan Thakkar in checking the steady state calculation algorithm and coupling the team generator and reactor models is deeply appreciated.

Many thanks go to Mrs. Juanita Rye for her effort in typing the rough drafts and the final form of the dissertation report.

The use of The University of Tennessee Computing Center facilities is highly acknowledged.

ABSTRACT

A number of lumped parameter dynamic models were developed for a vertical U-tube recirculation steam generator (UTSG) of the type used in most pressurized water reactor nuclear steam supply systems.

The models ranged in complexity from a simplified model (Model A) with only three lumps to represent the primary fluid (reactor coolant), tube metal and the secondary fluid to a detailed model (Model D) with fourteen lumps and a moving boundary between the subcooled and boiling sections of the heat exchange region. The models are linear and are in the state variable form which is convenient for using standard general purpose computer codes for time or frequency domain analysis.

The adequacy of the models was tested in several ways. The calculated response from the models was studied for physical plausibility. The adequacy of the analytical work was tested by comparing results from progressively more detailed models. The detailed model response was compared with the results of other UTSG dynamic models[6,32] and with test results obtained at the H. B. Robinson (739 MWe PWR) plant.[3,4,5]

All of the checks on model validity demonstrated the adequacy of the lumped parameter approach for the simulation of the dynamic response of a UTSG for normal operating transients involving small deviations from the steady state conditions.

TABLE OF CONTENTS

CHAPTER		PAGE
I.	INTRODUCTION	1
	General Considerations	1
	Description of the Physical System	3
	Statement of the Problem	8
	Importance of the Study	8
	Scope and Organization of the Text	9
II.	REVIEW OF PERTINENT LITERATURE	11
	Introduction	11
	Dynamic Models for Heat Exchangers and Fossil Fueled Boilers	11
	Dynamic Models for Boiling Water Reactor (BWR) Systems	14
	Dynamic Models for Recirculation Type Nuclear Steam Generators	18
	Remarks	24
III.	DEVELOPMENT OF THE MATHEMATICAL MODELS	25
	Introduction	25
	Basic Assumptions	25
	Structure of the Mathematical Models	26
	Simplified Steam Generating System Model (Model A)	27
	First Intermediate Model (Model B)	30

CHAPTER PAGE

Second Intermediate Model (Model C) 30

The Detailed Model (Model D) 33

Governing Equations for Model A 35

Primary Lump (PRL) 35

Tube Metal Lump (MTL) 36

Secondary Fluid Lump (SFL) 37

Summary of the Model Equations 42

Governing Equations for Model B 43

Primary Lump (PRL1) 43

Primary Lump (PRL2) 43

Tube Metal Lump (MTL1) 44

Tube Metal Lump (MTL2) 44

Secondary Fluid Lump (SFL) 44

Summary of the Model Equations 46

Governing Equations for Model C 48

General 48

Primary Lump (PRL1) 48

Primary Lump (PRL2) 49

Tube Metal Lump (MTL1) 49

Tube Metal Lump (MTL2) 49

Effective Heat Exchange Secondary Fluid Lump (SFEHEL) 49

Drum Equivalent Secondary Fluid Lump (SFDRL) . 56

CHAPTER PAGE

Downcomer Secondary Fluid Lump (SFDCL) 64
The Recirculation Loop Equation 65
Summary of the Model Equations 69
Governing Equations for Model D 74
Primary Side Equations 74
Tube Metal Equations 83
Secondary Side Equations 87
The Recirculation Loop Equation 95
Summary of the Model Equations 97
IV. CALCULATION PROCEDURE AND RESULTS 106
Introduction 106
Calculation Procedure for the Pure Differential
Formulation 107
Calculation Procedure for the Mixed Differential
and Algebraic Formulation 111
Time Response Calculation 112
Frequency Response Calculation 114
Geometrical Calculation 115
Primary Side 116
Tube Metal 118
Secondary Side 119
Results for H. B. Robinson Steam Generator . . .121
Calculation of Heat Transfer Coefficients 122
Film Heat Transfer Coefficients 123

HAPTER PAGE

Tube Metal Conductance 125

Overall Heat Transfer Coefficients 125

Combined Film and Tube Metal Conductances . . . 126

Results for H. B. Robinson Steam Generator . . . 129

Steady State Calculations 129

Introduction 129

Solution Using the Finite Difference Approach . 132

Solution Using Logarithmic Mean Temperature Difference (LMTD) 135

Results for H. B. Robinson Steam Generator . . . 137

General Remarks for Dynamic Response Calculations . 139

Dynamic Response Results 141

Response of Model A 141

Response of Model B 143

Response of Model C 146

Response of Model D 151

Comparison of Models Responses 158

V. COMPARISON OF DETAILED MODEL PREDICTIONS WITH EXPERIMENTAL RESULTS 160

Introduction 160

Description of the System 160

PWR Model 161

Coupling of Reactor and Steam Generator Models . . 167

Results 170

HAPTER PAGE

VI. COMPARISON OF DETAILED MODELS WITH OTHER UTSG MODELS 183

Introduction 183

Comparison with Christensen's UTSG Model 184

System Description 184

Model Description 184

Comparison of Model Formulation 186

Comparison of Dynamic Responses 188

Comparison with Arwood's IEUTSG Model 188

Description of the IEUTSG System 190

Comparison of Dynamic Responses 192

VII. REMARKS AND CONCLUSIONS 195

Evaluation of the Development Procedure 195

Possible Uses of the Current Work 196

Recommendations for Future Work 197

Conclusions 198

IST OF REFERENCES 199

PPENDIXES 205

A. NARROW RANGE LINEAR APPROXIMATION OF SATURATION, WATER AND STEAM PROPERTIES 206

B. THE CRITICAL FLOW ASSUMPTION 216

C. BASIC CONSERVATION EQUATIONS FOR TWO PHASE FLOW SYSTEMS 218

D. RECIRCULATION LOOP EQUATION 228

CHAPTER PAGE

E. AVERAGE DENSITY IN THE TWO-PHASE REGION 232

F. SUMMARY OF DYNAMIC RESPONSE RESULTS 236

G. INSTRUCTIONS FOR USING THE DETAILED MODEL DYNAMIC RESPONSE COMPUTER PROGRAM 271

VITA 280

LIST OF TABLES

ABLE		PAGE
II.1	System Variables for Model C	70
II.2	System Variables for the Detailed Model (Model D)	98
IV.1	H. B. Robinson Steam Generator Design Data	117
IV.2	Nonzero Elements of the Matrices A1 and A2 for Model C	147
IV.3	Nonzero Elements of the Matrices A1 and A2 for Model D	152
V.1	Definition of the State Variables Used in the Reactor Model	163
V.2	Nonzero Elements of the A Matrix for the Reactor Model	164
V.3	Nonzero Elements of the Forcing Vector for the Reactor Model	166
V.4	System Variables for the Steam Generator Model	169
V.5	Forcing Function for Steam Valve Perturbation (+10% Change in Steam Flow Rate)	171
F.1	Summary of Dynamic Response Results	237

LIST OF FIGURES

FIGURE		PAGE
I.1.	Pressurized Water Reactor Coolant Loop	2
I.2.	Details of a Vertical U-Tube Recirculation Steam Generator (UTSG)	4
I.3.	Schematic Diagram for a Vertical U-Tube Recirculation Steam Generator (UTSG)	5
II.1.	Simplified Steam Generator System for Model A	28
II.2.	Schematic Diagram for Model A	29
II.3.	Schematic Diagram for Model B	31
II.4.	Schematic Diagram for Model C	32
II.5.	Schematic Diagram for Model D	34
II.6.	Secondary Lumps for Model C	50
II.7.	Variation of Thermodynamic Properties of the Secondary Fluid in the Effective Heat Exchange Lump	53
II.8.	The Drum Equivalent Secondary Fluid Lump	57
IV.1.	Combining Film and Tube Metal Conductances	128
IV.2.	Schematic of the Effective Heat Exchange Region (Core)	131
IV.3.	Temperatures and Mass Quality Profiles Calculated by the Steady State Program	138
IV.4.	Step Response of Model A to +10% Change in Steam Valve Coefficient	142

GURE		PAGE
/.5.	Step Response of Model B to +10% Change in Steam Valve Coefficient	144
/.6.	Step Response of Model C to +10% Change in Steam Valve Coefficient	148
/.7.	Step Response of Model D to +10% Change in Steam Valve Coefficient	153
/.8.	Comparison of T_{Po} and P_s Responses in the Four Models	159
/.1.	Schematic of the H. B. Robinson Plant	162
/.2.	Lumped Structure for a PWR System Model	168
/.3.	Reactor Power/Reactivity ($\delta P/P_o/\delta\rho$) Frequency Response	172
/.4.	Steam Pressure/Reactivity ($\delta P_s/\delta\rho$) Frequency Response	174
/.5.	Reactor Power/Steam Flow ($\delta P/P_o/\delta W_{so}$) Frequency Response	176
/.6.	Steam Pressure/Steam Flow ($\delta P_s/\delta W_{so}$) Frequency Response	178
/.7.	Cold Leg Temperature/Steam Flow ($\delta T_{CL}/\delta W_{so}$) Frequency Response	180
I.1.	Simplified Diagram of the Physical System	185
I.2.	Comparison Between Model D and Christensen's Model	189
I.3.	Schematic Diagram of an IEUTSG	191
I.4.	Comparison Between UTSG and IEUTSG Models Using the Same Modeling Approach	193
A.1.	Variation of T_{sat} with Pressure	208
A.2.	Variation of V_f with Pressure	209

URE		PAGE
.3.	Variation of V_g with Pressure	210
.4.	Variation of V_{fg} with Pressure	211
.5.	Variation of h_f with Pressure	212
.6.	Variation of h_g with Pressure	213
.7.	Variation of h_{fg} with Pressure	214
.1.	Control Volume for the Application of the Continuity Equation	219
.2.	Control Volume for the Application of the Energy Equation	222
.3.	Control Volume for the Application of the Momentum Equation	226
.1.	Calculation of the Driving Pressure Head for the Recirculation Loop	230
.1.	Step Response for Case A.1	238
2.	Step Response for Case A.2	239
3.	Step Response for Case A.3	240
4.	Step Response for Case B.1	241
5.	Step Response for Case B.2	243
6.	Step Response for Case B.3	245
7.	Step Response for Case C.1	247
8.	Step Response for Case C.2	250
9.	Step Response for Case C.3	253
10.	Step Response for Case D.1	256
11.	Step Response for Case D.2	261
12.	Step Response for Case D.3	266

CHAPTER I

INTRODUCTION

I.1 General Considerations

Although steam generators have been used in power generating plants for a long time, the interest in their dynamic behavior has grown only since nuclear energy became a feasible substitute for fossil fuels as a load-following heat source for steam supply systems. Figure I.1 shows a pressurized water reactor (PWR) coolant loop. It is clear that the steam generator in this loop acts as a thermal coupling between the reactor primary coolant system and the secondary steam cycle. On the primary side, there is the nuclear power reactor where efficient and safe heat removal from the reactor core is of primary concern to the reactor designer. On the secondary side, there is the electrical energy consumer whose main interest is the reliability of service. It is because of this strategic position of the steam generator between these two sides that its dynamic behavior became of considerable interest for the safe design and reliable operation of PWR nuclear power plants.

The work reported in this dissertation was a part of a larger task for the dynamic analysis of both single and dual purpose (generating electricity and desalination of sea water), nuclear power plants that was carried out at the Nuclear Engineering Department

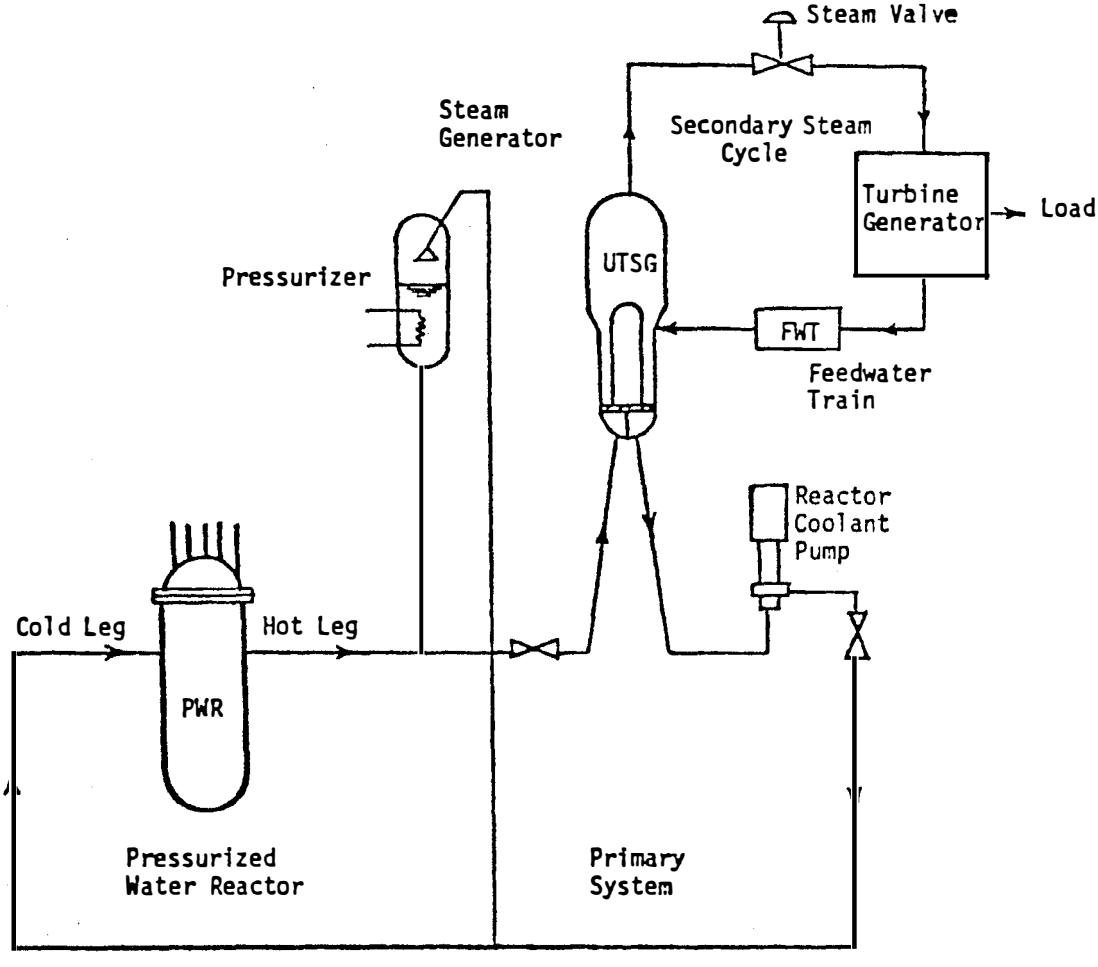

Figure I.1 Pressurized Water Reactor Coolant Loop.

f The University of Tennessee with the cooperation of Oak Ridge
ıtional Laboratory and the Power Systems Division of Combustion
ıgineering, Inc.

2 Description of the Physical System

The steam generator considered in this work is a vertical, tube, recirculation type steam generator (hereafter abbreviated UTSG). It is the type used in most of the current PWR nuclear eam supply systems (NSSS).

The details of such a steam generator are shown in Figure I.2 d a schematic is shown in Figure I.3. The hot reactor coolant rrying the heat generated in the core enters at the bottom of e steam generator through the inlet nozzle to an inlet plenum, ɔws through the U-tubes, transferring heat to the secondary fluid at flows outside the tubes and then enters an outlet plenum fore leaving the steam generator through the outlet nozzle(s). ɜ secondary feedwater to the steam generator enters at a level ;t above the U-tubes through a feedwater ring. It mixes with ɜ recirculated water and the slightly subcooled mixture passes nward through the annular region between the tube wrapper and ı shell before entering the U-tube region. Heat is transferred the secondary fluid as it flows upward outside the U-tubes, a steam water mixture is formed. The steam water mixture then ses through steam separators and dryers that limit the moisture tent of the steam leaving the steam generator to less than 0.25%.[2]

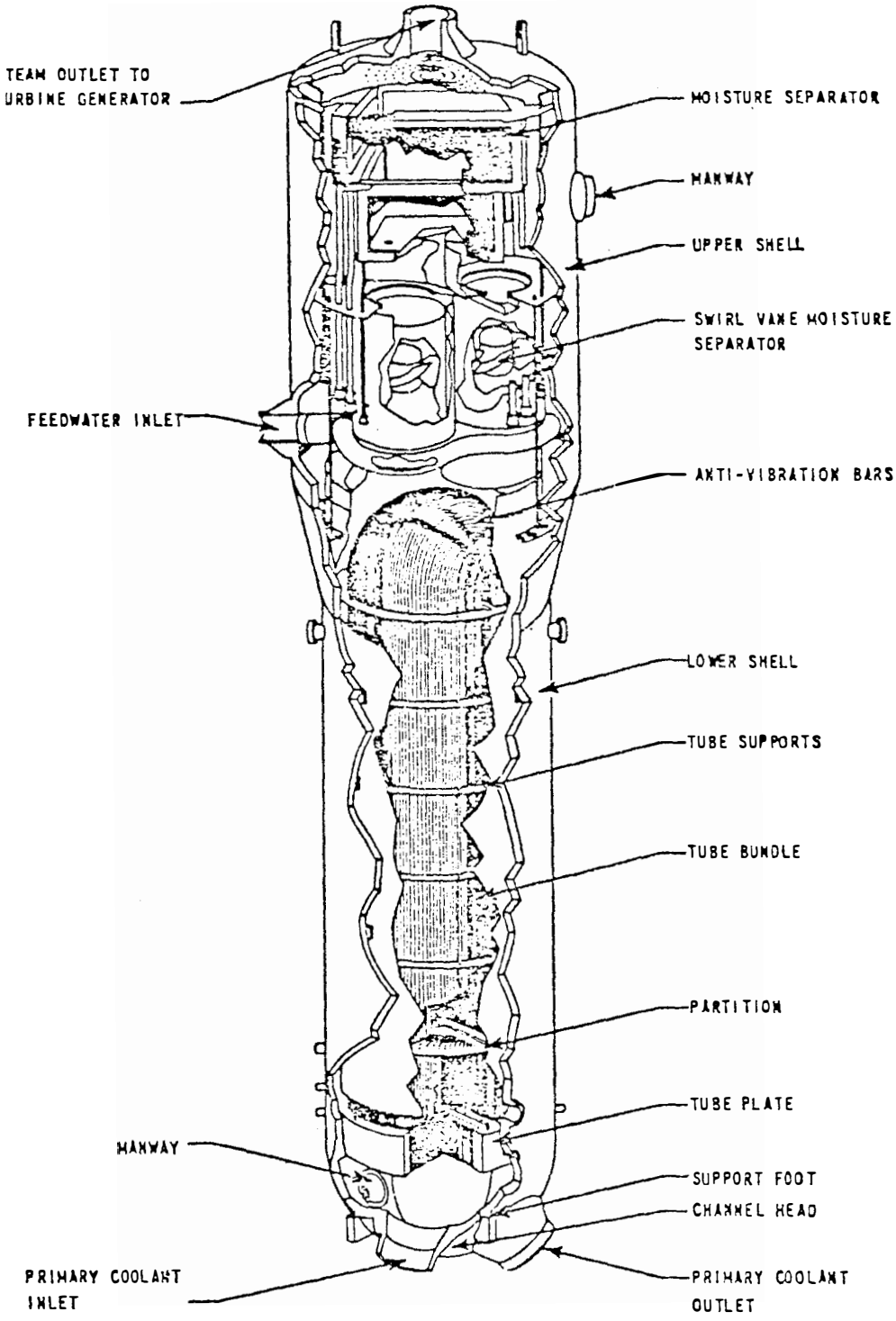

Figure I.2 Details of a Vertical U-Tube Recirculation Steam Generator (UTSG) (from Reference 1).

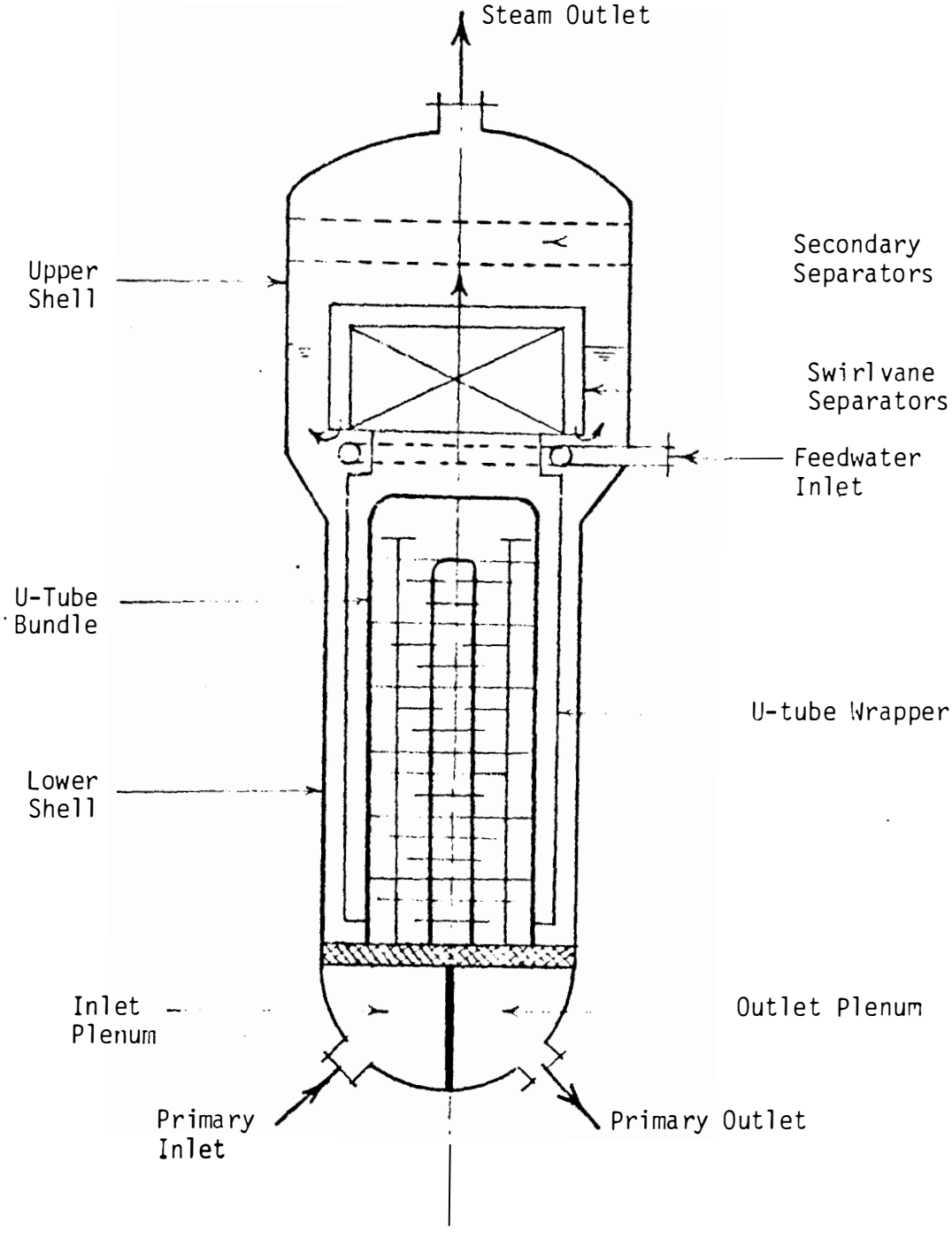

Figure I.3 Schematic Diagram for a Vertical U-tube Recirculation Steam Generator (UTSG).

The separated water returns to mix with the feedwater for another pass through the tube bundle region.

Referring to Figure I.3, one can summarize the different processes encountered in the functioning of this UTSG as follows:

A. Primary Side

1. Entrance of the primary water from the reactor hot leg to the inlet plenum.
2. Flow of the primary water through the U-tube bundle and heat transfer along its path to the secondary fluid. Notice that flow of the primary fluid is parallel to the secondary flow in the inlet branch of the U-tubes and opposite to it in the exit branch of the U-tubes. Therefore, the U-tube steam generator can be considered as composed of a parallel flow steam generator and a counter flow steam generator with a common secondary fluid.
3. Outlet of the primary water through the outlet plenum.

B. Tube Metal Walls

1. The tube metal separates the primary water and the secondary fluid. The tube conductance together with the film heat transfer coefficients determine the effective heat transfer coefficients relating the bulk mean temperatures in the primary and secondary sides and the tube metal temperature.

C. Secondary Side

1. Feedwater enters through the feedwater ring into the annulus between the U-tube wrapper and the shell, referred to as the downcomer section in this study.
2. Feedwater mixes with saturated water separated from the steam-water mixture in the steam separaters.
3. Secondary water enters from the downcomer into the tube bundle region.
4. Secondary water is heated as it flows upward around the U-tubes and the temperature is raised to the boiling point.
5. Boiling occurs in the flowing secondary fluid and steam is formed as more heat is transferred through the U-tubes from the primary fluid.
6. The steam-water mixture continues to flow upward to the steam separators where steam is separated and collected in the upper part of the steam generator shell and separated water is mixed with feedwater, then flows downward in the downcomer.
7. Steam exits from the upper part of the steam generator at a rate determined by the turbine stop valve opening.

Statement of the Problem

The purpose of the study and research work reported in this sertation was to investigate the dynamic behavior of a vertical G using the state variable, lumped parameter technique. The hematical models developed were required to be in a form suitable using existing state variable digital computer codes to obtain dynamic response in the time and frequency domains. Also, y were required to be in a form suitable for coupling with els for other subsystems so that the dynamic response of the egrated PWR system can be obtained using the same computer codes. validity of the model was to be checked against available erimental data from dynamic tests on the H. B. Robinson Nuclear er Plant.[3,4,5]

Importance of the Study

The need for efficient and practical techniques for assessment the dynamic behavior of nuclear steam generators is growing with growth of the nuclear power industry. The design of a steam erator within a nuclear power plant demands a detailed knowledge the thermohydraulic processes affecting its performance, not only steady state, but also during transients. Since a digital computer l be necessary to predict the dynamic response of large complex tems, an efficient mathematical model must have the following racteristics.

1. The number of equations should be the minimum that adequately simulates the dynamic behavior of the system.

2. The form of the model should allow the use of standard general purpose computer codes.
3. It should be easy to couple models for other subsystems.
4. The same model should be useable for transient, frequency response or stability analysis.

The lack of dynamic models with the above characteristics for nuclear UTSG's stimulated the need for the work reported in this dissertation.

I.5 Scope and Organization of the Text

Following this introductory chapter, a review of pertinent literature is presented in Chapter II. The development of the mathematical models is given in Chapter III. In Chapter IV, the calculation procedure is described and the application of these models for dynamic response simulation of an isolated UTSG is demonstrated. The response of a coupled PWR/steam generator system is examined in Chapter V for the purpose of testing the validity of the models. In this chapter, the correlation between the mathematical model's prediction and the results obtained from dynamic tests on H. B. Robinson Nuclear Power Plant[3] is discussed. In Chapter VI, the detailed model response is compared with the results obtained from a finite difference model.[32] Chapter VI also contains the comparison between the detailed UTSG model and a dynamic model for an Integral Economizer U-tube Steam Generator (IEUTSG) which was developed using the same modeling approach.[6] In Chapter VII a summary of the model evaluation is presented together with some concluding remarks.

The Appendixes contain the basic information and detailed calculations that would otherwise interfere with the smooth continuity of the discussion in the main text.

CHAPTER II

REVIEW OF PERTINENT LITERATURE

II.1 Introduction

The problem of developing dynamic models to predict the dynamic behavior of nuclear steam generators has received considerable attention in the past decade. In this chapter, a number of publications will be reviewed for the purpose of presenting a sample of the available literature pertinent to the area of dynamic simulation of two-phase natural circulation systems in general and of U-tube recirculation type steam generators in particular. The literature review is presented in three parts. In Section II.2, a review of some dynamic modeling approaches for heat exchangers and fossil fueled boilers are discussed. In Section II.3, some of the dynamic models for boiling water reactor (BWR) systems are discussed with the emphasis on the similarity between BWR and UTSG systems. In Section II.4, some of the modeling techniques for nuclear steam generator systems are reviewed with the emphasis on modeling approaches and the scarcity of published modeldescriptions that stimulated the need for the study and research work reported in this dissertation. General remarks about the literature review are given in Section II.5.

II.2 Dynamic Models for Heat Exchangers and Fossil Fueled Boilers

The interest in the dynamic behavior of heat exchangers and fossil fueled boilers has grown in the past two decades and a number of publications have been reported in the open literature.

Clark et al.[7] presented a number of papers where they derived analytical solutions for the dynamic response of heat exchangers as a function of position and time to three different perturbations in the heat generation rate (the perturbations were a step, an arbitrary function, and a sinusoid).

Chien et al.[8] presented the transient analysis for a boiler with an internal recirculating loop and a superheater bank in the load loop. The model includes a pressure drop equation for the superheater and recirculating loop together with a steam drum water level calculation. Analog solutions of the system were obtained for open loop and closed loop transient responses of the drum pressure and water level to changes in steam flow, fuel supply and feedwater flow.

Thal-Larson[9] examined the dynamic behavior of heat exchangers by deriving transfer functions for frequency response analysis using simple mathematical models. Important system time constants were identified for each model presented.

A detailed study by Masubuchi[10] treated the dynamic analysis of different configurations of heat exchangers. Transfer functions of a complex model were derived for frequency response analysis. He also presented a simplified model for simulating the transient response.

Enns[11] classified the many theoretical models of heat exchangers into distributed parameter and lumped parameter models. Transfer functions were derived which show the adequacy of lumped

parameter models for flow rate or heat flux induced transients while a distributed parameter model is recommended for temperature induced transients.

Dusinberre[12] approached the heat exchanger dynamics problem by presenting a numerical technique for calculating transient temperatures. He indicated that numerical methods are an excellent way for generating a family of solutions to a particular problem. He also hinted that there is often a great saving of time and effort in processing on a finite difference basis throughout when an analytical solution is not obtainable and when a digital computer is available.

Astrom[13] presented a simple nonlinear model for a drum boiler-turbine unit where the drum pressure is the state variable and fuel flow, control valve setting and feedwater flow are the control variables. The model was shown to agree well with measurements for an actual boiler in the range half power to full power. The model can be derived using physical arguments and is thus characterized by several parameters. A derivation of the simplified model based on physical consideration was given together with the assumptions required to arrive at the simplified model. A crude method of estimating the model parameters was also given.

Before leaving this section, the author would like to call attention to a number of excellent papers on the subject of boiler modeling given in Reference 14.

I.3 Dynamic Models for Boiling Water Reactor (BWR) Systems

An extensive research effort has been undertaken in the past twenty years in support of the boiling water reactor program with emphasis on hydrodynamic stability of natural circulation boiling systems.

The heat exchange process in a BWR core is somewhat similar to that in the tube bundle region of a UTSG. In both cases, heat is added from a primary source of heat to a flowing secondary fluid which enters the heat exchange region as subcooled water and leaves it as a two phase steam/water mixture. Some of the references dealing with the dynamic behavior of BWR systems are given below.

Thie[15] presented a theoretical analysis of the kinetic behavior of a number of operating boiling water reactors based on a simple model where steam void feedbacks dominate. It was concluded that it is possible within the framework of existing experimental and theoretical BWR dynamic technology to design these reactors with reduced instability limitations on the power.

Akcasu[16] investigated the dynamic behavior of boiling water reactors in a systematic way. General expressions for the transfer functions associated with the individual feedback mechanisms were obtained for an arbitrary flux distribution, weighting function and steam velocity distribution. Specific forms of the transfer functions were obtained and simplified by single time constant transfer functions. The error involved in the lumped time constant approximation was examined and was shown to be as large as 4 db in amplitude. The theoretical results were compared with experimental power-void transfer

ıctions and the agreement in some cases was proven to be better
ın 5 db in amplitude and 10 degrees in phase in the entire
:quency range from 0.01 to 100 rad/sec.

Fleck[17] used the laws of conservation of mass, energy, and
ıentum in the integral form to derive a set of ordinary differential
ıations governing the hydrodynamics of natural circulation boiling
;tems. The equations can be solved for the water velocities at
: inlet and outlet of the heated section, the outlet void fraction
l the total fluid momentum. These equations can be added to the
.ctor kinetics equation and the equations governing the transfer
heat from reactor fuel elements to water and the relation between
ıctivity and the average void fraction to obtain a model for the
ıamics of a boiling water reactor. The calculations using this
lel indicated that under certain conditions, boiling water reactors
ı operate stably even for very substantial reactivity additions.
: analysis also revealed that under proper conditions, purely hydro-
ıamic instability can occur independently of any coupling between
id and water. The onset of this unstable behavior would be
lependent of nuclear and thermal parameters although the dynamic
ıavior of the reactor would depend on them.

Muscettola[18] presented a theoretical formulation for the
ıamics of a boiling water reactor of the pressure tube and forced
·culation type. The model treated the neutron kinetics, fuel
:ment heat transfer dynamics, the boiling channel, steam drum,
ıncomer and recirculating pump. The author emphasized the need for
:oretical models to support both design and experimental programs.

Mida and Suda[19] presented simplified versions of the transfer function models derived by them in another report. The simplified models were used to investigate the dynamic characteristics of a BWR system from design parameters. The dynamic characteristics of the feedback transfer functions and the system stability were also investigated and some comparison with other studies were given.

Anderson et al.[20] examined the transient response and stability of a two phase natural circulation system for application to a boiling water reactor. The treatment is very similar to that required for a natural circulation steam generator. The model described the conservation of mass, energy, and momentum for a two-phase loop. The resulting equations were solved simultaneously with an analog computer. The model uses a slip ratio correlation for determining the two phase flow in the boiling portion of the loop.

Nahavandi and van Hollen[21] discussed the use of space-dependent dynamic analysis to study the dynamic behavior and stability of boiling water reactor systems where discrete space nodes along the axis of the core were used to determine local void fraction and thermohydraulic feedback effects.

Neal and Zivi[22] presented a comparative study of analytical models and experimental data for the hydrodynamic stability of natural circulation boiling systems. The authors examined the stability problem in natural circulation boiling systems and indicated that a large number of parameters in both the boiling and non-boiling portions of such a system jointly determine its stability, hence the complexity of the dynamic models. The study of hydrodynamic stability

problem was presented in three parts. In the first part, the mechanisms of instability considered by a number of authors were discussed and the experimentally observed effects of various system parameters were summarized. In the second part, the basic conservation equations were derived in general form, and each model was described relative to these equations. Finally, the model predictions were compared with experimental data, and the relative predicting power of each model was presented.

Spigt[23] presented the results of an experimental and theoretical study on the hydraulic characteristics of a single coolant channel of simple annular geometry in a boiling water reactor with main emphasis on the stability characteristics of the flow process in such a channel. The report included a description of the pressurized and atmospheric boiling loops which were used in the experimental part of the study. In the theoretical part of the study, the general equations describing the performance characteristics of a boiling system under steady state and non-steady state were derived with special attention to the formulation of boundary conditions and the introduction of pressure effects into the equations. The dynamic equations were linearized by assuming small disturbances from steady state and then numerically integrated by means of a digital computer.

Vassier[24] developed an analog model to study the dynamic behavior of a boiling loop with natural circulation. The model was constructed for a longer test loop then those used by Fleck[17] and Zivi[22] and was kept as simple as possible by isolating the most

important factors and neglecting the other factors. The model showed a rather good agreement with the experiments of Spigt[23] regarding the prediction of the onset of instability as well as the power/inlet velocity transfer function. The model has been expanded to include the neutron kinetics equations, fuel element and void feedback and the control system. The author indicated that when dealing with some phenomena in certain frequency ranges, it is not necessary to consider other components of the plant which have much lower natural frequencies.

II.4 Dynamic Models for Recirculation Type Nuclear Steam Generators

The problem of simulating the dynamic behavior of steam generator components of nuclear power plants has recently received a considerable attention both from industry and utility parties.

Westmoreland[25] developed a natural circulation steam generator model where he emphasized riser liquid-vapor volume fractions and circuit pressure losses in describing a closed secondary loop. This digital computer model of a shell and tube type unit used an annular two phase flow treatment in computing the steady state and transient steam flow, the recirculation ratio and the water level.

McGwan and Bodoia[26] have performed experimental studies of the stability of a natural circulation steam generator. Experimental data from the test loop were compared to predictions from a digital computer model of a steam generator. It was found that increased power level and riser resistance have adverse effects on stability while additional downcomer resistance improved stability.

Clark[27] presented a mathematical model for the steady state and transient analysis of a natural circulation, separate drum,

horizontal steam generator of the type used in the Shippingport Nuclear Power Plant. Equations describing the conservation of mass, energy, and momentum were written for a secondary side system to match a primary side heat balance and secondary power delivered to a turbine-generator load. Major aspects of the model include steady state and transient recirculation flow, single phase density and pressure drop calculation and automatic control of the steam drum water level. Both steady state conditions and the transient response of the steam generator model were obtained by means of a digital computer program, using a finite differencing method. The model response was compared with experimental data from the Shipping-port Nuclear Power Plant.

Nahavandi and Batenburg[28] presented a combined digital-analog mathematical model for the dynamic analysis of vertical U-tube natural circulation steam generator. In the first part, a space-dependent digital program simulation was used to describe the dynamic behavior of the steam generator recirculation loop. In the second part, an analog simulator consisting of five distinct blocks was used for feedwater controller parameter optimization studies. The five blocks of the analog simulator were (a) feedwater line; (b) steam drum, (c) steam main to turbine; (d) water level controller, and (e) recirculation loop model. In the analog model, the recirculation loop was represented by six transfer functions obtained by using analog/digital techniques and the time response from the digital program to specified input perturbations. The other four blocks were represented by analytical expressions using lumped parameter

odels. The fundamental equations and method of solution for the ecirculation loop space-dependent digital model were also presented y the authors.

Hargrov[29] presented a program to calculate multiloop detailed ransient behavior of a PWR system. The program simulated two eactor coolant loop including two steam generators and associated ystems. It also simulated reactor kinetics, reactor control and rotection systems. The thermal and hydraulic characteristics of he reactor coolant system were described by time and space ifferential equations, then reduced to nodal forms, the solution f which are tractable by means of finite differences. Each steam enerator was represented by six nodes, an inlet header, an outlet eader and four primary/secondary heat transfer nodes. The heat ransfer rate from each flow section to the secondary side was calcu-ated using the logarithmic mean temperature difference (LMTD) so hat the power transferred was computed correctly even at very low low conditions. The heat transfer coefficient and heat transfer rea were treated as variables and evaluated as functions of the epresentative parameters. Perturbations related to the steam enerator were taken as primary water inlet temperature (reactor hot eg temperature), steam flow rate, feedwater flow rate and feedwater nthalpy.

Ten Wolde[30] investigated various aspects of the simulation f the nonlinear transient thermal behavior of steam generators. Both he evaporator in a sodium cooled fast breeder reactor power plant

(LMFBR) and the steam generator in a pressurized water reactor plant (PWR) are considered in the investigation. Both a hybrid continuous space discrete time (CSDT) distributed parameter model and a lumped parameter model were considered in the study. The results from these models were compared with experimental results obtained from a 6 MW PWR steam generator.

Bauer et al.[31] described a digital model of the dynamic performance of gas and pressurized water reactors designed and developed by Electricite De France for its equipment studies. The model equations were partial differential equations and were solved by the finite difference technique. The paper showed the model equations, the method of solution, and the application of the model for two cases.

a. Explanation of the pulsating behavior of the heat exchanger originally intended for the Bugey graphite gas plant.
b. Analysis of instability of water level in the Chooz PWR steam generator under low output.

Christensen[32] developed a one dimensional model of a UTSG using a mixed distributed and lumped formulation. The governing equations for the heat transfer zone and the downcomer were described by partial differential equations while the other sections of the steam generator were described by ordinary differential equations. The partial differential equations were solved by sampling in time and division into subsections in space, thus transforming the equations into algebraic equations. The equations can be solved by pure digital or hybrid techniques. The model has the advantage of

calculating the steady state response as well as the dynamic response to specified perturbations. The work reported in this dissertation was developed independently from the work reported by Christensen. A comparison between the results presented in Reference 32 and the results obtained from the detailed lumped parameter model is given in Chapter VI.

Delene[33] developed a digital simulator for dual purpose desalination plants in which multistage flash (MSF) evaporators are coupled to a Pressurized Water Reactor (PWR) nuclear power plant through a back pressure turbine. This simulator included a state variable model for a U-tube, drum type recirculating boiler. The primary liquid was divided into three sections, each described by two ordinary differential equations with outlet and average temperatures of each section as the state variables. The secondary side was represented by four equations, two for the subcooled (non-boiling section), one for the downcomer temperature, and one for the steam mass. The author stated that "several simplifying assumptions are made in the steam generator model which may limit the simulator's ability to predict the results of wide ranging transients." The model was developed only for the purpose of an overall system representation and has not been explicitly tested against other models or test results.

Murrel[34] presented a description of the components comprising the simulation of PWR nuclear power plants. The reactor was represented by a single average channel defined as a fuel element and the coolant area associated with it. Average density in the

primary circuit was calculated as a function of average temperature and pressure. The flow from the primary circuit into the pressurizer was obtained from the rate of change of primary circuit density. The recirculation flow in the UTSG was calculated from a pressure balance of static head difference against frictional and acceleration head losses which were assumed proportional to the square of the flow.

Frei et al.[35] presented a description of a computer model for a 660 MWe nuclear power plant. The model included the pressurized water reactor, steam generator, pressurizer, secondary side (steam power plant side) and controls. The results obtained from the dynamic model were compared against test results obtained during the commissioning of the plant.

Matausek[36] developed a nonlinear lumped parameter model (SINOD) for analysis of two phase flow in natural circulation boiling water loops. The model consists of the equations for the conservation of mass, momentum, and energy. The resulting equations are solved with time and length along the loop as the only independent variables. The steady state calculations was performed by solving the same set of equations with the time derivative terms set equal to zero. The input data to the model are the parameters specifying the geometry of the system under consideration, physical properties of the fluid and pressure drop coefficients along the loop. Optional correlations are provided for the calculation of slip ratio and two phase friction multipliers. The models have a thorough investigation of the interaction between mass velocity and void fraction which is considered

the basic mechanism of hydrodynamic instability. When using the model, care must be taken to insure that the assumptions built into it are reasonable for the physical system under investigation.

II.5 Remarks

From the previous discussion, it can be seen that the problem of analytical and numerical simulation of the dynamic behavior of nuclear steam generators has recently received considerable attention as a tool for design and testing of PWR nuclear power plants. Three modeling approaches are now in competition.

1. Transfer function approach.
2. Numerical (finite difference) approach.
3. State variable lumped parameter approach.

The first approach is mainly an analytical approach suitable for the solution on analog computers. The system characteristics are hidden in the complex expressions of the transfer functions which make the interpretation of results rather difficult. The second approach is a numerical approach where the system of differential equations describing the system are discretized in space and/or time to obtain local effects of a given perturbation to the system.

The third approach combines some of the advantages of the analytical approach and the numerical approach. A physical insight into the system can be achieved by examining the dynamic behavior of the system state variables. The work reported in this dissertation is an independent contribution in the area of simulating the dynamic behavior of PWR nuclear power systems using the lumped parameter state variable approach.

CHAPTER III

DEVELOPMENT OF THE MATHEMATICAL MODELS

III.1 Introduction

An essential part of the dynamic analysis of an engineering system is modeling the physical process taking place within the system during a transient. The purpose of the modeling process is to obtain a mathematical description that can predict the response of the physical system to all anticipated inputs.

For a thermal hydraulic system like a nuclear steam generator, the mathematical model consists of the equations governing the storage and transportation of mass, momentum and energy (mainly thermal) within the system during a transient.

In this chapter, a number of mathematical models for a UTSG are developed using the state variable lumped parameter approach. The models range from a three-lump model of a simplified steam generating system to a fourteen-lump detailed model of a UTSG system.

III.2 Basic Assumptions

In the process of developing mathematical models for a complex system such as a UTSG, several assumptions have to be made. The following list includes the assumptions used in this work:

1. One dimensional flow for both primary and secondary fluids. This means that radial variations of thermal and hydraulic properties of the primary and secondary fluids are neglected.

2. For the pressurized primary water and the subcooled secondary fluid, constant density and specific heat are assumed.
3. Thermal conductivity of the tube bundle metal is assumed to be constant.
4. Heat transfer coefficients are adjusted to fit the heat transfer rates and temperature differences reported by the steam generator manufacturer. Heat transfer coefficients are assumed to be constant during transients.
5. Thermodynamic properties of saturated water and saturated steam are assumed to be linear functions of pressure over a narrow range about the steady state operating point.
6. The enthalpy and mass quality of the steam water mixture in the secondary fluid boiling region are taken as linear functions of position along the heat transfer path.
7. No heat transfer takes place between the tube bundle region and the downcomer.

III.3 Structure of the Mathematical Models

From the discussion in Chapter I, page 3, it can be seen that the UTSG is coupled to the reactor coolant system through the primary coolant flow rate and temperature. These primary loop conditions determine the rate at which thermal energy is input to the steam generator system. In the development that follows, the primary coolant flow rate is assumed constant. The UTSG is also

coupled to the steam cycle through the steam outlet flow rate and the feedwater input conditions. The steam outlet flow rate is determined by the steam demand signal to the turbine stop valve. The feedwater input conditions, mainly feedwater flow rate and the feedwater temperature, are determined by feedwater pump speed, feedwater heaters, and feedwater control system. Since the main emphasis in this work was the development of UTSG models, the feedwater control system is not included in the models and the feedwater flow rate was made equal to the steam flow rate. Thus, the turbine valve coefficient and the feedwater temperature are the only allowable secondary side forcing functions.

The modeling approach used in the development of the mathematical models documented in this chapter is the stepwise lumped parameter state variable approach. The models range from a three lump model for a simplified steam generating system (Model A) to a fourteen lump detailed model (Model D) for a UTSG system with two models of intermediate complexity (B and C). Progressive development of increasingly complex models and comparison of results created confidence in the validity of the formulation of the detailed model. The lumped structure of these models are described below.

III.3.1 Simplified Steam Generating System Model (Model A)

Model A was developed as a first step for the purpose of providing a "feel" for the dynamic response of the UTSG detailed model. In this model, the steam generator is represented by the simplified steam generating system shown in Figure III.1. The model consists of the following three lumps as shown in Figure III.2.

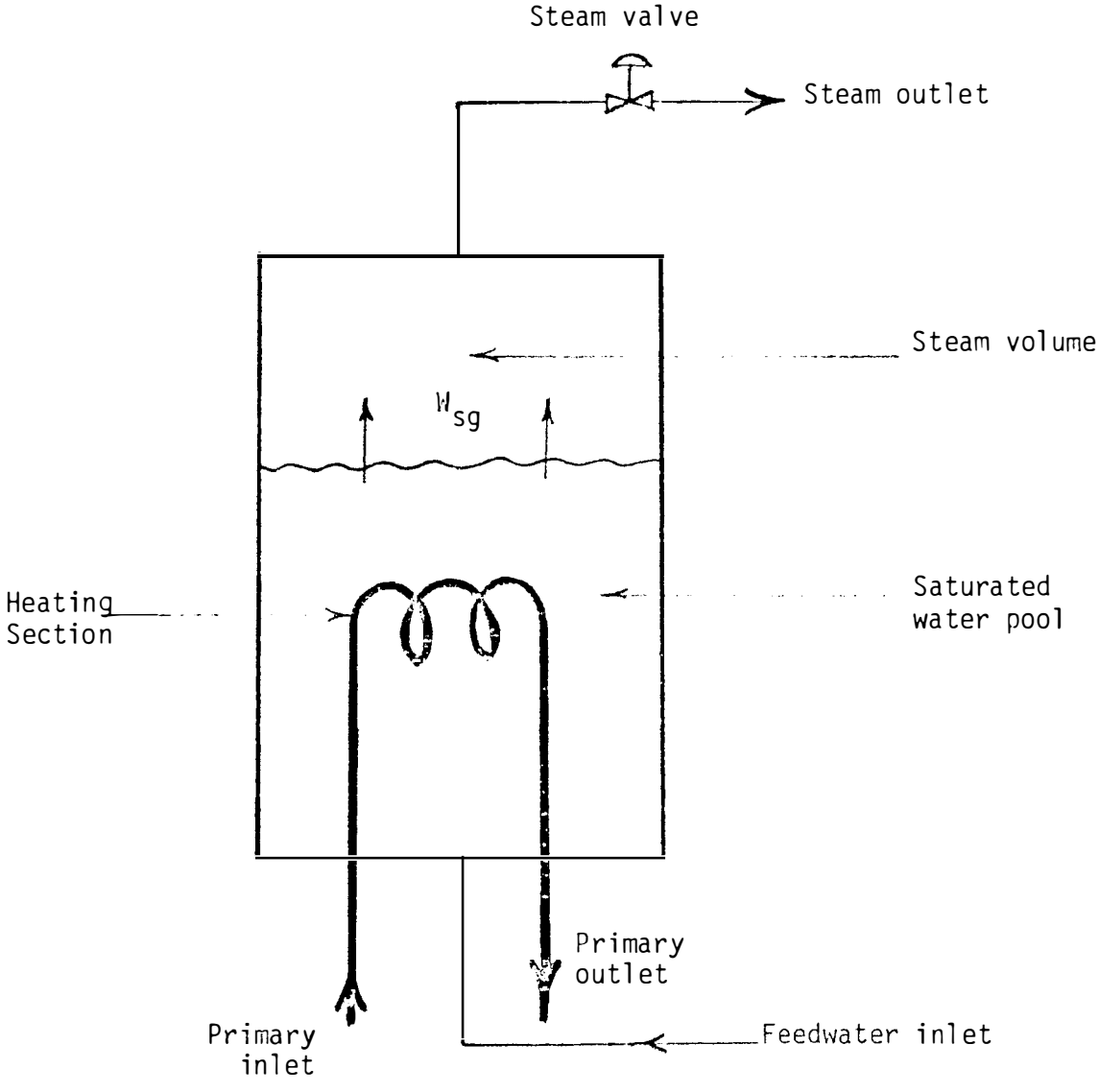

Figure III.1 Simplified Steam Generator System for Model A.

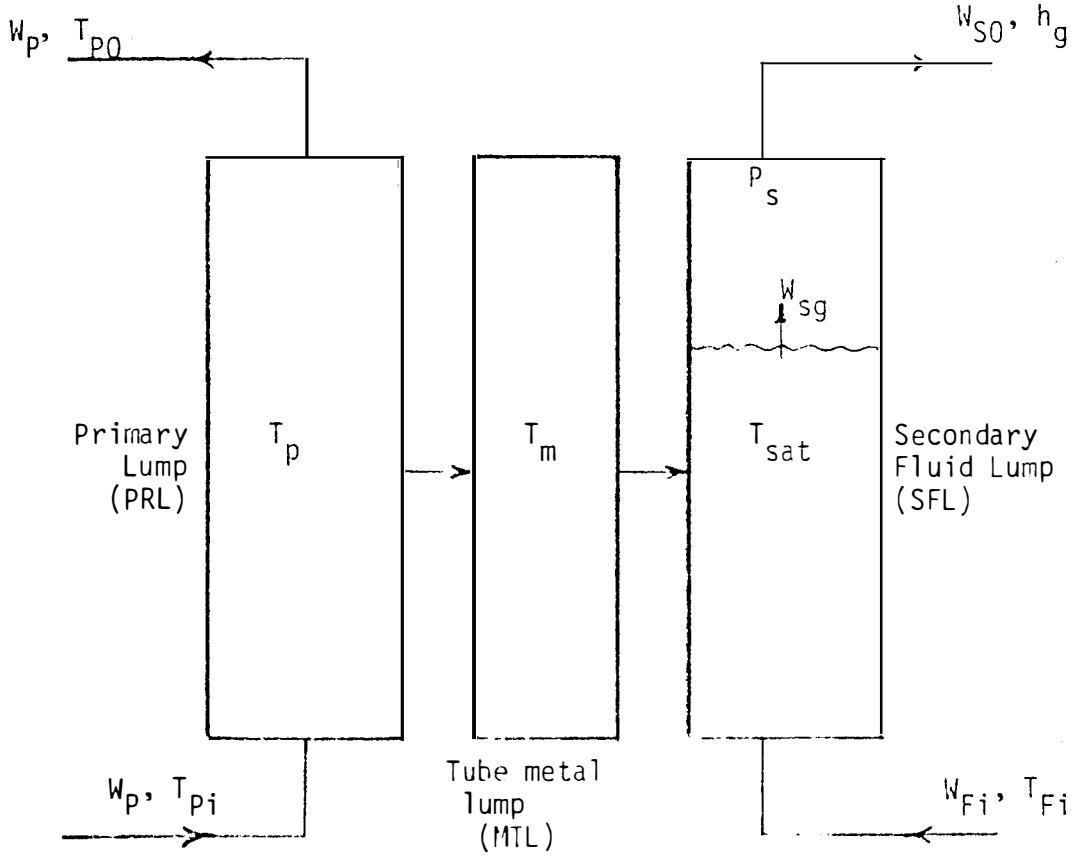

Figure III.2 Schematic Diagram for Model A.

1. Primary fluid lump (PRL).
2. Heat conducting tube metal lump (MTL).
3. Secondary fluid lump (SFL).

III.3.2 First Intermediate Model (Model B)

In Model B, the primary fluid lump and the conducting tube metal lump of Model A are each broken into two lumps to simulate the two branches of the U-tube bundle. The secondary fluid is still represented by one lump. The model consists of the following five lumps (also seen in Figure III.3):

1. Parallel flow branch primary fluid lump (PRL1)
2. Counter flow branch primary fluid lump (PRL2)
3. Parallel flow branch conducting tube metal lump (MTL1)
4. Counter flow branch conducting tube metal lump (MTL2)
5. Secondary fluid lump (SFL).

III.3.3 Second Intermediate Model (Model C)

In this model, the secondary fluid lump in Model B is broken into three lumps as shown in Figure III.4. The model thus consists of the following seven lumps.

1. Parallel flow branch primary fluid lump (PRL1)
2. Counterflow branch primary fluid lump (PRL2)
3. Parallel flow branch conducting tube metal lump (MTL1)
4. Counterflow branch conducting tube metal lump (MTL2)
5. Effective heat exchange secondary fluid lump (SFEHEL)
6. Drum equivalent secondary fluid lump (SFDRL)
7. Downcomer secondary fluid lump (SFDCL).

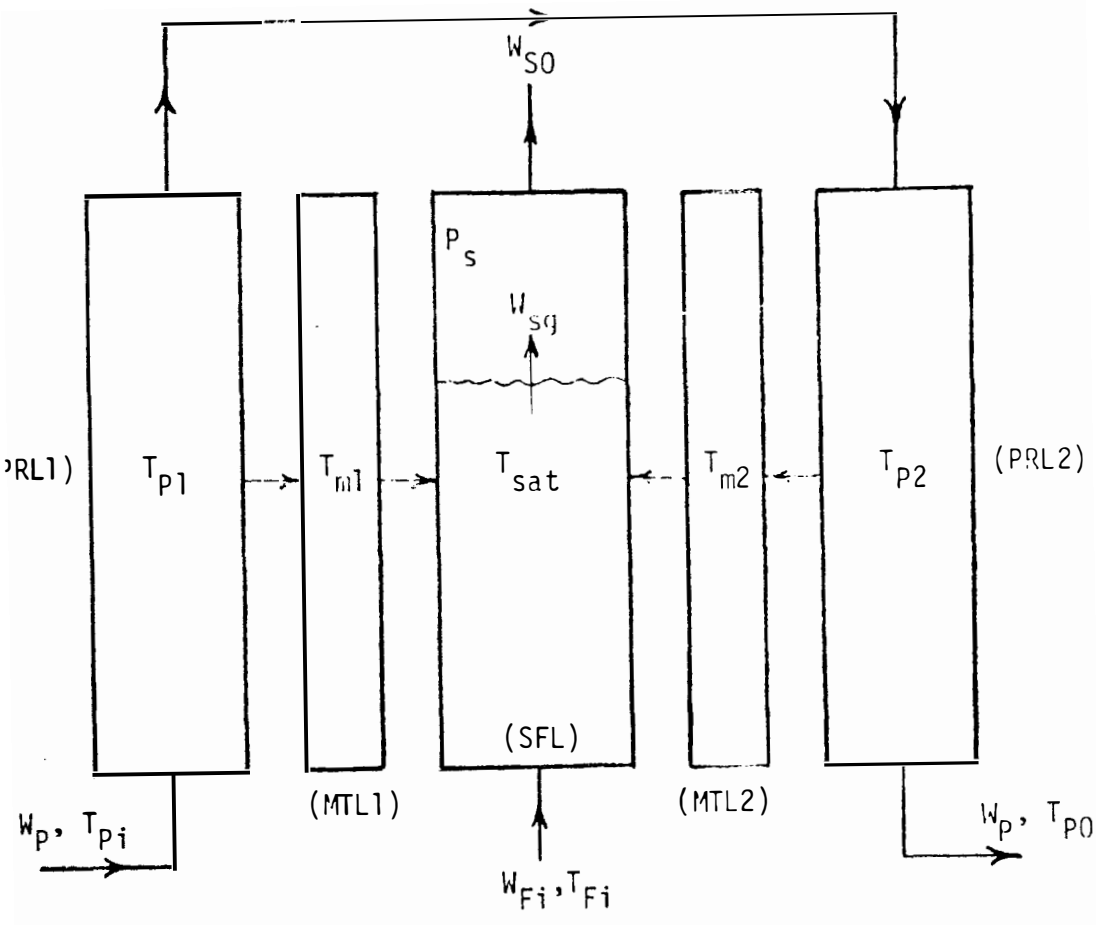

gure III.3 Schematic Diagram for Model B.

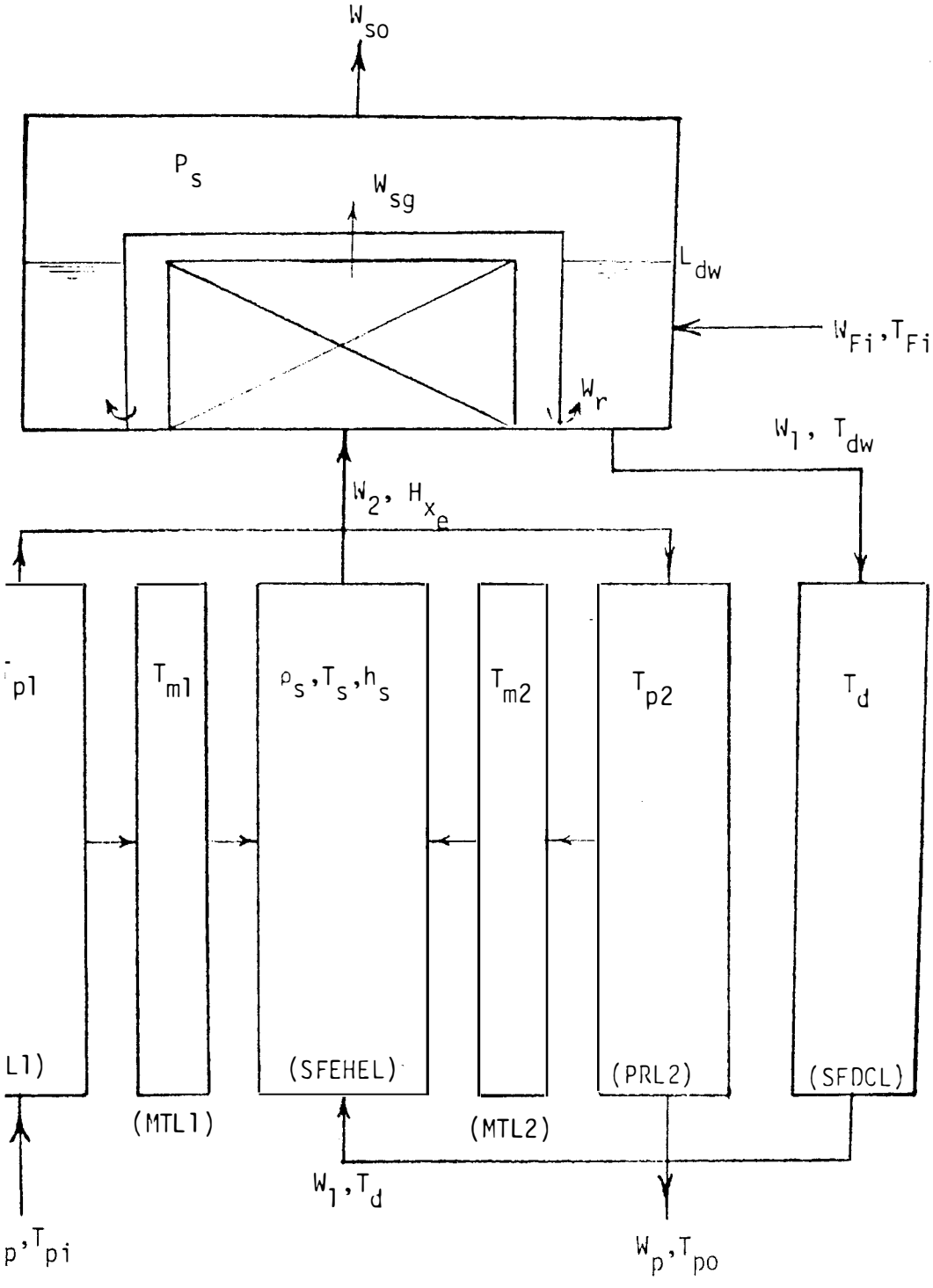

igure III.4 Schematic Diagram for Model C.

III.3.4 The Detailed Model (Model D)

In the detailed model, the effective heat exchange region (tube bundle region) is divided into a subcooled heat transfer section and a boiling heat transfer section with a dynamic boundary between the two sections. Also, the effect of primary coolant inlet and outlet plenums is examined by adding a lump for each plenum.

The detailed model structure is shown in Figure III.5 and is composed of the following lumps.

a. Primary side lumps
   1. primary inlet plenum (PRIN)
   2. parallel flow branch subcooled heat transfer section primary lump (PRL1)
   3. parallel flow branch boiling heat transfer section primary lump (PRL2)
   4. counter flow branch boiling heat transfer section primary lump (PRL3)
   5. counter flow branch subcooled heat transfer section primary lump (PRL4)
   6. primary outlet plenum (PROUT)

b. Conducting tube metal lumps.
   7. parallel flow branch subcooled heat transfer section tube metal lump (MTL1)
   8. parallel flow branch boiling heat transfer section tube metal lump (MTL2)
   9. counter flow branch boiling heat transfer section tube metal lump (MTL3)
   10. counter flow branch subcooled heat transfer section tube metal lump (MTL4)

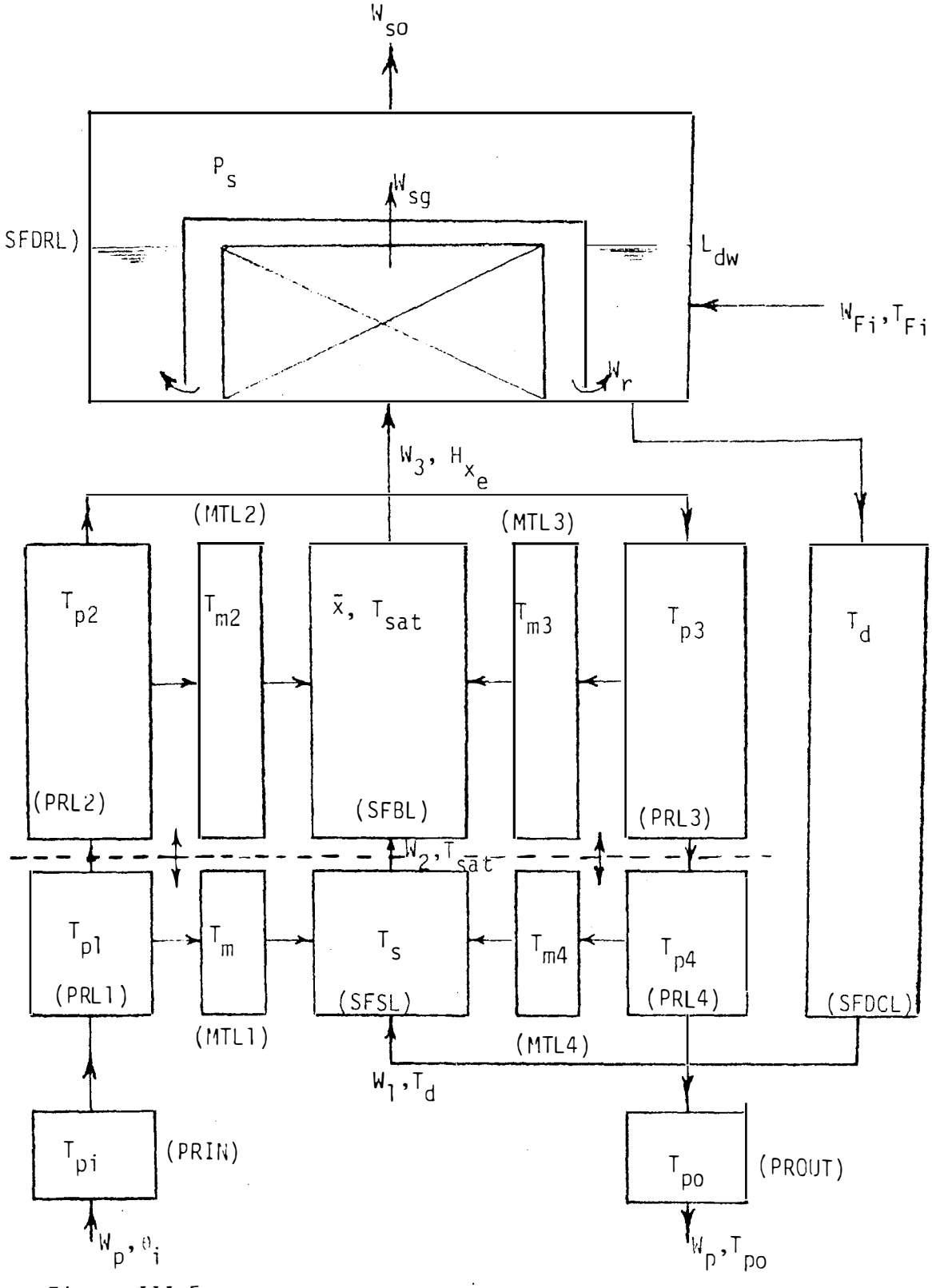

Figure III.5 Schematic Diagram for Model D.

c. Secondary side lumps

11. subcooled secondary fluid lump (SFSL)

12. boiling secondary fluid lump (SFBL)

13. drum equivalent secondary fluid lump (SFDRL)

14. downcomer secondary fluid lump (SFDCL).

III.4 Governing Equations for Model A

III.4.1 Primary Lump (PRL)

An energy balance on the primary water lump yields the following equation

$$\frac{d}{dt}(M_p C_{pl} T_p) = W_p C_{pl}(T_{pi} - T_p) - U_{pm} S_{pm}(T_p - T_m) \qquad \text{(III.4.1)}$$

where,

M_p = mass of primary water

C_{pl} = specific heat of primary water

T_p = bulk mean temperature of the primary water lump

W_p = mass flow rate of primary water

T_{pi} = inlet primary water temperature

U_{pm} = effective heat transfer coefficient between primary water and tube metal lumps

S_{pm} = heat transfer area between the primary water and tube metal lumps

T_m = average temperature of tube metal lump.

Since the density and specific heat of the primary water are assumed to be constant, then Equation (III.4.1) can be written in the form

$$\frac{dT_p}{dt} = -\left(\frac{1}{\tau_p} + \frac{U_{pm} S_{pm}}{M_p C_{pl}}\right) T_p + \frac{U_{pm} S_{pm}}{M_p C_{pl}} T_m + \frac{1}{\tau_p} T_{pi} \qquad \text{(III.4.2)}$$

where, $\tau_p = \frac{M_p}{W_p}$ = residence time of the primary water in the heating section.

Introducing perturbation variables, one obtains:

$$\frac{d\delta T_p}{dt} = -\left(\frac{1}{\tau_p} + \frac{U_{pm}S_{pm}}{M_p C_{pl}}\right) \delta T_p + \frac{U_{pm}S_{pm}}{M_p C_{pl}} \delta T_m + \frac{1}{\tau_p} \delta T_{pi} \qquad \text{(III.4.3)}$$

where δ means the deviation of the variable from its value at steady state.

III.4.2 Tube Metal Lump (MTL)

An energy balance on the tube metal lump yields the following equation

$$\frac{d}{dt}(M_m C_m T_m) = U_{pm}S_{pm}(T_p - T_m) - U_{ms}S_{ms}(T_m - T_s) \qquad \text{(III.4.4)}$$

where,

M_m = mass of tube metal

C_m = specific heat of tube metal

U_{ms} = effective heat transfer coefficient between the tube metal and secondary fluid lumps

S_{ms} = heat transfer area between the tube metal and secondary fluid lumps

T_s = bulk mean temperature in the secondary lump,

and other terms are as defined before.

For constant tube metal density and specific heat, we have

$$\frac{dT_m}{dt} = \left(\frac{U_{pm}S_{pm}}{M_m C_m}\right) T_p - \left(\frac{U_{pm}S_{pm} + U_{ms}S_{ms}}{M_m C_m}\right) T_m + \frac{U_{ms}S_{ms}}{M_m C_m} T_s. \qquad \text{(III.4.5)}$$

Thus, the perturbation form of the equation becomes

$$\frac{d\delta T_m}{dt} = \left(\frac{U_{pm} S_{pm}}{M_m C_m}\right) \delta T_p - \left(\frac{U_{pm} S_{pm} + U_{ms} S_{ms}}{M_m C_m}\right) \delta T_m + \frac{U_{ms} S_{ms}}{M_m C_m} \delta T_s. \quad \text{(III.4.6)}$$

It is assumed that the fluid in the secondary lump is a steam-water mixture at thermodynamic equilibrium. Therefore, a pressure change results in a change in saturation temperature:

$$\delta T_s = \left(\frac{\partial T_{sat}^*}{\partial P}\right) \delta P \quad \text{(III.4.7)}$$

where

P = steam pressure

$\left(\frac{\partial T_{sat}}{\partial P}\right)$ = slope of the straight line approximation of the curve of T_{sat} against P (see Appendix A).

Thus Equation (III.4.6) becomes

$$\frac{d\delta T_m}{dt} = \left(\frac{U_{pm} S_{pm}}{M_m C_m}\right) \delta T_p - \left(\frac{U_{pm} S_{pm} + U_{ms} S_{ms}}{M_m C_m}\right) \delta T_m + \left(\frac{U_{ms} S_{ms}}{M_m C_m}\right) \cdot \frac{\partial T_{sat}}{\partial P} \delta P. \quad \text{(III.4.8)}$$

III.4.3 Secondary Fluid Lump (SFL)

The governing equation for the secondary fluid lump is obtained by applying mass balances for the water and steam components, a volume balance, and an equation relating the steam generation rate W_{sg} to the heat transfer rate to the secondary fluid and the degree of subcooling of the feedwater entering the system (heat balance).

---

*Although T_{sat} and other saturation properties are considered as functions of one variable (P), the partial derivative symbol $(\partial/\partial P)$ is used for clarity of equations.

a. Mass balance

1. Water phase

$$\frac{d M_{sw}}{dt} = W_{Fi} - W_{sg} \qquad \text{(III.4.9)}$$

where,

M_{sw} = mass of water in the secondary lump

W_{Fi} = inlet feedwater flow rate

W_{sg} = steam generating (evaporation) rate

2. Steam phase

$$\frac{d M_{ss}}{dt} = W_{sg} - W_{so} \qquad \text{(III.4.10)}$$

where,

M_{ss} = mass of steam in the secondary lump

W_{so} = outlet steam flow rate

b. Volume balance

$$\frac{d V_{sw}}{dt} + \frac{d V_{ss}}{dt} = \frac{d V_{st}}{dt} = 0 \qquad \text{(III.4.11)}$$

where,

V_{sw} = volume of water in the secondary lump

V_{ss} = volume of steam in the secondary lump

V_{st} = total volume occupied by the secondary fluid.

Substituting $V_{sw} = M_{sw} \cdot v_f$

and $V_{ss} = M_{ss} \cdot v_g$,

where,

v_f = specific volume of saturated water

v_g = specific volume of saturated steam

we get

$$v_f \frac{d M_{sw}}{dt} + M_{sw} \frac{d v_f}{dt} + v_g \frac{d M_{ss}}{dt} + M_{ss} \frac{d v_g}{dt} = 0. \quad \text{(III.4.12)}$$

Neglecting the change in the specific volume of saturated water during a transient, one obtains:

$$v_f \frac{d M_{sw}}{dt} + v_g \frac{d M_{ss}}{dt} + M_{ss} \frac{d v_g}{dt} = 0 \quad \text{(III.4.13)}$$

using $\frac{d v_g}{dt} = \left(\frac{\partial v_g}{\partial P}\right) \cdot \frac{dP}{dt}$

and solving for $\frac{dP}{dt}$, we get

$$\frac{dP}{dt} = - \frac{1}{M_{ss} \frac{\partial v_g}{\partial P}} \left\{ v_f \frac{d M_{sw}}{dt} + v_g \frac{d M_{ss}}{dt} \right\} \quad \text{(III.4.14)}$$

and substituting from Equations (III.4.9) and (III.4.10) into Equation (III.4.14) and using the assumption $W_{Fi} = W_{so}$, we have

$$\frac{dP}{dt} = \frac{1}{M_{ss} \frac{\partial v_g}{\partial P}} \left\{ v_{fg} (W_{sg} - W_{so}) \right\} \quad \text{(III.4.15)}$$

where,

$$v_{fg} = v_g - v_f.$$

Using the critical flow assumption (see Appendix B), we have

$$W_{so} = C_L \cdot P$$

where,

C_L = steam valve coefficient.

Therefore,

$$\frac{dP}{dt} = \frac{-1}{M_{ss}\frac{\partial v_g}{\partial P}} \{v_{fg}(W_{sg} - C_L \cdot P)\}. \qquad \text{(III.4.16)}$$

c. Heat balance

$$\frac{d}{dt}(M_{sw}e_f + M_{ss}e_g) = U_{ms}S_{ms}(T_m - T_s) + W_{Fi}C_{P2}T_{Fi} - W_{so}h_g \qquad \text{(III.4.17)}$$

where,

e_f = internal energy of saturated water

e_g = internal energy of saturated steam

C_{P2} = specific heat of feedwater

T_{Fi} = inlet temperature of feedwater

and other terms are as defined before. The internal energy terms e_f and e_g can be replaced by the enthalpy terms h_f and h_g without significant error[22] due to the small value of the flow work term $(\frac{pv}{J})$ (see Appendix C). Since h_f and h_g are pressure dependent, we have

$$M_{sw}\frac{\partial h_f}{\partial P} \cdot \frac{dP}{dt} + h_f \frac{d M_{sw}}{dt} + M_{ss}\frac{\partial h_g}{\partial P} \cdot \frac{dP}{dt} +$$

$$+ h_g \frac{d M_{ss}}{dt} = U_{ms}S_{ms}(T_m - T_s) + W_{Fi}C_{P2}T_{Fi} - W_{so}h_g. \qquad \text{(III.4.18)}$$

Substituting from Equations (III.4.9) and (III.4.10) into Equation (III.4.18) and using the assumption $W_{Fi} = W_{so}$, we get

$$M_{sw} \frac{\partial h_f}{\partial P} \cdot \frac{dP}{dt} + M_{ss} \frac{\partial h_g}{\partial P} \cdot \frac{dP}{dt} + (W_{sg} - W_{so})(h_g - h_f) =$$

$$= U_{ms} S_{ms} (T_m - T_s) - W_{so}(h_g - C_{P2} T_{Fi}). \qquad \text{(III.4.19)}$$

From Equation (III.4.15) we have

$$(W_{sg} - W_{so}) = - \frac{M_{ss}}{v_{fg}} \frac{\partial v_g}{\partial P} \cdot \frac{dP}{dt} .$$

Thus, Equation (III.4.19) becomes

$$\left(M_{sw} \frac{\partial h_f}{\partial P} + M_{ss} \frac{\partial h_g}{\partial P} - M_{ss} \frac{h_{fg}}{v_{fg}} \cdot \frac{\partial v_g}{\partial P}\right) \frac{dP}{dt}$$

$$= U_{ms} S_{ms} (T_m - T_s) - W_{so}(h_g - C_{P2} T_{Fi}) \qquad \text{(III.4.20)}$$

where,

$$h_{fg} = h_g - h_f .$$

And, the perturbation equation becomes

$$\left(M_{sw} \frac{\partial h_f}{\partial P} + M_{ss} \frac{\partial h_g}{\partial P} - M_{ss} \frac{h_{fg}}{v_{fg}} \cdot \frac{\partial v_g}{\partial P}\right) \frac{d\delta P}{dt} =$$

$$= U_{ms} S_{ms} (\delta T_m - \delta T_s) - W_{so}\left(\frac{\partial h_g}{\partial P} \delta P - C_{P2} \delta T_{Fi}\right)$$

$$- (h_g - C_{P2} T_{Fi}) \delta W_{so}. \qquad \text{(III.4.21)}$$

Let $K = \left(M_{sw} \frac{\partial h_f}{\partial P} + M_{ss} \frac{\partial h_g}{\partial P} - M_{ss} \frac{h_{fg}}{v_{fg}} \cdot \frac{\partial v_g}{\partial P}\right)$

and substitute $\delta W_{so} = C_L \delta P + P \delta C_L$

and $\delta T_s = \frac{\partial T_{sat}}{\partial P} \delta P$ to obtain:

$$\frac{d\delta P}{dt} = \frac{1}{K} \left[U_{ms} S_{ms} \delta T_m - \left(U_{ms} S_{ms} \frac{\partial T_{sat}}{\partial P} + W_{so} \frac{\partial h_g}{\partial P}\right.\right.$$

$$\left.\left. + C_L (h_g - C_{P2} T_{Fi})\right) \delta P\right.$$

$$+ W_{so}C_{P2}\delta T_{Fi} - P(h_g - C_{P2}T_{Fi})\ \delta C_L. \quad \text{(III.4.22)}$$

III.4.4 Summary of the Model Equations

The first simplified model can be represented in the form of three first order differential equations that can be written in the matrix form

$$\frac{d\bar{x}}{dt} = A\,\bar{x} + B\,\bar{u} \quad \text{(III.4.23)}$$

where

$$\bar{x} = \begin{bmatrix} \delta T_p \\ \delta T_m \\ \delta P \end{bmatrix} \quad ; \quad \bar{u} = \begin{bmatrix} \delta T_{Pi} \\ \delta T_{Fi} \\ \delta C_L \end{bmatrix}$$

Each of the matrices, A and B, is a 3 x 3 matrix giving the coefficients of the state variable vector $\bar{x}$ and the forcing vector $\bar{u}$.

The nonzero elements of A and B are listed as follows:

$$A(1,1) = -\left(\frac{1}{\tau_p} + \frac{U_{pm}S_{pm}}{M_pC_{Pl}}\right)$$

$$A(1,2) = \frac{U_{pm}S_{pm}}{M_pC_{Pl}}$$

$$A(2,1) = \frac{U_{pm}S_{pm}}{M_mC_m}$$

$$A(2,2) = -\left(\frac{U_{pm}S_{pm} + U_{ms}S_{ms}}{M_mC_m}\right)$$

$$A(2,3) = (U_{ms}C_{ms}/M_mC_m) \cdot \frac{\partial T_{sat}}{\partial P}$$

$$A(3,2) = \frac{U_{ms}S_{ms}}{K}$$

$$A(3,3) = -\frac{1}{K}\left(U_{ms}S_{ms}\frac{\partial T_{sat}}{\partial P} + W_{so}\frac{\partial h_g}{\partial P} + C_L(h_g - C_{P2}T_{Fi})\right)$$

$$B(1,1) = \frac{1}{\tau_p}$$

$$B(3,2) = \frac{C_{P2} \cdot W_{so}}{K}$$

$$B(3,3) = -\frac{P}{K}(h_g - C_{P2}T_{Fi}).$$

III.5 Governing Equations for Model B

III.5.1 Primary Lump (PRL1)

Heat balance

$$\frac{d}{dt}(M_{P1}C_{P1}T_{P1}) = W_P C_{P1}T_{Pi} - U_{pm}(S_{pm})_1 (T_{P1} - T_{m1}) - W_P C_P T_{P1} \quad \text{(III.5.1)}$$

where,

M_{P1} = mass of primary water in PR1

T_{P1} = bulk mean temperature of PR1

$(S_{pm})_1$ = heat transfer area between PR1 and MTL1

Tm_1 = average temperature of MTL1,

and other terms are as defined before. Following the same procedure as in the first simplified model, we have

$$\frac{d\delta T_{P1}}{dt} = \frac{1}{\tau_{P1}}\delta T_{Pi} - \left(\frac{1}{\tau_{P1}} + \frac{U_{pm}(S_{pm})_1}{M_{P1}C_{P1}}\right)\delta T_{P1} + \frac{U_{pm}(S_{pm})_1}{M_{P1}C_{P1}}\delta T_{m1} \quad \text{(III.5.2)}$$

where

$\tau_{P1} = \frac{M_{P1}}{W_P}$ = residence time of the primary fluid in PR1.

III.5.2 Primary Lump (PRL2)

The equation for primary lump PRL2 can be obtained from Equation (III.5.2) by replacing T_{Pi} by T_{P1}, T_{P1} by T_{P2} and T_{m1} by T_{m2} as follows:

$$\frac{d\delta T_{P2}}{dt} = \frac{1}{\tau_{P2}}\delta T_{P1} - \left(\frac{1}{\tau_{P2}} + \frac{U_{pm}(S_{pm})_2}{M_{P2}C_{P1}}\right)\delta T_{P2} + \frac{U_{pm}(S_{pm})_2}{M_{P2}C_{P1}}\delta T_{m2}. \quad \text{(III.5.3)}$$

III.5.3 Tube Metal Lump (MTL1)

Heat balance

$$\frac{d}{dt}(M_{m1}C_m T_{m1}) = U_{pm}(S_{pm})_1 (T_{P1}-T_{m1}) - U_{ms}(S_{ms})_1 (T_{m1}-T_s) \quad \text{(III.5.4)}$$

where,

M_{m1} = mass of tube metal lump MTL1

T_s = bulk mean temperature of the secondary fluid lump.

Assuming that T_s is equal to T_{sat}, the saturation temperature, and using the same procedure as in the case of the first simplified model (Model A), we get:

$$\frac{d\,\delta T_{m1}}{dt} = \frac{U_{pm}(S_{pm})_1}{M_{m1}C_m}\delta T_{P1} - \left(\frac{U_{pm}(S_{pm})_1 + U_{ms}(S_{ms})_1}{M_{m1}C_m}\right)\delta T_m + \frac{U_{ms}(S_{ms})_1}{M_{m1}C_m}\frac{\partial T_{sat}}{\partial P}\delta P. \quad \text{(III.5.5)}$$

III.5.4 Tube Metal Lump (MTL2)

The equation for tube metal lump MTL2 can be obtained, by similarity, from Equation (III.5.5) as follows:

$$\frac{d\,\delta T_{m2}}{dt} = \frac{U_{pm}(S_{pm})_2}{M_{m2}C_m}\delta T_{P2} - \left(\frac{U_{pm}(S_{pm})_2 + U_{ms}(S_{ms})_2}{M_{m2}C_m}\right)\delta T_{m2} + \frac{U_{ms}(S_{ms})_2}{M_{m2}C_m}\cdot\frac{\partial T_{sat}}{\partial P}\cdot\delta P. \quad \text{(III.5.6)}$$

III.5.5 Secondary Fluid Lump (SFL)

The only difference in the formulation of the secondary lump equation between this model and the first one is that the heat is

transferred to the secondary lump from both metal lumps M_1 and M_2.

Thus, the heat balance equation becomes.

$$\frac{d}{dt}(M_{sw}h_f + M_{ss}h_g) = U_{ms}(S_{ms})_1 (T_{m1}-T_{sat}) + U_{ms}(S_{ms})_2 (T_{m2}-T_{sat}) + W_{Fi}C_{P2}T_{Fi} - W_{so}h_g. \quad \text{(III.5.7)}$$

That is:

$$M_{sw}\frac{dh_f}{dt} + h_f\frac{d\,M_{sw}}{dt} + M_{ss}\frac{dh_g}{dt} + h_g\frac{d\,M_{ss}}{dt} = U_{ms}(S_{ms})_1 (T_{m1}-T_{sat}) + U_{ms}(S_{ms})_2 (T_{m2}-T_{sat}) + W_{Fi}C_{P2}T_{Fi} - W_{so}h_g. \quad \text{(III.5.8)}$$

By using the relations

$$\frac{dh_g}{dt} = \frac{\partial h_g}{\partial P}\cdot\frac{dP}{dt}$$

and

$$\frac{dh_f}{dt} = \frac{\partial h_f}{\partial P}\cdot\frac{dP}{dt}$$

and substituting for $\frac{dM_{sw}}{dt}$ and $\frac{dM_{ss}}{dt}$ from Equation (III.4.9) and Equation (III.4.10) we get

$$(M_{sw}\frac{dh_f}{dP} + M_{ss}\frac{dh_g}{dP})\frac{dP}{dt} = U_{ms}(S_{ms})_1 (T_{m1}+T_{m2}-2T_{sat}) + W_{Fi}C_{P2}T_{Fi} - h_g(W_{sg}-W_{so}) - h_f(W_{Fi}-W_{sg}) - W_{so}h_g. \quad \text{(III.5.9)}$$

Using the assumption that feedwater is adjusted to match steam flow ($W_{Fi} = W_{so}$), and substituting for ($W_{sg} - W_{so}$) from Equation (III.4.15), we get

$$\left(M_{sw}\frac{dh_f}{dP} + M_{ss}\frac{dh_g}{dP} - M_{ss}\frac{h_{fg}}{v_{fg}}\cdot\frac{dv_g}{dP}\right)\frac{dP}{dt} =$$

$$U_{ms}(S_{ms})_1\,(T_{m1}+T_{m2}-2T_{sat}) - W_{so}(h_g - C_{P2}T_{Fi}). \qquad \text{(III.5.10)}$$

Introducing perturbation variables, we get:

$$\frac{d\delta P}{dt} = \frac{1}{K}\left[U_{ms}(S_{ms})_1\,\{\delta T_{m1} + \delta T_{m2}\} - \{2U_{ms}(S_{ms})_1\frac{\partial T_{sat}}{\partial P} + \right.$$

$$+ W_{so}\frac{\partial h_g}{\partial P} + C_L(h_g - C_{P2}T_{Fi})\}\,\delta P +$$

$$\left. + W_{so}\,C_{P2}\delta T_{Fi} - P(h_g - C_{P2}T_{Fi})\,\delta C_L\right]. \qquad \text{(III.5.11)}$$

III.5.6 Summary of the Model Equations

Model B can be represented in the form of five, first order differential equations that can be written in the matrix form given in Equation (III.4.23) where

$$\bar{x} = \begin{bmatrix} \delta T_{P1} \\ \delta T_{P2} \\ \delta T_{m1} \\ \delta T_{m2} \\ \delta P \end{bmatrix} \quad ; \quad \bar{u} = \begin{bmatrix} \delta T_{Pi} \\ \delta T_{Fi} \\ \delta C_L \end{bmatrix}$$

In this case, A is a 5x5 matrix and B is a 5x3 matrix giving the coefficients of the state variable vector $\bar{x}$ and the forcing vector $\bar{u}$, respectively.

The nonzero elements of A and B are listed as follows:

$$A(1,1) = -\left(\frac{1}{\tau_{P1}} + \frac{U_{pm}(S_{pm})}{M_{P1}C_{P1}}\right)$$

$$A(1,3) = \frac{U_{pm}(S_{pm})_1}{M_{P1}C_{P1}}$$

$$A(2,1) = \frac{1}{\tau_{P2}} = \frac{1}{\tau_{P1}}$$

$$A(2,2) = -\left(\frac{1}{\tau_{P2}} + \frac{U_{pm}(S_{pm})_2}{M_{P2}C_{P1}}\right) = A(1,1)$$

$$A(2,4) = \frac{U_{pm}(S_{pm})_2}{M_{P2}C_{P1}} = A(1,3)$$

$$A(3,1) = \frac{U_{pm}(S_{pm})_1}{M_{m1}C_m}$$

$$A(3,3) = -\left(\frac{U_{pm}(S_{pm})_1 + U_{ms}(S_{ms})_1}{M_{m1}C_m}\right.$$

$$A(3,5) = \frac{U_{ms}(S_{ms})_1}{M_{m1}C_m}\left(\frac{\partial T_{sat}}{\partial P}\right)$$

$$A(4,2) = \frac{U_{pm}(S_{pm})_2}{M_{m1}C_m} = A(3,1)$$

$$A(4,4) = -\left(\frac{U_{pm}(S_{pm})_2 + U_{ms}(S_{ms})_2}{M_{m2}C_m}\right) = A(3,3)$$

$$A(4,5) = A(3,5)$$

$$A(5,3) = \frac{U_{ms}(S_{ms})_1}{K}$$

$$A(5,4) = \frac{U_{ms}(S_{ms})_2}{K} = A(5,3)$$

$$A(5,5) = \frac{-1}{K}\{2\ U_{ms}(S_{ms})_1 \frac{\partial T_{sat}}{\partial P} + W_{so}\frac{\partial h_g}{\partial P} + C_L(h_g - C_{P2}T_{Fi})\}$$

$$B(1,1) = \frac{1}{\tau_{P1}}$$

$$B(5,2) = \frac{W_{so}C_{P2}}{K}$$

$$B(5,3) = -\frac{P(h_g - C_{P2}T_{Fi})}{K} \quad .$$

III.6 Governing Equations for Model C

III.6.1 General

The structure of this second intermediate model was described in Section III.3, page 26, and shown schematically in Figure III.4, page 32. The difference between this model and the first intermediate model (Model B) is that a more detailed lump structure of the secondary side is used. The governing equations for the primary fluid and tube metal lumps in Model C are similar to those in Model B and are repeated in this section for convenience. The governing equations for the secondary fluid lumps are derived in detail since they will be used in the development of the detailed model (Model D).

III.6.2 Primary Lump (PRL1)

The equation for the primary lump PRL1 in Model C is similar to Equation (III.5.2). That is:

$$\frac{d\delta T_{P1}}{dt} = \frac{1}{\tau_{P1}}\delta T_{Pi} - (\frac{1}{\tau_{P1}} + \frac{U_{pm}S_{pm1}}{M_{P1}C_{P1}})\ \delta T_{P1} + \frac{U_{pm}S_{pm1}}{M_{P1}C_{P1}}\delta T_{m1}. \qquad (III.6.1)$$

III.6.3 Primary Lump (PRL2)

The equation for the primary lump PRL2 in Model C is similar to Equation (III.5.3). That is:

$$\frac{d\delta T_{P2}}{dt} = \frac{1}{\tau_{P2}} \delta T_{P1} - \left(\frac{1}{\tau_{P2}} + \frac{U_{pm} S_{pm2}}{M_{P2} C_{P1}}\right) \delta T_{P2} + \frac{U_{pm} S_{pm2}}{M_{P2} C_{P1}} \delta T_{m2}. \quad \text{(III.6.2)}$$

III.6.4 Tube Metal Lump (MTL1)

The equation for the tube metal lump MTL1 in Model C is similar to Equation (III.5.5) except that T_s is considered a state variable (instead of pressure) to account for the change in secondary temperature between the subcooled and boiling regions of the effective heat exchange secondary fluid lump. That is:

$$\frac{d\delta T_{m1}}{dt} = \frac{U_{pm} S_{pm1}}{M_{m1} C_m} \delta T_{P1} - \left(\frac{U_{pm} S_{pm1} + U_{ms} S_{ms1}}{M_{m1} C_m}\right) \delta T_{m1} + \frac{U_{ms} S_{ms1}}{M_{m1} C_m} \delta T_s. \quad \text{(III.6.3)}$$

III.6.5 Tube Metal Lump (MTL2)

The equation for the tube metal lump MTL2 in Model C is similar to Equation (III.5.6) except for the use of T_s as a state variable (see above). That is:

$$\frac{d\delta T_{m2}}{dt} = \frac{U_{pm} S_{pm2}}{M_{m2} C_m} \delta T_{P2} - \left(\frac{U_{pm} S_{pm2} + U_{ms} S_{ms2}}{M_{m2} C_m}\right) \delta T_{m2} + \frac{U_{ms} S_{ms2}}{M_{m2} C_m} \delta T_s. \quad \text{(III.6.4)}$$

III.6.6 Effective Heat Exchange Secondary Fluid Lump (SFEHEL)

This lump represents the core of the steam generator secondary fluid where the main heat exchange process takes place as shown in Figure III.6. The secondary fluid that enters from the downcomer

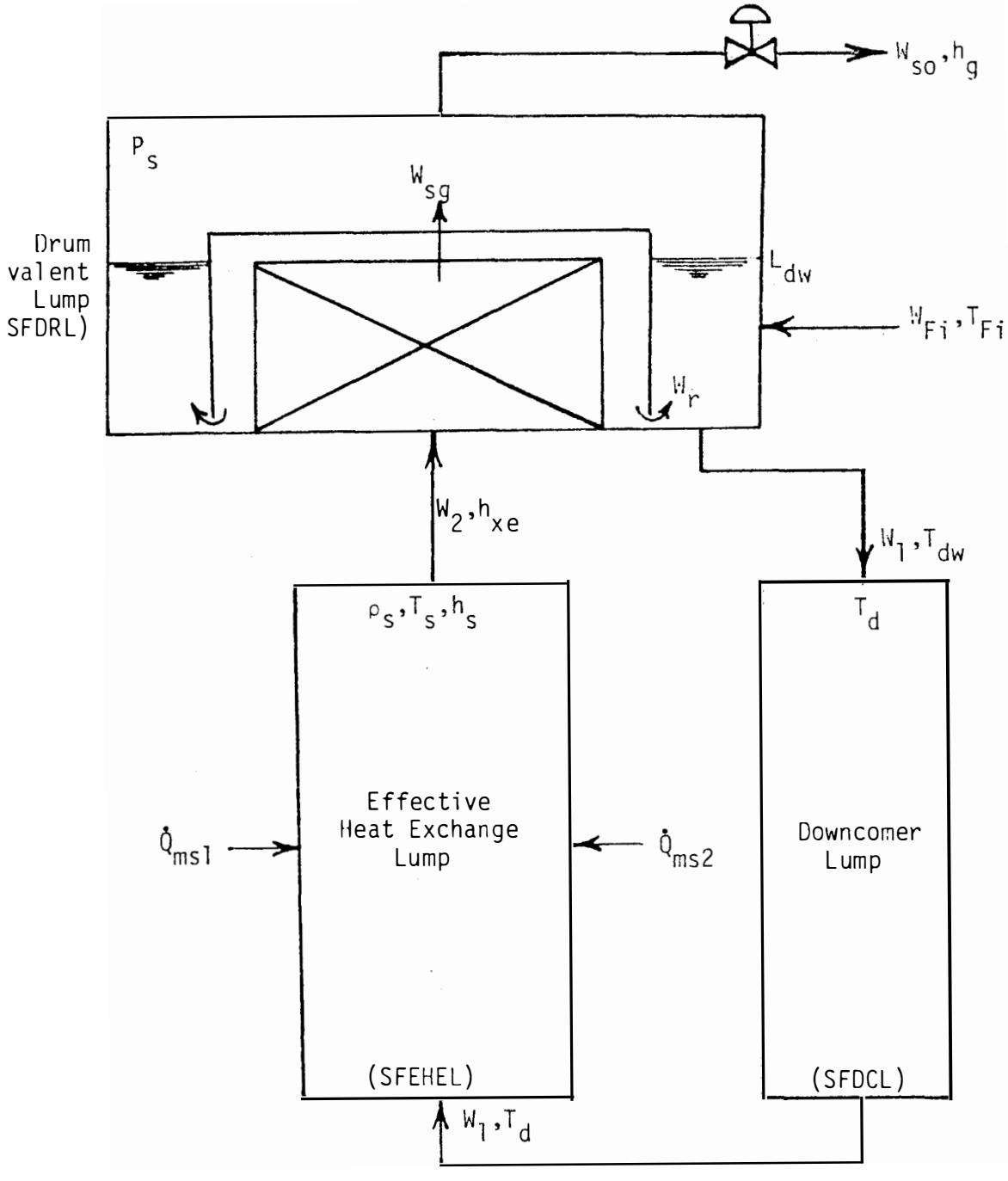

Figure III.6 Secondary Lumps for Model C.

section receives heat from both branches of the U-tube bundle and is converted from a slightly subcooled liquid into a two phase mixture that rises to enter the drum equivalent section. An energy balance on the control volume enclosing the effective heat exchange lump yields the following equation

$$\frac{d}{dt}(M_s h_s) = \dot{Q}_{ms1} + \dot{Q}_{ms2} + W_1 C_{P2} T_d - W_2 h_{xe} \qquad \text{(III.6.5)}$$

where,

M_s = mass of secondary fluid

h_s = average enthalpy of secondary fluid

$\dot{Q}_{ms1}$ = heat transfer rate from the parallel flow tube metal branch to the secondary fluid = $U_{ms} S_{ms} (T_{m1} - T_s)$

$\dot{Q}_{ms2}$ = heat transfer rate from the counter flow tube metal branch to the secondary fluid = $U_{ms} S_{ms} (T_{m2} - T_s)$

W_1 = mass flow rate of secondary fluid from the downcomer to the riser

C_{P2} = specific heat of the subcooled liquid leaving the downcomer section

T_d = temperature of the subcooled liquid leaving the downcomer section

W_2 = outlet secondary fluid mass flow rate

h_{xe} = enthalpy of the outlet secondary fluid.

Since the effective heat exchange lump is bounded at the bottom by the tube sheet and at the top by a hypothetical plane just above

the tube bundle, the volume of the lump is constant and Equation (III.6.5) becomes

$$V_s \frac{d}{dt}(\rho_s h_s) = U_{ms} S_{ms} (T_{m1} + T_{m2} - 2T_s) + W_1 C_{P2} T_d - W_2 h_e \quad \text{(III.6.6)}$$

where,

V_s = volume of the secondary fluid in the effective heat exchange lump

ρ_s = average density of the secondary fluid in the effective heat exchange lump

T_s = average temperature of the secondary fluid in the effective heat exchange lump.

The secondary fluid in the effective heat exchange lump is composed of two regions, a subcooled region where the bulk mean temperature of the subcooled water is raised from the downcomer temperature to the saturation temperature and a boiling region where part of the saturated water is converted into steam. Let L_{sub} be the length of subcooled region and L_{boil} be the length of the boiling region. L_{sub} (the level at which the boiling process starts) can be determined from a calculation of the secondary temperature profile in the effective heat exchange lump at steady state.

Since the dynamic response of the subcooled/boiling interface is not considered in this model, L_{sub} (and hence $\frac{L_{sub}}{L_{boil}}$) is assumed to be constant. The average thermodynamic properties of the secondary fluid in the effective heat exchange lump are derived from the weighted average of the properties in the subcooled and boiling regions. Figure III.7 shows the variation of the thermodynamic

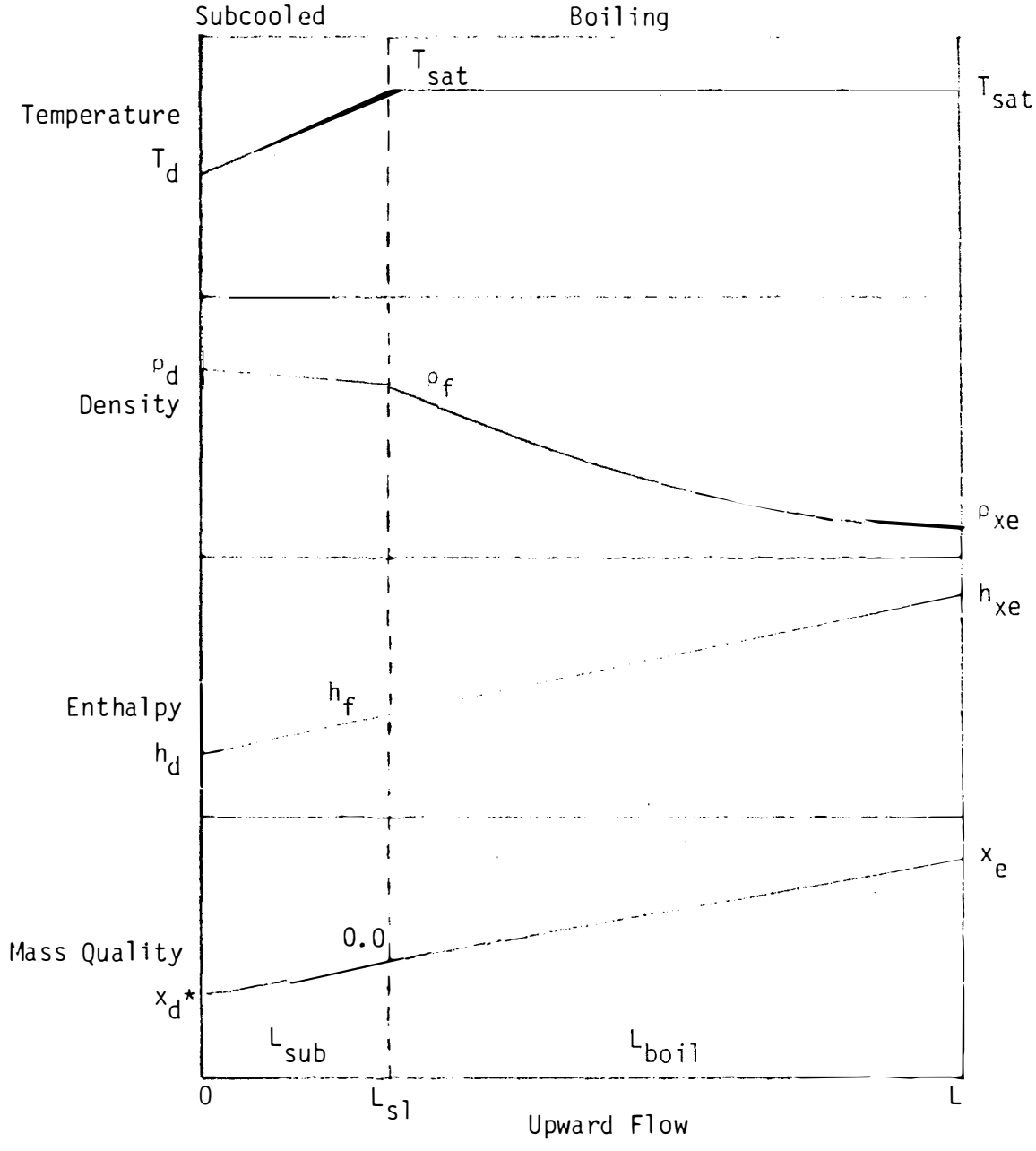

Figure III.7 Variation of Thermodynamic Properties of the Secondary Fluid in the Effective Heat Exchange Lump.

*$x_d \equiv \frac{h_d - h_f}{h_{fg}}$.

properties of the secondary fluid in the subcooled and boiling regions of the effective heat exchange lump. From this figure, the following equations are obtained for the average thermodynamic properties of the secondary fluid in the effective heat exchange lump.

$$T_s = \left(\frac{T_d+T_{sat}}{2}\right) \cdot \frac{L_{sub}}{L} + T_{sat} \cdot \frac{L_{boil}}{L} \qquad \text{(III.6.7)}$$

$$\rho_s = \left(\frac{\rho_d+\rho_f}{2}\right) \cdot \frac{L_{sub}}{L} + \frac{1}{v_f + \frac{x_e}{2} v_{fg}} \cdot \frac{L_{boil}}{L} \qquad \text{(III.6.8)}$$

$$h_s = C_{P2}\left(\frac{T_d+T_{sat}}{2}\right) \cdot \frac{L_{sub}}{L} + \left(h_f + \frac{x_e}{2} h_{fg}\right) \cdot \frac{L_{boil}}{L} \qquad \text{(III.6.9)}$$

$$x_s = \frac{C_{P2}(T_d-T_{sat})}{h_{fg}} \cdot \frac{L_{sub}}{L} + \frac{x_e}{2} \cdot \frac{L_{boil}}{L} . \qquad \text{(III.6.10)}$$

In the above equations, the subscript (s) indicates average properties in the effective heat exchange region and the subscript (d) indicates downcomer exit properties. Substituting from Equations (III.6.7) to (III.6.10) into Equation (III.6.6) and neglecting the changes in the subcooled density during the transient, one obtains the following equation:

$$M_s \frac{d}{dt}\left[C_{P2}\left(\frac{T_d+T_{sat}}{2}\right) \cdot \frac{L_{sub}}{L} + \left(h_f + \frac{x_e}{2} h_{fg}\right) \cdot \frac{L_{boil}}{L}\right]$$

$$+ V_s h_s \frac{d}{dt}\left[\frac{1}{v_f + \frac{x_e}{2} v_{fg}} \cdot \frac{L_{boil}}{L}\right]$$

$$= U_{ms} S_{ms}\left[T_{m1}+T_{m2}-2\left(\frac{T_d+T_{sat}}{2} \cdot \frac{L_{sub}}{L} + T_{sat} \cdot \frac{L_{boil}}{L}\right)\right] + W_1 C_{P2} T_d -$$

$$- W_2(h_f + x_e h_{fg}). \qquad \text{(III.6.11)}$$

Performing the differentiation in Equation (III.6.11) and using the assumption of linear change of the thermodynamic properties of saturated water and steam with the steam generator pressure (see Appendix A) one can write the equation describing the heat balance of the effective heat exchange lump in the form:

$$\left[M_s \cdot \frac{L_{sub}}{L} \cdot \frac{C_{P2}}{2} \frac{\partial T_{sat}}{\partial P} + M_s \cdot \frac{L_{boil}}{L} \cdot \left(\frac{\partial h_f}{\partial P} + \frac{x_e}{2} \frac{\partial h_{fg}}{\partial P}\right) + C_{1b} V_s h_s \cdot \frac{L_{boil}}{L}\right] \frac{d\delta P}{dt}$$

$$+ \left[M_s \frac{L_{sub}}{L} \cdot \frac{C_{P2}}{2}\right] \frac{d\delta T_d}{dt} + \left[M_s \frac{L_{boil}}{L} \cdot \frac{h_{fg}}{2} + C_{2b} V_s h_s \cdot \frac{L_{boil}}{L}\right] \frac{d\delta x_e}{dt}$$

$$= U_{ms} S_{ms} (\delta T_{m1} + \delta T_{m2} - 2\delta T_s) + C_{P2}[W_1 \delta T_d + T_d \delta W_1]$$

$$- W_2 \left[\frac{\partial h_f}{\partial P} + x_e \frac{\partial h_{fg}}{\partial P}\right] \delta P - W_2 h_{fg} \delta x_e - h x_e \delta W_2 \qquad \text{(III.6.12)}$$

where C_{1b} and C_{2b} are the coefficients of δP and δx_e in the derivative of the average density in the boiling region (see Appendix E). From Equation (III.6.7) we have

$$\delta T_s = \frac{L_{sub}}{2L} \delta T_d + \left(\frac{L_{sub}}{2L} + \frac{L_{boil}}{L}\right) \frac{\partial T_{sat}}{\partial P} \delta P. \qquad \text{(III.6.13)}$$

The relation between the flow rates W_1 and W_2 can be obtained from the mass balance equation as follows

$$V_s \frac{d\rho_s}{dt} = W_1 - W_2. \qquad \text{(III.6.14)}$$

Substituting for ρ_s from Equation (III.6.8) and introducing the perturbation variables

$$V_s\left[\frac{L_{boil}}{L}\left(C_{1b}\frac{d\delta p}{dt} + C_{2b}\frac{d\delta x_e}{dt}\right)\right] = \delta W_1 - \delta W_2. \qquad \text{(III.6.15)}$$

Equations (III.6.12), (III.6.13), and (III.6.15) are the describing equations for the effective heat exchange lump.

III.6.7 Drum Equivalent Secondary Fluid Lump (SFDRL)

The drum equivalent secondary fluid lump in this model is bounded by the hypothetical plane above the U-tube bundle and the steam generator shell inner surface as shown in Figure III.8. This lump can be divided into three parts

1. Riser/separator volume
2. Drum water volume
3. Drum steam volume.

The riser/separator volume represents the control volume bounded by the hypothetical plane at the exit of the effective heat exchange lump, the U-tube wrapper and the inner surface of the steam separators. The drum water volume represents the control volume bounded by the hypothetical plane at the exit of the effective heat exchange lump, the steam water interface, the housing of the steam separators and the steam generator shell inner surface (see Figure III.8). The drum steam volume represents the control volume bounded by the steam water interface, the steam separators and the steam generator inner surface. In the riser/separator volume, the two phase mixture leaving the effective heat exchanger lump is transported to the steam separators where the saturated steam part enters the drum steam volume and the saturated water part enters the drum water volume. In the drum water

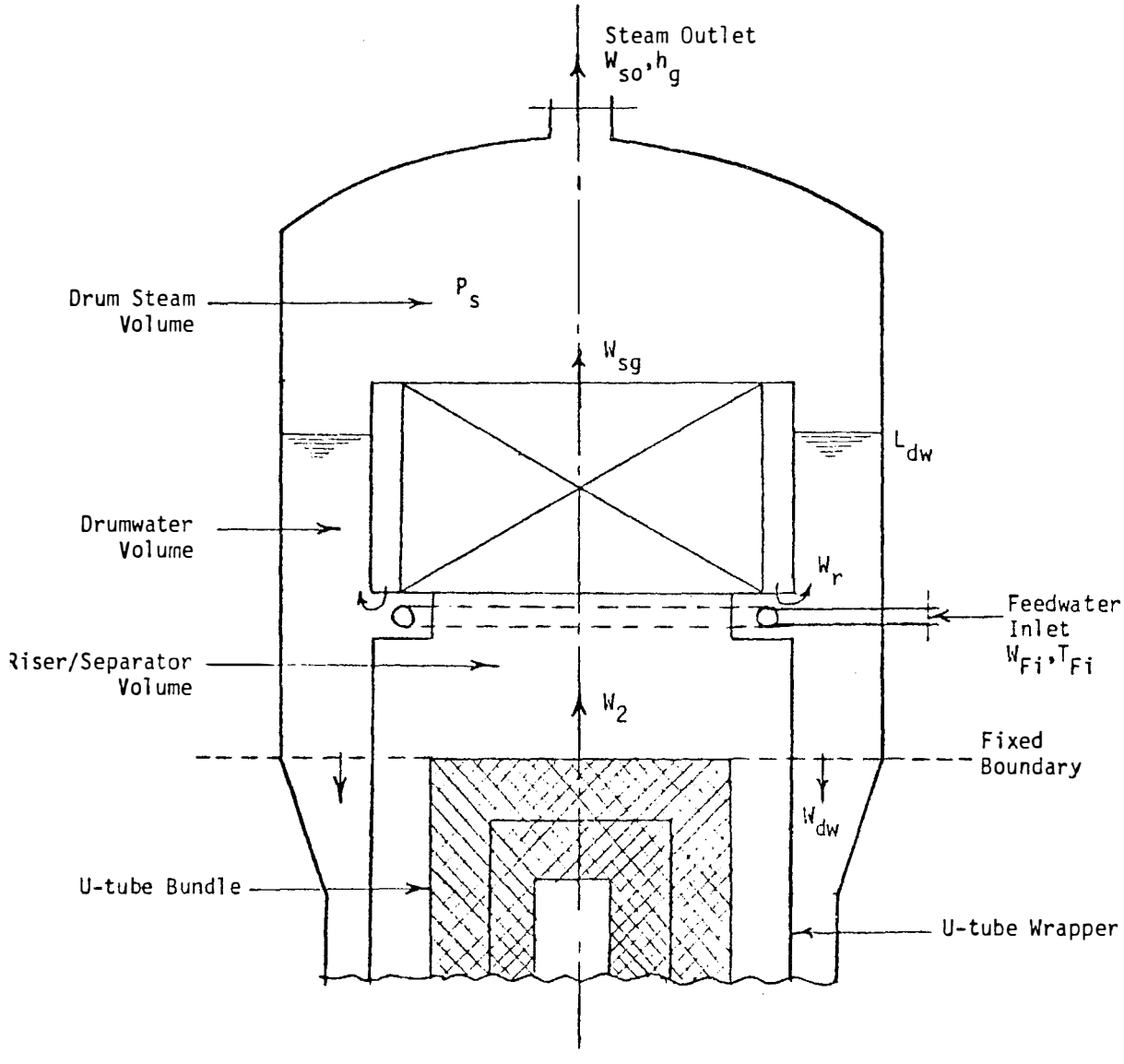

Figure III.8 The Drum Equivalent Secondary Fluid Lump.

volume, the saturated water from the steam separators is mixed with the feedwater entering through the feedwater ring and the slightly subcooled liquid thus formed flows downward to enter the downcomer lump. The drum steam volume acts as a steam storage and delivery section where the steam from the steam separators enters at a rate proportional to the exit quality of the evaporator section and leaves at a rate proportional to the turbine load demand. The governing equations for the above three volumes constituting the drum equivalent lump are developed below.

III.6.7.1 Riser/Separator Volume

This volume is mainly a transport section between the effective heat exchange lump and the steam and water volumes of the drum equivalent lump. The transport time delay associated with this volume can be accounted for by considering a mass balance on the riser/separator volume as follows:

$$\frac{d}{dt}(V_r \rho_r) = W_2 - W_3 \qquad \text{(III.6.16)}$$

where,

V_r = volume of the secondary fluid in the riser/separator volume

ρ_r = density of the secondary fluid in the riser/separator volume

W_2 = mass flow rate of the secondary fluid entering the riser/separator volume

W_3 = mass flow rate of secondary fluid leaving the riser/separator volume.

The density of the secondary fluid in the riser/separator volume can be expressed by the following equation:

$$\rho_r = \frac{1}{v_f + x_e v_{fg}} \qquad \text{(III.6.17)}$$

where

x_e = mass quality of the two phase mixture leaving the effective heat exchange lump

v_f = specific volume of saturated liquid

v_g = specific volume of saturated vapor.

From Equations (III.6.19) and (III.6.20), we have

$$V_r \frac{d}{dt}\left(\frac{1}{v_f+x_e v_{fg}}\right) + \frac{1}{(v_f+x_e v_{fg})} \frac{dV_r}{dt} = W_2 - W_3. \qquad \text{(III.6.18)}$$

Since the riser/separator volume is bounded by the hypothetical plane at the exit of the economizer-evaporator section and the U-tube wrapper then V_r is constant, and Equation (III.6.18) becomes

$$V_r \frac{d}{dt}\left(\frac{1}{v_f+x_e v_{fg}}\right) = W_2 - W_3. \qquad \text{(III.6.19)}$$

Differentiating and introducing the perturbation variables, we get

$$V_r\left(C_{1r} \frac{d\delta P}{dt} + C_{2r} \frac{d\delta x_e}{dt}\right) = \delta W_2 - \delta W_3 \qquad \text{(III.6.20)}$$

where

$$C_{1r} = -\frac{1}{(v_f+x_e v_{fg})^2}\left[\frac{\partial v_f}{\partial P} + x_e \frac{\partial v_{fg}}{\partial P}\right]$$

and

$$C_{2r} = -\frac{1}{(v_f+x_e v_{fg})^2}\left[v_{fg}\right] \text{ (see Appendix E).}$$

III.6.7.2 Drum Water Volume

The drum water volume is bounded at the bottom by the hypothetical plane separating the downcomer section from the drum section and is bounded at the top by the drum steam/water interface. Subcooled water from the feedwater train enters the drum water volume and mixes with the saturated water recirculated from the steam separators. The slightly subcooled water resulting from the mixing process leaves the drum water volume to the downcomer section. The mass and energy conservation equations applied to the drum water volumes yield:

$$\frac{d}{dt}(M_{dw}) = W_{Fi} + W_r - W_{dw} \qquad \text{(III.6.21)}$$

and

$$\frac{d}{dt}(M_{dw}C_{P2}T_{dw}) = W_{Fi}C_{P2}T_{Fi} + W_rC_{P2}T_{sat} - W_{dw}C_{P2}T_{dw} \qquad \text{(III.6.22)}$$

where

M_{dw} = mass of drum water

T_{dw} = drum water temperature

W_{Fi} = feedwater flow rate

T_{Fi} = feedwater inlet temperature

W_r = recirculated water flow rate

T_{sat} = saturation temperature

W_{dw} = drum water volume outlet flow rate

The recirculated water flow rate is determined by the secondary fluid mass flow rate entering the steam separation section and the evaporator exit quality thus

$$W_r = (1 - x_e)\, W_3 \qquad \text{(III.6.23)}$$

where

x_e = evaporator exit quality

and W_3 = secondary fluid mass flow rate entering the steam separation section.

Substituting from Equation (III.6.23) into Equations (III.6.21) and (III.6.22) and neglecting the difference in specific heat between subcooled and saturated water, we get:

$$\frac{d}{dt}(M_{dw}) = W_{Fi} + (1-x_e)\, W_3 - W_{dw} \qquad \text{(III.6.24)}$$

and

$$M_{dw}\frac{d}{dt}T_{dw} + T_{dw}\frac{dM_{dw}}{dt} = W_{Fi}T_{Fi} + (1-x_e)\, W_3 T_{sat} W_{di} T_{dw}. \qquad \text{(III.6.25)}$$

Substituting $M_{dw} = V_{dw}\rho_{dw}$

where

V_{dw} = volume of drum water

ρ_{dw} = density of drum water

and neglecting any change in ρ_{dw} during the transients considered in this analysis, we get

$$\rho_{dw}\frac{dV_{dw}}{dt} = W_{Fi} + (1-x_e)\, W_3 - W_{dw} \qquad \text{(III.6.26)}$$

and

$$M_{dw}\frac{dT_{dw}}{dt} + T_{dw}\rho_{dw}\frac{dV_{dw}}{dt} = W_{Fi}T_{Fi} + (1-x_e)\, W_3\, T_{sat} - W_{dw}T_{dw}. \qquad \text{(III.6.27)}$$

Assuming that the drum water volume has an effective area, A_{dw} and the level of the drum water is L_{dw}, then

$$V_{dw} = A_{dw}L_{dw}. \qquad \text{(III.6.28)}$$

Substituting from Equation (III.6.28) into Equations (III.6.26) and (III.6.27) and introducing perturbation variables, we get

$$\rho_d A_d \frac{d\delta L_{dw}}{dt} = - \delta W_{dw} + (1-x_e)\ \delta W_3 - W_3 \delta x_e + \delta W_{Fi} \qquad \text{(III.6.29)}$$

and

$$M_{dw} \frac{d\delta T_{dw}}{dt} + T_{dw}\rho_{dw}A_{dw} \frac{d\delta L_{dw}}{dt} = (1-x_e)\ W_3 \frac{\partial T_{sat}}{\partial P} \delta P - W_3 T_{sat} \delta x_e$$

$$+ (1-x_e)\ T_{sat}\delta W_3 + W_{Fi}\delta T_{Fi}$$

$$+ T_{Fi}\delta W_{Fi} - W_{dw}\delta T_{dw} - T_{dw}\delta W_{dw}. \qquad \text{(III.6.30)}$$

Equations (III.6.29) and (III.6.30) are the two governing equations for the drum water volume.

III.6.7.3 Drum Steam Volume

The drum steam volume is bounded by the steam generators' shell inside surface and the steam/water interface in the drum equivalent section. It acts as a storage and delivery section with the steam generator pressure as the dominant state variable. Steam leaving the steam separators accumulates in the drum steam volume which includes the steam dryers that limit the moisture content of the steam leaving the steam generator to less than 0.25%. The rate of steam leaving the steam generator from the steam outlet nozzle is a function of the turbine steam demand and is determined by the turbine valve opening which is adjusted according to the electrical load demand.

A mass balance on the drum steam volume yields

$$\frac{dM_{ds}}{dt} = x_e W_3 - W_{so} \qquad \text{(III.6.31)}$$

where,

M_{ds} = mass of drum steam

$X_e W_3$ = mass flow rate of steam from the steam separators

W_{so} = mass flow rate of steam leaving the steam generator.

Assuming that the steam in the drum steam volume is dry and saturated, then

$$M_{ds} = \rho_g \cdot V_{ds} \qquad \text{(III.6.32)}$$

where

ρ_g = density of dry saturated steam

V_{ds} = volume of drum steam.

The drum steam volume can be related to the drum water level through the equation:

$$V_{ds} = V_{dr} - A_{dw} L_{dw} \qquad \text{(III.6.33)}$$

where,

V_{dr} = volume of the equivalent drum section

A_{dw} = effective area of drum water volume

L_{dw} = drum water level.

Substituting from Equations (III.6.32) and (III.6.33) into Equation (III.6.31) and differentiating we get

$$\rho_g \frac{d}{dt} (V_{dr} - A_{dw} L_{dw}) + V_s \frac{d\rho_g}{dt} = x_e W_3 - W_{so}. \qquad \text{(III.6.34)}$$

Equation (III.6.34) is the governing equation for the drum steam volume, however, before it can be coupled to the other equations of the model, W_{so} may be either treated as a forcing element or related to other system state variables and forcing elements. In

this study, the critical flow equation is used to relate W_{so} to the steam generator pressure (P) and the turbine value coefficient (C_L). Thus

$$W_{so} = C_L \cdot P. \qquad \text{(III.6.35)}$$

Substituting from Equation (III.6.35) into Equation (III.6.34) and introducing perturbation variables, we get

$$V_{ds} \frac{\partial \rho_g}{\partial P} \frac{d\delta P}{dt} - \rho_g A_{dw} \frac{d\delta L_{dw}}{dt} = x_e \delta W_3 + W_3 \delta x_e - C_L \delta P - P \delta C_L. \qquad \text{(III.6.36)}$$

Equation (III.6.36) is the governing equation for the drum steam volume.

III.6.8 Downcomer Secondary Fluid Lump (SFDCL)

The downcomer secondary fluid lump in this model acts only as a time delay section between the exit of the drum water volume to the inlet of the effective heat exchange lump. Since the downcomer section has a fixed volume and the change in subcooled secondary water density is negligible then a mass balance on the downcomer secondary fluid lump yields

$$W_1 = W_{dw}. \qquad \text{(III.6.37)}$$

A heat balance on the downcomer secondary fluid lump results in the following:

$$\frac{d}{dt} (M_d C_{P2} T_d) = W_{dw} C_{P2} T_{dw} - W_1 C_{P2} T_d \qquad \text{(III.6.38)}$$

where,

M_d = mass of the secondary fluid in the downcomer lump

C_{P2} = specific heat of the secondary fluid in the downcomer lump

T_{dw} = temperature of the subcooled fluid entering the downcomer lump

T_d = temperature of the subcooled fluid leaving the downcomer lump.

Since M_d is constant, then

$$M_d \frac{dT_d}{dt} = W_{dw}T_{dw} - W_1T_d. \qquad \text{(III.6.39)}$$

Substituting from Equation (III.6.37) into Equation (III.6.39) and introducing perturbation variables, we get

$$M_d \frac{d\delta T_d}{dt} = W_1(\delta T_{dw} - \delta T_d). \qquad \text{(III.6.40)}$$

Equation (III.6.40) is the describing equation for the downcomer secondary fluid lump.

III.6.9 The Recirculation Loop Equation

In order to solve the equations for Model C, the variable W_1 (the flow from the downcomer into the riser) has to be related to other system state variables. The direct method for obtaining this relationship is to apply the momentum theory on the recirculation secondary fluid loop between the downcomer lump and the effective heat exchange lump. Since the recirculation ratio is assumed to be known from the steam generator design data, the momentum balance can be replaced by equating the driving pressure due to the static head difference to the acceleration and friction pressure drops along the loop. Since the dynamic pressure drops (friction and acceleration) are proportional to the square of the flow, then the momentum balance equation can be replaced by the following equation

$$\Delta P_d = C_d W_1^2 \qquad \text{(III.6.41)}$$

where,

ΔP_d = driving pressure due to static head difference

C_d = effective dynamic pressure coefficient

W_1 = recirculation mass flow rate.

From Equation (III.6.41) we have:

$$W_1 = \frac{1}{\sqrt{C_d}} \sqrt{\Delta P_d} \; . \qquad \text{(III.6.42)}$$

Let $C_1 = \frac{1}{\sqrt{C_d}}$ then,

$$W_1 = C_1 \sqrt{\Delta P_d} . \qquad \text{(III.6.43)}$$

The driving static head pressure ΔP_d can be calculated as follows:

$$\Delta P_d = (\Delta P)_{OTW} - (\Delta P)_{ITW} \qquad \text{(III.6.44)}$$

where,

$(\Delta P)_{OTW}$ = pressure head of the recirculation loop outside the tube wrapper

$(\Delta P)_{ITW}$ = pressure head of the recirculation loop inside the tube wrapper.

The secondary fluid outside the tube wrapper consists of two parts

1. the subcooled liquid in the drum water volume
2. the subcooled liquid in the downcomer lump.

Therefore, $(\Delta P)_{OTW}$ can be calculated from the following equation

$$(\Delta P)_{OTW}\Big|_{psi} = \frac{(\rho_{dw} L_{dw} + \rho_{dc} L_{dc})}{144} \cdot \frac{g}{g_c} \qquad \text{(III.6.45)}$$

where

ρ_{dw} = density of the secondary subcooled liquid in the drum water volume

L_{dw} = height of the secondary subcooled liquid in the drum water volume above the hypothetical plane at the effective heat exchange exit

ρ_{dc} = density of the subcooled secondary liquid in the downcomer lump

L_{dc} = height of the downcomer lump measured from the tube sheet

g = gravitational acceleration (32.2 ft/sec^2)

g_c = conversion factor (32.2 $\frac{\text{lbm ft/sec}^2}{\text{lb}_f}$).

Since g and g_c are numerically equal in the foot-pound-second (fps) unit system and ρ_{dw} and ρ_{dc} are equal, then Equation (III.6.45) reduces to

$$(\Delta P)_{OTW}\Big|_{psi} = \frac{\rho_d L_d}{144} \qquad \text{(III.6.46)}$$

where

$\rho_d = \rho_{dw} = \rho_{dc}$

and

$L_d = L_{dw} + L_{dc}$.

The secondary fluid inside the tube wrapper consists of two parts

1. the secondary fluid in the effective heat exchange lump
2. the secondary fluid in the riser/separator volume.

Therefore, $(\Delta P)_{ITW}$ can be calculated from the following equation:

$$(\Delta P)_{ITW}\Big|_{psi} = \frac{\rho_s L_s + \rho_r L_r}{144} \cdot \frac{g}{g_c} \qquad \text{(III.6.47)}$$

where

ρ_s = average density of secondary fluid in the effective heat exchange lump

L_s = length of the heat exchange lump

ρ_r = density of the secondary fluid in the riser/separator volume

L_r = height of the secondary fluid in the riser/separator volume.

Since g and g_c are numerically equal in the fps unit system, Equation (III.6.47) becomes

$$(\Delta P)_{ITW}\Big|_{psi} = \frac{\rho_s L_s + \rho_r L_r}{144} . \qquad \text{(III.6.48)}$$

Substituting from Equations (III.6.46) and (III.6.48) into Equation (III.6.44) and using the results in Equation (III.6.43), we get

$$W_l = \frac{C_l}{12} \sqrt{\rho_d L_d - (\rho_s L_s + \rho_r L_r)}. \qquad \text{(III.6.49)}$$

The value of the recirculation flow coefficient C_l can be estimated from the steady state conditions. The deviation of W_l from its steady state value can be obtained by taking the derivative of Equation (III.6.49) thus

$$\delta W_l = \frac{C_l}{12} \frac{\delta(\rho_d L_d) - \delta(\rho_s L_s + \rho_r L_r)}{2\sqrt{\rho_d L_d - (\rho_s L_s + \rho_r L_r)}} . \qquad \text{(III.6.50)}$$

When substituting the expressions for ρ_s and ρ_r from Equations (III.6.8) and (III.6.17) and assuming that the change in v_f and v_g with system pressure is linear, then Equation (III.6.50) can be reduced to the following equation which is suitable for coupling with other model equations

$$\delta W_1 = a_1 \delta L_{dw} + a_2 \delta P + a_3 \delta x_e \qquad \text{(III.6.51)}$$

where

δL_{dw} = deviation of drum water level from steady state

δP = deviation of steam pressure from steady state

δx_e = deviation of mass quality at the outlet of the effective heat exchange lump from steady state.

he expressions for the coefficients a_1, a_2, and a_3 are derived
1 Appendix D.

I.6.10 Summary of the Model Equations

The governing equations of Model C that were developed in the ceeding sections can be represented by the matrix equation

$$A_1 \frac{d\bar{x}}{dt} + A_2 \bar{x} = \bar{f}$$

e

$\bar{x}$ = system variables (differential + algebraic)* vector

id A_2 = coefficient matrices

$\bar{f}$ = forcing vector.

A list of the system variables is given in Table III.1 and the o elements of the matrices A_1 and A_2 and the forcing vector $\bar{f}$ ven below.

The definition of differential and algebraic variables will be ed in Chapter IV.

TABLE III.1

SYSTEM VARIABLES FOR MODEL C

State Variable Number	Symbol	Description
1	T_{p1}	Parallel flow branch primary water temperature
2	T_{p2}	Counterflow branch primary water temperature
3	T_{m1}	Parallel flow branch tube metal temperature
4	T_{m2}	Counterflow branch tube metal temperature
5	P	Steam pressure in the drum steam volume
6	x_e	Mass quality at the exit of the effective heat exchange lump
7	T_{dw}	Water temperature in the drum water volume
8	L_{dw}	Drum water level
9	T_d	Downcomer temperature
*10	T_s	Average temperature in the effective heat exchange lump
*11	W_1	Mass flow rate at the inlet of the effective heat exchange lump
*12	W_2	Mass flow rate at the exit of the effective heat exchange lump
13	W_3	Mass flow rate at the exit of the separator/riser volume

*Algebraic variables.

1. The A_1 Matrix

$$A_1(1,1) = 1.0$$

$$A_1(2,2) = 1.0$$

$$A_1(3,3) = 1.0$$

$$A_1(4,4) = 1.0$$

$$A_1(5,5) = \left[M_s \cdot \frac{L_{sub}}{L} \cdot \frac{C_{P2}}{2} \frac{\partial T_{sat}}{\partial P} + M_s \cdot \frac{L_{boil}}{L} \left(\frac{\partial h_f}{\partial P} + \frac{x_e}{2} \frac{\partial h_{fg}}{\partial P}\right)\right.$$
$$\left. + C_{1b} V_s h_s \cdot \frac{L_{boil}}{L}\right.$$

$$A_1(5,9) = M_s \cdot \frac{L_{sub}}{L} \cdot \frac{C_{P2}}{2}$$

$$A_1(5,6) = M_s \cdot \frac{L_{boil}}{L} \cdot \frac{h_{fg}}{2} + C_{2b} V_s h_s \cdot \frac{L_{boil}}{L}$$

$$A_1(7,5) = V_s \cdot \frac{L_{boil}}{L} \cdot C_{1b}$$

$$A_1(7,6) = V_s \cdot \frac{L_{boil}}{L} \cdot C_{2b}$$

$$A_1(8,5) = V_r \cdot C_{1r}$$

$$A_1(8,6) = V_r \cdot C_{2r}$$

$$A_1(9,8) = \rho_{dw} A_d$$

$$A_1(10,7) = M_{dw}$$

$$A_1(10,8) = T_{dw} \rho_{dw} A_{dw}$$

$$A_1(11,5) = V_s \frac{\partial \rho_g}{\partial P}$$

$$A_1(11,8) = - \rho_g A_{dw}$$

$$A_1(12,9) = M_d$$

2. The A_2 Matrix

$$A_2(1,1) = \left(\frac{1}{\tau_{P1}} + \frac{U_{pm}S_{pm1}}{M_{P1}C_{P1}}\right)$$

$$A_2(1,3) = -\frac{U_{pm}S_{pm1}}{M_{P1}C_{P1}}$$

$$A_2(2,1) = -\frac{1}{\tau_{P1}}$$

$$A_2(2,2) = \left(\frac{1}{\tau_{P1}} + \frac{U_{pm}S_{pm2}}{M_{P1}C_{P1}}\right)$$

$$A_2(2,4) = -\frac{U_{pm}S_{pm2}}{M_{P2}C_{P1}}$$

$$A_2(3,1) = -\frac{U_{pm}S_{pm1}}{M_{m1}C_m}$$

$$A_2(3,3) = \frac{U_{pm}S_{pm1} + U_{ms}S_{ms1}}{M_{m1}C_m}$$

$$A_2(3,10) = -\frac{U_{ms}S_{ms}}{M_{m1}C_m}$$

$$A_2(4,2) = -\frac{U_{pm}S_{pm2}}{M_{m2}C_m}$$

$$A_2(4,4) = \frac{U_{pm}S_{pm2} + U_{ms}S_{ms2}}{M_{m2}C_m}$$

$$A_2(4,10) = -\frac{U_{ms}S_{ms2}}{M_{m2}C_m}$$

$$A_2(5,3) = -U_{ms}S_{ms}$$

$$A_2(5,4) = -U_{ms}S_{ms}$$

$$A_2(5,5) = W_2\left[\frac{\partial h_f}{\partial P} + x_e\frac{\partial h_{fg}}{\partial P}\right]$$

$$A_2(5,6) = W_2 h_{fg}$$

$$A_2(5,9) = - W_1 C_{P2}$$

$$A_2(5,10) = 2\ U_{ms} S_{ms}$$

$$A_2(5,11) = - C_{P2} T_d$$

$$A_2(5,12) = h_f + x_e h_{fg}$$

$$A_2(6,5) = \left(\frac{L_{sub}}{2L} + \frac{L_{boil}}{L}\right) \frac{\partial T_{sat}}{\partial P}$$

$$A_2(6,9) = \frac{L_{sub}}{2L}$$

$$A_2(6.10) = - 1.0$$

$$A_2(7,11) = - 1.0$$

$$A_2(7,12) = 1.0$$

$$A_2(8,12) = - 1.0$$

$$A_2(8,13) = 1.0$$

$$A_2(9,6) = W_3 = W_1$$

$$A_2(9,11) = 1.0$$

$$A_2(9,13) = -(1 - x_e)$$

$$A_2(10,5) = - (1 - x_e)\ W_3 \frac{\partial T_{sat}}{\partial P}$$

$$A_2(10,6) = W_3\ T_{sat}$$

$$A_2(10,7) = W_{dw} = W_1$$

$$A_2(10,11) = T_{dw}$$

$$A_2(10,13) = (1 - x_e)\ T_{sat}$$

$A_2(11,5) = C_L$ (0.0 in case δW_{so} is used as forcing)

$A_2(11,6) = - W_3 = - W_1$

$A_2(11,13) = - x_e$

$A_2(12,7) = - W_1$

$A_2(12,9) = W_1$

$A_2(13,5) = - a_2$

$A_3(13,6) = - a_3$

$A_2(13,8) = - a_1$

$A_2(13,11) = 1.0$

3. The Forcing Vector $\bar{f}$

$f(1) = \frac{1}{\tau_{P1}} \delta T_{Pi}$

$f(9) = \delta W_{Fi}$

$f(10) = W_{Fi} \delta T_{Fi} + T_{Fi} \delta W_{Fi}$

$f(11) = - P \, \delta C_L$ ($-\delta W_{so}$ in case W_{so} is left as forcing).

III.7 Governing Equations for Model D

III.7.1 Primary Side Equations

The primary side equations consist of two equations for the inlet and outlet plenums and four equations for the primary fluid lumps in the tube bundle region. In developing the equations for the primary lumps in the heat transfer region, special consideration is given to the dynamic boundary between the primary lumps in the

subcooled region and those in the boiling region. Both continuity (mass balance) and energy (heat balance) equations are considered for describing the transient behavior of each lump. The formulation that results is a so-called moving boundary model. In this case, the boundary is determined by the heating length required to bring the subcooled water up to saturation temperature. This distance also fixes the length of the metal and primary lumps that are adjacent to the subcooled secondary section.

III.7.1.1 Inlet Plenum (PRIN)

The inlet plenum is considered as a well stirred tank. A heat balance yields the following equation

$$\frac{d}{dt}(M_{Pi}C_{Pl}T_{Pi}) = W_{Pi}C_{Pl}(\theta_i - T_{Pi}) \qquad \text{(III.7.1)}$$

where

M_{Pi} = mass of primary water in the inlet plenum

T_{Pi} = bulk mean temperature of the inlet plenum

θ_i = primary water inlet temperature

and other terms are as defined before..

Since the density and specific heat of the primary water are assumed constant, then

$$M_{Pi}C_{Pl}\frac{dT_{Pi}}{dt} = W_{Pi}C_{Pl}(\theta_i - T_{Pl}). \qquad \text{(III.7.2)}$$

Dividing through by $M_{Pi}C_{Pl}$ we get

$$\frac{dT_{Pi}}{dt} = \frac{1}{\tau_{Pi}}\delta T_{Pi}(\theta_i - T_{Pi}) \qquad \text{(III.7.3)}$$

where

$\tau_{Pi} = \frac{M_{Pi}}{W_{Pi}}$ = residence time of primary water in the inlet plenum.

And the perturbation form of the equation for the inlet plenum becomes

(III.7.4)

$$\frac{d\delta T_{Pi}}{dt} = -\frac{1}{\tau_{Pi}}\delta T_{Pi} + \frac{1}{\tau_{Pi}}\delta\theta_i. \qquad \text{(III.7.4)}$$

III.7.1.2 Primary Lump (PRL1)

a. Mass balance

$$\frac{d}{dt}(M_{Pl}) = W_{Pi} - W_{Pl} \qquad \text{(III.7.5)}$$

where

M_{Pl} = mass of primary water in the lump

W_{Pi} = mass flow rate at the entrance of the lump

W_{Pl} = mass flow rate at the exit of the lump.

But, $M_{Pl} = \rho_p A_p L_{sl}$ (III.7.6)

where

ρ_p = density of primary water

A_p = flow area of primary water

L_{sl} = length of the lump.

Since the flow area and the density of the primary water are constants, then Equation (III.7.5) becomes

$$\rho_p A_p \frac{dL_{sl}}{dt} = W_{Pi} - W_{Pl}. \qquad \text{(III.7.7)}$$

b. Heat balance

$$\frac{d}{dt}(M_{Pl}C_{Pl}T_{Pl}) = W_{Pi}C_{Pl}T_{Pi} - W_{Pl}C_{Pl}T_{Pl} - \dot{Q}_{pml} \qquad \text{(III.7.8)}$$

where

T_{Pl} = bulk mean temperature of the lump

$\dot{Q}_{pml}$ = heat transfer rate between (PRL1) and (MTL1) lumps.

Substituting from Equation (III.7.6) into Equation (III.7.8) we get

$$\rho_p A_p C_{Pl}\left(L_{sl}\frac{dT_{Pl}}{dt} + T_{Pl}\frac{dL_{sl}}{dt}\right) = W_{Pi}C_{Pl}T_{Pi} - W_{Pl}C_{Pl}T_{Pl} - \dot{Q}_{pml}. \qquad \text{(III.7.9)}$$

Substituting $\dot{Q}_{pm1} = U_{pm} P_{r1} L_{s1} (T_{P1} - T_{M1})$

where,

P_{r1} = heat transfer area/unit length between primary water lump (PRL1) and tube metal lump (MTL1)

T_{M1} = average temperature of lump (MTL1)

and using Equation (III.7.7) into Equation (III.7.9), we get

$$\rho_p A_p C_{P1} \left(L_{s1} \frac{dT_{P1}}{dt} + T_{P1} \frac{dL_{s1}}{dt}\right)$$

$$= W_p C_{P1} T_{Pi} - C_{P1} T_{P1} \left(W_{Pi} - \rho_p A_p \frac{dL_{s1}}{dt}\right)$$

$$- U_{pm} P_{r1} L_{s1} (T_{P1} - T_{M1}). \qquad \text{(III.7.10)}$$

Rearranging and dividing through by $M_{P1} C_{P1}$, then Equation (III.7.10) reduces to

$$\frac{d\delta T_{P1}}{dt} = \frac{1}{\tau_{P1}} \delta T_{Pi} - \left(\frac{1}{\tau_{P1}} + \frac{U_{pm} S_{pm1}}{M_{P1} C_{P1}}\right) \delta T_{P1} + \frac{U_{pm} S_{pm1}}{M_{p1} C_{P1}} \delta T_{M1}$$

$$- \frac{U_{pm} P_{r1}}{M_{P1} C_{P1}} (T_{P1} - T_{M1}) \delta L_{s1} \qquad \text{(III.7.11)}$$

where,

$$\tau_{P1} = \frac{M_{P1}}{W_{Pi}}$$

$$S_{pm1} = P_{r1} L_{s1}.$$

III.7.1.3 Primary Lump (PRL2)

a. Mass balance

$$\frac{d}{dt} (M_{p2}) = W_{P1} - W_{P2} \qquad \text{(III.7.12)}$$

where,

M_{P2} = mass of primary water in the lump

W_{P1}, W_{P2} = inlet and outlet mass flow rates.

Substituting

$$M_{P2} = \rho_p A_p L_{s2} \tag{III.7.13}$$

where,

L_{s2} = length of the lump, then

$$\rho_p A_p \frac{dL_{s2}}{dt} = W_{P1} - W_{P2}. \tag{III.7.14}$$

Since $L_{s1} + L_{s2}$ = constant, then

$$\frac{dL_{s2}}{dt} = - \frac{dL_{s1}}{dt} \tag{III.7.15}$$

and Equation (III.7.14) reduces to

$$W_{P2} = W_{P1} + \rho_p A_p \frac{dL_{s1}}{dt} . \tag{III.7.16}$$

But from Equation (III.7.7), we have

$$W_{Pi} = W_{P1} + \rho_p A_p \frac{dL_{s1}}{dt} . \tag{III.7.17}$$

Therefore, the mass balance equation for the primary water lump (PRL2) becomes

$$W_{P2} = W_{Pi}. \tag{III.7.18}$$

b. Heat balance

$$\frac{d}{dt} (M_{P2} C_{P1} T_{P2}) = W_{P1} C_{P1} T_{P1} - W_{P2} C_{P1} T_{P2} - \dot{Q}_{pm2} \tag{III.7.19}$$

where,

T_{P2} = bulk mean temperature of the lump

$\dot{Q}_{pm2}$ = heat transfer rate between (PRL2) and (MTL2) lumps.

Substituting for M_{P2} from Equation (III.7.13) and using Equations (III.7.17) and (III.7.18), we get

$$\rho_p A_p C_{P1}\left(L_{s2}\frac{dT_{P2}}{dt} + T_{P2}\frac{dL_{s2}}{dt}\right) = \left(W_{Pi} - \rho_p A_p \frac{dL_{s1}}{dt}\right) C_{P1}T_{P1} - W_{Pi}C_{P1}T_{P2} - \dot{Q}_{pm2}. \quad \text{(III.7.20)}$$

Substituting $\dot{Q}_{pm2} = U_{pm}P_{r1}L_{s2}(T_{P2} - T_{M2})$ (III.7.21)

where,

T_{M2} = average temperature of lump (MTL2)

and dividing through by $M_{P2}C_{P1}$, we get

$$\frac{dT_{P2}}{dt} + \left(\frac{T_{P1}-T_{P2}}{L_{s2}}\right)\frac{dL_{s1}}{dt} = \frac{W_{Pi}}{M_{P2}}(T_{P1} - T_{P2}) - \frac{U_{pm}P_{r1}L_{s2}}{M_{P2}C_{P1}}(T_{P2} - T_{M2}) \quad \text{(III.7.22)}$$

which upon introduction of perturbation variables becomes

$$\frac{d\delta T_{P2}}{dt} + \left(\frac{T_{P1}-T_{P2}}{L_{s2}}\right)\frac{d\delta L_{s1}}{dt} = \frac{1}{\tau_{P2}}\delta T_{P1} - \left(\frac{1}{\tau_{P2}} + \frac{U_{pm}S_{pm2}}{M_{P2}C_{P1}}\right)\delta T_{P2} + \frac{U_{pm}S_{pm2}}{M_{P2}C_{P1}}\delta T_{M2} + \frac{(T_{P2}-T_{M2})}{M_{P2}C_{P1}}U_{pm}P_{r1}\delta L_{s1} \quad \text{(III.7.23)}$$

where,

$$\tau_{P2} = \frac{M_{P2}}{W_{Pi}}$$

$$S_{pm2} = P_{rl} \cdot L_{s2}.$$

III.7.1.4 Primary Lump (PRL3)

a. Mass balance

$$\frac{d}{dt}(M_{P3}) = W_{P2} - W_{P3}. \qquad \text{(III.7.24)}$$

Since $M_{P3} = M_{P2} = \rho_p A_p L_{s2}$

and $W_{P2} = W_{Pi}$, then

$$\frac{d}{dt}(\rho_p A_p L_{s2}) = W_{Pi} - W_{P3} \qquad \text{(III.7.25)}$$

using the assumption of constant primary water density

and solving for W_{P3}, we get

$$W_{P3} = W_{Pi} - \rho_p A_p \frac{dL_{s2}}{dt}. \qquad \text{(III.7.26)}$$

Substituting from Equation (III.7.15) we get

$$W_{P3} = W_{Pi} + \rho_p A_p \frac{dL_{s1}}{dt}. \qquad \text{(III.7.27)}$$

b. Heat balance

$$\frac{d}{dt}(M_{P3}C_{Pl}T_{P3}) = W_{P2}C_{Pl}T_{P2} - W_{P3}C_{Pl}T_{P3} - \dot{Q}_{pm3}. \qquad \text{(III.7.28)}$$

Using Equations (III.7.18) and (III.7.26) to substitute

for W_{P2} and W_{P3}, we get

$$\rho_p A_p C_{Pl}\left(T_{P3}\frac{dL_{s2}}{dt} + L_{s2}\frac{dT_{P3}}{dt}\right) = W_{Pi}C_{Pl}T_{P2} - \dot{Q}_{pm3}$$

$$- C_{Pl}T_{P3}\left(W_{Pi} - \rho_p A_p \frac{dL_{s2}}{dt}\right). \qquad \text{(III.7.29)}$$

Dividing through by $M_{P3}C_{P1} = \rho_p A_p L_{s2} C_{P1}$, we get

$$\frac{dT_{P3}}{dt} = \frac{W_{Pi}}{M_{P3}} (T_{P2}-T_{P3}) - \frac{\dot{Q}_{pm3}}{M_{P3}C_{P1}} \qquad \text{(III.7.30)}$$

substituting $\dot{Q}_{pm3} = U_{pm} P_{rl} L_{s2} (T_{P3}-T_{M3})$ (III.7.31)

where

T_{M3} = average temperature of lump (MTL3),

and introducing perturbation variables, we get

$$\frac{d\delta T_{P3}}{dt} = \frac{1}{\tau_{P3}} \delta T_{P2} - \left(\frac{1}{\tau_{P3}} + \frac{U_{pm} S_{pm3}}{M_{P3}C_{P1}}\right) \delta T_{P3}$$

$$+ \frac{U_{pm} S_{pm3}}{M_{P3}C_{P1}} \delta T_{M3} = \frac{U_{pm} P_{rl}}{M_{P3}C_{P1}} (T_{P3}-T_{M3}) \delta L_{s1} \qquad \text{(III.7.32)}$$

where,

$\tau_{P3} = \tau_{P2}$

$S_{pm3} = S_{pm2}$.

III.7.1.5 Primary Lump (PRL4)

a. Mass balance

$$\frac{d}{dt} (M_{P4}) = W_{P3} - W_{P4} \qquad \text{(III.7.33)}$$

substituting $M_{P4} = \rho_p A_p L_{s1}$, we get

$$\rho_p A_p \frac{dL_{s1}}{dt} = W_{P3} - W_{P4}. \qquad \text{(III.7.34)}$$

From Equation (III.7.27), we have

$$\rho_p A_p \frac{dL_{s1}}{dt} = (W_{Pi} + \rho_p A_p \frac{dL_{s1}}{dt}) - W_{P4} \qquad \text{(III.7.35)}$$

from which we have

$$W_{P4} = W_{Pi}. \tag{III.7.36}$$

b. Heat balance

$$\frac{d}{dt}(M_{P4}C_{Pl}T_{P4}) = W_{P3}C_{Pl}T_{P3} - W_{P4}C_{Pl}T_{P4} - \dot{Q}_{pm4}. \tag{III.3.37}$$

Substituting for $M_{P4} = \rho_p A_p L_{sl}$ and using Equations (III.7.27) and (III.7.36), we get

$$\rho_p A_p C_{Pl}\left(T_{P4}\frac{dL_{sl}}{dt} + L_{sl}\frac{dT_{P4}}{dt}\right) = \left(W_{Pi} + \rho_p A_p \frac{dL_{sl}}{dt}\right) C_{Pl}T_{P3}$$

$$- W_{Pi}C_{Pl}T_{P4} - \dot{Q}_{pm4}. \tag{III.7.38}$$

Dividing through by $M_{P4}C_{Pl}$ and rearranging, we have

$$\frac{dT_{P4}}{dt} + \left(\frac{T_{P4}-T_{P3}}{L_{sl}}\right)\frac{dL_{sl}}{dt} = \frac{W_{Pi}}{M_{P4}}(T_{P3}-T_{P4}) - \frac{\dot{Q}_{pm4}}{M_{P4}C_{Pl}}. \tag{III.7.39}$$

Substituting for $\dot{Q}_{pm4} = U_{pm}P_{rl}L_{sl}(T_{P4}-T_{M4})$ and introducing perturbation variables, we get

$$\frac{d\delta T_{P4}}{dt} + \left(\frac{T_{P4}-T_{P3}}{L_{sl}}\right)\frac{d\delta L_{sl}}{dt} = \frac{1}{\tau_{P4}}\delta T_{P3} - \left(\frac{1}{\tau_{P4}} + \frac{U_{pm}S_{pm4}}{M_{P4}C_{Pl}}\right)\delta T_{P4}$$

$$+ \frac{U_{pm}S_{pm4}}{M_{P4}C_{Pl}}\delta T_{M4} - \frac{U_{pm}P_{rl}}{M_{P4}C_{Pl}}(T_{P4}-T_{M4})\,\delta L_{sl} \tag{III.7.40}$$

where,

$$\tau_{P4} = \tau_{Pl}$$

$$S_{pm4} = S_{pml}$$

$$M_{P4} = M_{Pl}.$$

III.7.1.6 Outlet Plenum (PROUT)

The equation for the outlet plenum is obtained in the same way as for the inlet plenum. The equation is as follows:

$$\frac{d\delta T_{Po}}{dt} = \frac{1}{\tau_{Po}} \delta T_{P4} - \frac{1}{\tau_{Po}} \delta T_{Po} \qquad \text{(III.7.41)}$$

where

$\tau_{Po} = \tau_{Pi}$

T_{Po} = primary water outlet temperature.

III.7.2 Tube Metal Equations

As in the case of the primary water lumps in the tube bundle region, special consideration is necessary for the treatment of the dynamic boundary between the subcooled and boiling sections. However, the treatment of the moving boundary is different from the case of the primary water lumps. Here, it was assumed that if the boundary is moving at a rate dL_{sl}/dt, it adds (or subtracts) a quantity of heat at a rate $\rho_m A_m C_m \bar{T}_m \frac{dL_{sl}}{dt}$ to the metal lump under consideration

where

ρ_m = density of tube metal

A_m = cross sectional area of tube metal lump

C_m = specific heat of tube metal

$\bar{T}_m$ = average temperature at the boundary.

This approach results in maintaining a dynamic heat balance for each lump during the transient.

III.7.2.1 Tube Metal Lump (MTL1)

Heat balance

$$\frac{d}{dt}(M_{m1}C_mT_{m1}) = \dot{Q}_{pm1} - (\dot{Q}_{ms1})_1 + \rho_m A_m C_m \bar{T}_{m1} \frac{dL_{s1}}{dt} . \qquad \text{(III.7.42)}$$

Substituting $M_{m1} = \rho_m A_m L_{s1}$ and $\bar{T}_{m1} = \frac{T_{m1} + T_{m2}}{2}$, then

$$\rho_m A_m C_m \left(T_{m1} \frac{dL_{s1}}{dt} + L_{s1} \frac{dT_{m1}}{dt}\right) = \dot{Q}_{pm1}$$

$$- (\dot{Q}_{ms1})_1 + \rho_m A_m C_m \left(\frac{T_{m1} + T_{m2}}{2}\right) \frac{dL_{s1}}{dt} . \qquad \text{(III.7.43)}$$

Dividing through by $M_{m1}C_m$ and collecting terms, then

$$\frac{dT_{m1}}{dt} + \left(\frac{T_{m1}-T_{m2}}{L_{s1}}\right) \frac{dL_{s1}}{dt} = \frac{\dot{Q}_{pm1} - (\dot{Q}_{ms1})_1}{M_{m1}C_m} . \qquad \text{(III.7.44)}$$

Substituting $\dot{Q}_{pm1} = U_{pm}P_{r1}L_{s1}(T_{P1}-T_{m1})$

and $(\dot{Q}_{ms1})_1 = U_{ms1}P_{r2}L_{s1}(T_{m1}-T_{s1})$, then

$$\frac{dT_{m1}}{dt} + \frac{(T_{m1}-T_{m2})}{L_{s1}} \frac{dL_{s1}}{dt} = \frac{1}{M_{m1}C_m} [U_{pm}P_{r1}L_{s1}(T_{P1}-T_{m1})$$

$$- U_{ms1}P_{r2}L_{s1}(T_{m1}-T_{s1})]. \qquad \text{(III.7.45)}$$

Introducing perturbation variables and replacing δT_{s1} by $\frac{1}{2}(\delta T_d + \delta T_{sat})$, where $\delta T_{sat} = \frac{\partial T_{sat}}{\partial P} \delta P$ then the describing equation for the first tube metal lump (MTL1) becomes

$$\frac{d\delta T_{m1}}{dt} + \left(\frac{T_{m1}-T_{m2}}{2L_{s1}}\right)\frac{d\delta L_{s1}}{dt} = \frac{U_{pm}S_{pm1}}{M_{m1}C_m}\delta T_{P1}$$

$$- \left(\frac{U_{pm}S_{pm1}+U_{ms1}S_{ms1}}{M_{m1}C_m}\right)\delta T_{m1}$$

$$+ \frac{U_{ms1}S_{ms1}}{2\,M_{m1}C_m}\delta T_d$$

$$+ \frac{U_{ms1}S_{ms1}}{2\,M_{m1}C_m}\frac{\partial T_{sat}}{\partial P}\delta P. \qquad \text{(III.7.46)}$$

III.7.2.2 Tube Metal Lump (MTL2)

Heat balance

$$\frac{d}{dt}\left(M_{m2}C_mT_{m2}\right) = \dot{Q}_{pm2} - \left(\dot{Q}_{ms2}\right)_2$$

$$- \delta_m A_m C_m \left(\frac{T_{m1}+T_{m2}}{2}\right)\frac{dL_{s1}}{dt}. \qquad \text{(III.7.47)}$$

Using the same procedure as in lump MTL1 results in the following equation

$$\frac{d\delta T_{m2}}{dt} + \left(\frac{T_{m1}-T_{m2}}{2L_{s2}}\right)\frac{d\delta L_{s1}}{dt} = \frac{U_{pm}S_{pm2}}{M_{m2}C_m}\delta T_{P2}$$

$$- \left(\frac{U_{pm}S_{pm2}+U_{ms2}S_{ms2}}{M_{m2}C_m}\right)\delta T_{m2}$$

$$+ \left(\frac{U_{ms2}S_{ms2}}{M_{m2}C_m}\right)\frac{\partial T_{sat}}{\partial P}\delta P. \qquad \text{(III.7.48)}$$

III.7.2.3 Tube Metal Lump (MTL3)

Heat balance

$$\frac{d}{dt}(M_{m3}C_mT_{m3}) = \dot{Q}_{pm3} - (\dot{Q}_{ms2})_3 - \rho_m A_m C_m \left(\frac{T_{m3}+T_{m4}}{2}\right)\frac{dL_{s1}}{dt}. \qquad \text{(III.7.49)}$$

Following the same procedure as in lump MTL2, we have

$$\frac{d\delta T_{m3}}{dt} - \left(\frac{T_{m3}-T_{m4}}{2L_{s2}}\right)\frac{d\delta L_{s1}}{dt} = \frac{U_{pm}S_{pm2}}{M_{m3}C_m}\delta T_{P3} - \left(\frac{U_{pm}S_{pm2}+U_{ms2}S_{ms2}}{M_{m3}C_m}\right)\delta T_{m3} + \left(\frac{U_{ms2}S_{ms2}}{M_{m3}C_m}\right)\frac{\partial T_{sat}}{\partial P}\delta P. \qquad \text{(III.7.50)}$$

III.7.2.4 Tube Metal Lump (MTL4)

Applying the heat balance and using the same procedure, then the governing equation for lump MTL4 can be written as

$$\frac{d\delta T_{m4}}{dt} - \left(\frac{T_{m3}-T_{m4}}{2L_{s1}}\right)\frac{d\delta L_{s1}}{dt} = \frac{U_{pm}S_{pm1}}{M_{m4}C_m}\delta T_{P4} - \left(\frac{U_{pm}S_{pm1}+U_{ms1}S_{ms1}}{M_{m4}C_m}\right)\delta T_{m4} + \frac{U_{ms1}S_{ms1}}{2M_{m4}C_m}\delta T_d + \left(\frac{U_{ms1}S_{ms1}}{2M_{m4}C_m}\right)\frac{\partial T_{sat}}{\partial P}\delta P. \qquad \text{(III.7.51)}$$

III.7.3 Secondary Side Equations

III.7.3.1 General Considerations

Heat is transferred from the hot primary fluid (reactor coolant) to the secondary fluid mainly in the tube bundle region sometimes referred to as the "Core."[32] Part of the heat transferred is used in removing the subcooling of the secondary water entering the tube region from the downcomer. The other part is used in the boiling process and converting part of the secondary water into steam. The steam water mixture thus formed continues to move upwards to the steam separators where the steam is separated and moves upwards to the steam storage and delivery section while the separated water moves downwards to mix with feedwater in the downcomer. The circulation between the downcomer and the tube region is achieved through the natural convection process due to the difference in density of the secondary fluid in these two regions.

Because of the two different heat transfer mechanisms between the tube metal and the secondary fluid, the active heat transfer region is divided into two sections; a subcooled (or preboiling) section and a boiling section (evaporator). In the subcooled section, the temperature of the secondary fluid rises from T_d at the downcomer outlet to T_{sat} at the starting of the boiling section. In the boiling section, the temperature stays at T_{sat} while the mass quality (x) or void fraction (α) increases as the secondary fluid moves upwards and more heat is transferred to it. At the end of the heat transfer region, the secondary fluid leaves the boiling section with an exit quality (x_e).

The length of the subcooled section is determined by the fraction of the heat transferred necessary to raise the secondary fluid temperature of the secondary fluid from T_d to T_{sat}.

The governing equations for the boiling section are simplified by assuming that the mass quality of the two phase mixture changes linearly with distance from the subcooled/boiling boundary.

III.7.3.2 Subcooled Secondary Fluid Lump (SFSL)

Slightly subcooled water from the downcomer enters the U-tube region at a flow rate W_1 and temperature T_d. Heat is transferred to the secondary fluid flowing upwards (by natural recirculation) from both branches of the U-tubes. As a result of this, the temperature of the secondary fluid rises until it reaches T_{sat}, which is a function of the secondary system pressure, and boiling takes place. The level at which boiling starts is a function of the following.

1. Flow rate and temperature of secondary fluid from the downcomer
2. Heat transfer rate from tube metal to the secondary fluid
3. Steam pressure which determines T_{sat}.

Since the length of the subcooled secondary lump is determined by the start of the boiling level, both mass balance and heat balance equations are required to represent the dynamics of the subcooled lump.

a. Mass balance

$$\frac{d}{dt}(M_{s1}) = W_1 - W_2 \qquad \text{(III.7.52)}$$

i.e., $$\frac{d}{dt}(\rho_{sl} A_{fs} L_{sl}) = W_1 - W_2 \qquad \text{(III.7.53)}$$

where,

ρ_{sl} = density of water in the subcooled lump

A_{fs} = secondary fluid flow area

L_{sl} = length of subcooled lump.

Neglecting the changes of subcooled water density during the transient, one obtains

$$\rho_{sl} A_{fs} \frac{dL_{sl}}{dt} = W_1 - W_2 \qquad \text{(III.7.54)}$$

which yields

$$\frac{d\delta L_{sl}}{dt} = \frac{1}{\rho_s A_{fs}} (\delta W_1 - \delta W_2). \qquad \text{(III.7.55)}$$

b. Heat balance

$$\frac{d}{dt}(M_{sl} C_{P2} T_{sl}) = (\dot{Q}_{msl})_1 + (\dot{Q}_{msl})_4 + W_1 C_{P2} T_d - W_2 C_{P2} T_{sat} \qquad \text{(III.7.56)}$$

where,

M_{sl} = mass of water in the subcooled lump

C_{P2} = specific heat of secondary water

T_{sl} = average temperature of water in the subcooled lump

$(\dot{Q}_{msl})_1$ = heat transfer rate between M_1 and S_1

$= U_{msl} Pr_2 L_{sl} (T_{m1} - T_{sl})$

$(\dot{Q}_{msl})_4$ = heat transfer rate between M_4 and S_1

$= U_{msl} Pr_2 L_{sl} (T_{m4} - T_{sl})$.

Since the difference between T_d and T_{sat} is usually small, then we can assume that

$$T_{sl} = \frac{T_d + T_{sat}}{2}. \qquad \text{(III.7.57)}$$

Substituting from Equation (III.7.57) into Equation (III.7.56) we get

$$\frac{d}{dt}\left[M_{sl}C_{P2}\left(\frac{T_d+T_{sat}}{2}\right)\right] = U_{msl}Pr_2L_{sl}(T_{ml} + T_{m4} - T_d - T_{sat}) + W_1C_{P2}T_d - W_2C_{P2}T_{sat}. \quad \text{(III.7.58)}$$

Since $M_{sl} = A_{fs}\rho_{sl}L_{sl}$, then

$$\frac{d}{dt}\left[A_{fs}\rho_{sl}L_{sl}C_{P2}\left(\frac{T_d+T_{sat}}{2}\right)\right] = U_{msl}P_{r2}L_{sl}(T_{ml} + T_{m4} - T_d - T_{sat}) + W_1C_{P2}T_d - W_2C_{P2}T_{sat}. \quad \text{(III.7.59)}$$

Using $\delta T_{sat} = \frac{\partial T_{sat}}{\partial P}\delta P$, we get

$$\frac{A_{fs}\rho_{sl}L_{sl}C_{P2}}{2}\left[\frac{d\delta T_d}{dt} + \frac{\partial T_{sat}}{\partial P}\frac{d\delta P}{dt}\right] + A_{fs}\rho_{sl}C_{P2}\left(\frac{T_d+T_{sat}}{2}\right)\frac{d\delta L_{sl}}{dt}$$

$$= U_{msl}Pr_2L_{sl}\left[\delta T_{ml} + \delta T_{m4} - \delta T_d - \frac{\partial T_{sat}}{\partial P}\delta P\right]$$

$$+ U_{msl}Pr_2[T_{ml} + T_{m4} - T_d - T_{sat}]\,\delta L_{sl} + W_1C_{P2}\delta T_d$$

$$+ C_{P2}T_d\delta W_1 - W_2C_{P2}\frac{\partial T_{sat}}{\partial P}\delta P - C_{P2}T_{sat}\delta W_2. \quad \text{(III.7.60)}$$

III.7.3.3 Boiling Secondary Fluid Lump (SFBL)

The secondary boiling starts when the temperature of the secondary fluid reaches T_{sat} and ends at the end of the active heat transfer region at a level just above the tube bundle. As the secondary fluid moves upwards, the quality of the two-phase mixture formed by the boiling process increases from 0 to an exit quality x_e.

Assuming the homogeneous flow model, we consider the secondary fluid in the boiling section as a homogeneous steam water mixture with an average quality $\bar{x}$, density ρ_b and enthalpy h_b where

$$\bar{x} = \frac{x_e}{2} , \tag{III.7.61}$$

$$\rho_b = \frac{1}{v_f + \bar{x}\, v_{fg}} , \tag{III.7.62}$$

and

$$h_b = h_f + \bar{x}\, h_{fg}. \tag{III.7.63}$$

Since the size and the density of the boiling lump change during the transient both mass balance and heat balance equations are necessary for the description of the boiling lump.

a. Mass balance

$$\frac{d}{dt} (\rho_b A_{fs} L_{s2}) = W_2 - W_3. \tag{III.7.64}$$

Since the flow area of the secondary fliud is constant, then

$$A_{fs}\left[L_{s2} \frac{d\rho_b}{dt} + \rho_b \frac{dL_{s2}}{dt}\right] = W_2 - W_3. \tag{III.7.65}$$

or, in terms of perturbation variables

$$A_{fs}\left[L_{s2} \frac{d\delta\rho_b}{dt} + \rho_b \frac{d\delta L_{s2}}{dt}\right] = \delta W_2 - \delta W_3. \tag{III.7.66}$$

Since $L_{s1} + L_{s2}$ = constant, then using the equation for $\delta\rho_b$ (see Appendix E), we get

$$- A_{fs}\rho_b \frac{d\delta L_{s1}}{dt} + A_{fs} L_{s2}\left[C_{1b} \frac{d\delta P}{dt} + C_{2b} \frac{d\delta x_e}{dt}\right] = \delta W_2 - \delta W_3. \tag{III.7.67}$$

b. Heat balance

$$\frac{d}{dt}\left[\rho_b A_{fs} L_{s2} h_b\right] = (\dot{Q}_{ms2})_2 + (\dot{Q}_{ms2})_3 + W_2 h_f - W_3 h_e \qquad \text{(III.7.68)}$$

where,

$(\dot{Q}_{ms2})_2$ = heat transfer rate between M_2 and S_2

$= U_{ms2} Pr_2 L_{s2} (T_{m2} - T_{sat})$

$(\dot{Q}_{ms2})_3$ = heat transfer rate between M_3 and S_2

$= U_{ms2} Pr_2 L_{s2} (T_{m2} - T_{sat})$

h_f = enthalpy of saturated water entering the boiling lump

h_{x_e} = enthalpy of secondary fluid leaving the boiling lump

$(h_{x_e} = h_f + x_e \; h_{fg})$

where,

h_{fg} = latent heat of vaporization.

Substituting for h_b, $(\dot{Q}_{ms2})_2$ and $(\dot{Q}_{ms2})_3$ in Equation (III.7.68), we get

$$\frac{d}{dt}\left[\rho_b A_{fs} L_{s2} \left(h_f + \frac{x_e}{2} h_{fg}\right)\right] = U_{ms2} Pr_2 L_{s2} (T_{m2} - T_{sat}) + U_{ms2} Pr_2 L_{s2} (T_{m3} - T_{sat}) + W_2 h_f - W_3 h_{x_e} \qquad \text{(III.7.69)}$$

which upon linearization and some algebraic manipulation yields the following equation

$$A_{fs}\rho_b L_{s2}\left[\frac{\partial h_f}{\partial P} + \frac{x_e}{2}\frac{\partial h_{fg}}{\partial P}\right]\frac{d\delta P}{dt} + A_{fs}\rho_b L_{s2}\frac{h_{fg}}{2}\frac{d\delta x_e}{dt}$$

$$+ h_b A_{fs}\left[-\rho_{s2}\frac{dL_{s1}}{dt} + L_{s2}\left(C_1\frac{d\delta P}{dt} - C_2\frac{d\delta x_e}{dt}\right)\right.$$

$$= U_{ms2}Pr_2 L_{s2}\left[\delta T_{m2} + \delta T_{m3} - 2\frac{\partial T_{sat}}{\partial P}\delta P\right]$$

$$- U_{ms2}Pr_2\left[T_{m2} + T_{m3} - 2T_{sat}\right]\delta L_{s1} + h_f\delta W_2 - h_{x_e}\delta W_3$$

$$+ W_2\frac{\partial h_f}{\partial P}\delta P - W_3 x_e\frac{\partial h_{fg}}{\partial P}\delta P - W_3 h_{fg}\delta x_e. \qquad \text{(III.7.70)}$$

III.7.3.4 Drum Equivalent Secondary Fluid Lump (SFDRL)

The drum equivalent secondary fluid lump in this model has the same geometrical boundaries as in Model C. It can also be divided into the following parts:

1. Riser/Separator volume
2. Drum water volume
3. Drum steam volume.

The equations describing these parts are developed using the same procedure as in Model C are repeated in this section for convenience.

1. Riser/Separator Volume

   The describing equation for the riser/separator volume is the same as Equation (III.6.20) derived in Section III.6.7.1, page 58, with δW_3 and δW_4 replacing δW_2 and δW_3 respectively, thus

$$V_r\left(C_{1r}\frac{d\delta P}{dt} + C_{2r}\frac{d\delta x_e}{dt}\right) = \delta W_3 - \delta W_4 \qquad \text{(III.7.71)}$$

where $C_{1r} = -\frac{1}{(v_f+x_e v_{fg})^2}\left[\frac{\partial v_f}{\partial P} + x_e \frac{\partial v_{fg}}{\partial P}\right]$

and $C_{2r} = -\frac{v_{fg}}{(v_f+x_e v_{fg})^2}$ (see Appendix E).

2. Drum Water Volume

The describing equations for the drum water volume are obtained from a mass balance equation relating the flows in, the flows out, and the water level and a heat balance equation describing the mixing between recirculated water and feedwater. The drum water lump is coupled to the secondary lumps in the effective heat exchange region through the downcomer lump and the recirculation loop equations.

Following the same procedure as in Section III.6.7.2, page 60, we have the following equations

$$\frac{d\delta L_{dw}}{dt} = \frac{1}{\rho_{dw} A_{dw}}\left[(1-x_e)\,\delta W_4 - W_4 \delta x_e - \delta W_{dw} + \delta W_{Fi}\right] \qquad \text{(III.7.72)}$$

$$L_{dw}\frac{d\delta T_{dw}}{dt} + T_{dw}\frac{d\delta L_d}{dt} = \frac{1}{\rho_{dw} A_{dw}}\left[T_{sat}\{(1-x_e)\,\delta W_4 - W_4 \delta x_e\}\right.$$

$$+ (1-x_e)\frac{\partial T_{sat}}{\partial P}\delta P - W_1 \delta T_d$$

$$\left. - T_d \delta W_1 + W_{Fi}\delta T_{Fi} + T_{Fi}\delta W_{Fi}\right]. \qquad \text{(III.7.73)}$$

The above equations are similar to Equations (III.6.29) and (III.6.30) with W_3 replaced by W_4 as the mass flow rate of the two phase mixture leaving the riser/separator volume.

3. Drum Steam Volume

The linearized equation for the drum steam volume is similar to Equation (III.6.36) developed in Section III.6.7.3, page 62, with W_4 replacing W_3 as the mass flow rate of the two phase mixture leaving the riser/separator volume, thus

$$V_s \frac{\partial \rho_g}{dt} \frac{d\delta P}{dt} - \rho_g A_{dw} \frac{d\delta L_{dw}}{dt} = x_e \delta W_4 + W_4 \delta x_e - C_L \delta P - P \delta C_L. \qquad \text{(III.7.74)}$$

III.7.3.5 Downcomer Secondary Fluid Lump (SFDCL)

As in the case with Model C, the downcomer secondary fluid lump acts as a transport time delay between the drum water volume and the effective heat exchange region. The equation for the downcomer lump is the same as Equation (III.6.40) and can be written in the form

$$\frac{d\delta T_d}{dt} = \frac{1}{\tau_d} (\delta T_{dw} - \delta T_d) \qquad \text{(III.7.75)}$$

where

$\tau_d = \frac{M_d}{W_1}$ = residence time of the secondary fluid in the downcomer lump.

III.7.4 The Recirculation Loop Equation

The recirculation loop equation is obtained by applying the momentum theory to the secondary fluid outside and inside the tube wrapper. Following the same procedure described for Model C in Section III.6.9, page 65, we notice that outside the tube wrapper the pressure head of the recirculation loop is identical for Model C and D, however, the secondary fluid inside the tube wrapper in Model D is composed of three parts.

1. Subcooled region of length L_{sl}, where the temperature of the subcooled fluid is raised from T_d at the inlet to T_{sat} at the outlet. The density is assumed constant in this region.
2. Nucleate boiling region of length $L_B = L - L_{sl}$, where boiling of the saturated water leaving the subcooled region takes place and the mass quality of the two phase mixture is assumed to change linearly from 0 at the inlet to x_e at the outlet.
3. Riser/separator region of length L_R, where the two phase mixture leaving the nucleate boiling continues to move upwards in the riser/separator volume.

Therefore $(\Delta P)_{OTW}$ can be calculated in the same way as in Equation (III.6.46), thus

$$(\Delta P)_{OTW}\Big|_{psi} = \frac{\rho_d L_d}{144} \qquad \text{(III.7.76)}$$

where,

$\rho_d = \rho_{dw} = \rho_{dc}$ = density of the secondary fluid outside the tube wrapper

$L_d = L_{dw} + L_{dc}$ = height of the secondary fluid in the drum water volume and the downcomer transport lump.

However, $(\Delta P)_{ITW}$ is now calculated from the following equation.

$$(\Delta P)_{ITW}\Big|_{psi} = \frac{\rho_s L_{sl} + \rho_b L_B + \rho_r L_r}{144} \qquad \text{(III.7.77)}$$

where,

ρ_s = density in the subcooled region

L_{sl} = length of the subcooled region

ρ_{bs} = average density in the nucleate boiling region

L_B = length of the boiling region

ρ_r = density in the riser/separator region

L_r = length of the riser/separator region.

Using the same method as discussed on page 68, the equation for δW_1 can be reduced to the form

$$\delta W_1 = a_1 \delta L_{dw} + a_2 \delta L_{sl} + a_3 \delta p + a_4 \delta x_e. \qquad \text{(III.7.78)}$$

The expressions for the coefficients a_1, a_2, a_3, and a_4 are derived in Appendix D.

III.7.5 Summary of the Model Equations

The governing equations of Model D that were developed in the preceeding sections can be represented by the matrix equation

$$A_1 \frac{d\bar{x}}{dt} + A_2 \bar{x} = \bar{f}$$

where

$\bar{x}$ = system variables (differential + algebraic)* vector

A_1 and A_2 = coefficient matrices

$\bar{f}$ = forcing vector.

A list of the system variables is given in Table III.2 and the nonzero elements of the matrices A_1 and A_2 and the forcing vector $\bar{f}$ are given below.

---

*The definition of differential and algebraic variables will be discussed in Chapter IV.

TABLE III.2

SYSTEM VARIABLES FOR THE DETAILED MODEL (MODEL D)

1.	T_{Pi}	:	primary water inlet plenum temperature
2.	T_{P1}	:	first primary water lump temperature
3.	T_{P2}	:	second primary water lump temperature
4.	T_{P3}	:	third primary water lump temperature
5.	T_{P4}	:	fourth primary water lump temperature
6.	T_{PO}	:	primary water outlet plenum temperature
7.	T_{m1}	:	first tube metal lump temperature
8.	T_{m2}	:	second tube metal lump temperature
9.	T_{m3}	:	third tube metal lump temperature
10.	T_{m4}	:	fourth tube metal lump temperature
11.	L_{dw}	:	drum water level
12.	L_{s1}	:	nonboiling (subcooled) length
13.	P	:	steam pressure
14.	x_e	:	boiling section exit quality
15.	T_{dw}	:	drum water temperature
16.	T_d	:	downcomer outlet temperature
*17.	W_1	:	flow rate to the nonboiling section
*18.	W_2	:	flow rate to the boiling section
*19.	W_3	:	flow rate from the boiling section
*20.	W_4	:	flow rate from the riser/separator volume

*Algebraic variables.

1. The A_1 Matrix

$$A_1(1,1) = 1.0$$

$$A_1(2,2) = 1.0$$

$$A_1(3,3) = 1.0$$

$$A_1(3,12) = \left(\frac{T_{P1}-T_{P2}}{L_{s2}}\right)$$

$$A_1(4,4) = 1.0$$

$$A_1(5,5) = 1.0$$

$$A_1(5,12) = \frac{T_{P4}-T_{P3}}{L_{s1}}$$

$$A_1(6,6) = 1.0$$

$$A_1(7,7) = 1.0$$

$$A_1(7,12) = \left(\frac{T_{m1}-T_{m2}}{2L_{s1}}\right)$$

$$A_1(8,8) = 1.0$$

$$A_1(8,12) = \frac{T_{m1}-T_{m2}}{2L_{s2}}$$

$$A_1(9,9) = 1.0$$

$$A_1(9,12) = -\left(\frac{T_{m3}-T_{m4}}{2L_{s2}}\right)$$

$$A_1(10,10) = 1.0$$

$$A_1(10,12) = -\left(\frac{T_{m3}-T_{m4}}{2L_{s1}}\right)$$

$$A_1(11,11) = 1.0$$

$$A_1(12,12) = \frac{M_{s1}C_{P3}}{2}\left(\frac{T_{dt}T_{sat}}{L_{s1}}\right)$$

$$A_1(12,13) = \frac{M_{s1} C_{P2}}{2} \frac{\partial T_{sat}}{\partial P}$$

$$A_1(12,16) = \frac{M_{s1} C_{P2}}{2}$$

$$A_1(13,12) = - A_{fs} \rho_b$$

$$A_1(13,13) = A_{fs} L_{s2} C_{1b}$$

$$A_1(13,14) = A_{fs} L_{s2} C_{2b}$$

$$A_1(14,12) = - A_{fs} h_b \rho_b$$

$$A_1(14,13) = A_{fs} \rho_b L_{s2} \left(\frac{\partial h_f}{\partial P} + \frac{x_e}{2} \frac{\partial h_{fg}}{\partial P}\right) + A_{fs} L_{s2} h_b C_{1b}$$

$$A_1(14,14) = A_{fs} \rho_b L_{s2} \cdot \frac{h_{fg}}{2} + A_{fs} L_{s2} h_b C_{2b}$$

$$A_1(15,13) = V_r C_{1r}$$

$$A_1(15,14) = V_r C_{2r}$$

$$A_1(16,11) = 1.0$$

$$A_1(17,11) = T_{dw}$$

$$A_1(17,15) = L_{dw}$$

$$A_1(18,11) = - \rho_g A_{dw}$$

$$A_1(18,13) = V_s \frac{\partial \rho_g}{\partial P}$$

$$A_1(19,16) = 1.0.$$

2. The A_2 Matrix

$$A_2(1,1) = \frac{1}{\tau_{Pi}} = \frac{W_{Pi}}{M_{Pi}}$$

$$A_2(2,1) = - \frac{1}{\tau_{P1}} = - \frac{W_{Pi}}{M_{P1}}$$

$$A_2(2,2) = \left(\frac{1}{\tau_{P1}} + \frac{U_{pm} S_{pm1}}{M_{P1} C_{P1}}\right)$$

$$A_2(2,7) = -\frac{U_{pm} S_{pm1}}{M_{P1} C_{P1}}$$

$$A_2(2,12) = \frac{U_{pm} P_{r1}}{M_{P1} C_{P1}} (T_{P1} - T_{m1})$$

$$A_2(3,2) = -\frac{1}{\tau_{P2}} = -\frac{W_{Pi}}{M_{P2}}$$

$$A_2(3,3) = \left(\frac{1}{\tau_{P2}} + \frac{U_{pm} S_{pm2}}{M_{P2} C_{P1}}\right)$$

$$A_2(3,8) = -\frac{U_{pm} S_{pm2}}{M_{P2} C_{P1}}$$

$$A_2(3,12) = -\frac{U_{pm} P_{r1}}{M_{P2} C_{P1}} (T_{P2} - T_{m2})$$

$$A_2(4,3) = -\frac{1}{\tau_{P3}} = \frac{W_{Pi}}{M_{P3}}$$

$$A_2(4,4) = \left(\frac{1}{\tau_{P3}} + \frac{U_{pm} S_{pm3}}{M_{P3} C_{P1}}\right)$$

$$A_2(4,9) = -\frac{U_{pm} S_{pm3}}{M_{P3} C_{P1}}$$

$$A_2(4,12) = -\frac{U_{pm} P_{r1}}{M_{P3} C_{P1}} (T_{P3} - T_{m3})$$

$$A_2(5,4) = -\frac{1}{\tau_{P4}} = \frac{W_{Pi}}{M_{P4}}$$

$$A_2(5,5) = \left(\frac{1}{\tau_{P4}} + \frac{U_{pm} S_{pm4}}{M_{P4} C_{P1}}\right)$$

$$A_2(5,10) = - \frac{U_{pm} S_{pm4}}{M_{P4} C_{P1}}$$

$$A_2(5,12) = \frac{U_{pm} P_{rl}}{M_{P4} C_{P1}} (T_{P4} - T_{m4})$$

$$A_2(6,5) = - \frac{1}{\tau_{P0}} = - \frac{W_{Pi}}{M_{P0}}$$

$$A_2(6,6) = \frac{1}{\tau_{P0}}$$

$$A_2(7,2) = - \frac{U_{pm} S_{pm1}}{M_{m1} C_m}$$

$$A_2(7,7) = \left(\frac{U_{pm} S_{pm1} + U_{ms1} S_{ms1}}{M_{m1} C_m}\right)$$

$$A_2(7,13) = - \left(\frac{U_{ms1} S_{ms1}}{2 M_{m1} C_m}\right) \cdot \frac{\partial T_{sat}}{\partial P}$$

$$A_2(7,16) = - \frac{U_{ms1} S_{ms1}}{2 M_{m1} C_m}$$

$$A_2(8,3) = - \frac{U_{pm} S_{pm2}}{M_{m2} C_m}$$

$$A_2(8,8) = \left(\frac{U_{pm} S_{pm2} + U_{ms2} S_{ms2}}{M_{m2} C_m}\right)$$

$$A_2(8,13) = - \left(\frac{U_{ms2} S_{ms2}}{M_{m2} C_m}\right) \cdot \frac{\partial T_{sat}}{\partial P}$$

$$A_2(9,4) = - \frac{U_{pm} S_{pm2}}{M_{m3} C_m}$$

$$A_2(9,9) = \left(\frac{U_{pm}S_{pm2} + U_{ms2}S_{ms2}}{M_{m3}C_m}\right)$$

$$A_2(9,13) = -\left(\frac{U_{ms2}S_{ms2}}{M_{m3}C_m}\right) \cdot \frac{\partial T_{sat}}{\partial P}$$

$$A_2(10,5) = -\frac{U_{pm}S_{pm1}}{M_{m4}C_m}$$

$$A_2(10,10) = \left(\frac{U_{pm}S_{pm1} + U_{ms1}S_{ms1}}{M_{m4}C_m}\right)$$

$$A_2(10,13) = -\left(\frac{U_{ms1}S_{ms1}}{2M_{m4}C_m}\right) \cdot \frac{\partial T_{sat}}{\partial P}$$

$$A_2(10,16) = -\frac{U_{ms1}S_{ms1}}{2M_{m4}C_m}$$

$$A_2(11,17) = -\frac{1}{\rho_s A_{fs}}$$

$$A_2(11,18) = \frac{1}{\rho_s A_{fs}}$$

$$A_2(12,7) = -U_{ms1}S_{ms1}$$

$$A_2(12,10) = -U_{ms1}S_{ms1}$$

$$A_2(12,12) = -\left(\frac{U_{ms1}S_{ms1}}{L_{s1}}\right)\left[T_{m1} + T_{m4} - T_d - T_{sat}\right]$$

$$A_2(12,13) = \left(U_{ms1}S_{ms1} + W_2C_{P2}\right)\frac{\partial T_{sat}}{\partial P}$$

$$A_2(12,16) = \left(U_{ms1}S_{ms1} - W_1C_{P2}\right)$$

$$A_2(12,17) = -C_{P2}T_d$$

$$A_2(13,18) = -1.0$$

$$A_2(13,19) = 1.0$$

$$A_2(14,8) = -U_{ms2}S_{ms2}$$

$$A_2(14,9) = -U_{ms2}S_{ms2}$$

$$A_2(14,12) = \frac{U_{ms2}S_{ms2}}{L_{s2}}(T_{m2} + T_{m3} - 2T_{sat})$$

$$A_2(14,13) = 2U_{ms2}S_{ms2}\frac{\partial T_{sat}}{\partial P} + W_3 x_e \frac{\partial h_{fg}}{\partial P}$$

$$A_2(14,14) = W_3 h_{fg}$$

$$A_2(14,18) = -h_f$$

$$A_2(14,19) = hx_e = h_f + x_e h_{fg}$$

$$A_2(15,19) = -1.0$$

$$A_2(15,20) = 1.0$$

$$A_2(16,14) = \frac{W_4}{\rho_{dw}A_{dw}}$$

$$A_2(16,17) = \frac{1}{\rho_{dw}A_{dw}}$$

$$A_2(16,20) = -\frac{(1-x_e)}{\rho_{dw}A_{dw}}$$

$$A_2(17,13) = -\frac{(1-x_e)}{\rho_{dw}A_{dw}}\frac{\partial T_{sat}}{\partial P}$$

$$A_2(17,14) = \frac{W_4}{\rho_{dw}A_{dw}} \cdot T_{sat}$$

$$A_2(17,16) = \frac{W_1}{\rho_{dw}A_{dw}}$$

$$A_2(17,17) = \frac{T_d}{\rho_{dw} A_{dw}}$$

$$A_2(17,20) = -\frac{(1-x_e)}{\rho_{dw} A_{dw}} \cdot T_{sat}$$

$$A_2(18,13) = C_L$$

$$A_2(18,14) = -W_4$$

$$A_2(18,20) = x_e$$

$$A_2(19,15) = -\frac{1}{\tau_d} = -\frac{W_1}{M_d}$$

$$A_2(19,16) = \frac{1}{\tau_d}$$

$$A_2(20,11) = a_1$$

$$A_2(20,12) = a_2$$

$$A_2(20,13) = a_3$$

$$A_2(20,14) = a_4$$

$$A_2(20,17) = -1.0.$$

3. The Forcing Vector $\bar{f}$

$$f(1) = \frac{1}{\tau_{Pi}} \delta\theta_i = \frac{W_{Pi}}{M_{Pi}} \delta\theta_i$$

$$f(16) = \frac{1}{\rho_{dw} A_{dw}} \delta W_{Fi}$$

$$f(17) = \frac{1}{\rho_{dw} A_{dw}} (W_{Fi} \delta T_{Fi} + T_{Fi} \delta W_{Fi})$$

$$f(18) = -P\, \delta C_L.$$

CHAPTER IV

CALCULATION PROCEDURE AND RESULTS

IV.1 Introduction

As was seen in Chapter III, page 25, the lumped parameter state variable approach results in two different types of model formulations:

1. Pure Differential Formulation. In this case, all of the model equations are differential. Models A and B belong to this group.
2. Mixed Differential and Algebraic Formulation. In this case, some of the model equations are differential and some are algebraic. The system variables consist of differential (or state) variables and algebraic (or intermediate) variables. A differential variable is defined[37] as a variable whose derivative appears at least once in the system equations while an algebraic variable is defined as a variable whose derivative does not appear anywhere in the system equations. Models C and D belong to this group. As the model complexity increases, the mixed differential and algebraic formulation has the advantage of reducing the amount of mathematical manipulation required by the system analyst and accordingly reducing the possibility of algebraic or numerical errors in the process of dynamic system analysis. The calculation procedure for obtaining the system time response and frequency response for both

formulation groups and the results obtained from the mathematical models are described in the following sections.

IV.2 Calculation Procedure for the Pure Differential Formulation

A system of coupled first order differential equations can, in general, be written in the form

$$C \frac{d\bar{x}}{dt} = D \bar{x} + E \bar{f} \qquad \text{(IV.1)}$$

where

$\bar{x}$ = state variables vector

$\bar{f}$ = forcing vector

C, D and E = coefficient matrixes.

Provided that C is a nonsingular matrix,[38] both sides of Equation (IV.1) can be pre-multiplied by C^{-1} (inverse of C) to get the following equation

$$\frac{d\bar{x}}{dt} = A \bar{x} + B \bar{f} \qquad \text{(IV.2)}$$

where

$A = C^{-1} D$ = state coefficient matrix

and $B = C^{-1} E$ = forcing coefficient matrix.

Equation (IV.2) is the "classical" form for the mathematical representation of a system of first order differential equations. This equation forms the basis for the computer codes MATEXP[39] and SFR-3[40] that are used in this study to calculate the time response and frequency response respectively.

The general solution of Equation (IV.2) in the time domain is given by[41]

$$\bar{x}(t) = e^{A(t-t_o)}\,\bar{x}(t_o) + \int_{t_o}^{t} e^{A(t-\tau)}\,B\,\bar{f}(\tau)\,d\tau \qquad \text{(IV.3)}$$

where

$\bar{x}(t_o)$ = initial conditions vector

and

$$e^{A(t-t_o)} = \sum_{k=0}^{\infty} \frac{\{A(t-t_o)\}}{k!} . \qquad \text{(IV.4)}$$

The following conventions are used in the matrix exponential in Equation (IV.4)

$\{A(t-t_o)\}^0$ = I = identity matrix

and $0! = 1$.

From Equation (IV.3), it can be seen that given the initial condition vector $\bar{x}(t_o)$, the coefficient matrices A and B and the forcing vector $\bar{f}(t)$, the solution at a later instant t can be found. The degree of accuracy of the solution depends on the number of terms used in the calculation of the matrix exponential in Equation (IV.4) and the method of numerical integration used to calculate the integral in Equation (IV.3). The method for handling the integral term in the MATEXP computer program is to assume that the forcing function is piecewise constant. This gives:

$$\int_{t_o}^{t} e^{A(t-\tau)}\,B\,\bar{f}(\tau)\,d\tau = [I - e^{A(t-t_o)}]\,A^{-1}\,B\,\bar{f}(t_o). \qquad \text{(IV.5)}$$

The frequency response can be obtained by starting with Equation (IV.2) and Laplace transforming[42] both sides, thus

$$S\,\bar{x}(S) = A\,\bar{x}(S) + B\,\bar{F}(S) \qquad \text{(IV.6)}$$

where

S = Laplace transformation variable

$\bar{x}(S)$ = Laplace transform of $\bar{x}(t)$

$\bar{F}(S)$ = Laplace transform of $\bar{f}(t)$

A,B = coefficient matrices, assumed constant.

Rearranging Equation (IV.5) and solving for $\bar{x}(S)$, we get

$$\bar{x}(S) = [SI - A]^{-1}\,B\,\bar{F}(S). \qquad \text{(IV.7)}$$

For a single forcing element $f_m(t)$ in the forcing vector $\bar{f}(t)$, Equation (IV.7) can be written as

$$\bar{x}(S) = [SI - A]^{-1}\,\bar{b}_m\,F_m(S) \qquad \text{(IV.8)}$$

where

$F_m(S)$ = Laplace transform of $f_m(t)$

$$\bar{b}_m = \begin{bmatrix} b_{1m} \\ b_{2m} \\ \cdot \\ \cdot \\ \cdot \\ b_{nm} \end{bmatrix} .$$

The frequency response vector of the system state variables with respect to the forcing element f_m can be obtained from Equation (IV.8) by replacing S by $j\omega$, thus

$$\bar{G}_m(j\omega) \equiv \left\{\frac{\bar{x}(j\omega)}{F_m(j\omega)}\right\} = [j\omega\ I - A]^{-1}\ \bar{b}_m. \qquad \text{(IV.9)}$$

From Equations (IV.3) and (IV.9), the calculation procedure for obtaining the dynamic response when the mathematical model consists of a system of first order differential equations (Models A and B) can be summarized as follows:

1. Calculate the geometrical parameters needed to estimate the volumes of the different lumps in the model using available design data and/or engineering judgement.
2. Calculate the thermal and hydraulic parameters required for the calculation of the coefficient matrices and forcing vectors. This calculation includes the calculation of the heat transfer coefficients and steady state parameters.
3. For time response analysis, input the coefficient matrix and forcing function to the computer code MATEXP[39] together with the program control cards described in Reference 39.
4. For frequency response analysis, input the coefficient matrix and the forcing function to the computer code SFR-3[40] together with the program control cards described in Reference 40.

IV.3 Calculation Procedure for the Mixed Differential and Algebraic Formulation

As the dynamic model complexity increases, the mathematical manipulation effort can be considerably reduced when the algebraic equations relating system intermediate variables to system state variables are left in the model. In this case, the mathematical model of the system consists of a set of first order equations having both differential and algebraic variables that can be written in the form:

$$A_1 \frac{d\bar{z}}{dt} + A_2 \bar{z} = \bar{g}\, u(t) \qquad \text{(IV.10)}$$

where

$\bar{z}$ = vector of system variables (differential + algebraic)

$\bar{g}$ = vector of constant multipliers of the time varying forcing function

$u(t)$ = arbitrary function of time representing system input (forcing function)

A_1 and A_2 = coefficient matrices.

If the system variables are composed of n differential (or state) variables and r algebraic (or intermediate) variables, then matrix Equation (IV.10) has the order m which is equal to (n+r).

The method of obtaining the time response and the frequency response when the system dynamic model can be represented by Equation (IV.10) is described in Reference 37 and is summarized below for convenience.

IV.3.1 Time Response Calculation

The set of equations represented by matrix Equation (IV.10) is first reordered into m differential equations followed by r algebraic equations and then reduced to a system of n differential equations using the computer code PUREDIFF.[37] Then the reduced set of pure differential equations is solved using the computer code MATEXP.[39] The method of removing the algebraic variables from the equations is described below.

After reordering Equation (IV.10) can be written in the partitioned matrix form

$$\frac{d}{dt}\left[\begin{array}{c|c} R_{11} & \underline{0} \\ \hline R_{21} & \underline{0} \end{array}\right]\left[\begin{array}{c} \bar{x} \\ \hline \bar{y} \end{array}\right] + \left[\begin{array}{c|c} T_{11} & T_{12} \\ \hline T_{21} & T_{22} \end{array}\right]\left[\begin{array}{c} \bar{x} \\ \hline \bar{y} \end{array}\right] = \left[\begin{array}{c} \bar{g}_1 \\ \hline \bar{g}_2 \end{array}\right] u(t) \qquad \text{(IV.11)}$$

where

$\bar{x}$ = differential variable vector

$\bar{y}$ = algebraic variable vector.

Equation (IV.11) can be expanded to obtain the following equations

$$R_{11}\frac{d\bar{x}}{dt} + T_{11}\bar{x} + T_{12}\bar{y} = g_1 u(t) \qquad \text{(IV.12)}$$

$$R_{21}\frac{d\bar{x}}{dt} + T_{21}\bar{x} + T_{22}\bar{y} = g_2 u(t). \qquad \text{(IV.13)}$$

The algebraic variable vector $\bar{y}$ is eliminated by pre-multiplying both sides of Equation (IV.12) by the inverse of T_{12} and pre-multiplying both sides of Equation (IV.13) by the inverse of T_{22} and subtracting the resulting equations to get

$$[T_{12}^{-1} R_{11} - T_{22}^{-1} R_{21}] \frac{d\bar{x}}{dt} + [T_{12}^{-1} T_{11} - T_{22}^{-1} T_{21}] \bar{x} =$$

$$[T_{12}^{-1} \bar{g}_1 - T_{22}^{-1} g_2] u(t) \qquad \text{(IV.14)}$$

pre-multiplying Equation (IV.14) by T_{12} we get

$$[R_{11} = T_{12}^{-1} T_{22}^{-1} R_{21}] \frac{d\bar{x}}{dt} + [T_{11} - T_{12}^{-1} T_{22}^{-1} T_{21}] \bar{x} =$$

$$[g_1 - T_{12}^{-1} T_{22}^{-1} g_2] u(t). \qquad \text{(IV.15)}$$

Equation (IV.14) can be written in the concise form

$$B \frac{d\bar{x}}{dt} + C \bar{x} = \bar{b} u(t) \qquad \text{(IV.16)}$$

where

$$B = [R_{11} - T_{12} T_{22}^{-1} R_{21}]$$

$$C = [T_{11} - T_{12} T_{22}^{-1} T_{21}]$$

$$\bar{b} = [\bar{g}_1 - T_{12} T_{22}^{-1} \bar{g}_2]$$

Multiplying both sides of Equation (IV.16) by B^{-1} gives

$$\frac{d\bar{x}}{dt} + B^{-1} C \bar{x} = B^{-1} \bar{b} u(t). \qquad \text{(IV.17)}$$

Equation (IV.17) is in the "classical" form suitable for using the time response code MATEXP.[39]

An important feature of the above method is that it involves matrix inversion which may produce error in the results when any of the matrices involved are ill-conditioned.[43] This problem may be avoided by changing the ordering of the system equations.

IV.3.2 Frequency Response Calculation

The frequency response vector for the dynamic system represented by Equation (IV.10) can be obtained by replacing S by $j\omega$ in the transfer function vector $\bar{G}(S)$ defined as

$$\bar{G}(S) = \frac{\bar{z}(S)}{u(S)} . \qquad \text{(IV.18)}$$

The transfer function vector can be obtained by two methods.

1. Following the same procedure as in the time response calculation, one can reduce the system of combined differential and algebraic equations to a set of pure differential equations of the form

$$\frac{d\bar{x}}{dt} = A\,\bar{x} + \bar{g}\,u(t). \qquad \text{(IV.19)}$$

The computer code, SFR-3,[40] can then be used to obtain the frequency response vector $\bar{G}(j\omega)$ using the following relation

$$\bar{G}(j\omega) = [j\omega\, I - A]^{-1}\,\bar{g}. \qquad \text{(IV.20)}$$

2. The system equations can be kept in the original mixed mode (differential + algebraic) formulation and a modified version of the SFR-3 code developed in Reference 37 can be used to obtain the frequency response vector $\bar{G}(j\omega)$ using the following relation

$$\bar{G}(j\omega) = [j\omega\, A_1 - A_2]\,\bar{g}. \qquad \text{(IV.21)}$$

From the above discussion, it can be seen that the calculation procedure for obtaining the dynamic response when the mathematical model consists of a mixed set of differential and algebraic equations (Models C and D) can be summarized as follows.

1. Calculate the geometric parameters needed to estimate the volumes of the different lumps in the model using available design data and/or engineering judgement.
2. Calculate the thermal and hydraulic parameters required for the calculation of the coefficient matrices and forcing vectors. This calculation includes the calculation of the heat transfer coefficients and steady state parameters.
3. For the time response analysis, input the coefficient matrices A_1 and A_2 together with the forcing function to the computer code PUREDIFF[37] to reduce the system to pure differential form. Then use the computer code MATEXP[39] to obtain the time response.
4. For the frequency response analysis, either use the modified version of the SFR-3 code[37] or use the reduced system matrix and forcing vector obtained from step 3 as input to the computer code SFR-3.[40]

V.4 Geometrical Calculation

When the design details of the steam generator are known to the ıalyst, the task of calculating the lengths, areas and volumes ecessary for the dynamic response calculation reduces to a simple ısk that has to be repeated when the dimensions and/or ometrical configuration change. However, since the design details

of nuclear steam generators are often considered as proprietory information, the method of calculating geometrical input data for dynamic response calculation from the design details is ruled out when this information is not available. In this study, the only information available to the author is the scoping design data usually listed in the safety analysis report of a nuclear power plant.[2] Therefore, engineering judgement and proportionality principles are used to obtain the geometrical parameters used as input to the dynamic response calculation algorithms. In this section, the method of calculating the geometrical parameters is described and then applied to the H. B. Robinson Unit 2 steam generator using the steam generator design data obtained from Reference 2 and shown in Table IV.1.

IV.4.1 Primary Side

On the primary side, it is required to determine the volume of the primary water in the inlet and outlet plenums and flow area in the effective heat exchange region (U-tube region). The U-tubes are replaced by two straight-tube branches and the average length of each branch is calculated as follows

$$S_o = \frac{\pi D_o}{12} \cdot N \cdot 2L \qquad \text{(IV.21)}$$

where

S_o = total heat transfer surface, ft^2

D_o = U-tube diameter, in.

N = number of U-tubes

L = length of straight tube branch, ft.

TABLE IV.1

H. B. ROBINSON STEAM GENERATOR
DESIGN DATA*

Number of Steam Generators	3
Design Pressure, Reactor Coolant/Steam, psig	2485/1085
Design Temperature, Reactor Coolant/Steam, °F	650/556
Reactor Coolant Flow, lb/hr	33.93×10^6
Total Heat Transfer Surface Area, ft^2	44,430
Steam Conditions at Full Load, Outlet Nozzle:	
Steam Flow, lb/hr	3.196×10^6
Steam Temperature, °F	516
Steam Pressure, psig	770
Feedwater Temperature, °F	435
Overall Height, ft-in.	63 - 1.6
Shell OD, upper/lower, in.	166/127.5
Shell Thickness, upper/lower, in.	3.5/2.63
Number of U-tubes	3260
U-tube Diameter, in.	0.875
Tube Wall Thickness, (average) in.	0.050

	2200 MWt	Zero Power
Reactor Coolant Water Volume, ft^3	928	928
Secondary Side Water Volume, ft^3	1536	3089
Secondary Side Steam Volume, ft^3	3203	1640

*Table 4.1-4, Reference 2.

The flow area of the primary water in the tube region is determined by the following equation

$$A_p = \frac{\pi D_i^2}{4x144} \cdot N \qquad \text{(IV.23)}$$

where

A_p = primary flow area, ft^2

D_i = U-tube inside diameter, in

N = number of tubes.

The tube inside diameter is obtained from the tube outside diameter and the tube wall thickens. The inlet and outlet plenums are each assumed to have the same volume which is given by

$$V_{PL} = \frac{V_p - V_t}{2} \qquad \text{(IV.24)}$$

where

V_{PL} = volume of inlet or outlet plenum, ft^3

V_p = steam generator primary water volume, ft^3

V_t = volume of primary water inside the U-tubes, ft^3.

IV.4.2 Tube Metal

The cross section area of the tube metal (A_m) is given by

$$A_m = \frac{\pi (D_o^2 - D_i^2)}{4x144} \cdot N. \qquad \text{(IV.25)}$$

The surface area per unit length is used in the calculation in the heat transfer area and can be determined as follows

$$P_{ri} = \frac{\pi D_i}{12} \cdot N \qquad \text{(IV.26)}$$

$$P_{ro} = \frac{\pi D_o}{12} \cdot N. \qquad \text{(IV.27)}$$

IV.4.3 Secondary Side

The secondary side is divided into three parts.

1. Secondary fluid in the effective heat exchange region.
2. Secondary fluid in the downcomer region.
3. Secondary fluid in the drum equivalent region.

For the effective heat exchange region and the downcomer region, it is possible to determine the flow area and therefore the volume of any secondary fluid lump in these regions from a knowledge of the length of the lump. However, for the drum equivalent region, it is only possible to estimate lumped volumes due to the complex geometrical configuration in that region since it includes the feed-water ring and the steam separators and driers. The calculation of the geometrical parameters in the above regions is described below.

1. Effective Heat Exchange Region. The effective heat exchange region is bounded by the tube-wrapper, the tube plate and a fixed plane just above the U-tubes. The secondary fluid flow area in this region can be estimated from the area inside the tube wrapper and the area occupied by the U-tubes, thus,

$$A_s = A_w - A_t \qquad \text{(IV.28)}$$

where

A_s = secondary fluid flow area, ft^2

A_w = area inside the tube wrapper, ft^2

A_t = area occupied by the U-tubes, ft^2.

The area inside the tube wrapper can be estimated from the tubes arrangement, number and outside diameter. The length of the effective heat exchange region is assumed to be the same as the straight tube branch length calculated by Equation (IV.22).

2. Downcomer Region. The downcomer region is defined by the annular space between the steam generator lower shell section and the tube wrapper. The downcomer flow area is determined by

$$A_d = A_{LS} - A_w \qquad \text{(IV.29)}$$

where

A_d = downcomer flow area, ft^2

A_{LS} = inside area of the lower shell section, ft^2

A_w = area of the tube wrapper, ft^2.

The length of the downcomer section is assumed to be equal to the same as the length of the effective heat exchange region.

3. Drum Equivalent Region. As described in Chapter III, page 56, the drum equivalent region is composed of three sections.

   a. Riser/separator volume

   b. Drum water volume

   c. Drum steam volume.

The dimensions for these sections were estimated using engineering judgement and proportionality principles using the steam generator dimensions and the secondary side water and steam volumes given in Table IV.1.

IV.4.4 Results for H. B. Robinson Steam Generator

The geometrical data calculated for the H. B. Robinson steam generator can be summarized as follows.

A. Primary Side

1. Number of tubes = 3260
2. Straight tube branch length = 29.75 ft
3. Primary flow area = 10.68 ft^2
4. Primary inlet plenum volume = 146.27 ft^3
5. Primary outlet plenum volume = 146.27 ft^3.

B. Tube Metal

1. Tube metal cross section = 2.934 ft^2
2. Primary/metal heat transfer area per unit length = 661.436 ft
3. Metal/secondary heat transfer area per unit length = 746.783 ft.

C. Secondary Side

1. Effective exchange region

   Flow area (A_S) = 52.93 ft^2

   Total length (L_t) = 29.75 ft.

2. Downcomer region

   Flow area (A_d) = 7.614 ft^2

   Length (L_d) = 29.75

3. Drum equivalent region

   Drum water volume (V_{dw}) = 973.88 ft^3

   Drum water area (A_{dw}) = 101.13 ft^2

   Drum water length (L_{dw}) = 9.63 ft

   Drum steam volume (V_{ss}) = 2966.38 ft^3

   Riser/separator volume (V_r) = 408.5 ft^3

   Riser/separator area = 42.42 ft^2

   Riser/separator length = 9.63 ft.

IV.5 Calculation of Heat Transfer Coefficients

In the effective heat exchange region, heat is transferred from the primary side to the secondary side through the U-tube walls. On the primary side, pressurized water passes inside the U-tubes and transfers heat to the tube metal. Across the tube thickness, heat is transferred by radial conduction. On the secondary side, slightly subcooled water, then two phase steam/water mixture flows by natural circulation outside the U-tubes. Metal-to-liquid heat transfer occurs in the subcooled secondary region while nucleate boiling is the primary heat transfer mechanism in the boiling secondary region.

In this section, the method used in calculating the heat transfer coefficients is described and the results used as input for the dynamic response calculations are reported.

IV.5.1 Film Heat Transfer Coefficients

The Dittus-Boelter Correlation is the most desirable correlation[27] for calculating film heat transfer coefficients when convection is the primary heat transfer mechanism. This correlation can be written in the form

$$U_{FC} = 0.023 \left(\frac{K}{D}\right) \left(\frac{G\ D}{\mu}\right)^{0.8} \left(\frac{\mu\ C_p}{K}\right)^{n} \qquad \text{(IV.30)}$$

where

U_{FC} = film heat transfer coefficient, Btu/hr ft^2 °F

K = thermal conductivity, Btu/hr ft °F

G = mass velocity, lbm/hr ft^2

D = hydraulic diameter, ft

μ = viscosity, lbm/ft hr

C_p = specific heat at constant pressure, Btu/lbm °F.

The value of the index n is taken as 0.3 for calculating the heat transfer coefficient between the primary water and the inner surface of the tubes and as 0.4 for calculating the heat transfer coefficient between the outside surface of the tubes and the secondary fluid in the subcooled region. In the boiling region of the secondary fluid, the heat transfer is enhanced by the boiling mechanism. In this region, the film heat transfer coefficient can be calculating using a correlation proposed by Chen.[44] In

this correlation, the heat transfer coefficient in the saturated nucleate boiling region is assumed to have contribution from both nucleate boiling and convection, thus

$$U_{TP} = U_{NCB} + U_C \tag{IV.31}$$

where

U_{TP} = heat transfer coefficient in the boiling region

U_{NCB} = contribution due to nucleate boiling

U_C = contribution due to convection.

It was assumed that the convection component, U_C, could be represented by a modified Dittus-Boelter type equation

$$U_C = 0.023 \left[\frac{G(1-x)}{\mu f}\right]^{0.8} \left[\frac{\mu C_p}{K}\right]_f^{0.4} \left(\frac{K_f}{D}\right) F \tag{IV.32}$$

where F is a parameter defined such that

$$F = \left[\frac{R_{eTP}}{G(1-x)\ D/\mu f}\right]^{0.8} \tag{IV.33}$$

F is a function of the Martinelli factor X_{tt} defined as

$$X_{tt} = \left(\frac{1-x}{x}\right)^{0.9} \left(\frac{vf}{vg}\right)^{0.5} \left(\frac{\mu f}{\mu g}\right)^{0.1} \tag{IV.34}$$

where

x = mass quality

vf = specific volume of saturated liquid

vg = specific volume of saturated steam

μf = viscosity of saturated liquid

μg = viscosity of saturated steam.

The nucleate boiling contribution h_{NCB} is given by[44]

$$U_{NCB} = 0.172 \left[\frac{K_f^{0.79} C_{pf}^{0.45} \rho_f^{0.49}}{\sigma^{0.5} \mu_f^{0.29} h_{fg}^{0.24} \rho_g^{0.24}}\right] S \cdot \Delta T_{sat}^{0.24} \cdot \Delta P_{sat}^{0.75} \cdot \quad \text{(IV.35)}$$

The reader is referred to Reference 44 for the details of calculating the heat transfer coefficient in the boiling region using Chen's correlation.

IV.5.2 Tube Metal Conductance

Since the thickness of the tube wall is very small relative to the tube length, the tube metal conductance can be estimated using the following equation[45]

$$U_m = \frac{12 K_w}{b_w} \quad \text{(IV.36)}$$

where

K_w = thermal conductivity of tube metal

b_w = thickness of tube wall (inches).

Effective area for heat conduction through the tube wall is given by

$$A_m = \frac{A_0 - A_i}{\ln (\frac{A_0}{A_i})} . \quad \text{(IV.37)}$$

IV.5.3 Overall Heat Transfer Coefficients

The overall heat transfer resistance is the sum of the resistances of the primary side film, the tube wall, fouling and the secondary side film. Based on the secondary side heat transfer area we have

$$\frac{1}{U} = \frac{1}{U_i} \frac{A_0}{A_i} + \frac{1}{U_m} \cdot \frac{A_0}{A_m} + f + \frac{1}{U_0} \quad \text{(IV.38)}$$

where

U = overall heat transfer coefficient

U_i = primary side film heat transfer coefficient

U_m = tube metal conductance

U_o = secondary side film heat transfer coefficient

f = fouling factor

A_i = inside tube area

A_o = outside tube area.

The secondary side film heat transfer coefficient depends on whether the secondary fluid is subcooled or boiling.

Fouling factors may be considered to represent safety factors that increase the design area of the steam generator to compensate for possible scale build up on the tube metal surfaces. Since the primary coolant is maintained at extremely high purity level, fouling on the primary side is often negligible. Secondary side system purity is lower and some fouling allowance must be considered in calculating the overall heat transfer coefficients. Fraas et al.[45] stated that an allowance of 0.0003 (°F ft^2 ht/Btu) is generally considered reasonable.

IV.5.4 Combined Film and Tube Metal Conductances

When the mean temperature of the tube metal lump is considered as a state variable in the dynamic model, it is necessary to combine the film heat transfer conductance (coefficient) with the tube metal conductance to obtain an effective heat transfer coefficient between the bulk mean temperatures of the primary and secondary fluids and the tube mean temperature. The calculation for this effective heat

transfer coefficient can be derived from the analogy between the flow of heat energy through thermal resistance to the flow of electric current in an electrical resistor,[46] thus

$$\text{Heat Transfer Rate} = \frac{\text{Temperature Difference}}{\text{Thermal Resistance}} .$$

Referring to Figure IV.1 we have

$$\dot{Q}_{pm} = \frac{T_p - T_m}{R_i + R_m(\frac{A_{ml}}{A_i})} = U_{pm}A_i(T_p - T_m) \qquad \text{(IV.39)}$$

and

$$\dot{Q}_{ms} = \frac{T_m - T_s}{R_o + R_m(\frac{A_{m2}}{A_o})} = U_{ms}A_o(T_m - T_s). \qquad \text{(IV.40)}$$

From these equations we have

$$\frac{1}{U_{pm}} = \frac{1}{U_i} + (\frac{A_i}{A_{ml}}) \cdot \frac{1}{U_m} \qquad \text{(IV.41)}$$

and

$$\frac{1}{U_{ms}} = (\frac{A_o}{A_{m2}}) \cdot \frac{1}{U_m} + \frac{1}{U_o} \qquad \text{(IV.42)}$$

where

$$A_{ml} = \frac{A_m - A_i}{\ln(\frac{A_m}{A_i})} = \frac{A_i(\frac{A_m}{A_i} - 1)}{\ln(\frac{A_m}{A_i})} \qquad \text{(IV.43)}$$

and

$$A_{m2} = \frac{A_o - A_m}{\ln(\frac{A_o}{A_m})} = \frac{A_o(1 - \frac{A_m}{A_o})}{\ln(\frac{A_o}{A_m})} \qquad \text{(IV.44)}$$

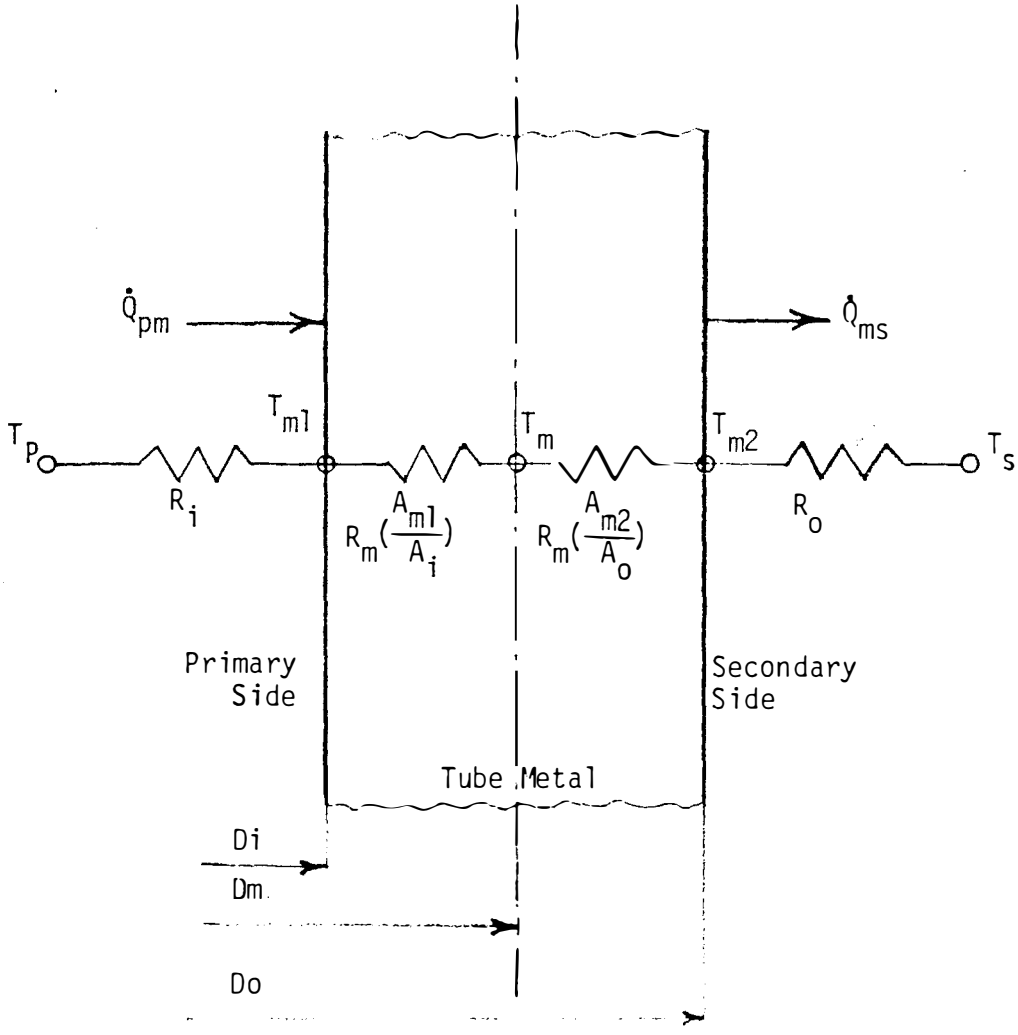

Figure IV.1 Combining Film and Tube Metal Conductances.

where

U_i = primary side film conductance = $1/R_i$

U_m = tube metal conductance = $1/R_m$

U_o = secondary side film conductance = $1/R_o$

A_i = tube inside surface area

A_m = tube mean surface area

A_o = tube outside surface area.

IV.5.5 Results for H. B. Robinson Steam Generator

The following values of the heat transfer coefficients are used as input for the reference case dynamic calculation.

Primary film heat transfer coefficient = 4500 Btu/hr ft^2°F

Tube metal conductance = 2160 Btu/hr ft^2°F

Tube outside heat transfer area = 44430 ft^2

Tube metal/subcooled secondary film heat transfer coefficient = 1972 Btu/hr ft^2°F

Tube metal/boiling secondary film heat transfer coefficient = 6000 Btu/hr ft^2°F

IV.6 Steady State Calculations

IV.6.1 Introduction

When the moving boundary approach is used in the development of dynamic models for a UTSG, the conditions at steady state are prerequisites for the dynamic calculation algorithm. In this section, it is assumed that the recirculation ratio of the steam generator is known and the purpose of the steady state calculation is to determine the temperature profiles along the primary and

subcooled secondary flow paths and also the mass quality profile along the boiling secondary flow path after finding the level at which the boiling process in the secondary fluid starts (L_{S1}). Figure IV.2 shows a schematic diagram of the effective heat exchange region (core) of a UTSG. Primary water from the reactor hot leg enters the heat exchange region from the steam generator inlet plenum at temperature T_{Pi} and after exchanging heat to the secondary fluid passing outside the U-tubes, it leaves the heat exchange region to the steam generator outlet plenum at temperature T_{Po}. The secondary fluid enters the heat exchange region from the downcomer section at a temperature T_d which is lower than the saturation temperature corresponding to the steam generator pressure. As the secondary fluid flows upwards in the core region (by natural circulation) its temperature increases until the saturation temperature T_{sat} is reached at a level L_{S1} which is considered as the subcooled/boiling boundary. The primary temperatures at the subcooled/boiling boundary are denoted by T_{P1} and T_{P4} in the parallel and counter flow branches respectively. Above L_{S1}, the heat added to the secondary fluid is used in increasing the mass quality of the steam/water mixture from xso at the onset of bulk nucleate boiling to $x = x_e$ at the end of the boiling section of the heat exchange region. The primary temperatures at the end of the boiling section are denoted by T_{P2} and T_{P3} in the parallel and counterflow branches respectively. Since the primary temperature at the exit of the parallel flow branch must be equal to the inlet temperature to the counterflow branch, T_{P2} and T_{P3} should be equal. Since the

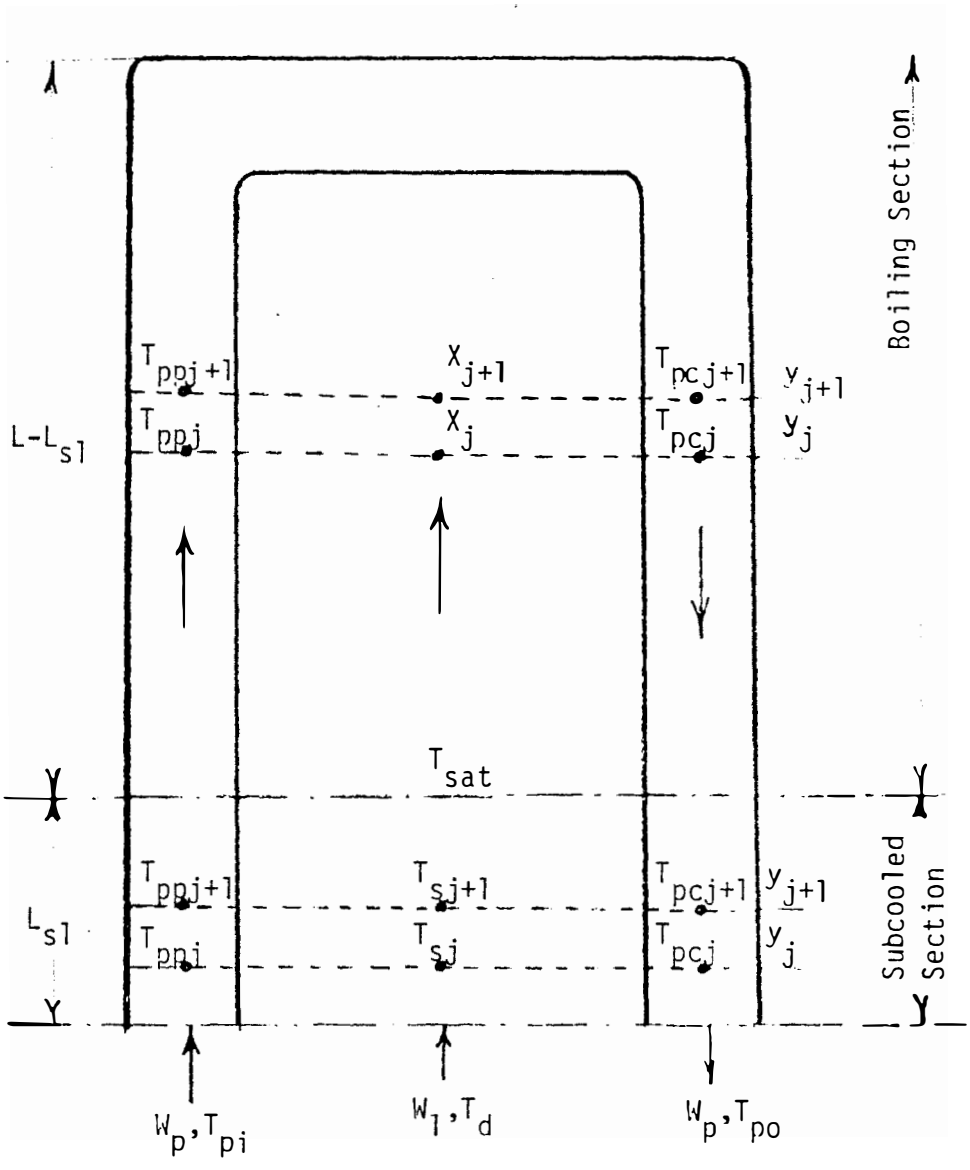

Figure IV.2 Schematic of the Effective Heat Exchange Region (Core).

secondary inlet temperature T_d is dependent on the mass quality at the exit of the boiling section, an iteration technique is necessary to satisfy an overall heat balance between the primary and secondary sides of the steam generator.

IV.6.2 Solution Using the Finite Difference Approach

In this method, the path along the heat exchange region is divided into a number of finite sections. The heat balance equations for each section are solved for the exit conditions using the inlet conditions and the other known system parameters. The secondary temperature at the exit of the finite section is compared with the saturation temperature. There are three possible conditions:

1. The secondary temperature is less than T_{sat}.
2. The secondary temperature is equal to T_{sat} (within a reasonable convergence allowance).
3. The secondary temperature is greater than T_{sat}.

In the first case, the height along the heat exchange path is incremented and the calculations are repeated for another finite section using the exit conditions of the previous sections as the new inlet conditions. In the second case, the subcooled/boiling boundary is reached and new heat balance equations are solved where the mass quality is the unknown variable for the secondary fluid. In the third case, the incremental height of the finite section is decreased and the calculations are repeated until the secondary temperature at the exit of the calculation section converges to the saturation temperature within a reasonable convergence allowance.

In the boiling section, the finite element calculation continues until the total height of the U-tube branch is reached. At this point, the primary exit temperatures, T_{P2} and T_{P3} are tested for equality in case they are unequal, the primary outlet temperature is adjusted and the calculation loop is repeated. This approach causes a slight adjustment of the primary average temperature in order to achieve balanced conditions in the steam generator.

The heat balance equations for a finite element in the subcooled section are given by (see Figure IV.2, page 131)

$$W_p C_{pl}(T_{ppj}-T_{ppj+1}) = U_1 A_{ij}(T_{ppmj}-T_{smj}) \qquad (IV.45)$$

$$W_p C_{pl}(T_{pcj+1}-P_{pcj}) = U_1 A_{ij}(T_{pcmj}-T_{smj}) \qquad (IV.46)$$

$$W_p C_{pl}\{(T_{ppj}-T_{ppj+1}) + (T_{pcj+1}-T_{pcj})\} = \frac{W_s}{x_e} C_{p2}(T_{sj+1}-T_{sj}) \qquad (IV.47)$$

where,

$$A_{ij} = \pi D_o N(y_{j+1}-y_j) \qquad (IV.48)$$

$$T_{ppmj} = \frac{T_{ppj} + T_{ppj+1}}{2} \qquad (IV.49)$$

$$T_{pcmj} = \frac{T_{pcj} + T_{pcj+1}}{2} \qquad (IV.50)$$

and $$T_{smj} = \frac{T_{sj} + T_{sj+1}}{2} . \qquad (IV.51)$$

The initial conditions for the subcooled section calculation are

$$T_{pp1} = T_{pi}$$

$$T_{pc1} = T_{po}$$

and $$T_{s1} = T_d .$$

Equations (IV.45) through (IV.47) are solved for the exit conditions (at y_{j+1}) knowing the inlet conditions (at y_j).

The heat balance equations for a finite element in the boiling section are given by (see Figure IV.2)

$$W_p C_{pl}(T_{ppj}-T_{ppj+1}) = U_2 A_{ij}(T_{ppmj}-T_{sat}) \qquad (IV.52)$$

$$W_p C_{pl}(T_{pcj+1}-T_{pcj}) = U_2 A_{ij}(T_{pcmj}-T_{sat}) \qquad (IV.53)$$

$$W_p C_{pl}\{(T_{ppj}-T_{ppj+1}) + (T_{pcj+1}-T_{pcj})\} = \frac{W_s}{x_e}(X_{j+1}-X_j) \qquad (IV.54)$$

where the definitions in Equations (IV.45) through (IV.51) apply with the following initial conditions

$$T_{ppl} = T_{pl}$$
$$T_{pcl} = T_{p4}$$
$$X_1 = 0.0.$$

Equations (IV.52) through (IV.54) are solved for the exit conditions (at y_{j+1}) knowing the inlet conditions (at y_i) until y_{j+1} is equal to the tube branch length and T_{p2} is equal to T_{p3} within a reasonable convergence tolerance.

The above method was programmed on the IBM/360 digital computer of The University of Tennessee and is used as a subroutine which provides the steady state boundary conditions needed for the dynamic calculation algorithm for Models C and D.

IV.6.3 Solution Using Logarithmic Mean Temperature Difference (LMTD)

In this method, the effective heat exchange region is divided into two sections, a subcooled section and a boiling section as seen in Figure IV.2. Each section has a parallel flow branch and a counterflow branch with a common secondary fluid passing outside the tubes.

The heat balance equations for the subcooled section are given by

$$\dot{Q}_{ps1} = W_p C_{p1}(T_{pi}-T_{pi}) = U_1 A_{s1}(LMTD)_{ps1} \qquad (IV.55)$$

$$\dot{Q}_{cs1} = W_p C_{p1}(T_{p4}-T_{po}) = U_1 A_{s1}(LMTD)_{cs1} \qquad (IV.56)$$

$$\dot{Q}_{ps1} + \dot{Q}_{cs1} = W_s(h_f-h_{si}) \qquad (IV.57)$$

where the logarithmic mean temperature difference in the parallel and counterflow branches of the subcooled section are given by[45]

$$(LMTD)_{ps1} = \frac{(T_{pi}-T_d) - (T_{p1}-T_{sat})}{\ln\left(\frac{T_{pi}-T_d}{T_{p1}-T_{sat}}\right)} \qquad (IV.58)$$

and

$$(LMTD)_{cs1} = \frac{(T_{p4}-T_{sat}) - (T_{po}-T_d)}{\ln\left(\frac{T_{p4}-T_{sat}}{T_{po}-T_d}\right)} . \qquad (IV.59)$$

In the boiling section, the heat balance equations are given by

$$\dot{Q}_{ps2} = W_p C_{p1}(T_{p1}-T_{pm}) = U_2 A_{s2}(LMTD)_{ps2} \qquad (IV.60)$$

$$\dot{Q}_{cs2} = W_p C_{pl}(T_{pm}-T_{p4}) = U_2 A_{s2}(LMTD)_{cs2} \tag{IV.61}$$

$$\dot{Q}_{ps2} + \dot{Q}_{cs2} = W_{sg} h_{fg}. \tag{IV.62}$$

Since the bulk mean temperature of the secondary fluid in the boiling section is equal to T_{sat}, the logarithmic mean temperature difference in the parallel and counterflow branches of the boiling section are given by

$$(LMTD)_{ps2} = \frac{(T_{pl} - T_{pm})}{\ln(\frac{T_{pm}-T_{sat}}{T_{pm}-T_{sat}})} \tag{IV.63}$$

$$(LMTD)_{cs2} = \frac{(T_{pm}-T_{p4})}{\ln(\frac{T_{pm}-T_{sat}}{T_{p4}-T_{sat}})}. \tag{IV.64}$$

where $T_{pm} = T_{p2} = T_{p3}$.

The above equations were programmed on the IBM/360 digital computer of The University of Tennessee. Either the finite difference of the log mean temperature difference method can be used to calculate the temperature and mass quality profiles in a UTSG. However, since the finite difference method can be easily implemented in the dynamic calculation algorithm, it was decided to use it in obtaining the results of the dynamic response calculations reported in the following section. A comparison between the two methods is given in the next section where the steady state results for H. B. Robinson Nuxlear Power Plant is presented.

IV.7 Results for H. B. Robinson Steam Generator

The primary and subcooled secondary temperature variation along the heat transfer path as well as the variation of the mass quality of the secondary fluid in the boiling region were calculated using the finite element method and the results are shown in Figure IV.3. The conditions describing the inlet and outlet of the subcooled and boiling sections are as follows.

A. Primary Side

T_{Pi} = 601.2 °F

T_{Pl} = 597.2 °F

T_{Pm} = 566.9 °F

T_{P4} = 548.1 °F

T_{Po} = 546.2 °F

B. Secondary Side

T_{d} = 500.6 °F

T_{sat} = 517 °F

x_{e} = 0.1993 (0.2 starting value)

L_{sl} = 3.966 ft.

When the LMTD method was used to obtain the subcooled/boiling lumps boundary conditions, the following results were obtained.

A. Primary Side

T_{Pi} = 602.1 °F

T_{Pl} = 597.33 °F

T_{Pm} = 567.06 °F

T_{P4} = 548.2 °F

T_{Po} = 546.2 °F

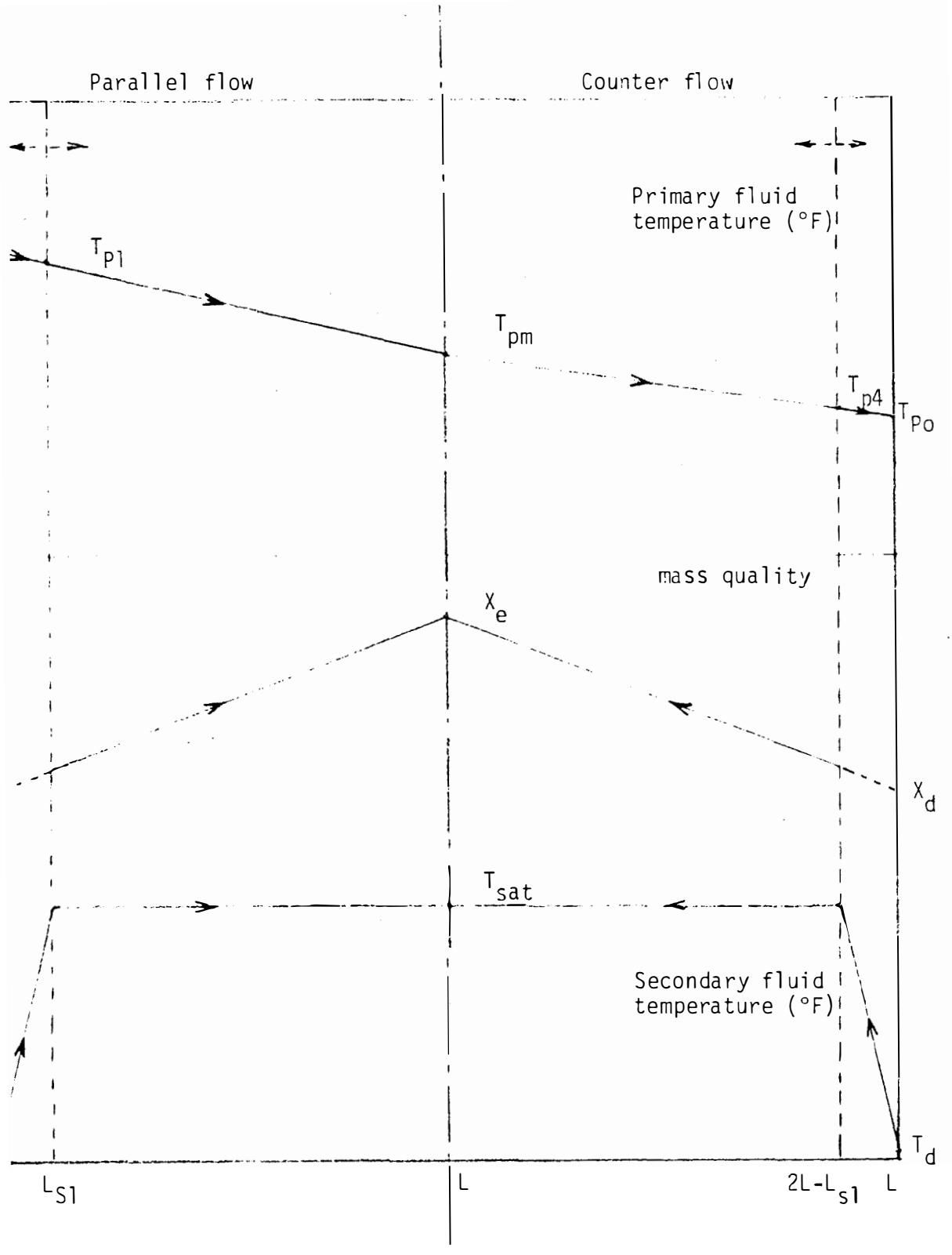

Figure IV. 3 Temperatures and Mass Quality Profiles Calculated by the Steady State Program.

B. Secondary Side

T_d = 500.6 °F

T_{sat} = 517 °F

X_e = 0.2

L_{sl} = 3.95 ft.

From the above results, we can see that the results obtained from the finite elements method or the LMTD method are in agreement to within 0.2% in the boundary temperature calculation and within 0.5% in estimating the subcooled length. It is noticed that the use of the finite element method resulted in a slight modification of the primary water average temperature.

IV.8 General Remarks on Dynamic Response Calculations

The following remarks are needed before presenting the results of the dynamic response calculations obtained from the UTSG mathematical models developed in Chapter III, page 25.

1. When the critical flow assumption was used to furnish the steam flow rate leaving the steam generator, the term δW_{so} was expressed by the following equation

$$\delta W_{so} = C_L \, \delta P + P \, \delta C_L . \qquad \text{(IV.65)}$$

2. There are two ways to handle the feedwater flow term, δW_{Fi}.

   a. Uncontrolled case. In this case δW_{Fi} is a forcing function (if the perturbation of interest is a feedwater flow perturbation), or δW_{Fi} is zero (no change in feedwater flow).

b. Perfect controller case. In this case, the feedwater flow rate is continuously set equal to the steam flow rate ($\delta W_{Fi} = \delta W_{so}$). For the case of the critical flow assumption, $\delta W_{Fi} = \delta W_{so} = C_L \delta P + P_o \delta C_L$. This means that terms involving δP now appear in the Λ matrix to represent this control assumption because of the $C_L \delta P$ term.

3. In obtaining the dynamic response from Model C, it was found necessary to remove the algebraic equation expressing δT_s in terms of δT_d and δP. Also, the equations are reordered in order to avoid the inversion of ill-conditioned matrices which may result in erroneous results from PUREDIFF.[37]

4. From the experience gained from Model C, it was found that combining the drum water volume with the downcomer lump and combining the evaporator/riser volume with the boiling secondary fluid lump in Model D reduces the order of the system equations from 20 to 18 and solves the problem of the inversion of ill-conditioned matrices in PUREDIFF.[37]

5. A complete summary of the dynamic response results as obtained from the mathematical models is given in Appendix F. In the following section, the step response results of the four models, to a +10% change in steam valve coefficient, are presented for the purpose of checking the physical plausibility of the mathematical development and comparing the model's capabilities.

IV.9 Dynamic Response Results

IV.9.1 Response of Model A

The nonzero elements of the A matrix and B matrix for Model A (using input data for H. B. Robinson steam generator) are given by:

A(1,1) = - 0.9783

A(1,2) = 0.6486

A(2,1) = 2.406

A(2,2) = -5.400

A(2,3) = 0.4342

A(3,2) = 1.651

A(3,3) = -0.2864

B(1,1) = 0.3296

B(3,2) = 0.05579

B(3,3) = -33.28.

The step response of Model A to a +10% change in steam valve coefficient is given in Figure IV.4. It shows a stable response with a time constant of approximately 15 seconds. It can be seen that the steam pressure shows the earliest response to the perturbation. This is to be expected since the steam valve perturbation is a secondary side perturbation. The primary outlet temperature response shows a slight delay of about 1.25 seconds. Then it starts to fall down following the decrease in the secondary side temperature caused by the pressure decay due to the steam valve perturbation.

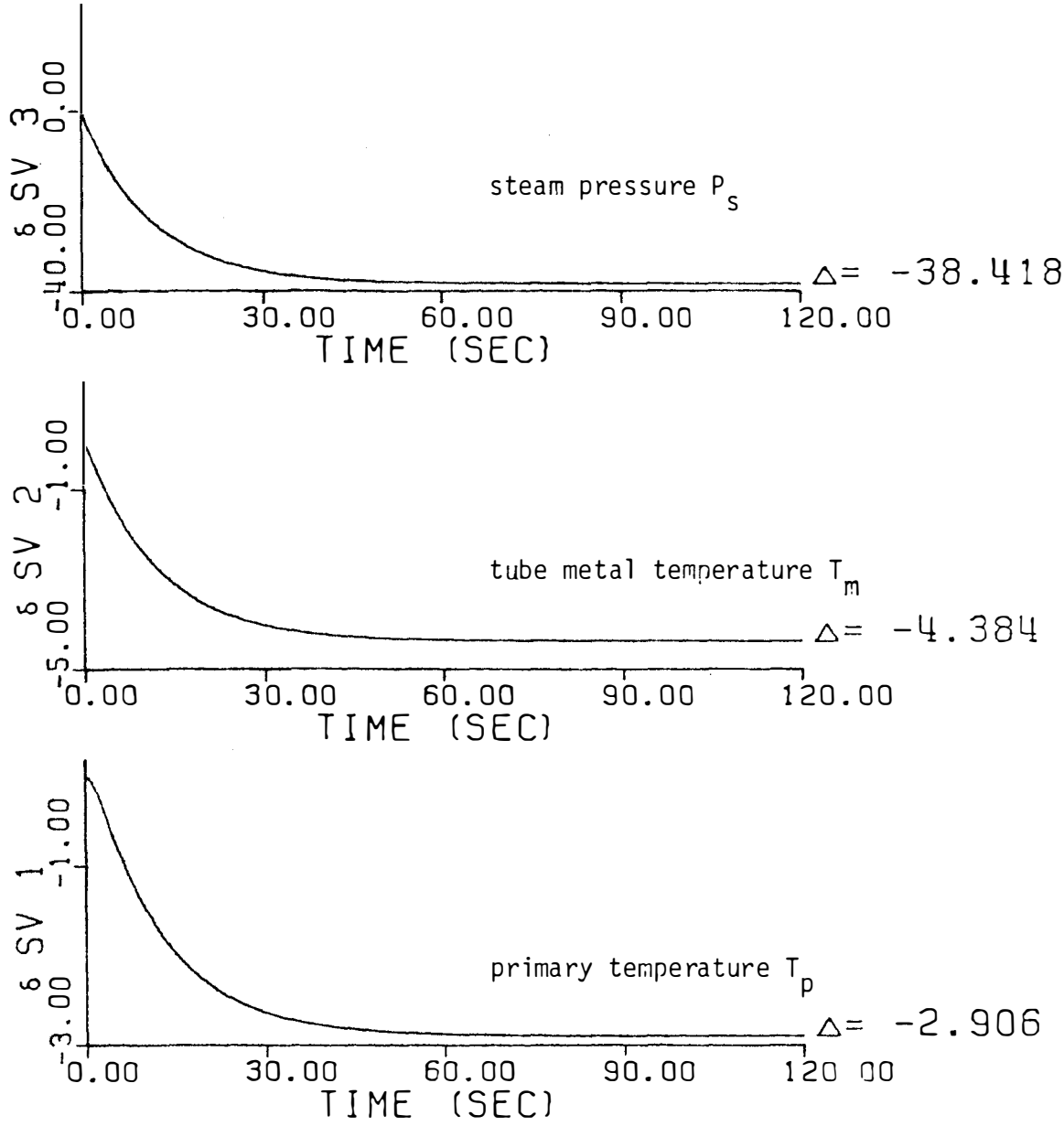

Figure IV.4 Step Response of Model A to +10% Change in Steam Valve Coefficient.

IV.9.2 Response of Model B

The nonzero elements of the coefficient matrices A and B for Model B (calculated using the H. B. Robinson steam generator data) are given by:

A(1,1) = -1.308

A(1,3) = 0.6486

A(2,1) = 0.6593

A(2,2) = -1.308

A(2,4) = 0.6486

A(3,1) = 2.406

A(3,3) = -5.400

A(3,5) = 0.4342

A(4,2) = 2.406

A(4,4) = -5.400

A(4,5) = 0.4342

A(5,3) = 0.8254

A(5,4) = 0.8254

A(5,5) = -0.2864

B(1,1) = 0.6593

B(5,2) = 0.0558

B(5,3) = -33.28

The response of Model B to +10% step change in steam valve coefficient is shown in Figure IV.5. The general trend of the response is similar to Model A except for the more delayed primary outlet temperature (about 2 seconds) and the slight change in the new steady state values. This change is the result of using two lumps to represent the primary water and tube metal instead of one lump as used in Model A.

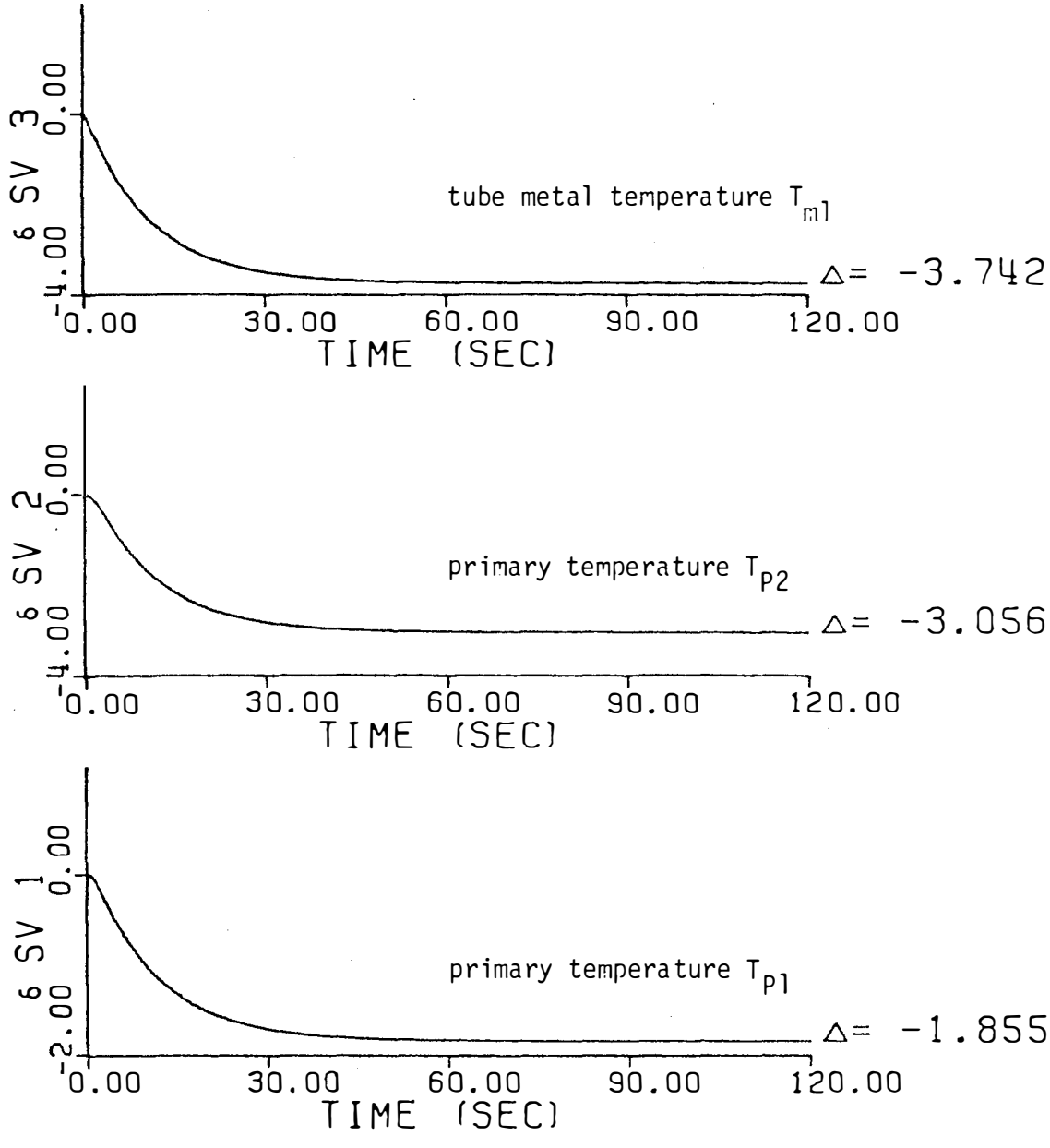

Figure IV.5 Step Response of Model B to +10% Change in Steam Valve Coefficient.

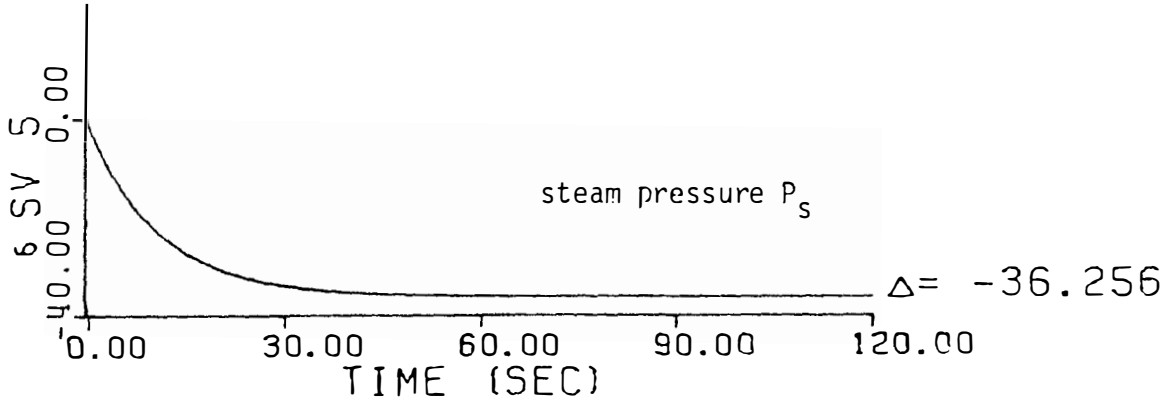

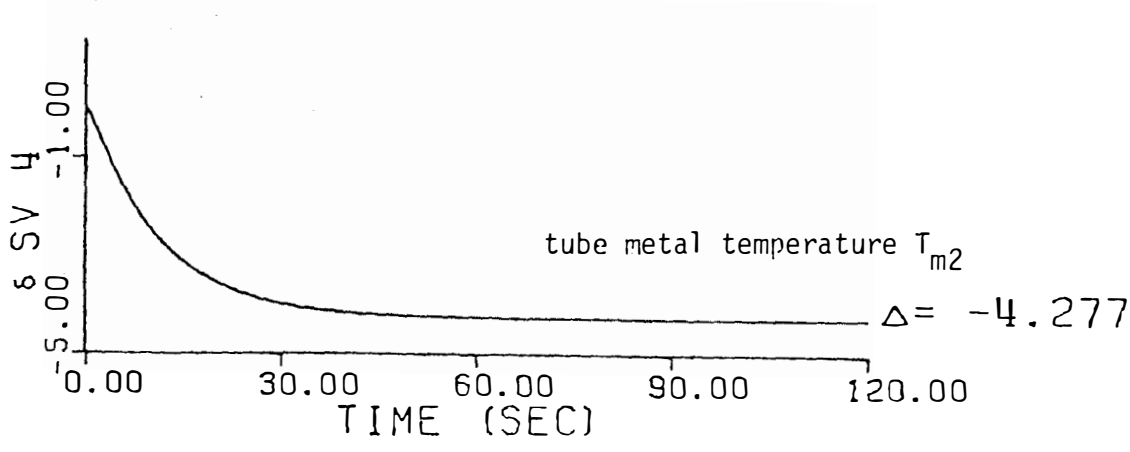

Figure IV.5 (Continued).

IV.9.3 Response of Model C

Since Model C was developed in the mixed algebraic plus differential formulation, there are two coefficient matrices, A_1 and A_2, to be calculated as input to PUREDIFF.[37] The nonzero elements of A_1 and A_2 are given in Table IV.2. The nonzero elements of the forcing vector for the case of +10% step change in the valve coefficient and assuming that the feedwater flow always matches the steam flow are given below

$f(6) = -89.06$

$f(8) = 89.06$

$f(9) = 7.967 \times 10^4$.

Note that the output from PUREDIFF is a 9x9 reduced matrix and a 9x1 forcing vector that is used by MATEXP to calculate the time response. This step is done within the dynamic response calculation algorithm without external interference. The results of the step response calculations are shown in Figure IV.6. It is noticed that the response of the primary and tube metal lumps are almost the same as in Model B. This is to be expected since the difference between Models B and C is only in the treatment of the secondary side.

For the secondary side lumps, it is noticed that the deviation of the steam pressure in the new steady state is about 4.5 psi less than for Model A and 2.4 psi less than Model B. This can be explained by the fact that in Models A and B, the secondary side temperature is assumed to be the saturation temperature. While in Model C, it is taken as a weighted average between the downcomer temperature and the saturation temperature.

TABLE IV.2

NONZERO ELEMENTS OF THE MATRICES A1 AND A2 FOR MODEL C

THE NONZERO ELEMENTS OF THE A1 MATRIX ARE:

1	1	0.1000E 01	2	2	0.1000E 01	3	3	0.1000E 01	4	4	0.1000E 01
5	5	0.2377E 05	5	6	-0.6456E 08	5	9	0.1415E 05	6	5	0.7687E 01
6	7	-0.1777E 03	7	9	0.1028E 05	8	7	0.4854E 04	9	7	0.4662E 07
9	8	0.4675E 05	10	5	0.1758E 02	10	6	-0.6558E 05	11	5	0.4057E 01

THE NONZERO ELEMENTS OF THE A2 MATRIX ARE:

1	1	0.1308E 01	1	3	-0.6490E 00	2	1	-0.6593E 00	2	2	0.1308E 01
2	4	-0.6490E 00	3	1	-0.2406E 01	3	3	0.5400E 01	3	5	-0.4053E 00
3	9	-0.1996E 00	4	2	-0.2406E 01	4	4	0.5400E 01	4	5	-0.4053E 00
4	9	-0.1996E 00	5	3	-0.1895E 05	5	4	-0.1895E 05	5	5	0.5753E 04
5	6	0.3069E 07	5	9	-0.2641E 04	5	10	-0.1114E 04	5	11	0.1270E 04
6	5	0.1132E 01	6	6	-0.4454E 04	6	12	-0.1993E 00	7	8	-0.4454E 04
7	9	0.4454E 04	8	5	-0.1132E 01	8	6	0.4454E 04	8	10	0.1000E 01
8	12	-0.8007E 00	9	5	-0.1529E 04	9	6	0.4351E 07	9	8	0.4454E 04
9	10	0.9604E 03	9	12	-0.7820E 03	10	10	-0.1000E 01	10	11	0.1000E 01
11	11	-0.1000E 01	11	12	0.1000E 01	12	5	0.7239E 00	12	6	-0.2689E 04
12	7	-0.8323E 02	12	10	0.1000E 01						

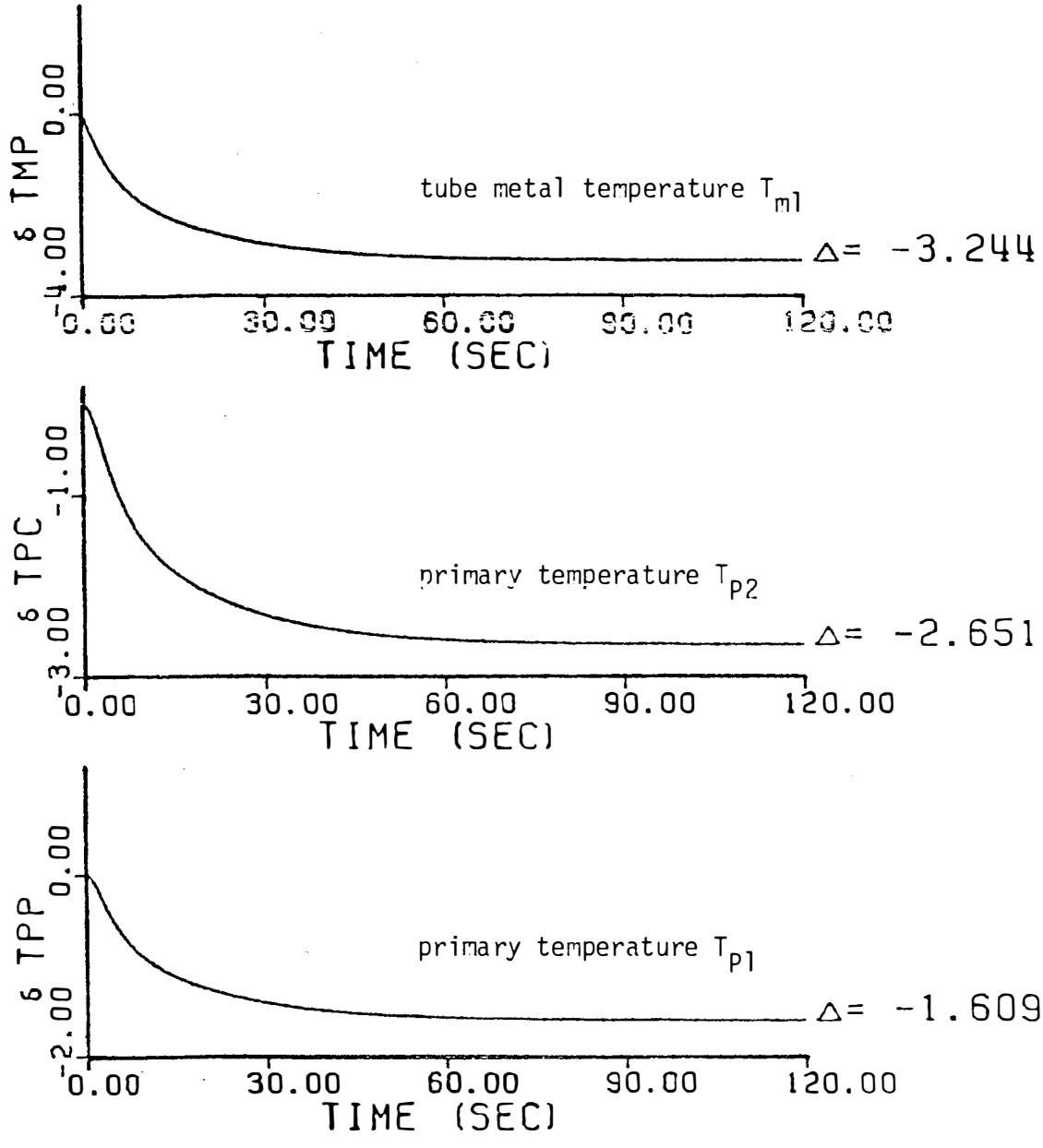

Figure IV.6 Step Response of Model C to +10% Change in Steam Valve Coefficient.

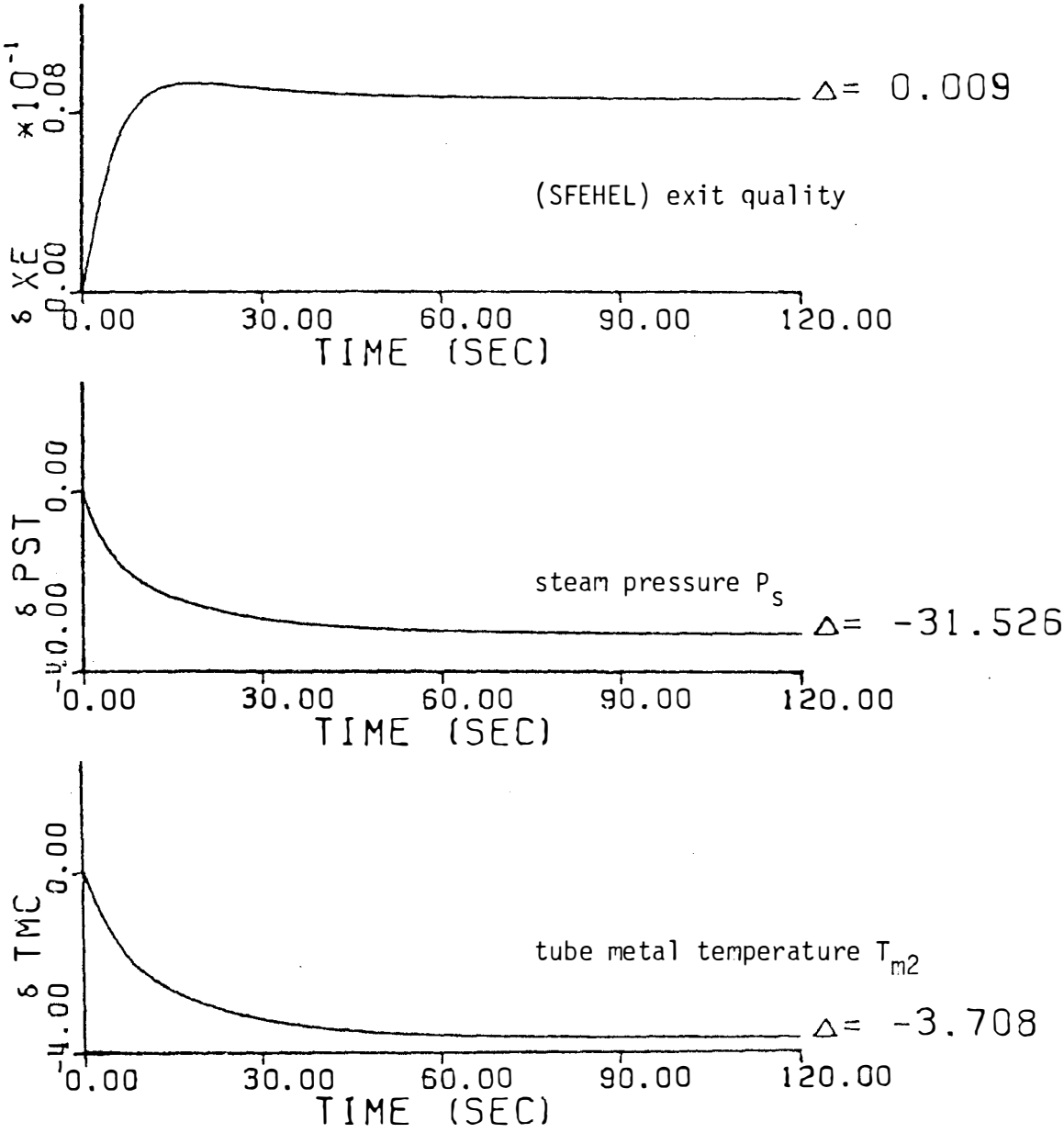

Figure IV.6 (Continued).

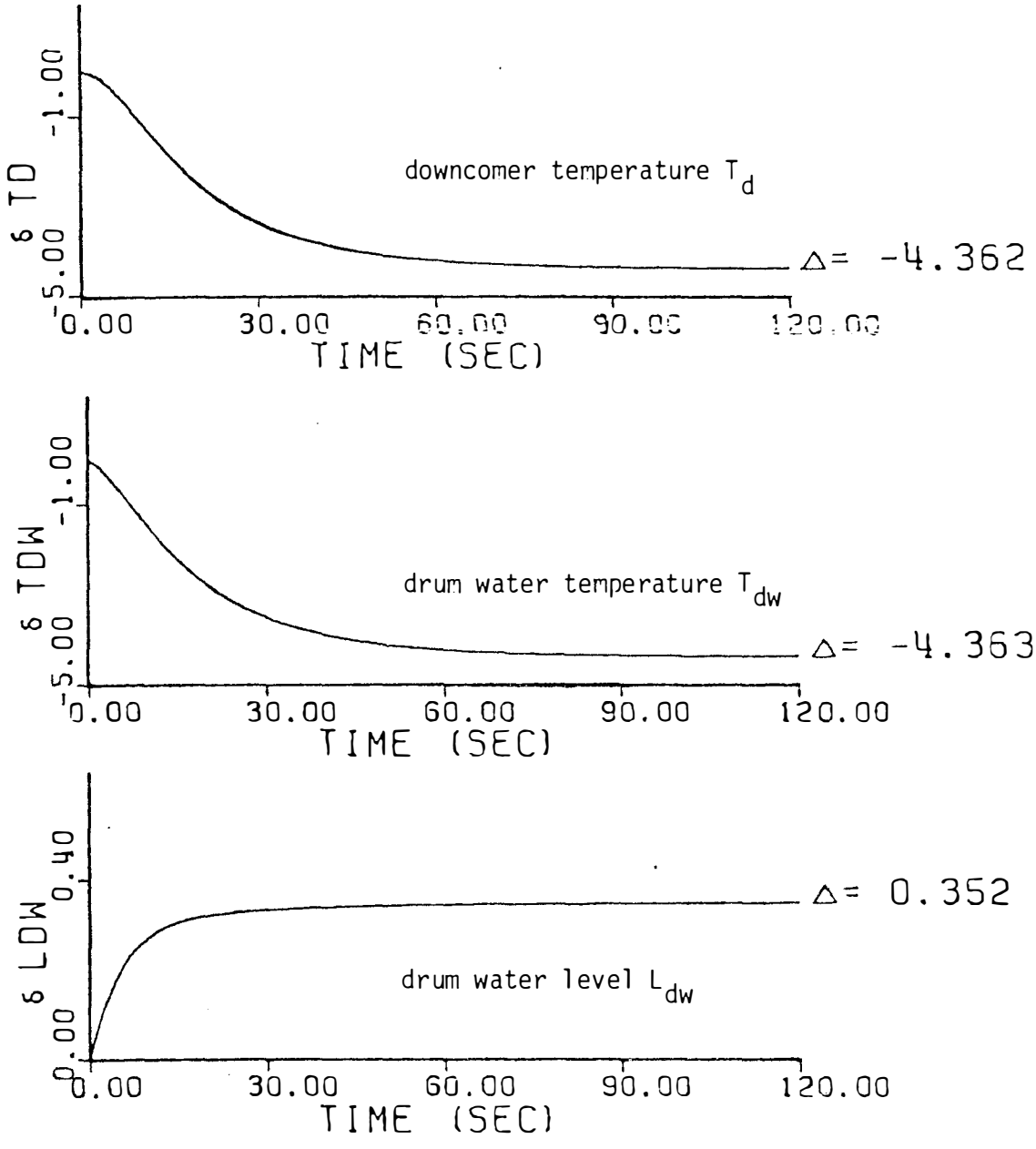

Figure IV.6 (Continued).

The increased exit quality at the end of the effective heat exchange lump can be explained by the reduction of the saturation temperature due to the pressure decrease. This causes more heat to be available for steam evaporation. The increase in the downcomer level and the decrease in downcomer temperature are due to the increase in feedwater flow into the steam generator to match the increase of steam flow rate due to the step change in the valve opening. The downcomer temperature lags behind the drum water temperature by about three seconds which is the transport time in the downcomer lump.

IV.9.4 Response of Model D

The nonzero elements of the coefficient matrices, A_1 and A_2, for Model D are given in Table IV.3. The nonzero elements of the forcing vector for a +10% step change in the steam valve coefficient are given by

f(11) = 0.0667

f(12) = 59.67

f(17) = -89.06.

The step response is shown in Figure IV.7. The primary inlet plenum has a zero response because it acts only as a mixing lump between the reactor hot leg temperature and the primary inlet temperature. The behavior of the primary temperature in the first primary lump T_{P1} looks different than the other primary lumps, This is due to the moving boundary that determines the length of the lump. A look at the response of the subcooled length

TABLE IV.3

NONZERO ELEMENTS OF THE MATRICES A1 AND A2 FOR MODEL D

THE NONZERO ELEMENTS OF THE A1 MATRIX ARE:

1	1	0.1000E 01	2	2	0.1000E 01	3	3	0.1000E 01	3	12	0.1174E 01
4	4	0.1000E 01	5	5	0.1000E 01	5	12	-0.5065E 00	6	6	0.1000E 01
7	7	0.1000E 01	7	12	0.2059E 01	8	8	0.1000E 01	8	12	0.3167E 00
9	9	0.1000E 01	9	12	-0.7084E-01	10	10	0.1000E 01	10	12	-0.4605E 00
11	11	0.1000E 01	12	11	0.9604E 03	12	15	0.4024E 02	13	12	0.1000E 01
14	12	0.2854E 07	14	13	0.8475E 03	14	15	0.5845E 04	15	12	0.7010E 03
15	13	-0.1758E 02	15	14	0.6558E 05	16	12	-0.8423E 06	16	13	0.2401E 05
16	14	-0.7258E 08	17	11	-0.4890E 02	17	13	0.7687E 01			

THE NONZERO ELEMENTS OF THE A2 MATRIX ARE:

1	1	0.1431E 01	2	1	-0.4945E 01	2	2	0.5593E 01	2	7	-0.6486E 00
2	12	0.6001E 01	3	2	-0.7607E 00	3	3	0.1409E 01	3	8	-0.6486E 00
3	12	-0.8928E 00	4	3	-0.7607E 00	4	4	0.1409E 01	4	9	-0.6486E 00
4	12	-0.5554E 00	5	4	-0.4945E 01	5	5	0.5593E 01	5	10	-0.6486E 00
5	12	0.2504E 01	6	5	-0.1431E 01	6	6	0.1431E 01	7	2	-0.2406E 01
7	7	0.3871E 01	7	13	-0.1062E 00	7	15	-0.7325E 00	8	3	-0.2406E 01
8	8	0.5400E 01	8	13	-0.4342E 00	9	4	-0.2406E 01	9	9	0.5400E 01
9	13	-0.4342E 00	10	5	-0.2406E 01	10	10	0.3871E 01	10	13	-0.1062E 00
10	15	-0.7325E 00	11	13	-0.8472E-03	11	14	0.3335E 01	11	16	0.7487E-03
11	18	-0.5995E-03	12	13	-0.1145E 01	12	14	0.3258E 04	12	15	0.3335E 01
12	16	0.7190E 00	12	18	-0.5855E 00	13	16	-0.3936E-03	13	17	0.3936E-03
14	7	-0.9939E 03	14	10	-0.9939E 03	14	12	-0.1930E 05	14	13	0.8934E 03
14	15	-0.4173E 04	14	16	-0.1114E 04	14	17	0.1133E 04	15	17	0.1000E 01
15	18	-0.1000E 01	16	8	-0.1320E 05	16	9	-0.1320E 05	16	12	0.2459E 05
16	13	0.3652E 04	16	14	0.3069E 07	16	17	-0.1133E 04	16	18	0.1270E 04
17	13	0.1132E 01	17	14	-0.4455E 04	17	18	-0.1993E 00	18	11	0.7638E 02
18	12	-0.5531E 02	18	13	-0.5284E 00	18	14	0.1972E 04	18	16	-0.1000E 01

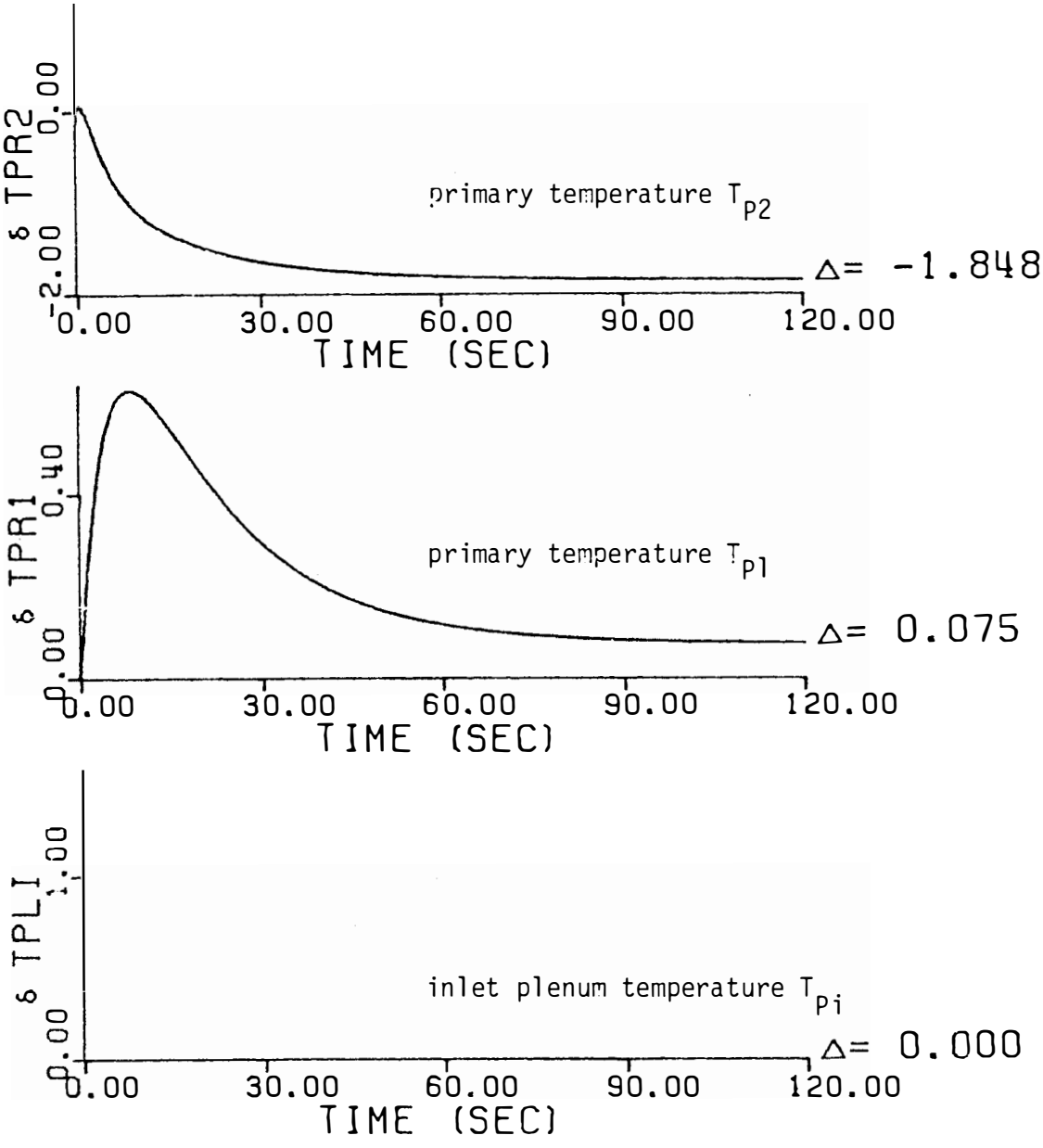

Figure IV.7 Step Response of Model D to +10% Change in Steam Valve Coefficient.

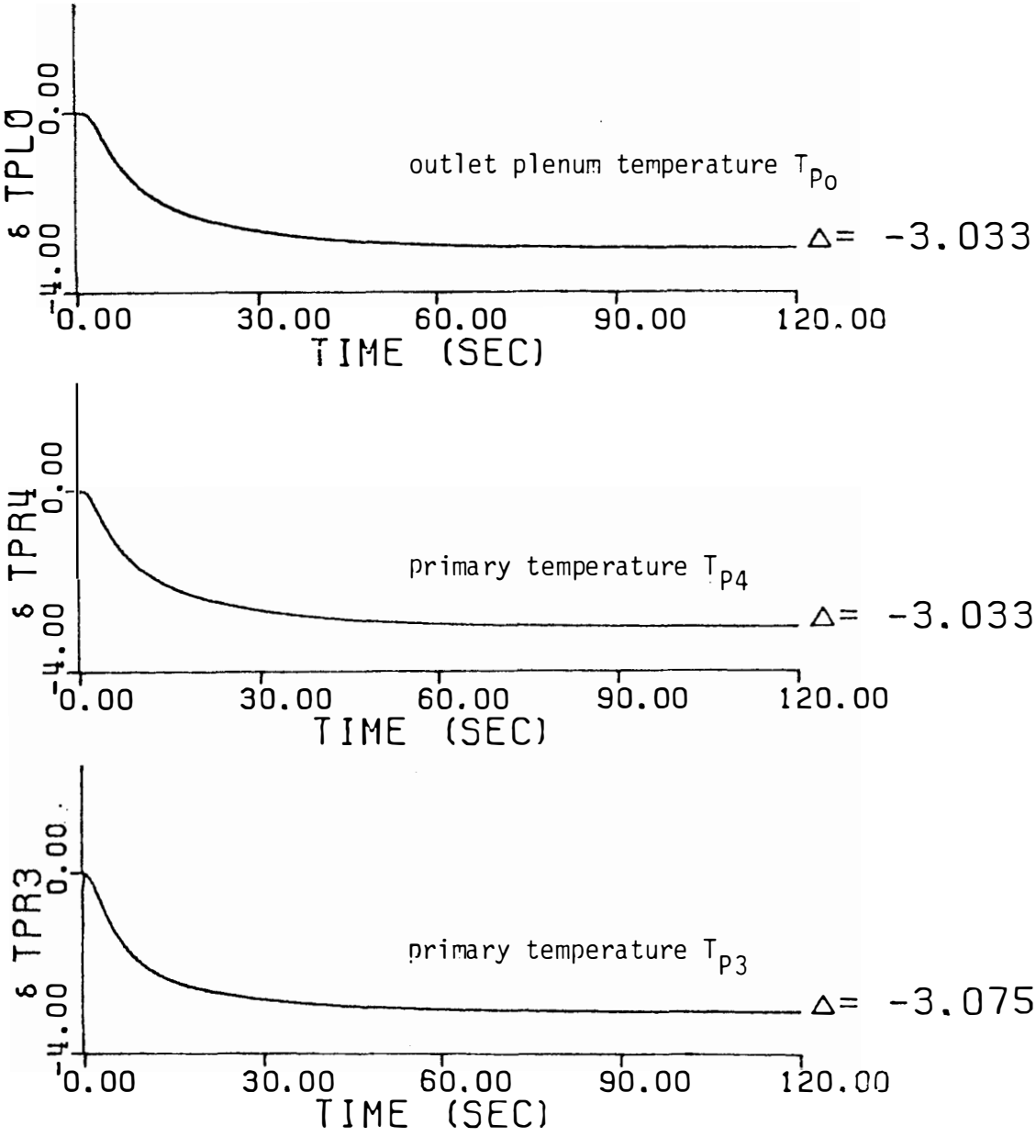

Figure IV.7 (Continued).

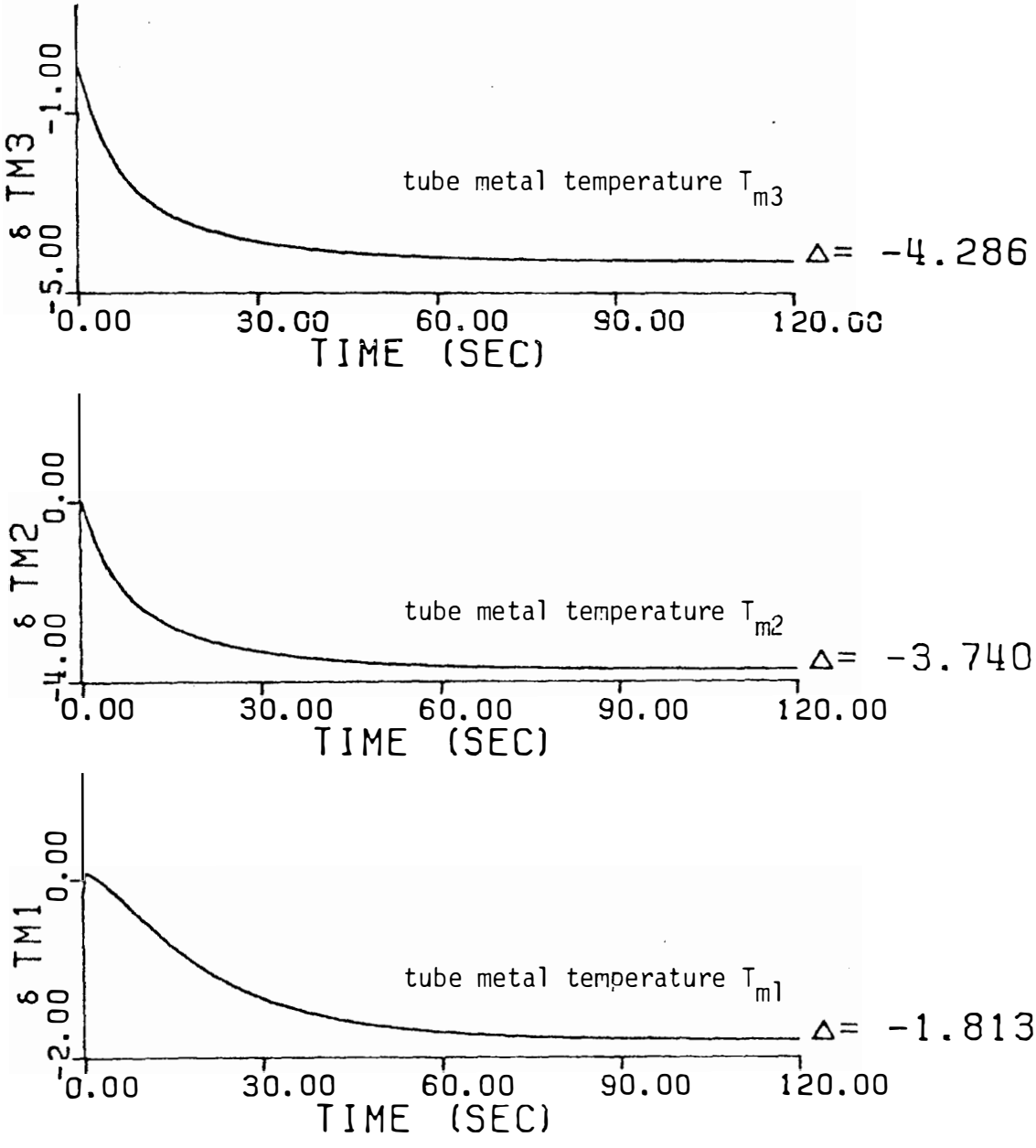

Figure IV.7 (Continued).

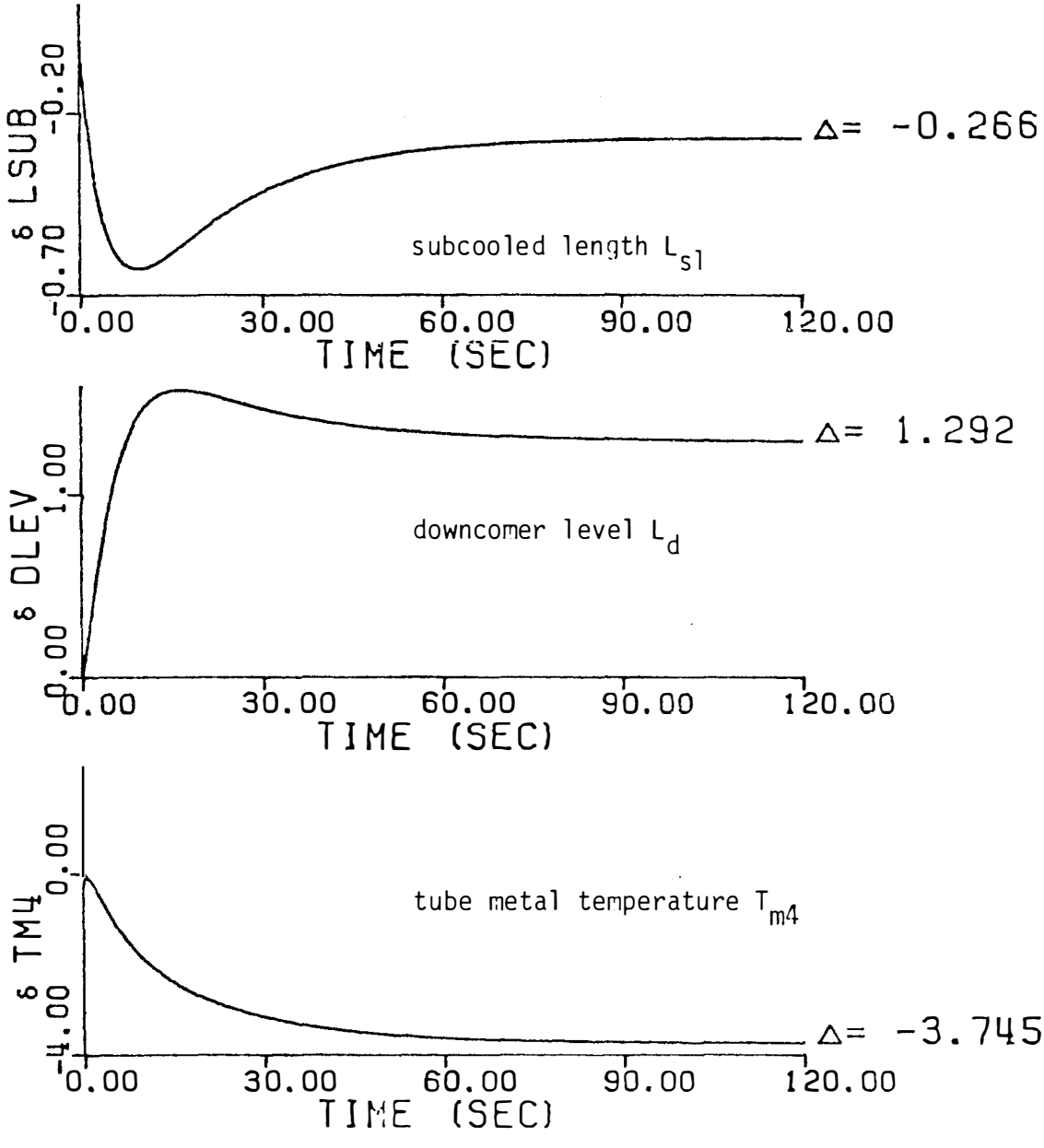

Figure IV.7 (Continued).

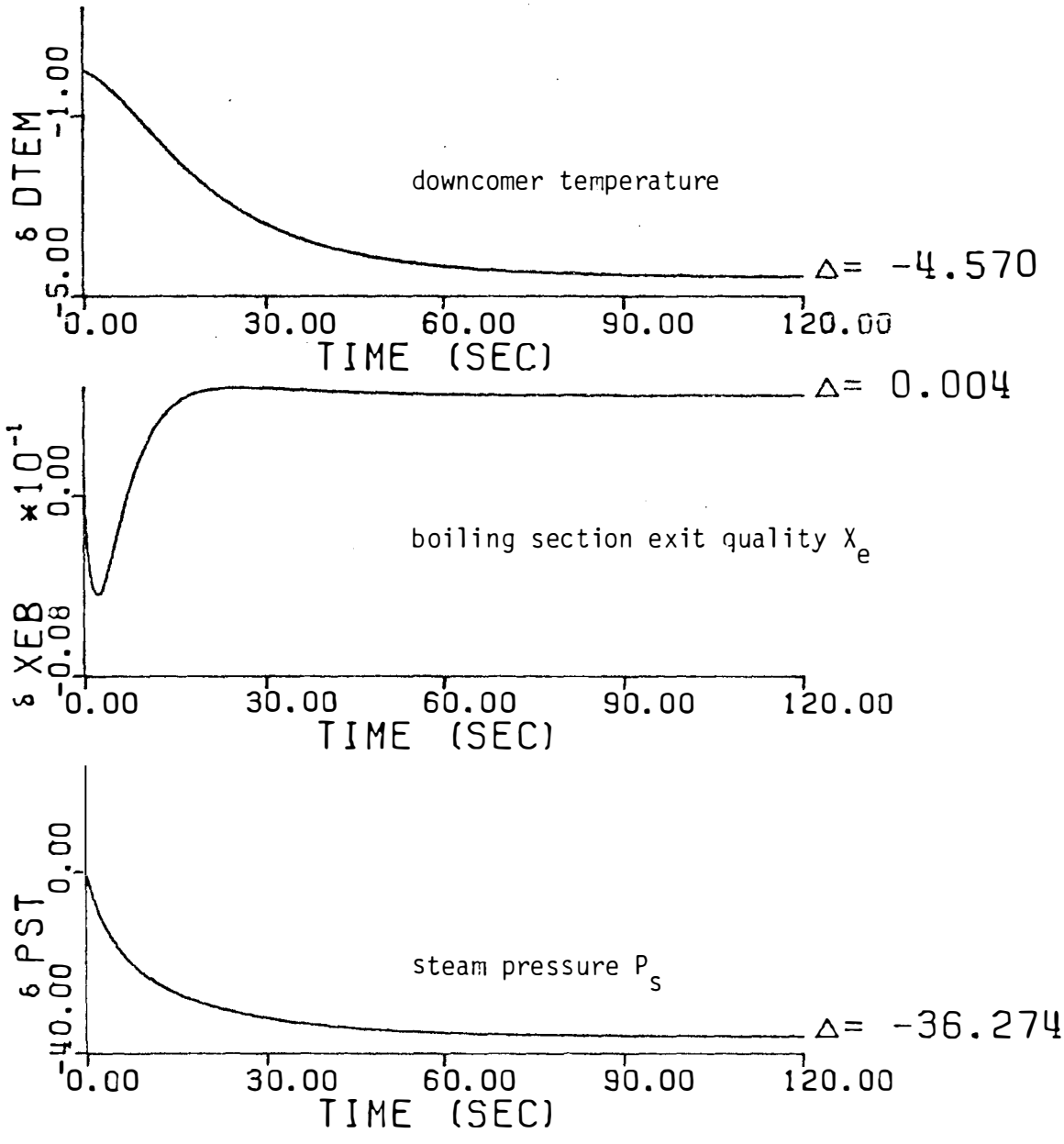

Figure IV.7 (Continued).

shows a sharp drop then a gradual increase until it settles at a lower level at the new steady state. The downcomer level and the downcomer temperature behave in a similar way as in Model C.

IV.9.5 Comparison of Models Responses

Since each dynamic model has state variables to represent different sections of the system, a one-to-one correspondence for comparing the results obtained from the four models is not possible. The only two state variables that are common to all four models are the primary outlet temperature (T_{Po}) and the steam pressure (P_s). A comparison of these two state variables to a +10% change in the steam valve coefficient is shown in Figure IV.8. In Model D, the primary outlet temperature is taken as the temperature of the last primary lump (P_4) since the inlet and outlet plenum lumps were not considered in the other models.

Referring to Figure IV.8, it can be seen that the response of the primary outlet temperature and the steam pressure is consistent for all four models. The maximum deviation in the new steady state for the primary outlet temperature is less than 0.5°F and for the steam pressure is less than 8 psi. This shows the lumped nature of the UTSG. The difference in response between Models A and B is due to the use of the backward differencing with a single primary lump for Model A and two primary lumps for Model B. The difference in response between Models C and D is due to the assumption of a fixed boundary between the subcooled and the boiling sections of the effective heat exchange lump in Model C while a moving boundary is considered for Model D.

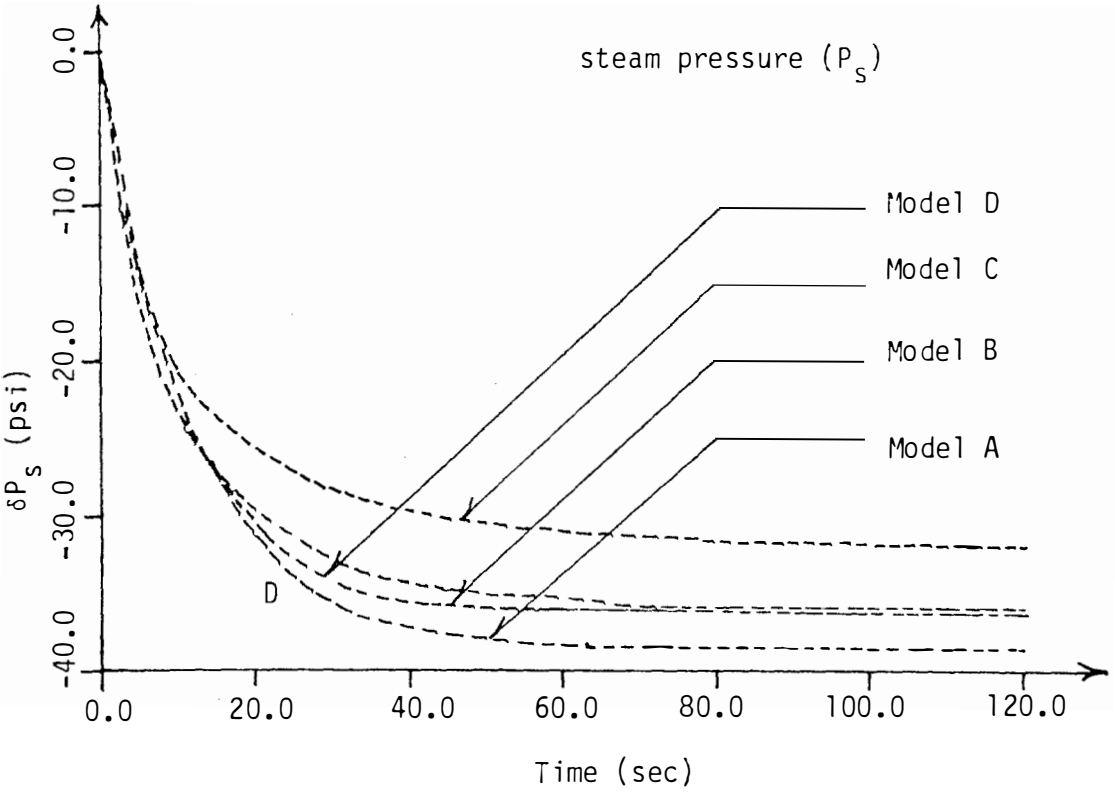

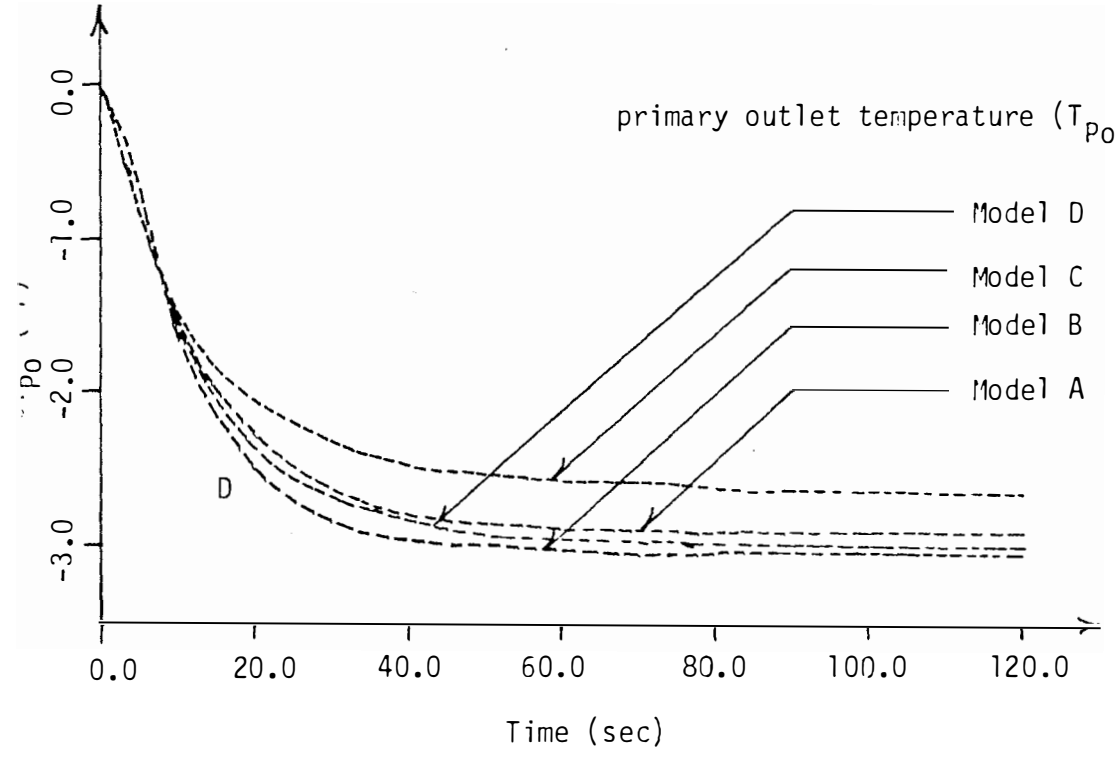

Figure IV.8 Comparison of T_{Po} and P_s Responses in the Four Models.

CHAPTER V

COMPARISON OF DETAILED MODEL PREDICTIONS WITH EXPERIMENTAL RESULTS

V.I Introduction

A mathematical model of an engineering system is as good as its capability of predicting the dynamic response of the actual system. Therefore, the comparison between theoretical model predictions and experimental results is the best method for testing the adequacy of the dynamic simulation models of an engineering system.

In Chapter IV, page 106, the mathematical models developed in Chapter III, page 25, were applied to simulate the step response and frequency response of a UTSG with a perfect feedwater controller. In this chapter, the end product UTSG model (Model D) is coupled with a model for a pressurized water reactor,[3,4] and the frequency response of the combined system is compared with the experimental results obtained from dynamic tests performed on the H. B. Robinson nuclear power plant.[5] The objective of the comparison is to check the adequacy of the UTSG model.

V.2 Description of the System

The Nuclear Steam Supply System (NSSS) of the H. B. Robinson Nuclear Power Plant[2] is a three-loop 2200 MWt (739 MWe) Westinghouse PWR system owned and operated by Carolina Power and Light Company. Each loop includes a vertical UTSG. The dynamic tests were performed during full power operation using normal plant equipment to measure

system responses at several locations of the loop as shown in Figure V.1. The dynamic tests involved the perturbation of reactivity and steam demand using multifrequency binary signals[4] and monitoring the system outputs at the junction box where the signals enter the plant computer.

V.3 PWR Model[3]

The reactor power was modeled using the point kinetics equations with six groups of delayed neutrons and reactivity feedbacks due to changes in fuel temperature, coolant/moderator temperature and primary coolant system pressure. The core heat transfer model used a nodal approximation for fuel and coolant temperature. Each axial section included a fuel temperature node and two coolant temperature nodes. This formulation was used to obtain a good approximation to the average coolant temperature. The reactor lower and upper plenums and the piping between the reactor and steam generator were modeled to account for the transport time delays between the reactor core and steam generator. The reactor model used for coupling with the detailed steam generator model (Model D) consists of fourteen first order differential equations that can be expressed in the form

$$\frac{d\bar{x}}{dt} = A\bar{x} + \bar{f}(t) \qquad (V.1)$$

where $\bar{x}$ and $\bar{f}(t)$ are the state variables and forcing vectors respectively and A is the coefficient matrix. The definitions of the state variables used in the reactor model are given in Table V.1. The nonzero elements of the A matrix and the forcing vector $\bar{f}$ as obtained from Reference 3 are given in Tables V.2 and V.3, respectively.

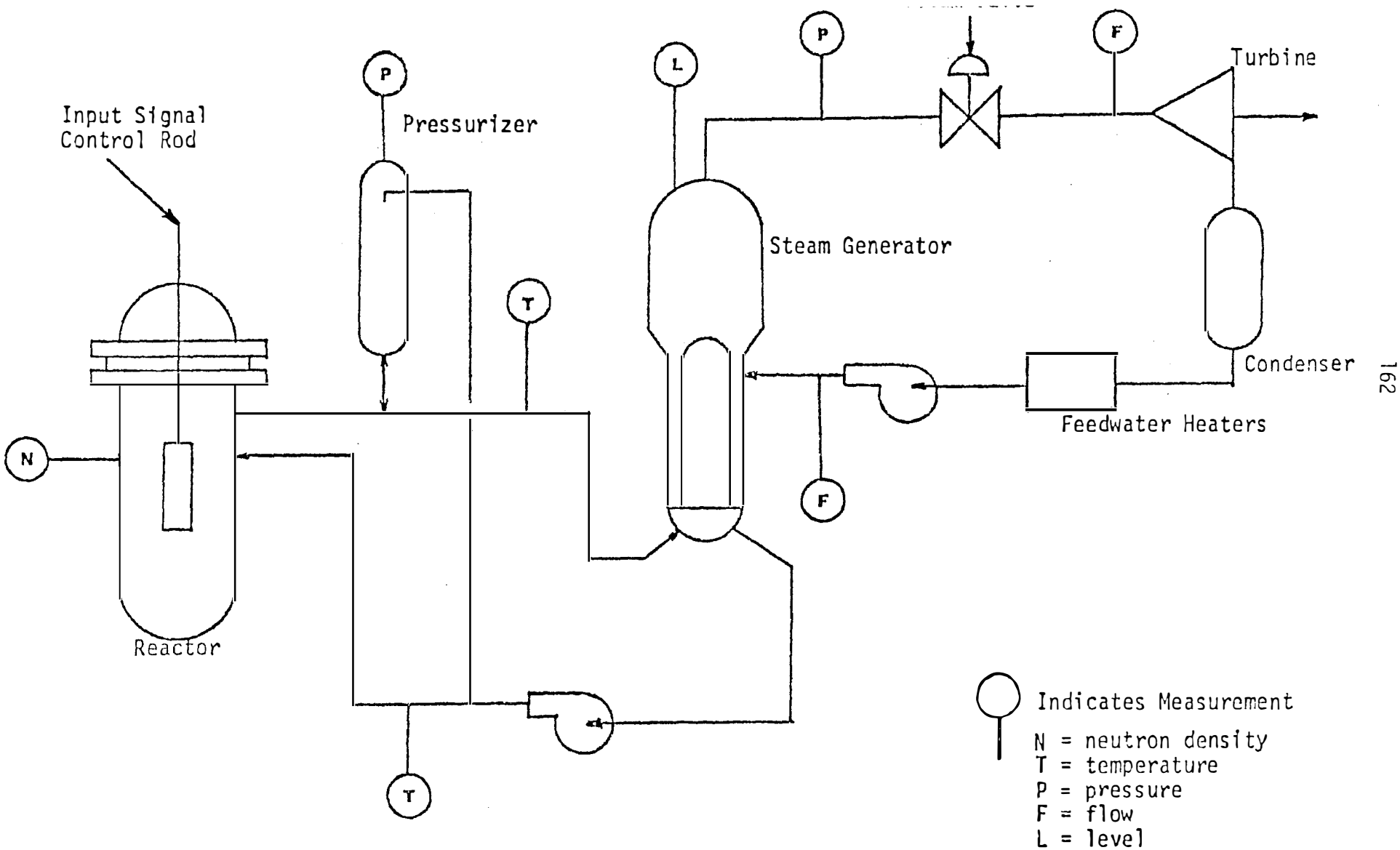

Figure V.1 Schematic of the H. B. Robinson Plant.

TABLE V.1

DEFINITION OF THE STATE VARIABLES USED IN THE REACTOR MODEL

State Variable Number	Symbol	Definitions
1	$\delta P/P_o$	δP = deviation in reactor power
2	$\delta C_1/P_o$	P_o = steady state reactor power
3	$\delta C_2/P_o$	δC_i = deviation in precursor concentration of group i, i=1, 2,...,6
4	$\delta C_3/P_o$	δT_f = deviation in fuel temperature
5	$\delta C_4/P_o$	δT_{C1} = deviation in reactor coolant temperature of the first coolant lump
6	$\delta C_5/P_o$	
7	$\delta C_6/P_o$	δT_{C2} = deviation in reactor coolant temperature of the second reactor coolant lump
8	δT_f	
9	δT_{C1}	δT_{UP} = deviation in reactor upper plenum temperature
10	δT_{C2}	
11	δT_{UP}	δT_{HL} = deviation in reactor hot leg temperature
12	δT_{LP}	δT_{CL} = deviation in reactor cold leg temperature
13	δT_{HL}*	
14	δT_{CL}**	δT_{LP} = deviation in reactor lower plenum temperature

*To be coupled with steam generator primary inlet plenum.

**To be coupled with steam generator primary outlet plenum.

TABLE V.2

NONZERO ELEMENTS OF THE A MATRIX FOR THE REACTOR MODEL[3]

Row Number	Column Number	Element Value
1	1	-400.0
1	2	0.0125
1	3	0.0305
1	4	0.1110
1	5	0.3010
1	6	1.140
1	7	3.01
1	8	-0.8095
1	9	-6.227
1	10	-6.227
2	1	13.125
2	2	-0.0125
3	1	87.50
3	3	-0.0305
4	1	78.130
4	4	-0.1110
5	1	158.10
5	5	-0.301
6	1	46.25
6	6	-1.140
7	1	16.88

TABLE V.2 (Continued)

Row Number	Column Number	Element Value
7	7	-3.01
8	1	166.30
8	8	-0.1647
8	9	0.1647
9	8	0.05707
9	9	-2.440
9	12	2.383
10	8	0.05707
10	9	2.326
10	10	-2.383
11	10	0.3365
11	11	-0.3365
12	12	-0.516
12	14	0.516
13	11	2.500
13	13	-2.500
14	14	-1.48

TABLE V.3

NONZERO ELEMENTS OF THE FORCING VECTOR
FOR THE REACTOR MODEL

$f(1) = 400.0$

V.4 Coupling of Reactor and Steam Generator Models

Figure V.2 shows a schematic of the reactor and steam generator lumps used in the dynamic models. It can be seen that the output from the reactor hot leg lump feeds into the steam generator primary inlet plenum and the output from the steam generator primary outlet plenum feeds into the reactor cold leg lump. This constitutes the coupling mechanism between the reactor model and the steam generator model. The steam generator model used for coupling with the reactor model is the reduced version of Model D. It was obtained as an output from the PUREDIFF[37] computer program when the mixed differential and algebraic equations described in Section III.7, page 74, are used as input. The mixed algebraic and differential form of the model consists of eighteen differential and algebraic equations involving fifteen differential variables and three algebraic variables as shown in Table V.4. After eliminating the algebraic variables in PUREDIFF, the model is reduced to fifteen first order differential equations involving the first fifteen variables in Table V.4. The state variables involved in the coupling with the reactor model are marked with the superscript "c". The combined reactor-steam generator model can be expressed in the form given in Equation (V.1), page 161, when in this case $\bar{x}$ is a (29x1) state variable vector where the first 14 elements are the reactor variables described in Table V.1 and the next 15 elements are the steam generator differential variables given in Table V.4.

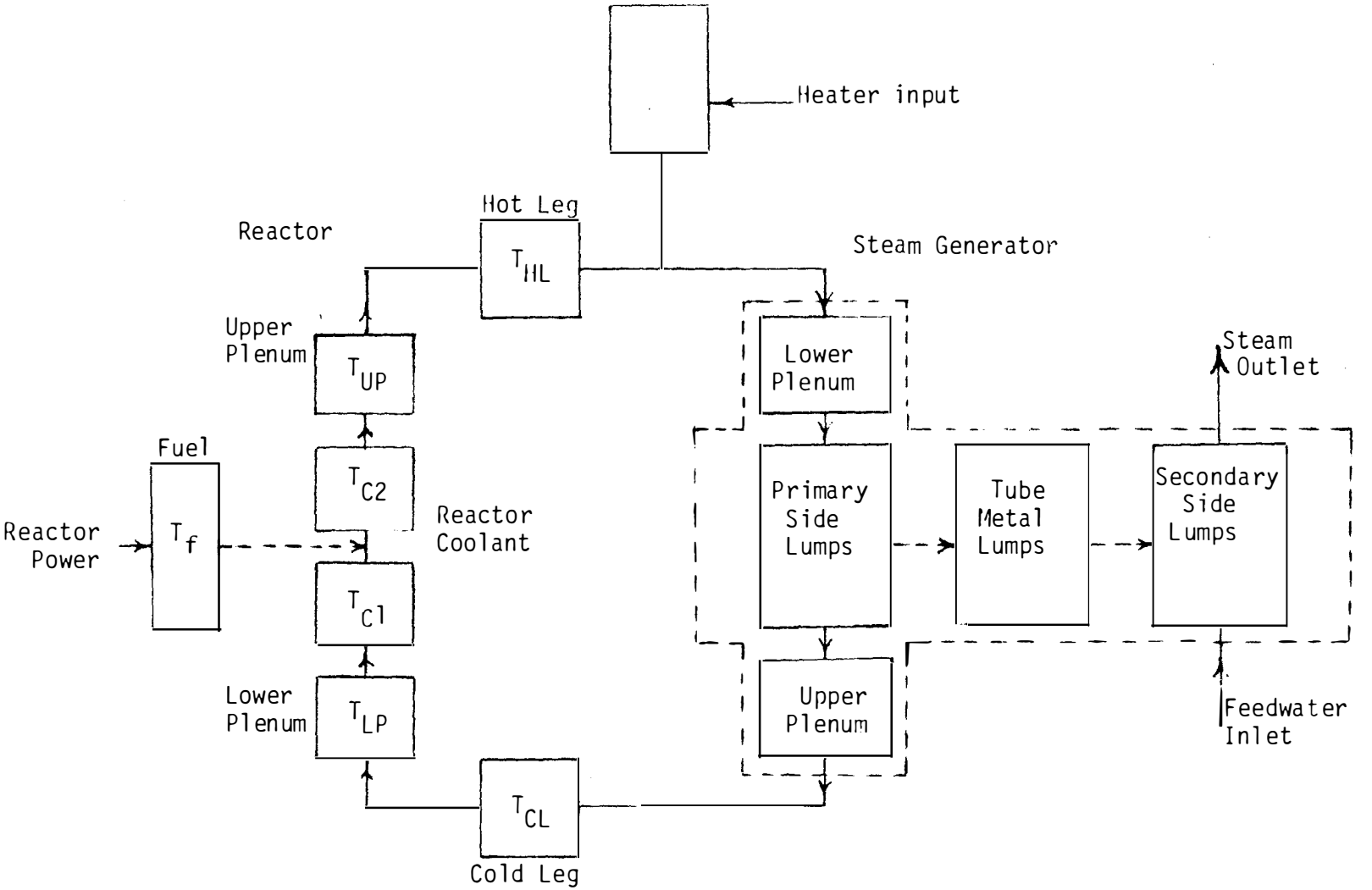

Figure V.2 Lumped Structure for a PWR System Model.

TABLE V.4

SYSTEM VARIABLES FOR THE STEAM GENERATOR MODEL

1.	T_{Pi}^{C}	:	primary water inlet plenum temperature
2.	T_{P1}	:	first primary water lump temperature
3.	T_{P2}	:	second primary water lump temperature
4.	T_{P3}	:	third primary water lump temperature
5.	T_{P4}	:	fourth primary water lump temperature
6.	T_{PO}^{C}	:	primary water outlet plenum temperature
7.	T_{m1}	:	first tube metal lump temperature
8.	T_{m2}	:	second tube metal lump temperature
9.	T_{m3}	:	third tube metal lump temperature
10.	T_{m4}	:	fourth tube metal lump temperature
11.	L_d	:	downcomer level
12.	L_{s1}	:	nonboiling (subcooled) length
13.	P_s	:	steam pressure
14.	x_e	:	boiling section exit quality
15.	T_d	:	downcomer temperature
*16.	W_1	:	flow rate to the nonboiling section
*17.	W_2	:	flow rate to the boiling section
*18.	W_3	:	flow rate from the boiling section

*Algebraic variables.

V.5 Results

The frequency response of the combined reactor steam generator model was calculated for two perturbations, a reactor side reactivity perturbation and a steam generator side steam flow perturbation, using the SFR-3 code.[40] The forcing vector for the reactivity perturbation has only one nonzero element as given in Table V.3. For the steam flow perturbation, the forcing vector was obtained from the time response analysis of the steam generator model and the nonzero elements are given in Table V.5.

Figures V.3 and V.4 show the frequency response of reactor power and steam generator pressure for the reactivity perturbation and Figures V.5 through V.7 show the frequency response of reactor power, cold leg temperature and steam pressure for the steam valve perturbation.

For the reactivity perturbation, it was found that the agreement between the theoretical model predictions and the experimental results in the lower frequency range depends on the value of the moderator coefficient of reactivity (α_c). The theoretical response was calculated for two values of α_c, the reference value (α_{cr}) used by Kerlin et al.[5] and 60% of this reference value. It can be seen from Figure V.3 that the agreement between the theoretical model response and the experimental results is better for the smaller α_c, especially in the lower frequency range. Clearly, one would need a better value of α_c than was available for this work to permit conclusive comparisons of theory and experiment at low frequencies. The following comments on the comparison with test results are in order.

TABLE V.5

FORCING FUNCTION FOR STEAM VALVE PERTURBATION
(+10% Change in Steam Flow Rate)

f(17) = 2.697999E-01
f(19) = -1.163999E-01
f(21) = 4.732000E-01
f(22) = 7.279998E-02
f(23) = -1.628000E-02
f(24) = -1.058000E-01
f(25) = 1.681000E-01
f(26) = -2.298000E-01
f(27) = -6.072000E-00
f(28) = -5.488999E-03
f(29) = -6.673998E-02

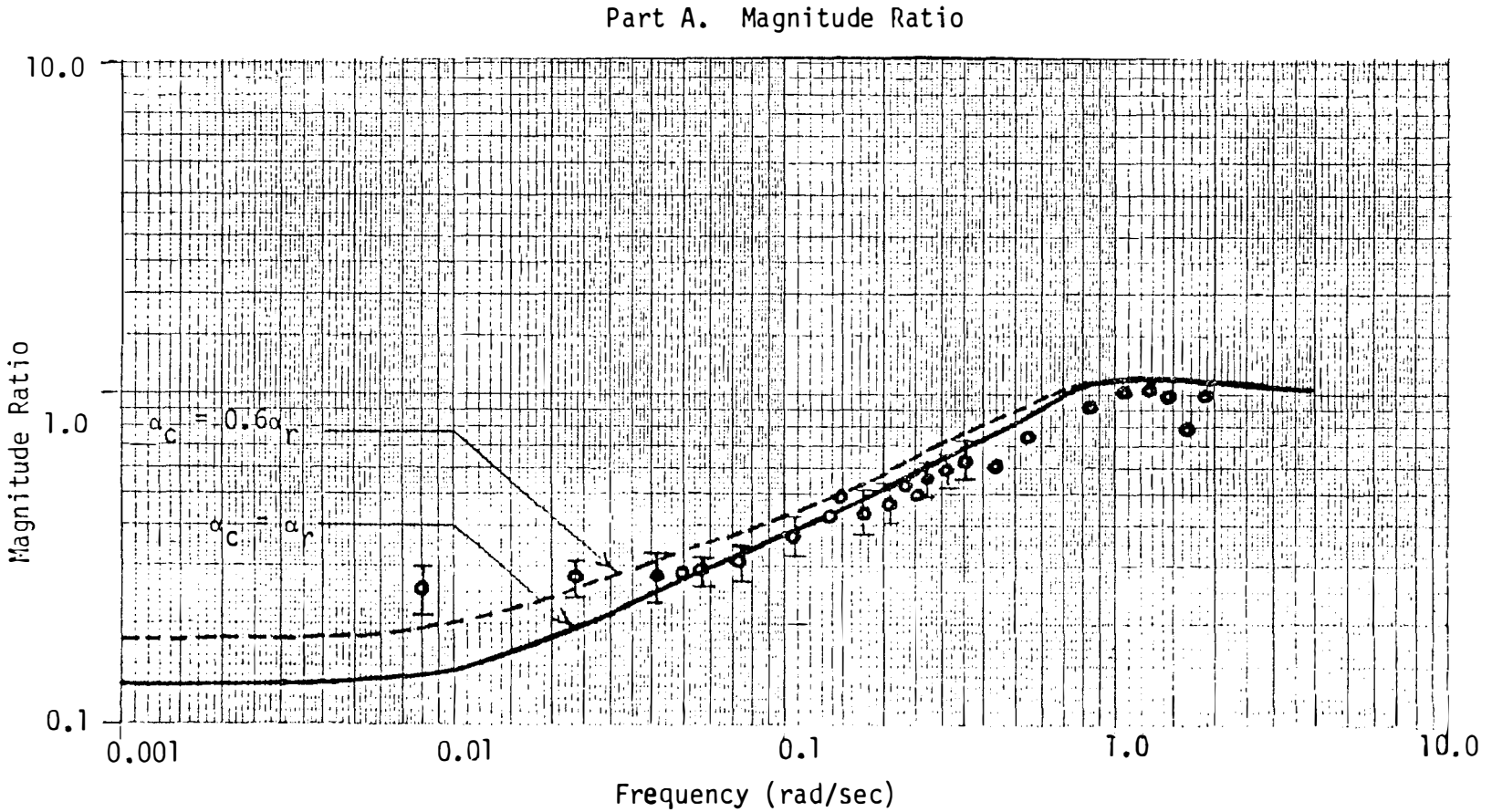

Figure V.3 Reactor Power/Reactivity ($\delta P/P_o/\delta\rho$) Frequency Response.

Part B. Phase

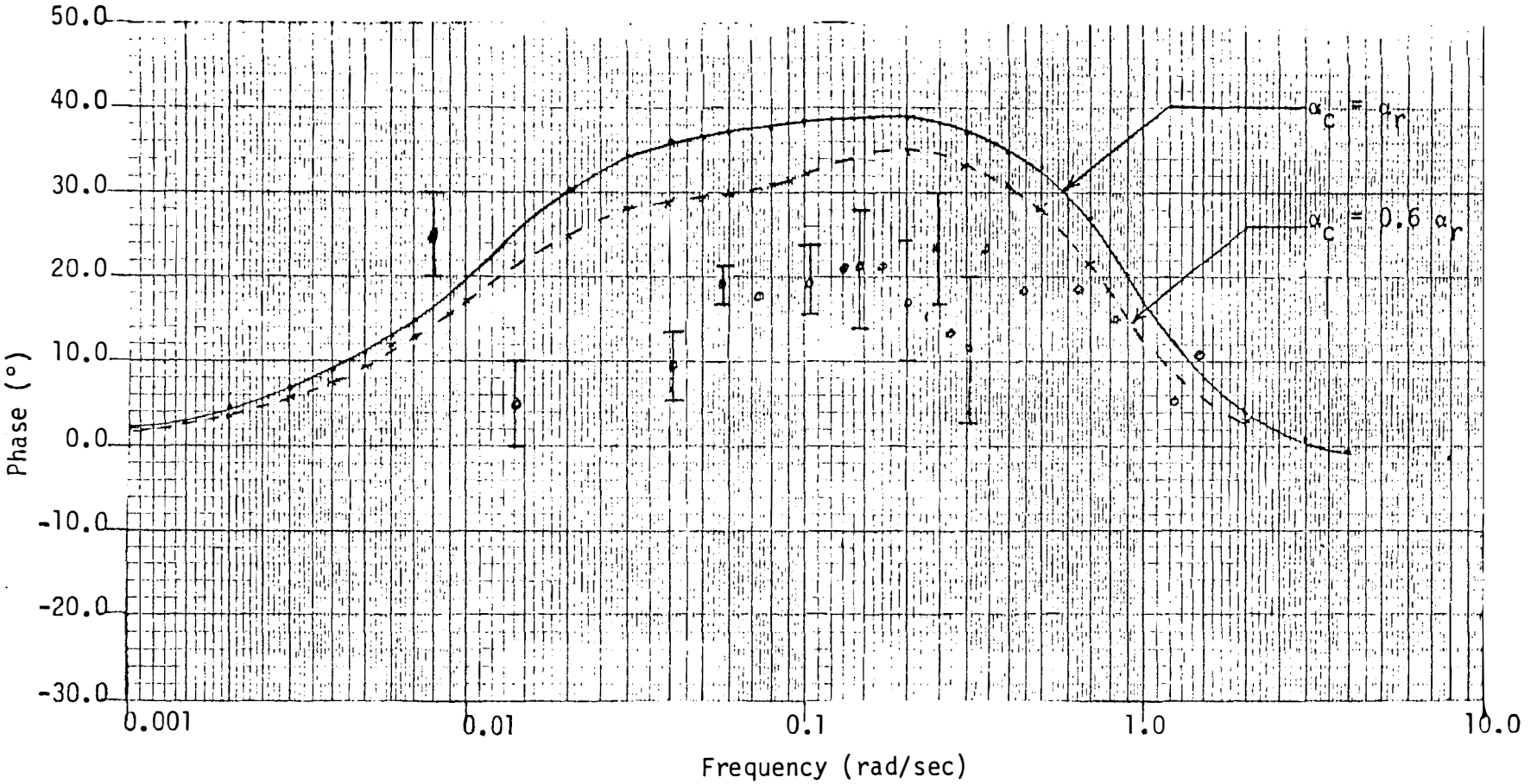

Figure V.3 (Continued).

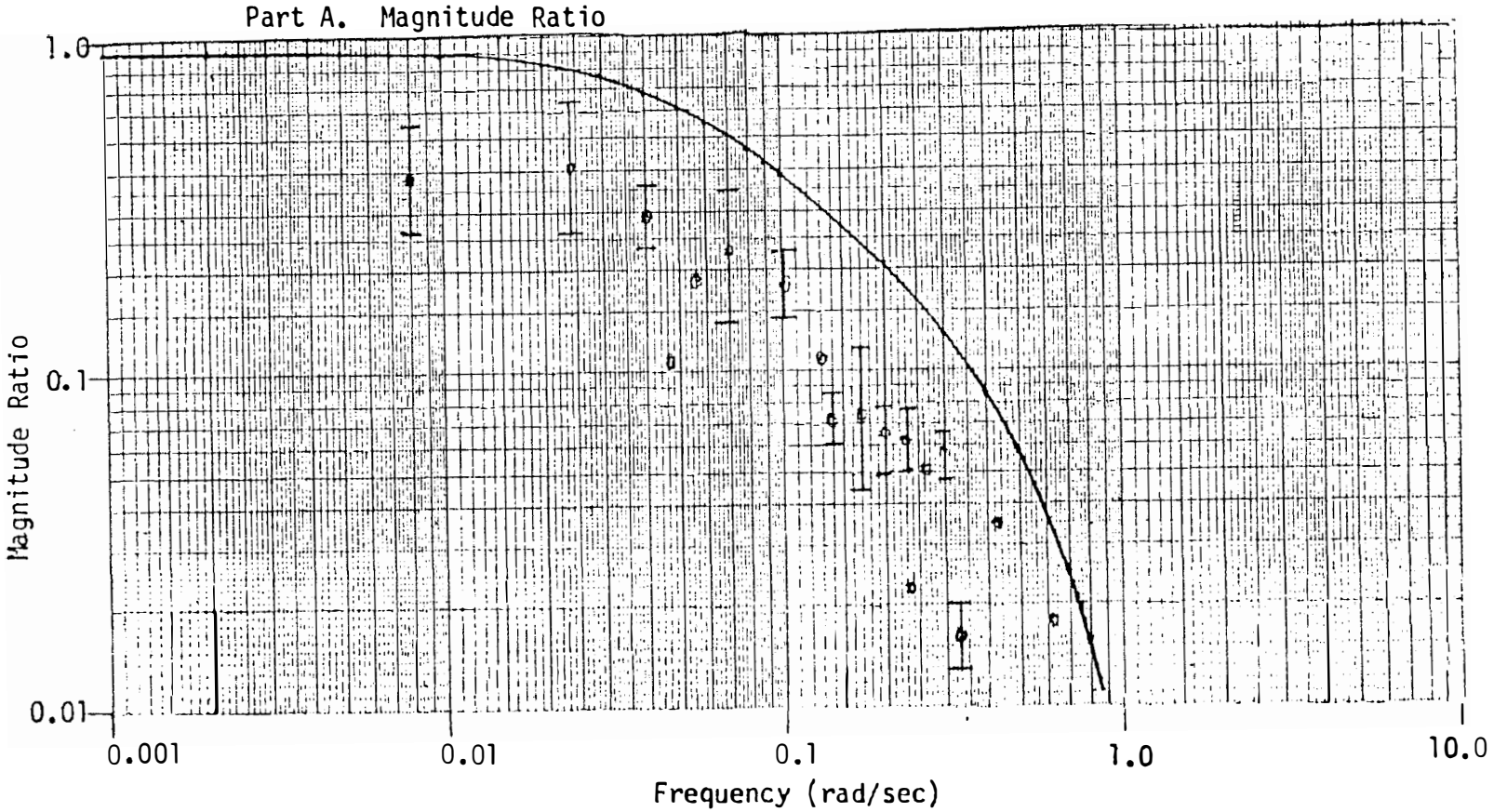

Figure V.4 Steam Pressure/Reactivity ($\delta P_s/\delta\rho$) Frequency Response.

Part B. Phase

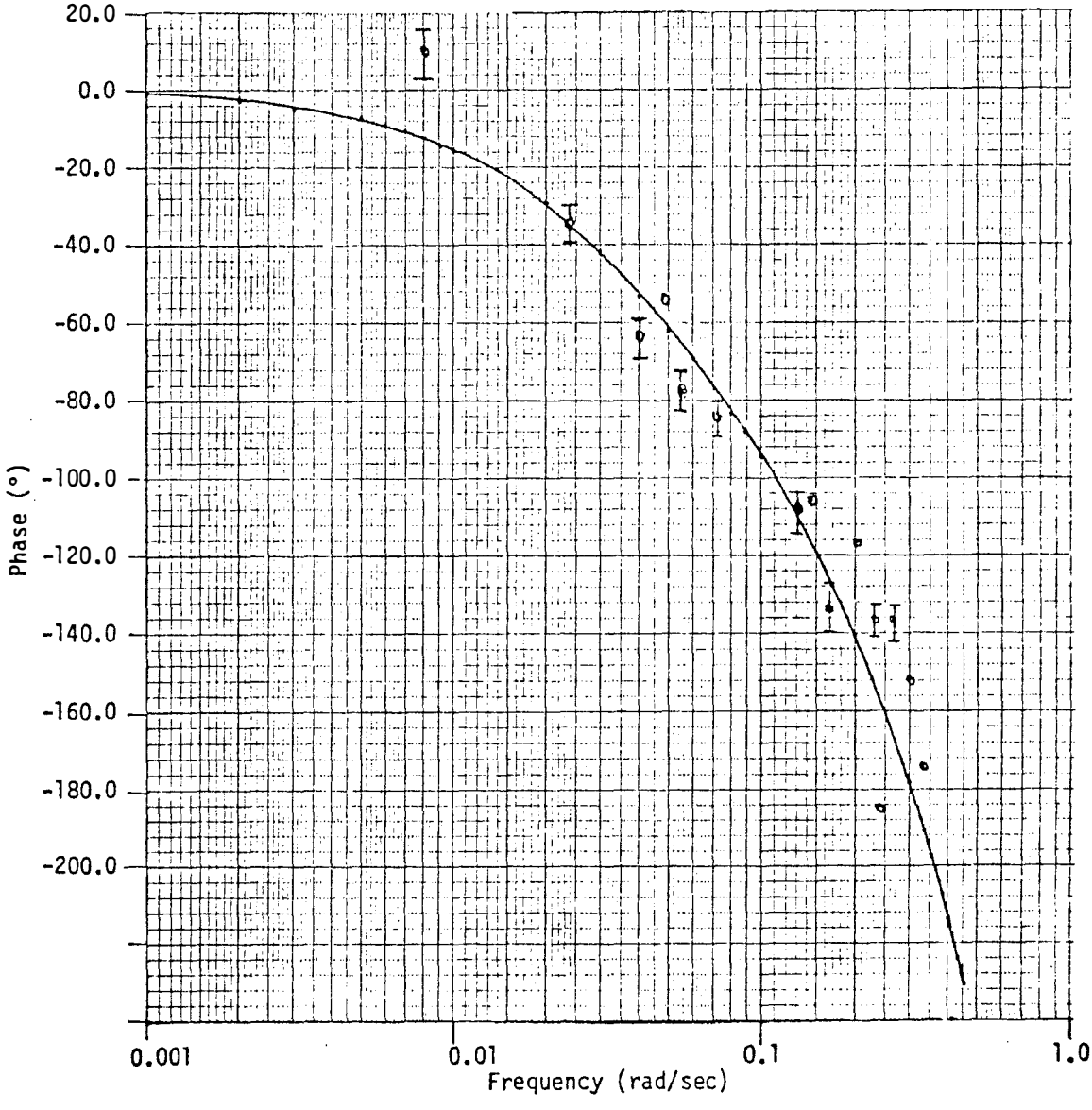

Figure V.4 (Continued).

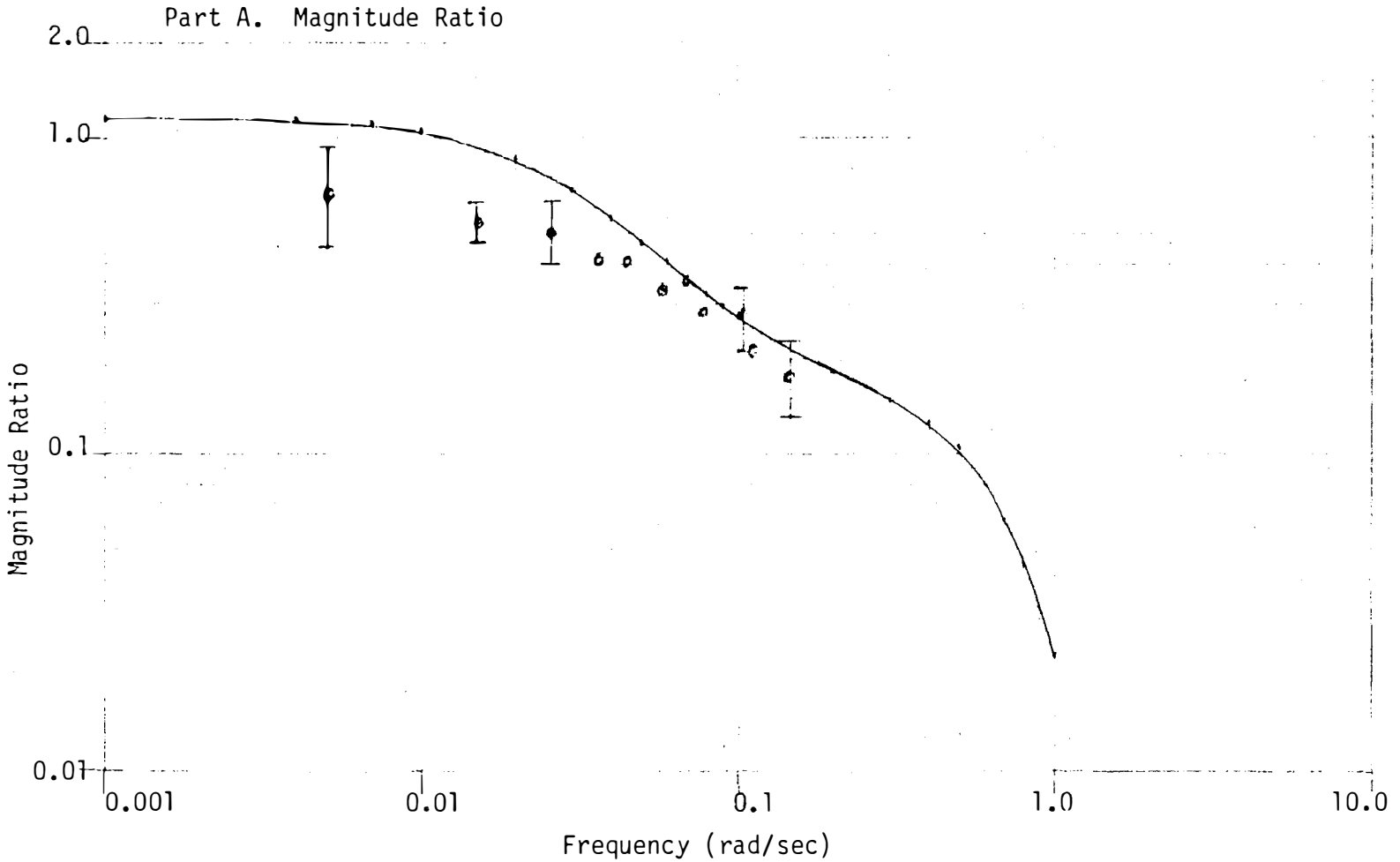

Figure V.5 Reactor Power/Steam Flow ($\delta P/P_o/\delta W_{so}$) Frequency Response.

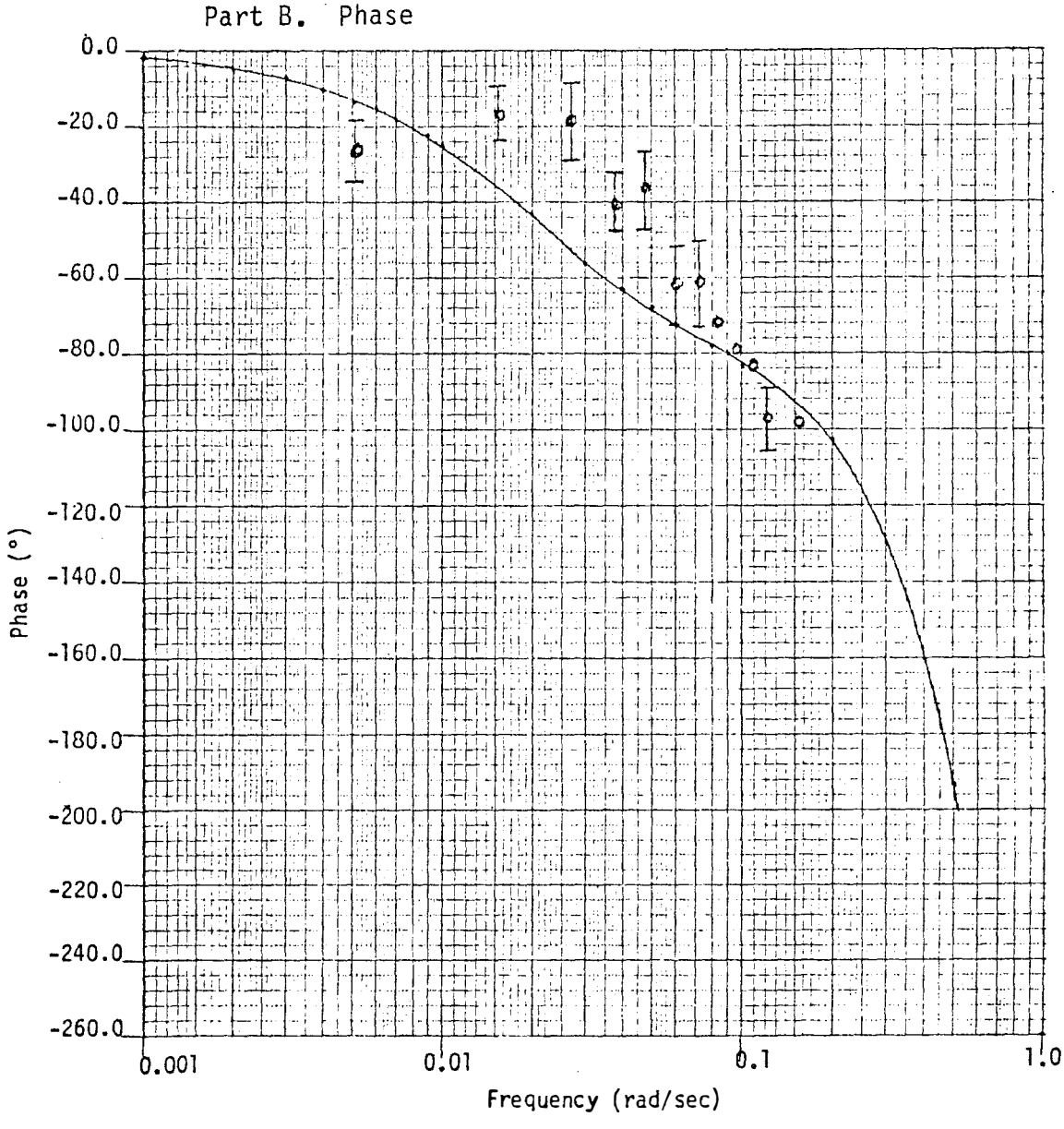

Figure V.5 (Continued).

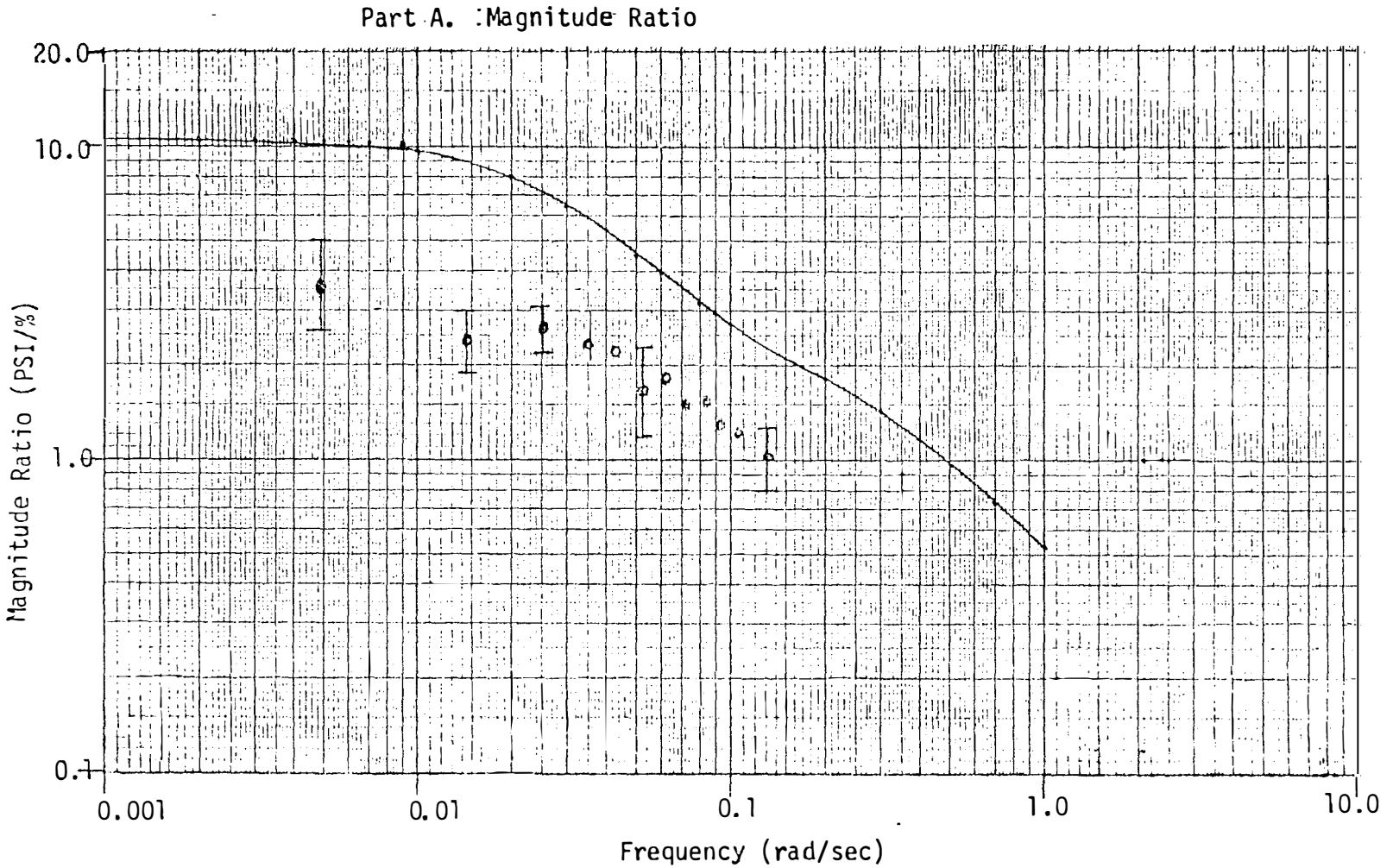

Figure V.6 Steam Pressure/Steam Flow ($\delta P_s/\delta W_{so}$) Frequency Response.

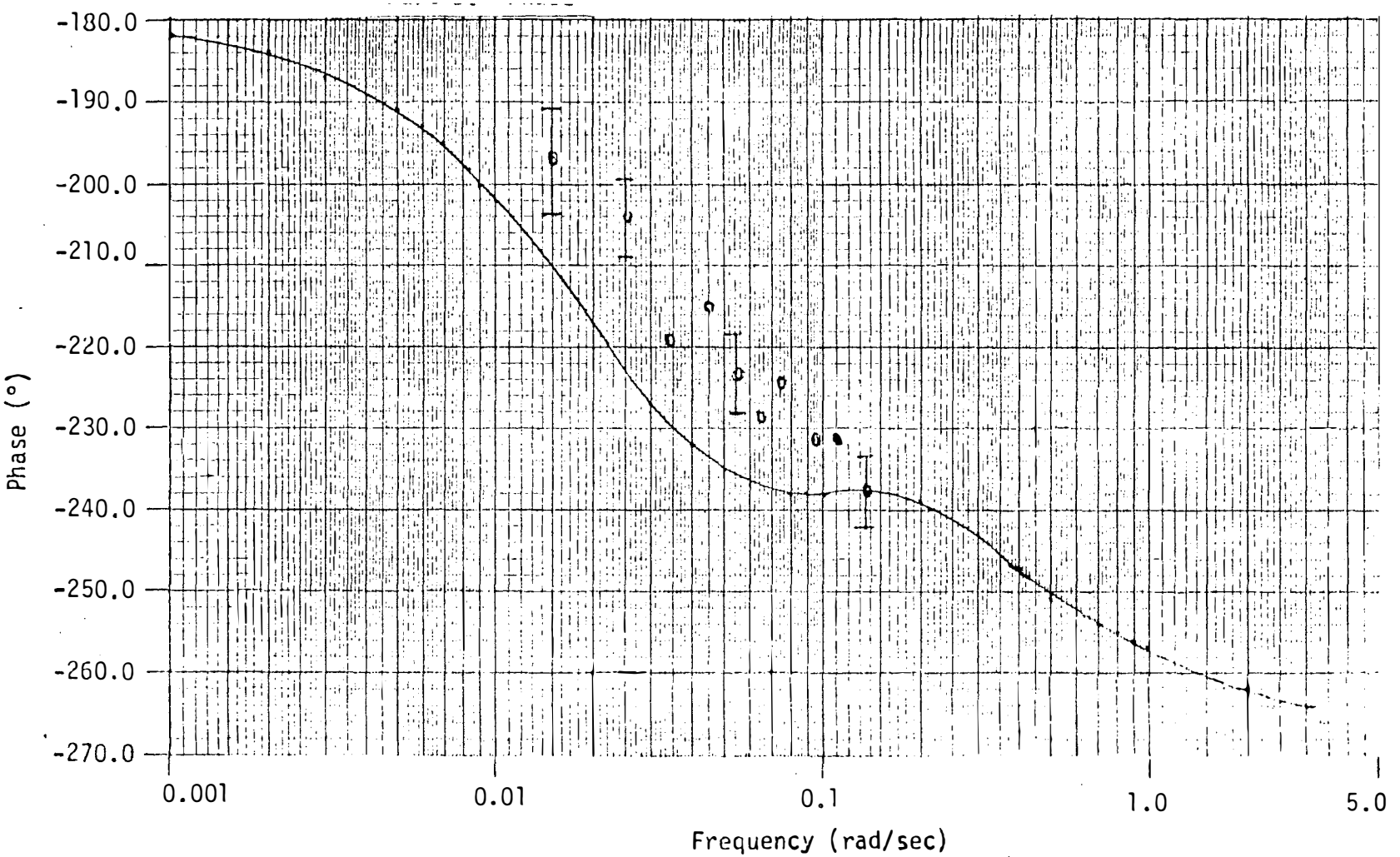

Figure V.6 (Continued).

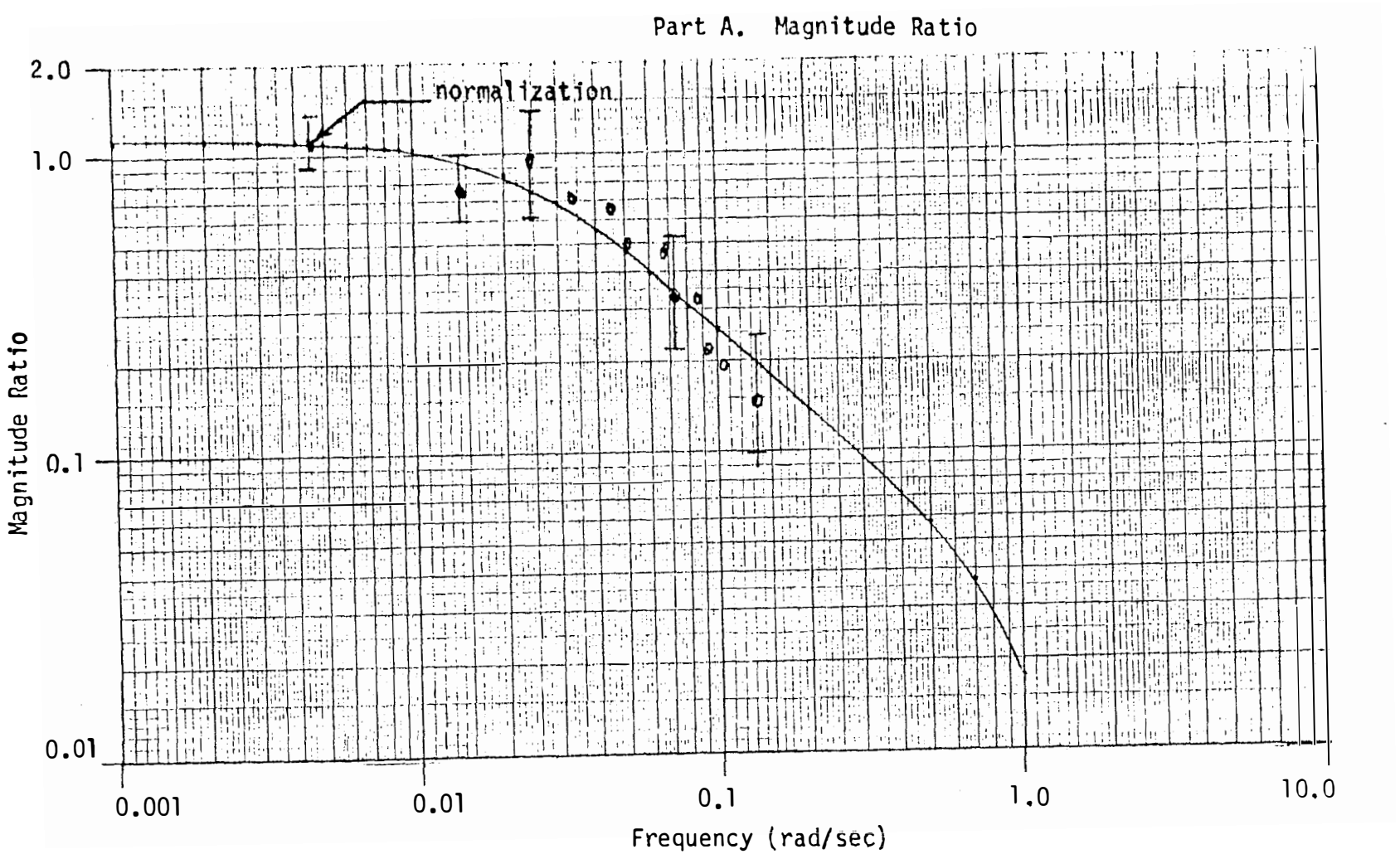

Figure V.7 Cold Leg Temperature/Steam Flow ($\delta T_{CL}/\delta W_{so}$) Frequency Response.

Part B. Phase

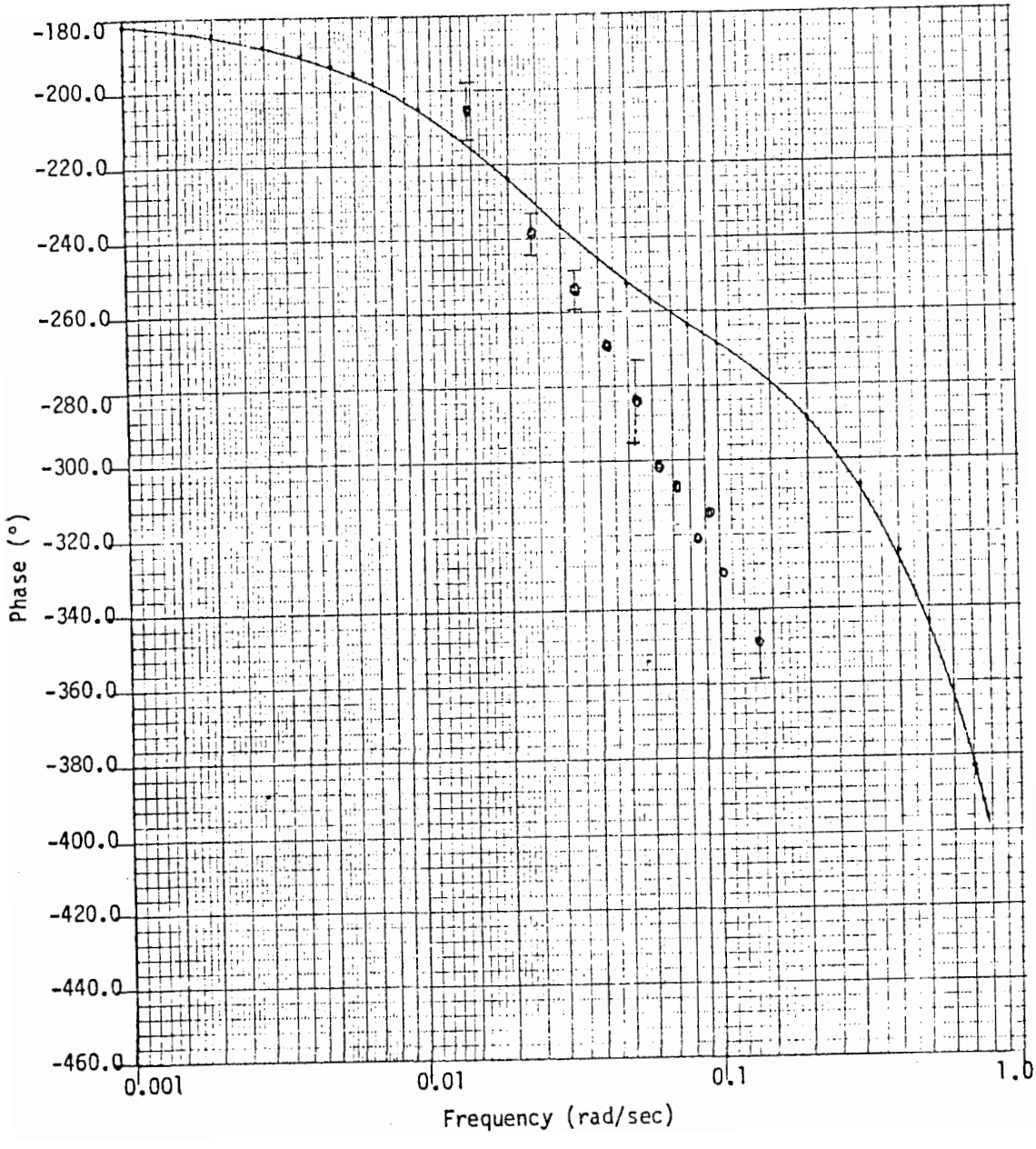

Figure V.7 (Continued).

1. A complete statistical analysis of the experimental data from the H. B. Robinson dynamic tests[3] has not been made. However, the standard deviation was calculated for some of the data and the selected results are shown in Figures V.3 through V.7.
2. The comparison with test results presented in this chapter can only serve the purpose of checking for gross inadequacies in the steam generator model because of the following factors.
   a. Limited accuracy of the test results due to experimental noise in some signals.
   b. The effects of the control systems were not included in the theoretical model results, and control system inputs have a significant effect on steam generator response.
   c. Models for other components of the system such as the pressurizer, reactor coolants, pumps and turbine generator were not included in the theoretical model results.

It can be concluded that no gross differences in qualitative behavior were observed that would indicate major inadequacies in the development of the detailed steam generator model.

CHAPTER VI

COMPARISON OF DETAILED MODELS WITH OTHER UTSG MODELS

VI.1 Introduction

In Chapter V, page 160, the frequency response of the UTSG detailed model (Model D), coupled with a PWR model was compared with the experimental results obtained from dynamic tests performed on the H. B. Robinson Nuclear Power Plant.[5] In this chapter, another approach for checking the mathematical development of the UTSG detailed model is considered. The step response of Model D is compared with the step response obtained with two other models.

1. A one dimensional finite difference model of a Westinghouse design UTSG developed independently by Christensen.[32]
2. A state variable lumped parameter model of a new Combustion Engineering (CE) integral economizer U-tube steam generator (IEUTSG) developed at The University of Tennessee by Arwood.[6]

The comparison with the first model is to check the lumped parameter, homogeneous flow, state variable approach against a finite difference, slip flow approach. The comparison with the second model is done for the purpose of comparing the behavior of the conventional type (UTSG) with that of the new design (IEUTSG).

In each case, a brief description of the system and the mathematical model is introduced followed by the comparison of the step response of selected state variables.

VI.2 Comparison with Christensen's UTSG Model

VI.2.1 System Description

The UTSG system considered by Christensen[32] in his model development is a Westinghouse UTSG[1] similar to that described in Section I.2, page 3. A simplified diagram of the physical system is given in Reference 32 and is reproduced as Figure VI.1.

VI.2.2 Model Description[32]

The steam generator is divided into eight sections as shown in Figure VI.1. The central "core" and the downcomer sections are described by partial differential equations, while the other sections are described by ordinary differential equations. The partial differential equations are solved by sampling in time and division into subsections (finite differencing) in space, thus transforming the differential equations into algebraic equations.

The main approximations used for the formulation of the equations are:

1. Uniform water and steam velocity in the primary and the secondary side and constant steam to water velocity ratio (slip factor) are used.
2. No subcooled boiling is included. The water is heated to saturation and afterwards all the energy is used for steam production.
3. Thermal equilibrium at the saturation point is assumed in the boiling part of the "core," the riser, the steam volume, and the upper part of the feedwater chamber.

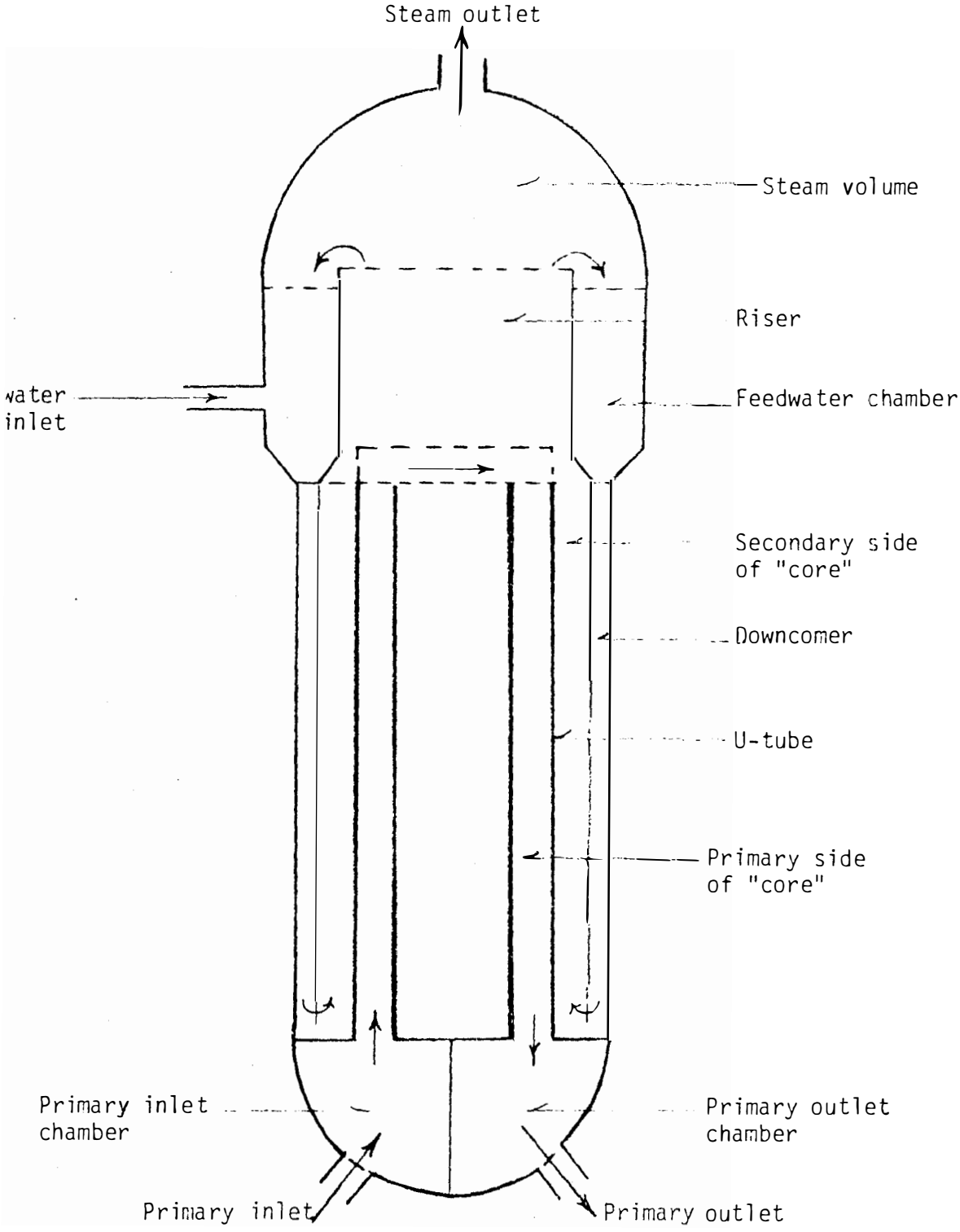

igure VI.1 Simplified Diagram of the Physical System.(32)

4. No heat conduction along the tubes takes place. The tubes are divided in two shells, each with half of the heat capacity and all of the heat resistance assigned to the coupling between the shells.
5. No boiling is allowed in the downcomer and no heat transmission from the "core" to the downcomer takes place. This assumption limits the working range of the pressure derivative to values less than 1-2 bar/s.
6. All heat exchange with the wall and the steel constructions in the steam volume is neglected.

The basic equations are derived by applying the mass, energy and/or momentum conservation principles to the eight sections of the steam generator. The equations for the "core" and downcomer sections are partial differential equations while those for the other sections are ordinary differential equations. The details of the model equations are given in Reference 32.

VI.2.3 Comparison of Model Formulation

The main differences between Christensen's model and Model D can be summarized as follows.

1. Model D uses a homogenous flow model where average density and average enthalpy in the boiling region are expressed in terms of mass quality (x) and the saturation properties while Christensen's model utilizes a slip flow model with constant slip factor (S). In Christensen's work, the average density and average enthalpy in the boiling region

are expressed in terms of the void ratio (α). The relation between x, α, and S can be derived from the basic definitions of these quantities and is given by

$$S = \left(\frac{x}{1-x}\right) \cdot \frac{\rho_f}{\rho_g} \cdot \frac{(1-\alpha)}{\alpha} . \qquad \text{(VI.1)}$$

2. In Model D, the heat transfer coefficients are assumed constant during the transient. In Christensen's model, they are calculated at each time step using instantaneous values of temperature and pressure.
3. The recirculation flow in Model D is calculated from a quasi-static momentum balance assuming that the differential gravity head equals the dynamic pressure drops in the recirculation loop. In Christensen's model, the dynamic pressure drops are treated explicitly with the flow velocity as a variable which should equal the total mass flow divided by the flow area and density.
4. The method of solution for Model D is described in Section IV.3, page 111. Christensen's model may be solved either by a digital program or by hybrid simulation. Partial differential equations are solved by division of space into subsections, 20 "core" and downcomer sections, and sampling in the time domain with a sampling rate of 10-20 per second. The time derivatives are replaced by first order differences in both cases, while the space derivatives are handled in different ways. Details of both digital and hybrid solution procedures are given in Reference 32.

VI.2.4 Comparison of Dynamic Responses

In Reference 32, Christensen presented the step response of a UTSG model to changes in the primary inlet temperature and the steam valve coefficient. The steam valve perturbation results are used for the comparison of the dynamic model as predicted by Model D and Christensen's model. It is noticed that the results given in Reference 32 are based on steam generator design data that is somewhat different from the H. B. Robinson data (Christensen's system is larger and operates at higher pressure). Therefore, the responses can be compared only on a qualitative basis. The system variables used for the comparison are primary outlet temperature (T_{Po}) and steam pressure (P_s).

The results of the comparison are given in Figure VI.2. It can be seen that the results obtained from the detailed lumped parameter model (Model D) agree fairly well with the results reported by Christensen using the finite difference formulation.

VI.3 Comparison with Arwood's IEUTSG Model

Arwood[6] developed a mathematical model for an Integral Economizer U-Tube Steam Generator (IEUTSG) using the state variable lumped parameter approach. Arwood used Model D of this study as a starting point and made the necessary changes to the lump structure to include the integral economizer section and to simulate the new steam generator design features. In this section, the step response of Model D will be compared with the results reported by Arwood for the IEUTSG. The main objective of this comparison is to highlight the similarities and differences between the two UTSG designs.

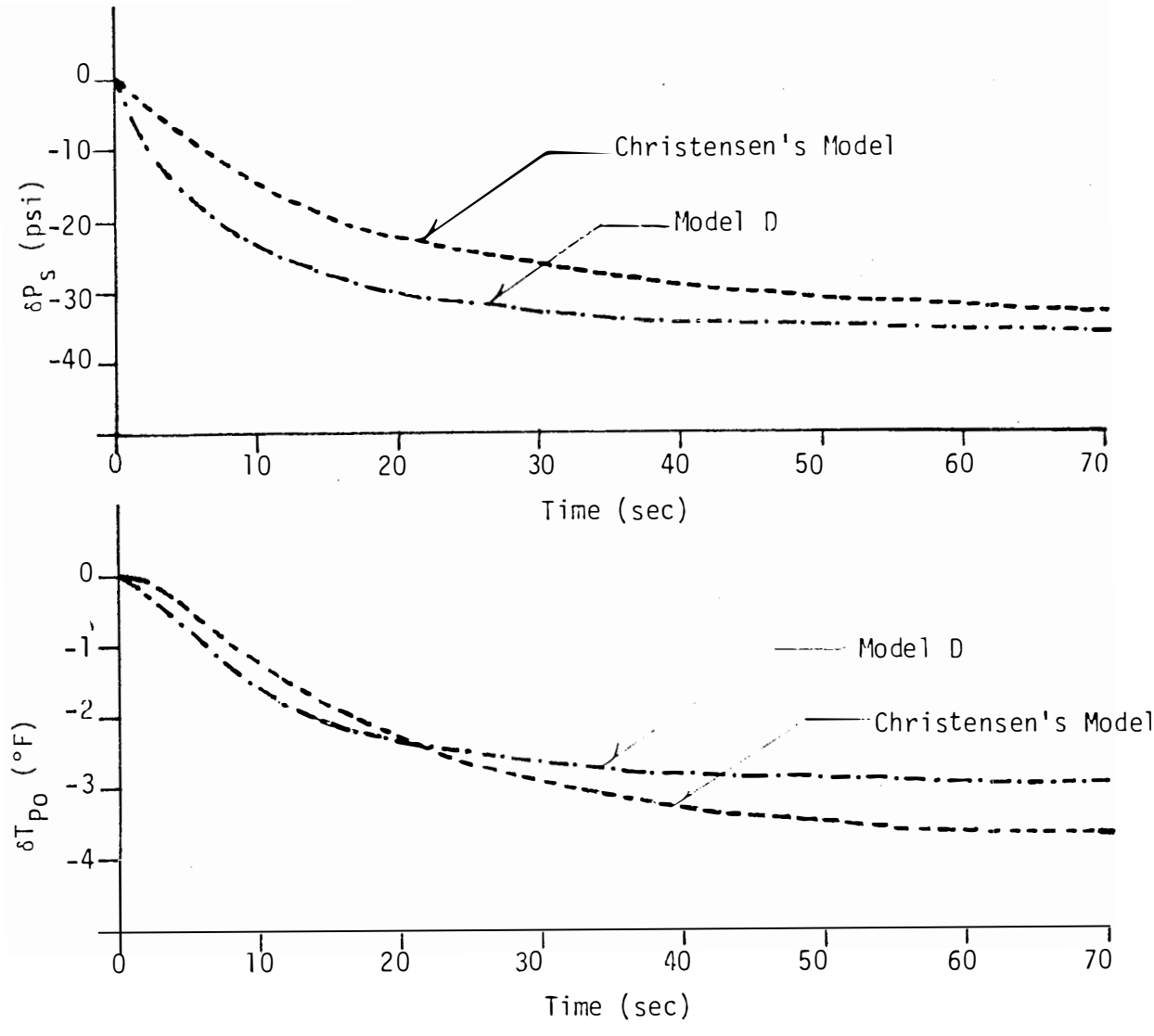

Figure VI.2 Comparison Between Model D and Christensen's Model.

VI.3.1 Description of the IEUTSG System

The integral economizer steam generator is an advanced UTSG design that will be installed in future PWR systems.[47] The IEUTSG is illustrated in Figure VI.3. A steam generator with an integral economizer is similar in most respects to the standard U-tube recirculating steam generator (UTSG). The basic difference is that instead of introducing feedwater only through a sparger ring to mix with the recirculating water flow in the downcomer channel, feedwater is also introduced into a separate, but integral section of the steam generator. A semi-cylindrical section of the tube bundle at the exit end of the U-tubes is separated from the remainder of the tube bundle by vertical divider plates and horizontal baffle plates. Feedwater is introduced directly into this section and preheated before discharge into the evaporator section. The economizer section is divided into two halves, in the upper or counterflow section feedwater flows in three paths across the tubes and generally counter current to the direction of primary flow inside the tubes. In the lower or parallel flow section, feedwater also flows in three paths across the tubes and generally parallel to the primary flow inside the tubes. This split feed arrangement prevents introduction of cold feedwater on the tube sheet with the associated thermal stress problems and at the same time retains partially the advantage of higher log mean temperature difference associated with the counterflow arrangement. The remainder of the steam generator is little different from the UTSG type except that the lower portion of the

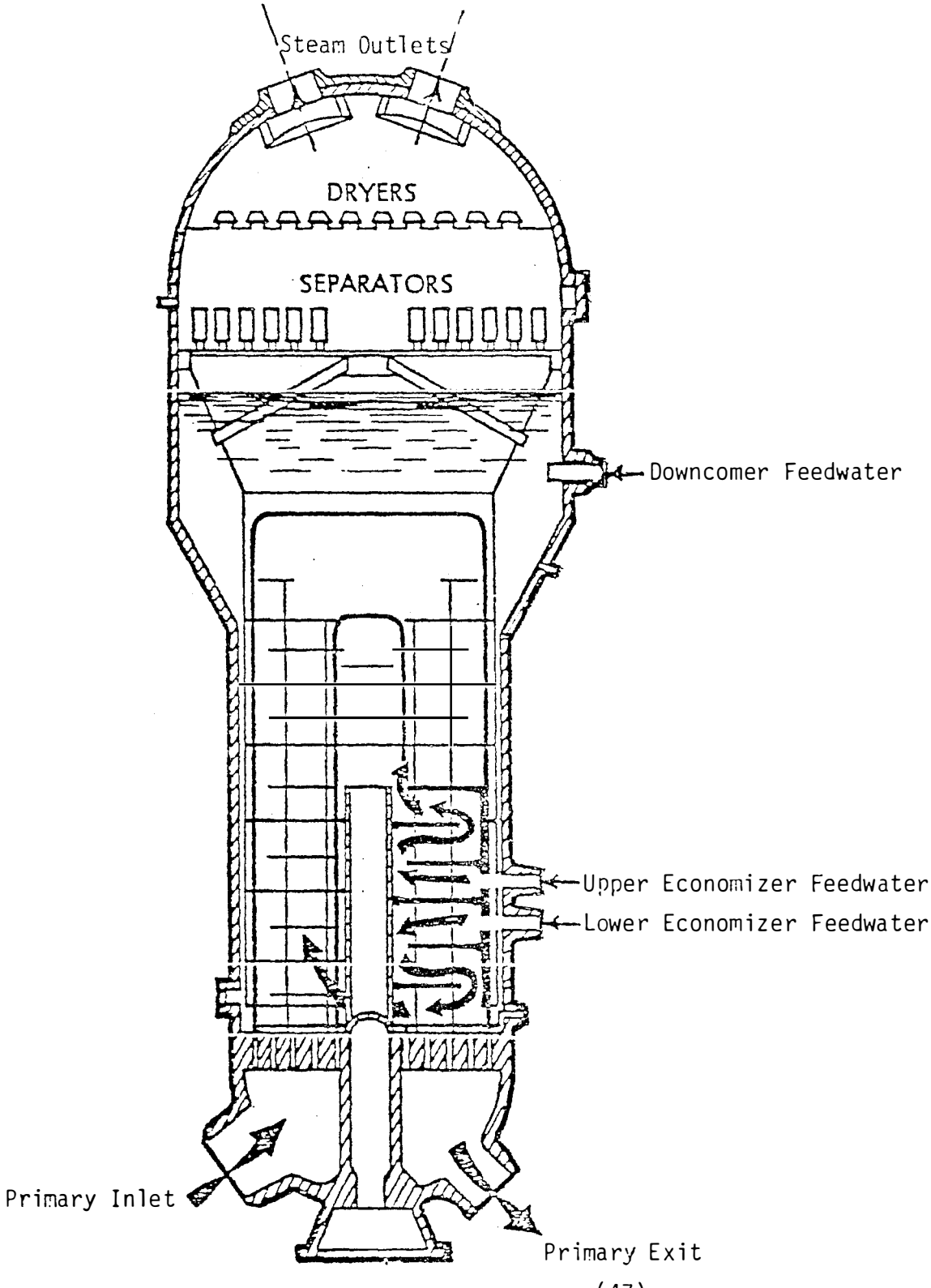

Figure VI.3 Schematic Diagram of an IEUTSG.(47)

evaporator section and the downcomer channel occupies only one half of the steam generator cross section.

VI.3.2 Comparison of Dynamic Responses

Figure VI.4 show the comparison between the IEUTSG and UTSG models step response to +10°F change in primary inlet temperature. A primary side perturbation was chosen so that both steam generator models can be compared on similar basis. The state variables chosen for comparison purposes are:

1. Primary outlet temperature (TPO).
2. Steam generator pressure (PS).
3. Downcomer level (LD).
4. Downcomer temperature (TD).

It can be seen that the response of the primary TPO and PS are similar in both steam generator models. This is to be expected since the only difference between the IEUTSG and the UTSG is in the feedwater preheating mechanism. The difference in the final steady state values is due to the difference in the design input parameters used for the dynamic response calculation.

The basic design difference between the UTSG and the IEUTSG can be seen from the response of the downcomer level and downcomer temperature as seen in Figure VI.4. Since only a small fraction of the feedwater is introduced into the downcomer section in the IEUTSG, it shows a larger change in the downcomer level due to the decrease of the recirculated water due to the increase in evaporation rate because of the increase in heat input rate. The downcomer temperature

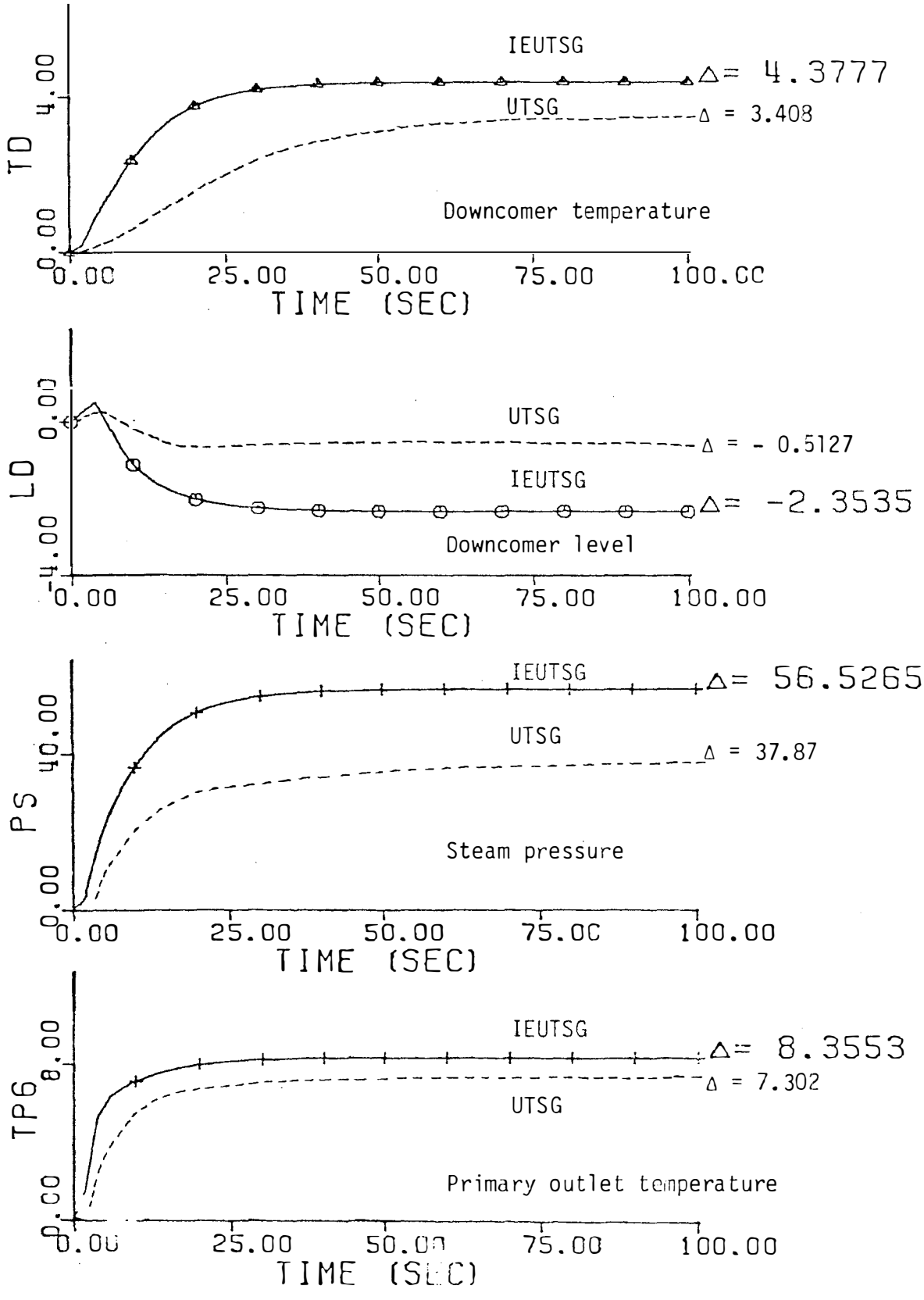

Figure VI.4 Comparison Between UTSG and IEUTSG Models Using the Same Modeling Approach.

in the IEUTSG is largely determined by the saturation temperature and therefore it shows a larger increase than in the case of the UTSG. The above comparison provided a second check on the modeling approach used for the detailed model (Model D) development.

CHAPTER VII

REMARKS AND CONCLUSIONS

VII.1 Evaluation of the Development Procedure

In the previous chapters, an approach was described that involved stepwise development of increasingly detailed models for a UTSG. This approach starts with identifying the physical process taking place within the system during anticipated transient. The approach proceeds by dividing the system into the minimum number of lumps that can describe the response to anticipated inputs. After analyzing the response of the system as obtained from this first step (simplest) model, further subdivision into more lumps can proceed in order to study spatial effects and/or add new system variables that are needed for design purposes. The above approach has the following advantages.

1. An idea of the response characteristics can be obtained from a simple model. The simplicity makes it possible to check the formulation in detail to insure that there are no blunders in the formulation or the algebraic manipulation of the equations. As progressively more detailed models are developed, their performance can be compared with results from eariler, simpler models. Major differences in comparable outputs would indicate probable errors in the formulation of the more detailed model.

2. This progressive approach allows an assessment of model complexity vs. fidelity. This information can assist in selecting the model with the appropriate detail and cost for a particular application.

VII.2 Possible Uses of the Current Work

Possible uses of the mathematical models developed in this dissertation depend on the purpose of performing the dynamic analysis.

Models A and B are the simplest UTSG models. They can be used for scoping analysis and when a simplified model for the steam generator is needed to simulate an overall PWR system. The models do not include the steam generator level as a state variable, therefore, they cannot be used for analysis involving the dynamic response of this quantity.

Model C combines the simplicity of using the primary and tube metal structure of Model B with the treatment of water level since the secondary fluid lump is broken into three lumps.

a. Effective heat exchange lump.

b. Drum equivalent lump.

c. Downcomer lump.

The model is represented by 9 differential equations compared to 15 for Model D. Therefore, it can be used for parametric steam generator controller work without introducing the complexities of the subcooled/boiling moving boundary considered in Model D.

Model D can be considered as the end product of the work reported in this dissertation. It is now programmed such that it

receives steam generator design data and produces the steady state temperature and mass quality profile along the heat exchange path, then uses the steady state output for the transient response calculations. The model represents a fairly detailed lumped parameter approach that can be used for the dynamic analysis of UTSG associated with PWR nuclear power plants.

VII.3 Recommendations for Future Work

The work reported in this dissertation can be expanded in several directions. Possible future work may include the following:

1. The steady state profile calculations can be modified to include the momentum equation and can be used to estimate the recirculation ratio at different load conditions.
2. The steam flow rate can be related to the turbine electrical load by means of a turbine model and thus the steam generator model can be coupled to the reactor on the primary side and to the turbine on the secondary side to simulate load following capabilities of PWR system.
3. A feedwater controller can be coupled to the steam generator model and the closed loop response can be used to determine and optimize the controller parameters.
4. The nonlinear terms that were eliminated in this work can be identified and re-introduced into the model.
5. The effect of subcooled boiling and the effect shrink and swell can be added to the model by introducing the void fraction (α) instead of the mass quality (x) as a state variable in the boiling secondary fluid lumps.

VII.4 Conclusions

A set of linear, lumped parameter, state variable models of varying complexity was developed for simulation of U-tube steam generators. The models appear capable of predicting the response of this type of system. The suitability of these models was examined by:

- assessing the physical plausibility of the transient results
- comparison with independently-developed, more detailed model results
- comparison with available test data.

The models are cast in the state variable form, making it convenient to couple them with other subsystem models for use in studying overall plant performance.

LIST OF REFERENCES

REFERENCES

1. RESAR, Reference Safety Analysis Report, Vol. 1, Westinghouse Nuclear Energy Systems, Pittsburgh, Pennsylvania (1970).

2. Final Facility Description and Safety Analysis Report, Vol. 1, H. B. Robinson Unit No. 2, Carolina Power and Light Company.

3. Thakkar, J. G., "Correlation of Theory and Experiment for the Dynamics of a Pressurized Water Reactor, M. S. Thesis, Nuclear Engineering Department, The University of Tennessee (March 1975).

4. Katz, E. Marcia, "Planning, Performing and Interpreting Dynamic Measurements in Pressurized Water Reactors," Ph. D. Dissertation, Nuclear Engineering Department, The University of Tennessee (June 1976).

5. Kerlin, T. W., E. M. Katz, J. G. Thakkar, "Dynamic Testing of Nuclear Power Plant," Proceedings of the 1974 Joint Automatic Control Conference, Austin, Texas, June 18-28, 1974.

6. Arwood, Don C., "A Mathematical Model for an Integral Economizer Steam Generator," M. S. Thesis, Nuclear Engineering Department, The University of Tennessee, Knoxville, Tennessee (March 1975).

7. Clark, J. A., V. S. Arpaci and K. M. Treadwall, "Dynamic Response of Heat Exchangers Having Internal Heat Source," Part I, Trans. ASME, Vol. 80, pp. 612-624 (1958), Part II, Trans. ASME, Vol. 80, pp. 625-634 (1958), Part III, Trans. ASME, Series C. Vol. 91, pp. 253-266 (1959), Part IV, Journal of Heat Transfer Trans. ASME, Series C. Vol. 83, pp. 321-336 (1961).

8. Chien, K. L., E. I. Ergin, C. Ling, and A. Lee, "Dynamic Analysis of a Boiler," Trans. ASME, Vol. 80, pp. 1809-1819 (1958).

9. Thal-Larson, H., "Dynamics of Heat Exchangers and their Models," Journal of Basic Engineering, Trans. ASME, Series D, Vol. 82, pp. 489-504 (1960).

10. Masubuchi, M., "Dynamic Response and Control of Multipass Heat Exchangers," Journal of Basic Engineering Trans., ASME, Series D., Vol. 82, pp. 51-65 (1960).

11. Enns, Mark, "Comparison of Dynamic Models of a Superheater," Journal of Heat Transfer, Trans. ASME, Series C., Vol. 84, pp. 373-385.

12. Dusinberre, G. M., "Calculations of Transient Temperatures in Pipes and Heat Exchangers by Numerical Methods," Trans. ASME, Vol. 76, pp. 421-426 (1954)

13. Astrom, K. J. and K. Eklund, "A Simplified Nonlinear Model of a Drum Boiler-Turbine Unit," Int. J. Control 1972, Vol. 16, No. 1 (pp. 145-169).

14. Berkowitz, David A., (Editor) "Proceedings of the Seminar on Boiler Modeling," The MITRE Corporation, November 6-7, 1974.

15. Thie, J. A., "Dynamic Behavior of Boiling Reactors," AEC Research and Development Report ANL-5849, May 1959.

16. Akcasu, A. Ziya, "Theoretical Feedback Analysis in Boiling Water Reactors," AEC Research and Development Report ANL-6221, October 1960.

17. Fleck, J. A., Jr., "The Dynamic Behavior of Boiling Water Reactors," J. Nucl. Energy, Part A.: Reactor Sciences, 1960, Vol. 11, pp. 114-130.

18. Muscettola, M., "Dynamic Model for a Boiling Water Reactor," United Kingdom Atomic Energy Authority Reactor Group, AEEW-R-285, 1963.

19. Junichi, Mida and Nobuhide Suda, "Dynamic Analysis of Natural Circulation Boiling Water Reactor," Japan Atomic Energy Research Institute (JAERI) 1061, December 1963.

20. Anderson, R. P., L. T. Bryant, J. C. Carter, and J. F. Marchaltere, "An Analog Simulation of the Transient Behavior of Two-Phase Natural Circulation Systems," Chemical Engineering Progress Symposium Series No. 41, Vol. 59, pp. 96-103, 1963.

21. Nahavandi, A. N. and R. F. von Hollen, "A Space-Dependent Dynamic Analysis of Boiling Water Reactor Systems," Nuclear Science and Engineering, 20, pp. 392-413 (1964).

22. Neal, L. G. and S. M. Zivi, "Hydrodynamic Stability of Natural Circulation Boiling Systems," Vol. 1, A Comparative Study of Analytical Models and Experimental Data, STL-312-14 (1), June 1965.

23. Spigt, C. L., "On the Hydraulic Characteristics of a Boiling Water Channel with Natural Circulation," EURAEC Report EUR 2842.e (1966).

24. Vayssier, G., "A Nonlinear Analog Model for Boiling Loop Dynamics and Its Application in Reactor Stability," Paper submitted to the Symposium on Two-Phase Flow Dynamics at Technological University of Eindhaven, September 1967.

25. Westmoreland, J. C., "Natural Circulation Steam Generators for Nuclear Power Plants," Nuclear Science and Engineering, Vol. 2, pp. 533-546 (1957).

26. McGwan, E. J. and J. R. Bodoia, "An Investigation of Stability in a Glass Model Steam Generator," Bettis Technical Review, WAPD-BT-27, pp. 1-19, December 1962.

27. Clarke, W. G., "Transient Analysis of Steam Generators in Nuclear Power Plants Using Digital Computer Techniques," WAPD-T-1648 (1965).

28. Nahavandi, Amir N. and Abram Batenburg, "Steam Generator Water Level Control," Journal of Basic Engineering, June 1966 (pp. 343-354).

29. Hargrove, H. G., "MARVEL: A Digital Computer Code for Transient Analysis of a Multiloop PWR System," WCAP-7909, October 1972.

30. Ten Wolde, D. G., "Transient Behavior of Nuclear Steam Generator Dynamics," WTHD-36, Ph. D. Thesis, Delft University of Technology, Department of Mechanical Engineering, April 1972.

31. Bauer, M. M., Larminaux, Lemoine et Sureau, "Simulation Numerique Des Generateurs de Vapeur Nucleaires," Societe Hydrotechnique de France XII mes Journees de L'Hydraulique (Paris 1972).

32. Christensen, P. La Cour, "Description of a Model of a U-Tube Steam Generator," Report No. RISO-M-1564, Library of the Danish Atomic Energy Commission, Riso, Riskilde, Denmark, 1973.

33. Delene, J. G., "A Digital Computer Code for Simulating the Dynamics of Demonstration Size Duel-Purpose Desalting Plants Using a Pressurized Water Reactor as a Heat Source," ORNL-TM-4104, September 1973.

34. Murrell, M. D., "Boiler Simulation, PWR Station Dynamics," Paper No. 4, Boiling Dynamics and Control in Nuclear Power Stations, Proceedings of International Conference organized by the British Nuclear Energy Society, March 22-23, London, 1973.

35. Frei, G., J. Weber and F. Hirmer, "Dynamic Behavior of a 660 MW Nuclear Power Station," Paper No. 5, Boiling Dynamics and Control in Nuclear Power Stations, Proceedings of International Conference organized by the British Nuclear Energy Society, March 22-23, 1973, London.

36. Matausek, M. R., "SINOD-A Nonlinear Lumped Parameter Model for Analysis of Two-Phase Flow in Natural Circulation Boiling Water Loop," Nuclear Science and Engineering: 53, 1974, pp. 440-457.

37. Harrington, R. M., "Analysis of the Fort St. Vrain Nuclear Plant in Support of a Dynamic Testing Program," M. S. Thesis, Nuclear Engineering Department, The University of Tennessee, Knoxville, Tennessee (August 1974).

38. Kreyszig, E., Advanced Engineering Mathematics, John Wiley and Sons, Inc., New York, Second Edition, 1967).

39. Ball, S. J. and R. K. Adams, "MATEXP: A General Purpose Digital Computer Program for Solving Ordinary Differential Equations by the Matrix Exponential Method," ORNL-TM-1933, Oak Ridge National Laboratory (August 1967).

40. Kerlin, T. W. and J. L. Lucius, The SFR-3 Code-A Fortran Program for Calculating the Frequency Response of a Multivariable System and its Sensitivities to Parameter Changes, USAEC Report ORNL-TM-1575 (1966).

41. Weaver, L. E., Reactor Dynamics and Control, American Elsevier Publishing Company, Inc., New York (1968).

42. Melsa, J. L. and D. G. Shultz, Linear Control Systems, McGraw Hill Book Company, Inc., New York (1969).

43. Ralston, A. and H. S. Wilf, ed., Mathematical Methods for Digital Computers, Vol. 2, John Wiley and Sons, Inc., New York (1967).

44. Collier, John G., Connective Boiling and Condensation, McGraw Hill Book Company (UK) Limited, London (1972).

45. Fraas, A. P. and M. Necatiozisik, Heat Exchanger Design, John Wiley and Sons, Inc., New York, 1965.

46. Arpaci, Vedat S., Conduction Heat Transfer, Addison-Wesley Publishing Company, Reading, Massachusetts (1966).

47. "CESSAR CE Standard Safety Analysis Report for System 80 NSSS, CE Power Systems, Windsor, Connecticut, 1974.

48. El-Wakil, M. M., Nuclear Heat Transport, International Textbook Company, Scranton, Pennsylvania, 1971.

49. Kays, W. M., Convective Heat and Mass Transfer, McGraw-Hill Book Company, New York (1966).

APPENDIXES

APPENDIX A

NARROW RANGE LINEAR APPROXIMATION OF SATURATION, WATER AND STEAM PROPERTIES

One of the prerequisites for the solution of the dynamic analysis models for UTSG systems is the expressions for the equation of state for saturated water and steam. The most direct and accurate method for satisfying the above requirement is to input the thermodynamic properties of saturated water and steam in tabular form into the digital computer and use standard table lookup algorithms to obtain the value of a certain property at a given thermodynamic state. This method is suitable for numerical solution of dynamic analysis models.

Another method to obtain the thermodynamic properties is to use polynomial fitting of the steam tables data. Obviously, the higher the order of the fitting polynomial, the more accurate the solution (at the expense of computation time). In this study, intuition and engineering judgement were used to arrive at the least expensive method for obtaining the saturation properties of water and steam in the range of interest (600-1000 psia).

The method was arrived at by first studying the behavior of the saturation thermodynamic properties as a function of pressure over a wider range than the range of interest for a particular application. After that the wide range was divided into a number of narrow ranges and the behavior of the saturation properties was reexamined over these

narrow ranges to determine the least order polynomial that can adequately represent the relation between the saturation properties and the system pressure. The above method was applied to obtain an approximation for the equations of state for saturated water and steam over the pressure range 600-1000 psi. This range is suitable for normal operation transients of steam generator systems where the steady state pressure is about 800 psi. The following saturation properties were plotted as a function of pressure using the ASME 1967 steam tables.

1. T_{sat} = saturation temperature (°F)
2. V_f = specific volume of saturated water (ft^3/lbm)
3. V_g = specific volume of saturated steam (ft^3/lbm)
4. $V_{fg} = V_g - V_f$
5. h_f = enthalpy of saturated water (Btu/lbm)
6. h_g = enthalpy of saturated steam (Btu/lbm)
7. $h_{fg} = h_g - h_f$.

The results are shown in Figures A.1 through A.7. From these results, it can be seen that the change of the above properties, over the range of interest is fairly linear. The following values are representative of the rate of change of the above saturation properties with respect to pressure for the H. B. Robinson steam generator.

1. $\frac{\partial T^*_{sat}}{\partial P} = 0.145$ °F/psia
2. $\frac{\partial V_f}{\partial P} = 3.6 \times 10^{-6}$ ft^3/lbm/psia

*Although T_{sat} and other saturation properties are considered as functions of one variable (P), the partial derivative symbol ($\partial/\partial P$) is used for clarity of equations.

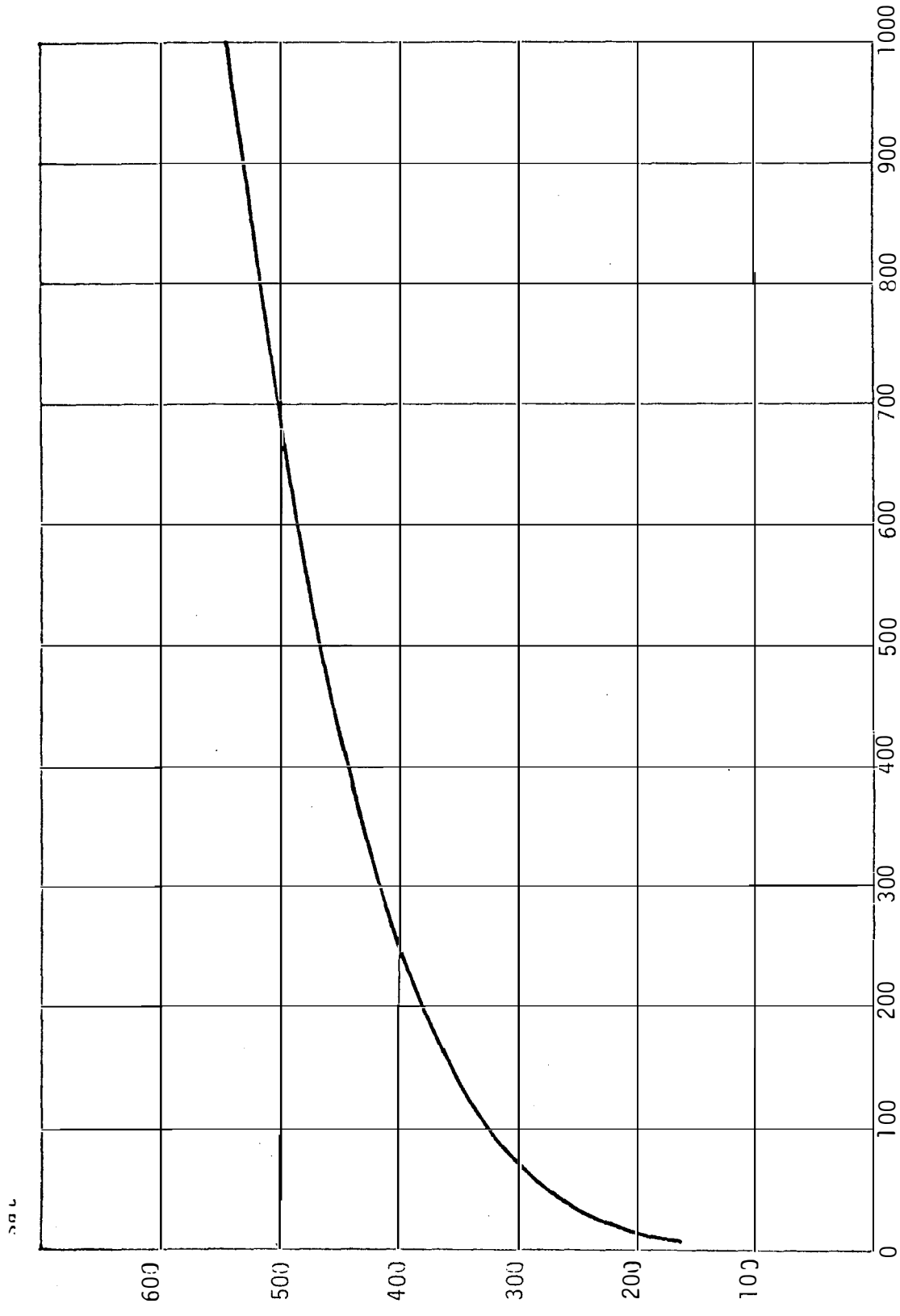

Figure A.1 Variation of T_{sat} with Pressure.

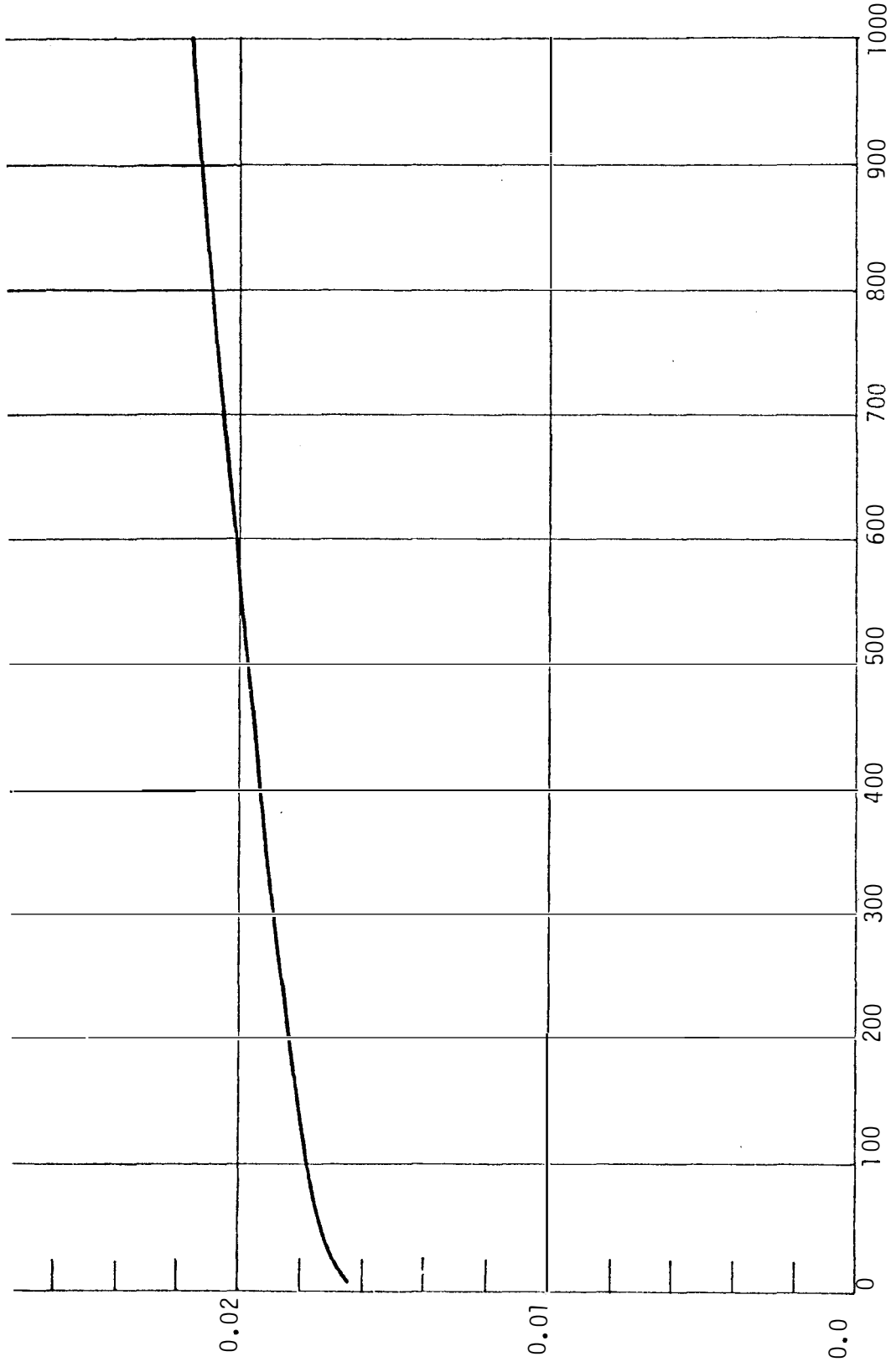

Figure A.2 Variation of V_f with Pressure.

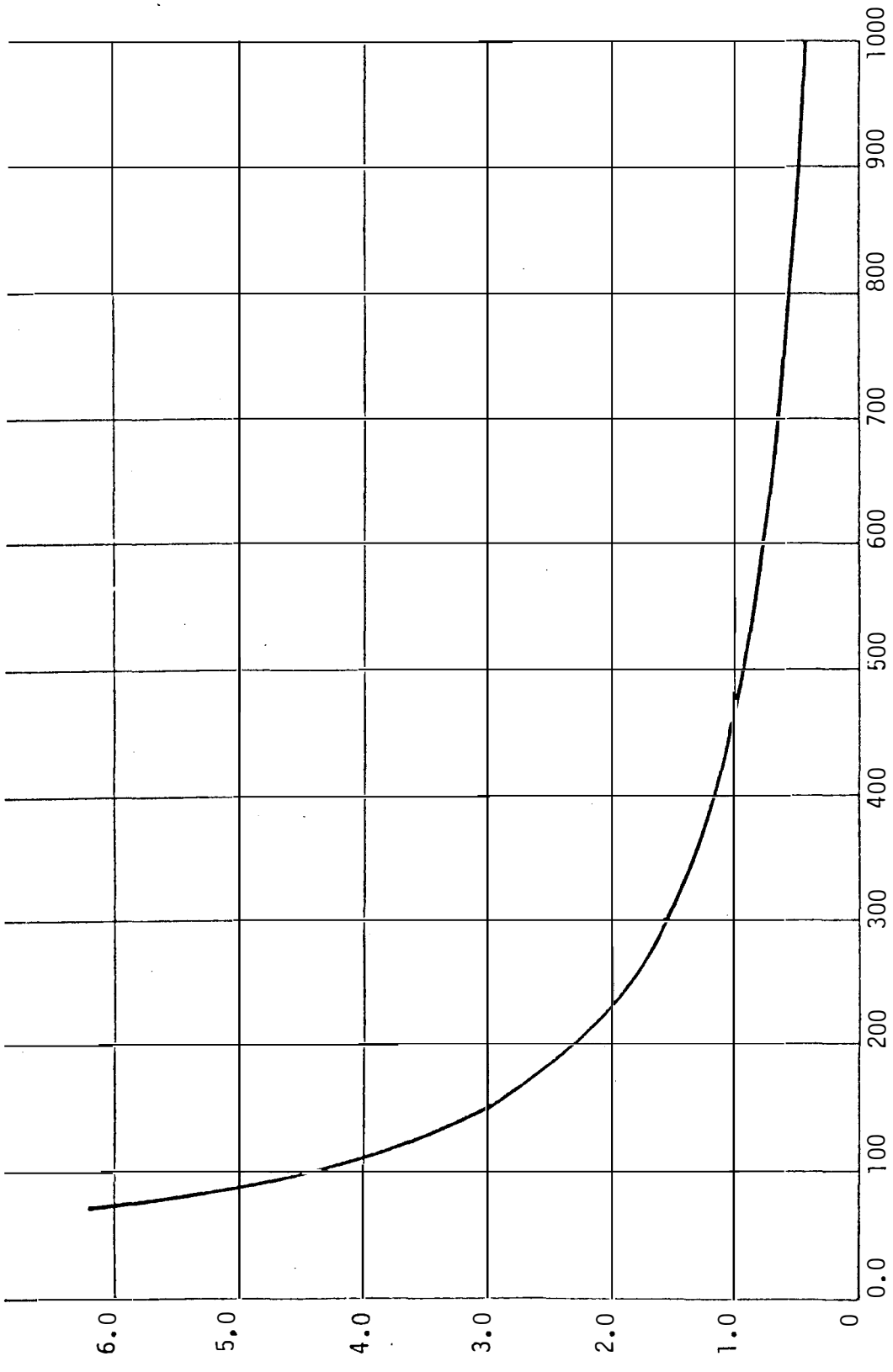

Figure A.3 Variation of V_g with Pressure.

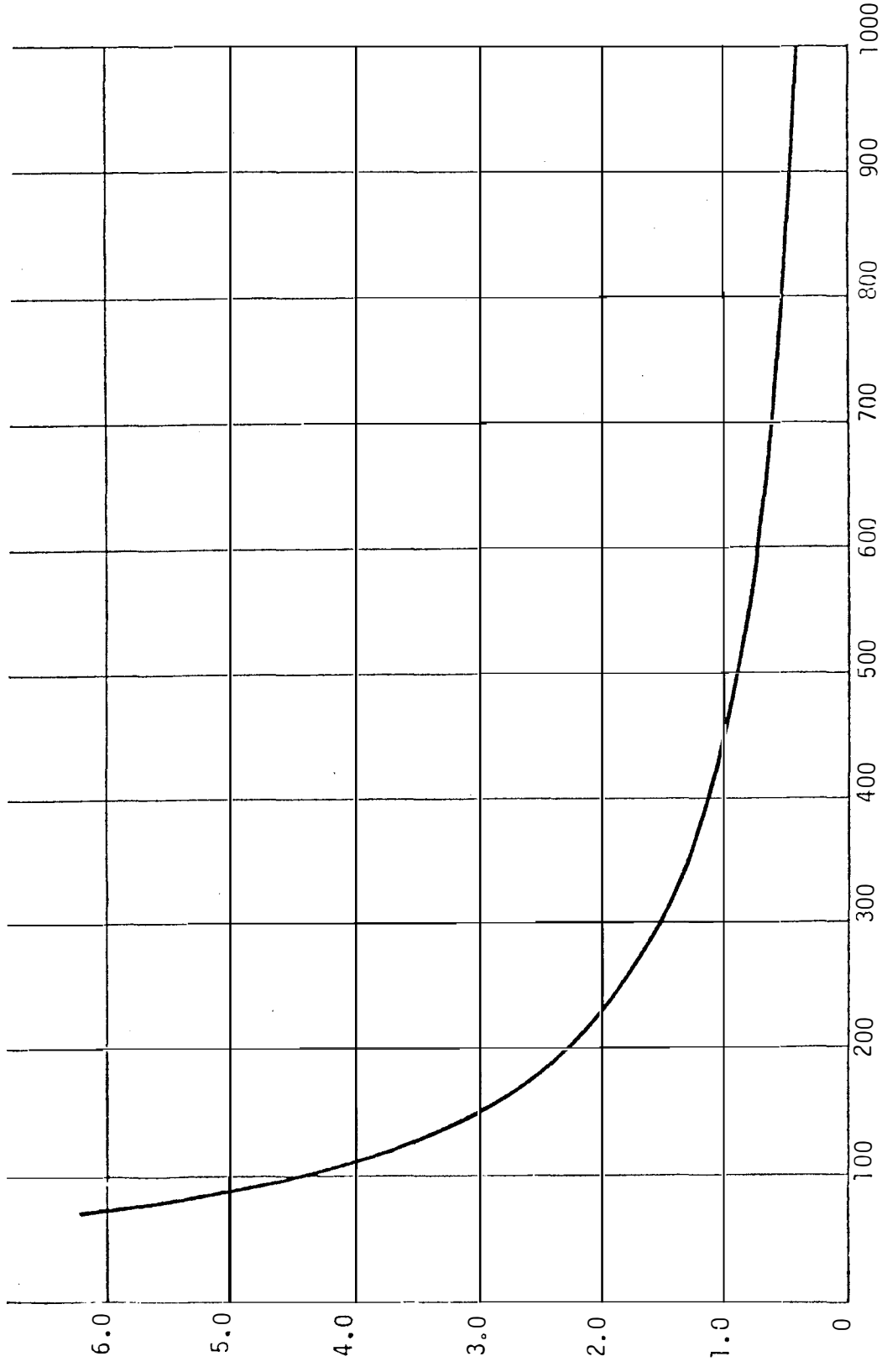

Figure A.4 Variation of V_{fg} with Pressure.

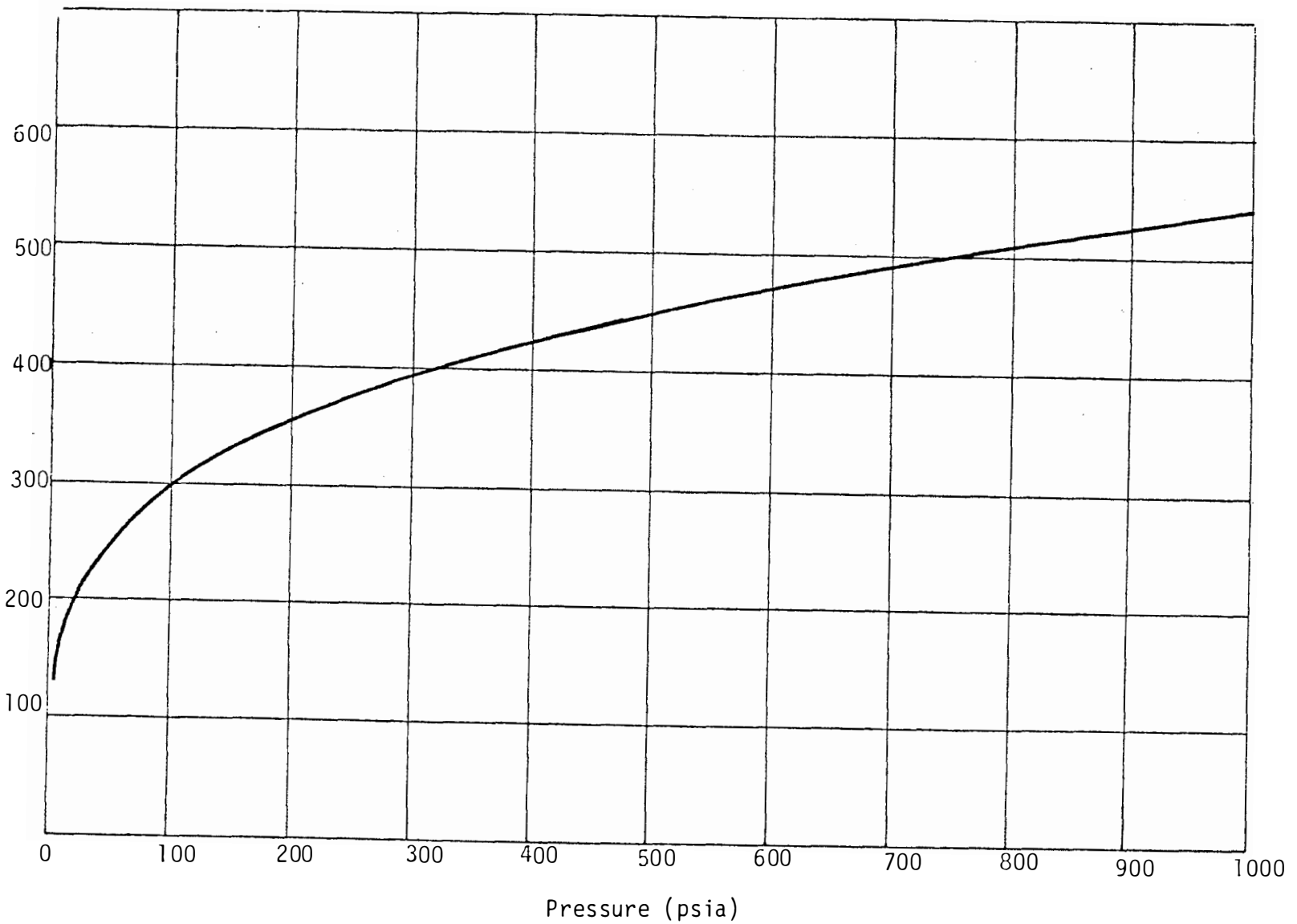

Figure A.5 Variation of h_f with Pressure.

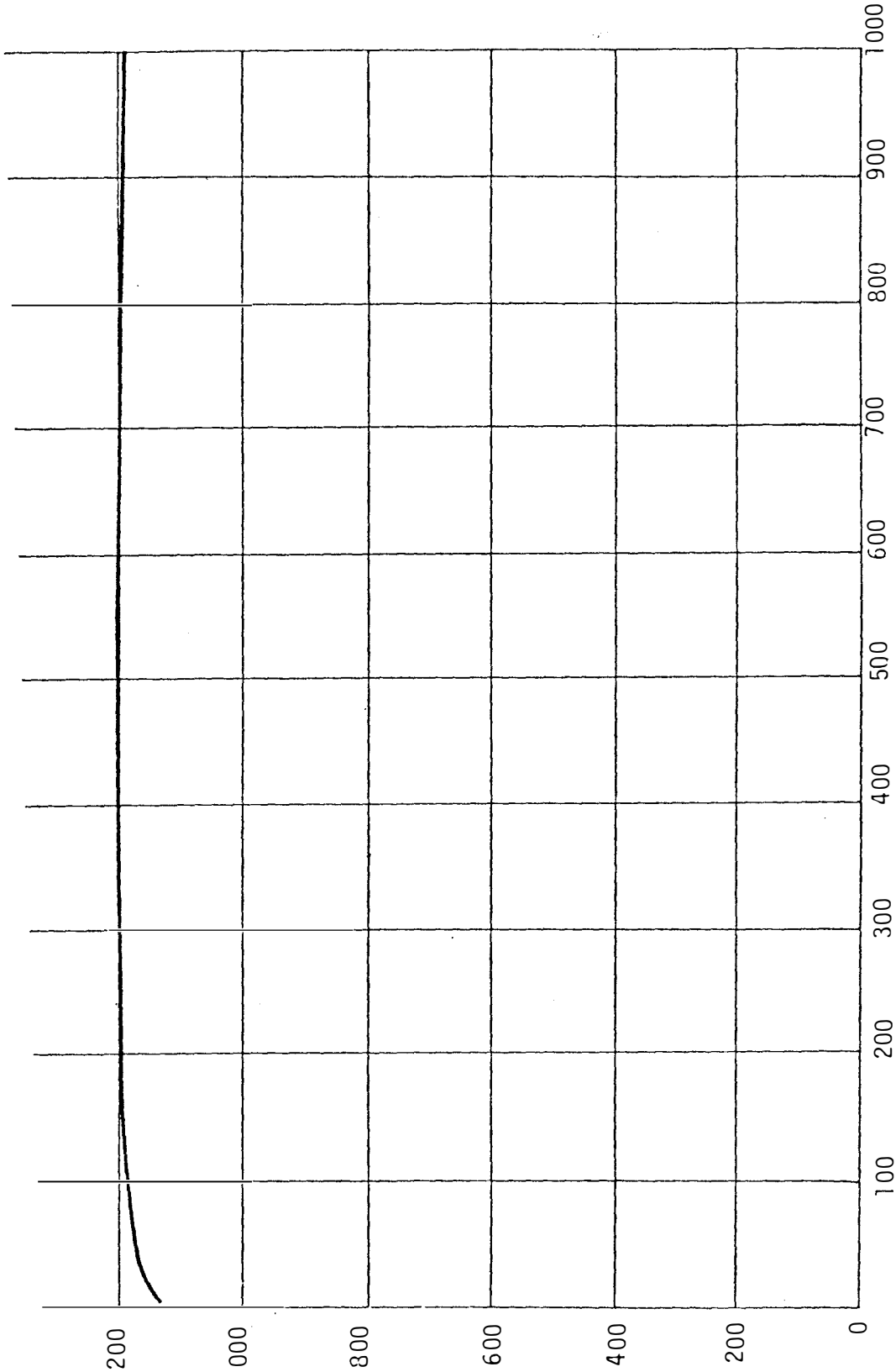

Figure A.6 Variation of h_g with Pressure.

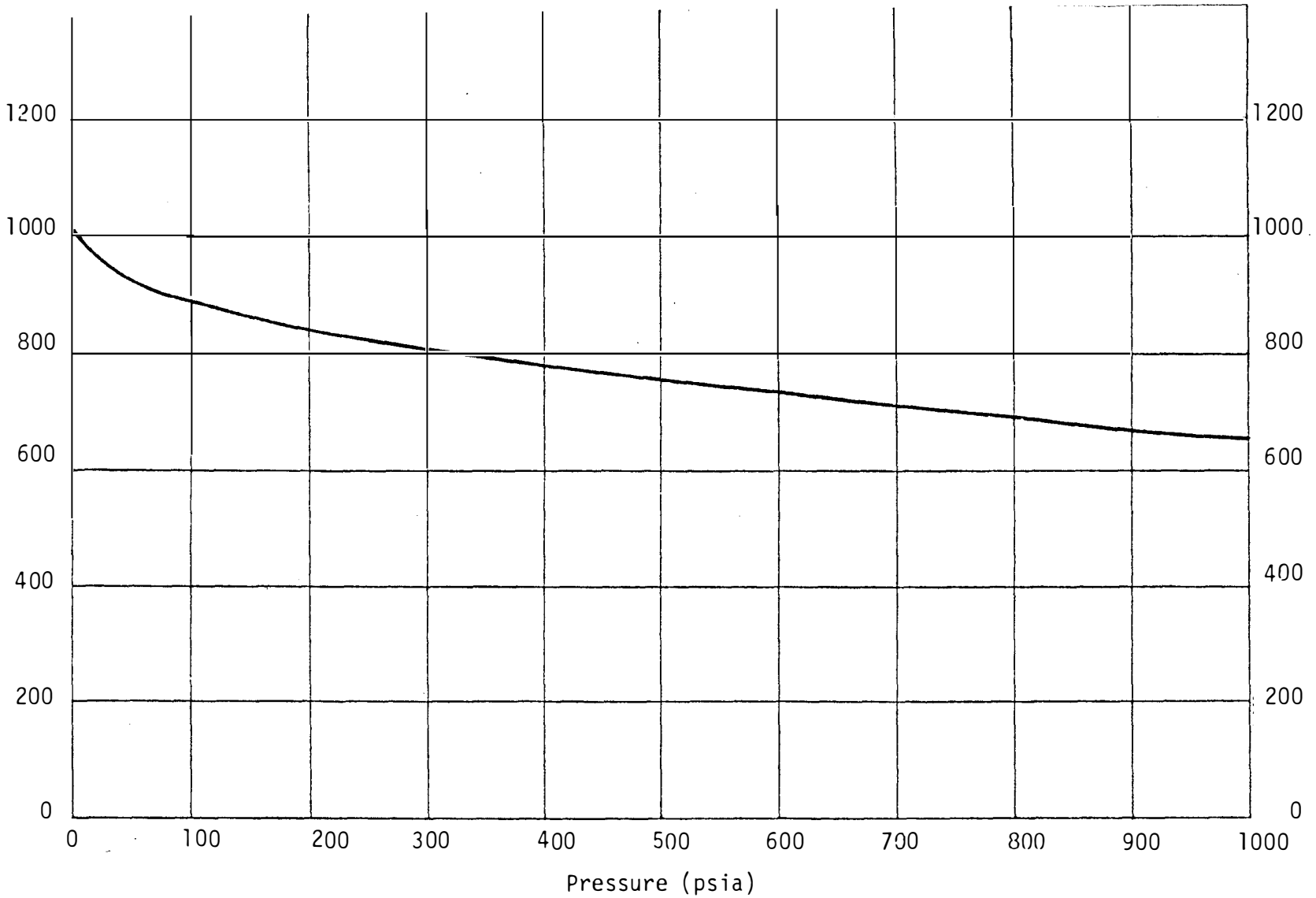

Figure A.7 Variation of h_{fg} with Pressure.

3. $\frac{\partial V_g}{\partial P} = -7.65 \times 10^{-4}$ $ft^3/lbm/psia$

4. $\frac{\partial V_{fg}}{\partial P} = -7.7 \times 10^{-4}$ $ft^3/lbm/psia$

5. $\frac{\partial h_f}{\partial P} = 0.175$ Btu/lbm/psia

6. $\frac{\partial h_g}{\partial P} = -2.7 \times 10^{-2}$ Btu/lbm/psia

7. $\frac{\partial h_{fg}}{\partial P} = -0.203$ Btu/lbm/psia.

APPENDIX B

THE CRITICAL FLOW ASSUMPTION

In the absence of a turbine model that can be used to relate the steam flow rate from the steam generator to the turbine load, some assumptions have to be made to relate the steam flow rate to other system variables and/or forcing functions.

The simplest method to achieve this relation is to leave the steam flow rate in the equations as a forcing function. This method is suitable when using the steam generator model for feedwater controller design and optimization. Another method is to relate the steam flow rate to the steam generator pressure and the turbine first stage pressure using the orifice flow equation

$$W_{so} = C_f\sqrt{P_s - P_t} \tag{B.1}$$

where

W_{so} = steam flow rate

P_s = steam generator pressure

P_t = turbine first stage pressure.

When Equation (B.1) is linearized, we get

$$\delta W_{so} = C_{f1}\,\delta P_s + C_{f2}\,\delta P_t \tag{B.2}$$

where C_{f1} and C_{f2} are constant coefficients that can be calculated from steady state conditions. From Equation (B.2), it can be seen that the steam flow rate term in the governing equations for the steam generator model is replaced by two terms. The first includes

the steam generator pressure which is one of the state variables and the other includes the turbine first stage pressure which now serves as a forcing function.

The method used in the mathematical developments in Chapter III, page 25, is to assume that the steam flow rate is determined only by the upstream (steam generator) pressure and any drop in the downstream (turbine) pressure no longer results in an increase in the steam flow rate from the steam generator. This is usually known as the "critical flow" assumption. This condition is reached when the ratio between the turbine pressure to the steam generator pressure reaches a critical value.[48] For saturated steam, this critical pressure ratio is about 0.545.[48] When the central flow assumption is used, the steam flow rated is considered to be a function of the upstream (steam generator) pressure only, thus

$$W_{so} = C_L \cdot P_s. \tag{B.3}$$

Equation (B.3) when linearized yields the following equation.

$$\delta W_{so} = C_L \, \delta P_s + P_s \, \delta C_L \tag{B.4}$$

Thus, the steam flow term is replaced by a term including the steam pressure P_s and another term involving the flow (or valve) coefficient C_L which is now taken as the forcing function.

APPENDIX C

BASIC CONSERVATION EQUATIONS FOR TWO PHASE FLOW SYSTEMS

The basic conservation equations are the building blocks in the development of dynamic models for thermal hydraulic systems. They express the storage and transport of mass, energy, and momentum which are the major factors governing the dynamic behavior of the system. In this appendix, the general statement of the basic conservation equations is given and applied to derive the mathematical expressions for the conservation equations in a one dimensional two phase flow system.

C.1 Principle of Conservation of Mass (Continuity Equation)

The principle of conservation of mass equation can be stated as follows

(Rate of increase of mass storage) = (flow in) - (flow out). (C.1)

Consider the control volume bounded by the horizontal levels (z) and (z+L) in the vertical flow system shown in Figure C.1, application of Equation (C.1) to this control volume yields the following equation

$$\frac{d}{dt}\left[\bar{\rho}\ AL\right] = W_z - W_{z+L} \qquad (C.2)$$

where

$\bar{\rho}$ = average density of the fluid in the control volume

A = cross section area

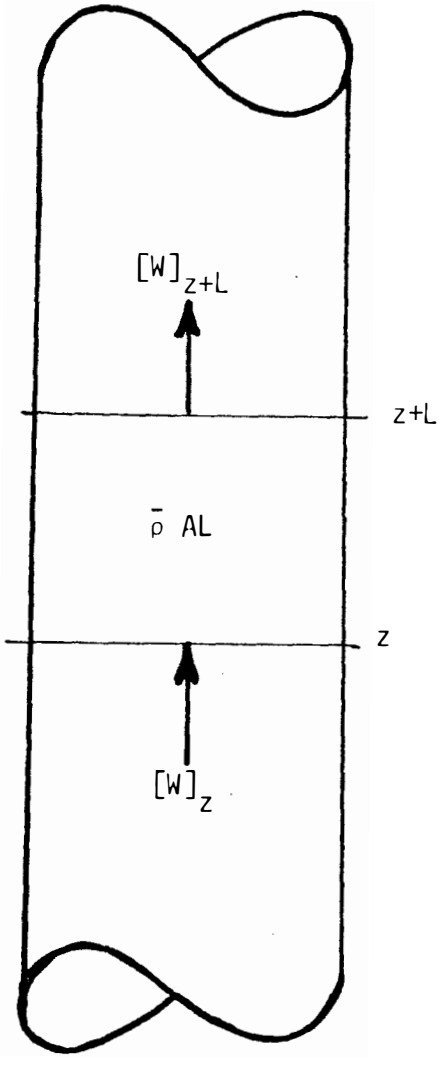

Figure C.1 Control Volume for the Application of the Continuity Equation.

L = length of the control volume

W_z = flow in

W_{z+L} = flow out.

For constant cross section area, we can divide both sides of Equation (C.2) by A to get

$$\frac{d}{dt}[\bar{\rho} L] = G_z - G_{z+L} \tag{C.3}$$

where

G_z = inlet mass velocity

G_{z+L} = outlet mass velocity.

For a homogeneous flow model, we have

$$\bar{\rho} = \frac{1}{v_f + \bar{x} v_{fg}} \tag{C.4}$$

$$G_z = \left[\frac{u}{v_f + x v_{fg}}\right]_z \tag{C.5}$$

$$G_{z+L} = \left[\frac{u}{v_f + x v_{fg}}\right]_{z+L} \tag{C.6}$$

where

v_f = specific volume of saturated water

v_g = specific volume of saturated steam

$v_{fg} = (v_g - v_f)$

$\bar{x}$ = average mass quality

u = flow velocity

x = local mass quality.

For a slip flow model, we have

$$\bar{\rho} = \rho_f(1-\bar{\alpha}) + \rho_g \bar{\alpha} \tag{C.7}$$

$$G_z = [\rho_f u_f(1-\alpha) + \rho_g u_g \alpha]_z \tag{C.8}$$

$$G_{z+L} = [\rho_f u_f(1-\alpha) + \rho_g u_g \alpha]_{z+L} \tag{C.9}$$

where

$\bar{\rho}$ = average density

$\bar{\alpha}$ = average void friction

ρ_f = density of saturated water

ρ_g = density of saturated steam

u_f = velocity of water phase

u_g = velocity of steam phase.

C.2 Principle of Conservation of Energy (Energy Equation)

The principle of conservation of energy can be stated as follows

$$\text{Rate of Creation of Energy} = 0 \tag{C.10}$$

where the term creation is defined as[49]

$$\text{Creation} = (\text{outflow}) - (\text{inflow}) + (\text{increase of storage}). \tag{C.11}$$

The application of Equation (C.10) to the control volume shown in Figure C.2, yields the following equation

$$\frac{d}{dt}[\bar{\rho}\, AL \cdot \bar{e}] = [W \cdot (e + \frac{pv}{J})]_z - [W \cdot (e + \frac{pv}{J})]_{z+L} + \dot{Q} \tag{C.12}$$

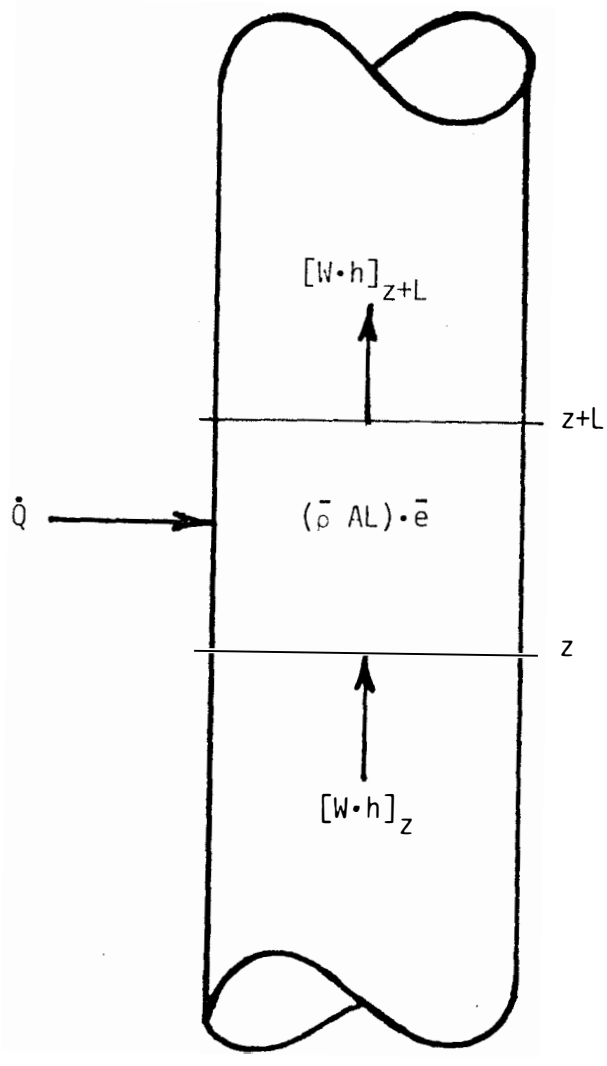

Figure C.2 Control Volume for the Application of the Energy Equation.

where

$\bar{e}$ = average internal thermal energy

e = local internal thermal energy

$\dot{Q}$ = heat input rate

$\frac{pv}{J}$ = flow work (in thermal energy units).

The combination $e + \frac{pv}{J}$ is known as the enthalpy and is denoted by h, thus, Equation (C.12) can be written in the form

$$\frac{d}{dt}[\bar{\rho}\ AL \cdot e] = [W \cdot h]_z - [W \cdot h]_{z+L} + \dot{Q}. \qquad (C.13)$$

The flow work term can be shown to be negligible compared to the enthalpy term in typical UTSG operation. Therefore, the enthalpy h can be used in both sides of Equation (C.13), thus

$$\frac{d}{dt}[\rho\ AL \cdot \bar{h}] = [W \cdot h]_z - [W \cdot h]_{z+L} + \dot{Q}. \qquad (C.14)$$

The relative importance of the flow work term for applications involving low mass quality two phase mixtures can be examined from the following example.

For P = 800 psia, we have,

h_f = 509.7 Btu/lbm

h_g = 1199.3 Btu/lbm

v_f = 0.02087 ft^3/lbm

v_g = 0.5691 ft^3/lbm

then $\frac{pv_f}{J} = \frac{800 \times 144 \times 0.02087}{778.16}$ = 3.09 Btu/lbm

$$\frac{pv_g}{J} = \frac{800 \times 144 \times 0.5691}{778.16} = 84.26 \text{ Btu/lbm}$$

and

$$\left(\frac{pv_f}{J}/h_f\right) = \frac{3.09}{509.7} = 0.00606 \text{ (or 0.606\%)}$$

$$\left(\frac{pv_g}{J}/h_g\right) = \frac{84.26}{1199.3} = 0.07026 \text{ (or 7.026\%)}$$

for a mass quality $X_e = 0.2$, the weighted error involved in using enthalpy instead of internal energy can be estimated as follows

$$\varepsilon_e = 0.8(0.606) + 0.2(7.026) = 1.89\%$$

and for an average mass quality $\bar{x} = 0.1$, we have

$$\bar{\varepsilon} = 0.9(0.606) + 0.1(7.026) = 1.25\%.$$

From the above example, it can be seen that the error involved in using the enthalpy instead of the internal energy term for UTSG applications is less than 2%.

Dividing both sides of Equation (C.14) by A, we get

$$\frac{d}{dt}[L \cdot \bar{\rho}\ \bar{h}] = [Gh]_z - (G \cdot h]_{z+L}. \qquad (C.15)$$

For the homogeneous flow model, we have

$$\bar{h} = h_f + \bar{x}(h_g - h_f) \qquad (C.16)$$

$$[h]_z = h_f + x_i(h_g - h_f) \qquad (C.17)$$

$$[h]_{z+L} = h_f + x_o(h_g - h_f). \qquad (C.18)$$

For the slip flow model

$$\bar{\rho}\bar{h} = (\rho_f(1-\bar{\alpha})\ h_f + \rho_g\ \bar{\alpha} h_g) \tag{C.19}$$

$$[hG]_z = [\rho_f(1-\alpha)\ u_f\ h_f + \rho_g\ \alpha u_g\ h_g]_z \tag{C.20}$$

$$[hG]_{z+L} = [\rho_f(1-\alpha)\ u_f\ h_f + \rho_g\ \alpha u_g\ h_g]_{z+L}. \tag{C.21}$$

C.3 The Momentum Principle (Momentun Equation)

The momentum equation can generally be stated as follows.

"Rate of momentum accumulation in a control volume is equal to the net rate at which momentum flows into the control volume plus the sum of the surface and body forces acting upon the control volume."

When the above statement is applied to the control volume shown in Figure C.3, we obtain the following mathematical expressions for the momentum equation

$$A\frac{d}{dt}[L\ \bar{\rho}\bar{u}] = A[\rho u^2 + P]_z - A[\rho u^2 + P]_{z+L}$$

$$- \bar{\tau}_\omega\ P_{\gamma\omega}\ L - g\ \bar{\rho}\ AL \tag{C.22}$$

where

$\bar{u}$ = average velocity of the fluid in the control volume

$\bar{\tau}_\omega$ = wall sheer stress

$P_{\gamma\omega}$ = wall wetted parameter

g = acceleration due to gravity

and other terms are as defined before.

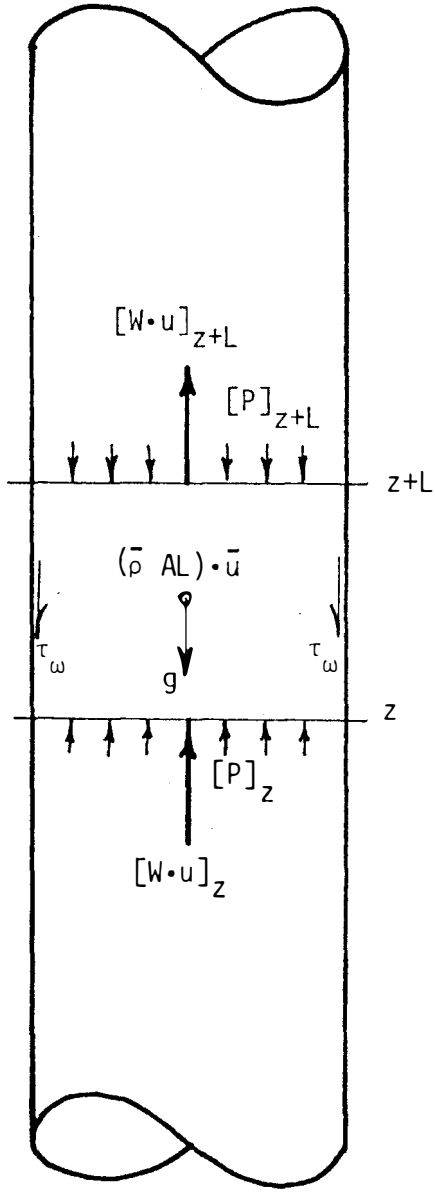

Figure C.3 Control Volume for the Application of the Momentum Equation.

In the current application, the momentum equation is used in its steady state form (no time derivative) to calculate the secondary fluid mass flow rate at the entrance of the tube bundle region as described in Appendix D.

APPENDIX D

RECIRCULATION LOOP EQUATION

The mass flow rate of the secondary fluid entering the tube bundle region from the downcomer section (W_1) is considered as an inlet condition for the solution of the mass and energy balance equations in the effective heat exchange region. The relation between W_1 and other state variables in the UTSG model is derived here using the assumption that the net pressure drop along the recirculation loop is equal to zero during the transient. This assumption means that the driving static head due to the difference in density between the downcomer section and the tube bundle region is equal to the total dynamic head loss along the recirculation loop. That is

$$\Delta P_d = \Delta P_f + \Delta P_a \qquad (D.1)$$

where,

ΔP_d = static pressure drop along the loop

ΔP_f = frictional pressure drop along the loop

ΔP_a = acceleration pressure drop along the loop.

Since the friction and acceleration pressure drops are proportional to the square of the mass flow rate, then Equation (D.1) can be written as

$$\Delta P_d = C_d W_1^2 \qquad (D.2)$$

where

C_d = effective dynamic head loss coefficient.

Solving Equation (D.2) for W_1, we get

$$W_1 = \frac{1}{\sqrt{C_d}} \sqrt{\Delta P_d} \ . \tag{D.3}$$

Let $C_1 = \frac{1}{\sqrt{C_d}}$, then

$$W_1 = C_1 \sqrt{\Delta P_d} \ . \tag{D.4}$$

Referring to Figure D.1, we have

$$\Delta P_d = \frac{\rho_d(L_{dw}+L_d) - \rho_{S1}L_{S1} - L_b\rho_b - L_r\rho_r}{144} \text{ psia} \tag{D.5}$$

where

ρ_d = density in the downcomer section

L_{dw} = drum water level

L_d = downcomer length

ρ_{S1} = density of the secondary fluid in the subcooled region

L_{S1} = length of the subcooled region

ρ_b = density in the secondary fluid in the boiling region

L_b = length of the boiling region

L_r = effective length of the riser/separator volume

ρ_f = density of the secondary fluid in the riser/separator volume.

Since the density of the subcooled liquid in the downcomer region is nearly equal to the density in the subcooled region, then Equation (D.5) can be written as follows

$$\Delta P_d = \frac{\rho_d(L_{dw}+L_d-L_{S1}) - L_b\rho_b - L_r\rho_r}{144} \ . \tag{D.6}$$

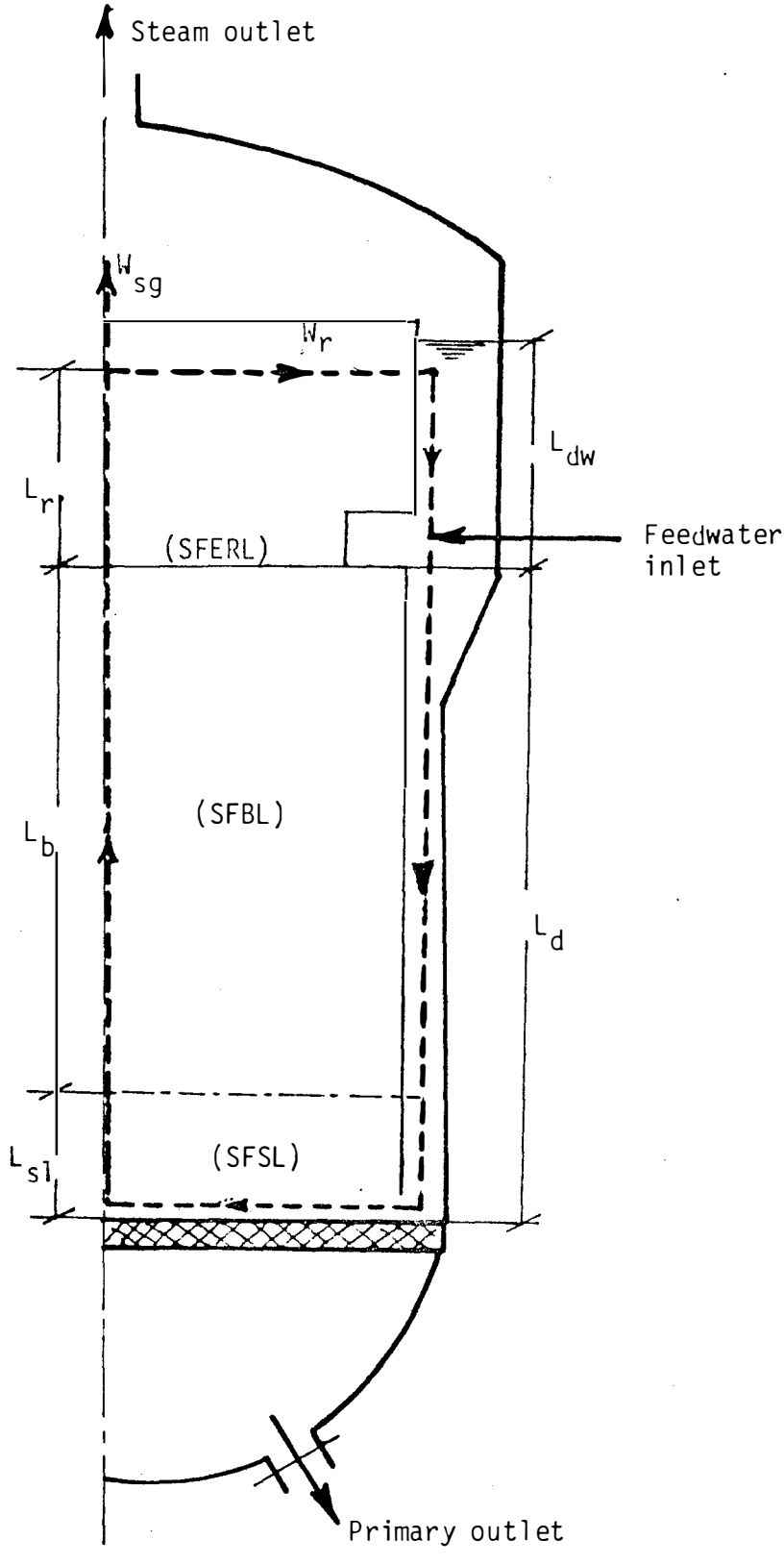

Figure D.1 Calculation of the Driving Pressure Head for the Recirculation Loop.

Substituting from Equation (D.6) into Equation (D.4), we get

$$W_1 = \frac{C_1}{12} (\rho_d(L_{dw}+L_d-L_{S1}) - L_b\rho_b - L_r\rho_r)^{1/2}. \qquad (D.7)$$

The deviation of W_1 from steady state can be obtained from Equation (D.7) as follows

$$\delta W_1 = \frac{C_1}{24R} \{\rho_d(\delta L_{dw}-\delta L_{S1}) - (\rho_b L_b+L_b\delta\rho_b) - L_r\delta\rho_r\} \qquad (D.8)$$

where

$$R = (\rho_d(L_{dw}+L_d-L_{S1}) - L_b\rho_b - L_r\rho_r)^{1/2}. \qquad (D.9)$$

The deviation in the two-phase density in the boiling region and in the riser/separator volume can be expressed as (see Appendix E)

$$\delta\rho_b = C_{1b}\ \delta P + C_{2b}\ \delta X_e \qquad (D.10)$$

and

$$\delta\rho_r = C_{1r}\ \delta P + C_{2r}\ \delta X_e. \qquad (D.11)$$

When Equations (D.10) and (D.11) are substituted into Equation (D.8), we get

$$\delta W_1 = a_1\ \delta L_{dw} + a_2\ \delta L_{S1} + a_3\ \delta P + a_4\ \delta L_{S1} \qquad (D.12)$$

where

$$a_1 = \frac{C_1\ \rho_d}{24R}$$

$$a_2 = -\frac{C_1(\rho_d-\rho_b)}{24R}$$

$$a_3 = -\frac{C_1(C_{1b}L_b+C_{1r}L_r)}{24R}$$

$$a_4 = -\frac{C_1(C_{2b}L_b+C_{2r}L_r)}{24R} \quad .$$

APPENDIX E

AVERAGE DENSITY IN THE TWO-PHASE REGION

An expression for the density in the two-phase region, in terms of system pressure and bubble population in the two-phase mixture, is necessary for the solution of the describing equations in the two phase secondary fluid lumps.

In the slip flow model, the bubble population is represented by the void fraction α defined by the equation

$$\alpha = \frac{A_g}{A} \tag{E.1}$$

where

α = void fraction

A_g = area occupied by the vapor phase

A = total flow area.

The density of the two-phase mixture is given by[44]

$$\rho = \alpha \rho_g + (1-\alpha) \rho_f \tag{E.2}$$

where

ρ = two-phase mixture density

ρ_f = density of the liquid phase (water)

ρ_g = density of the vapor phase (steam).

Assuming that ρ_f and ρ_g are linear functions of system pressure P_s (see Appendix A, page 206) differentiating Equation (E.2) and linearizing gives

$$\frac{d\delta\rho}{dt} = \frac{\partial\rho_f}{\partial P}\frac{d\delta P}{dt} - \left[\alpha\left(\frac{\partial\rho_f}{\partial P} - \frac{\partial\rho_g}{\partial P}\right)\delta P + (\rho_f-\rho_g)\frac{d\delta\alpha}{dt}\right]. \qquad (E.3)$$

Neglecting the change in liquid phase density with pressure, we have

$$\frac{d\delta\rho}{dt} = \frac{\partial\rho_g}{\partial P}\frac{d\delta P}{dt} - (\rho_f-\rho_g)\frac{d\delta\alpha}{dt}. \qquad (E.4)$$

The perturbation equation for the two phase mixture density can be written as

$$\delta\rho = \frac{\partial\rho_g}{\partial P}\delta P - (\rho_f-\rho_g)\delta\alpha. \qquad (E.5)$$

Equation (E.5) relates the perturbations in ρ with the perturbation in P and α.

In the homogeneous flow model, we have[49]

$$\rho = \frac{1}{v_f+x(v_g-v_f)} \qquad (E.6)$$

where

ρ = density of the two phase mixture

v_f = specific volume of liquid phase

v_g = specific volume of vapor phase

x = mass quality = $\frac{\text{mass flow note of vapor phase}}{\text{total mass flow rate}}$.

Differentiating Equation (E.6) gives

$$\frac{d\delta\rho}{dt} = \frac{-1}{[v_f+x(v_g-v_f)]^2}\left\{\left(\frac{\partial v_f}{\partial P} + x\frac{\partial v_{fg}}{\partial P}\right)\frac{d\delta P}{dt} + v_{fg}\frac{d\delta x}{dt}\right\} \qquad (E.7)$$

where

$$v_{fg} = (v_g - v_f).$$

If we neglect the change in v_f with pressure, the perturbation equation for the two phase mixture density can be written as

$$\delta\rho = \frac{-1}{(v_f + x\, v_{fg})^2} \{x \frac{\partial v_{fg}}{\partial P} \delta P + v_{fg}\, \delta x\}. \qquad (E.8)$$

In the boiling secondary fluid lump, we have $x = \bar{x} = \frac{x_e}{2}$ and Equation (E.8) becomes

$$\delta\rho_b = \frac{-1}{(v_f + \bar{x}\, v_{fg})^2} \{\bar{x} \frac{\partial v_{fg}}{\partial P} \delta P + \frac{v_{fg}}{2} \delta x_e\}. \qquad (E.9)$$

Equation (E.9) can be written in the simple form

$$\delta\rho_b = C_{1b}\, \delta P + C_{2b}\, \delta x_e \qquad (E.10)$$

where

$$C_{1b} = \frac{-\bar{x}}{(v_f + \bar{x}\, v_{fg})^2} \left.\frac{\partial v_{fg}}{\partial P}\right|_{s_{sl}}$$

and

$$C_{2b} = \left.\frac{-v_{fg}}{2(v_f + \bar{x}\, v_{fg})^2}\right|_{s_s}.$$

In the riser/separator lump $x = x_e$ and Equation (E.8) becomes

$$\delta\rho_r = \frac{-1}{(v_f + x_e v_{fg})^2} \{x_e \frac{\partial v_{fg}}{\partial P} + v_{fg}\, \delta x_e\}. \qquad (E.11)$$

Equation (E.11) can be written in the simple form

$$\delta\rho_r = C_{1\gamma}\,\delta P + C_{2\gamma}\,\delta x_e$$

where

$$C_{1\gamma} = \frac{-x_e}{(v_f + x_e\, v_{fg})^2} \cdot \left.\frac{\partial v_{fg}}{\partial P}\right|_{ss}$$

and

$$C_{2\gamma} = \left.\frac{-v_{fg}}{(v_f + x_e\, v_{fg})^2}\right|_{ss}.$$

When using the above expressions, it is understood that the unperturbed parameters are calculated at the steady state conditions corresponding to the system pressure, even when the subscript (ss.) is not shown in the expression for these parameters.

APPENDIX F

SUMMARY OF DYNAMIC RESPONSE RESULTS

In Chapter IV, page 141, the step response of the four UTSG dynamic models to a steam valve perturbation was presented for models comparison. In this appendix, a summary of the dynamic response of the four models to all anticipated perturbations is presented for future reference. The four models are designated as follows:

Model A: Simplified model

Model B: First intermediate model

Model C: Second intermediate model

Model D: Detailed model.

The input perturbations are

1. Primary inlet temperature perturbation
2. Feedwater temperature perturbation
3. Steam valve perturbation.

Table F.1 gives the case identifications and Figures F.1 through F.12 show the results of the dynamic response for these cases.

TABLE F.I

SUMMARY OF DYNAMIC RESPONSE RESULTS

Case No.	Model	Perturbations	Figure
A-1	A	1	F-1
A-2	A	2	F-2
A-3	A	3	F-3
B-1	B	1	F-4
B-2	B	2	F-5
B-3	B	3	F-6
C-1	C	1	F-7
C-2	C	2	F-8
C-3	C	3	F-9
D-1	D	1	F-10
D-2	D	2	F-11
D-3	D	3	F-12

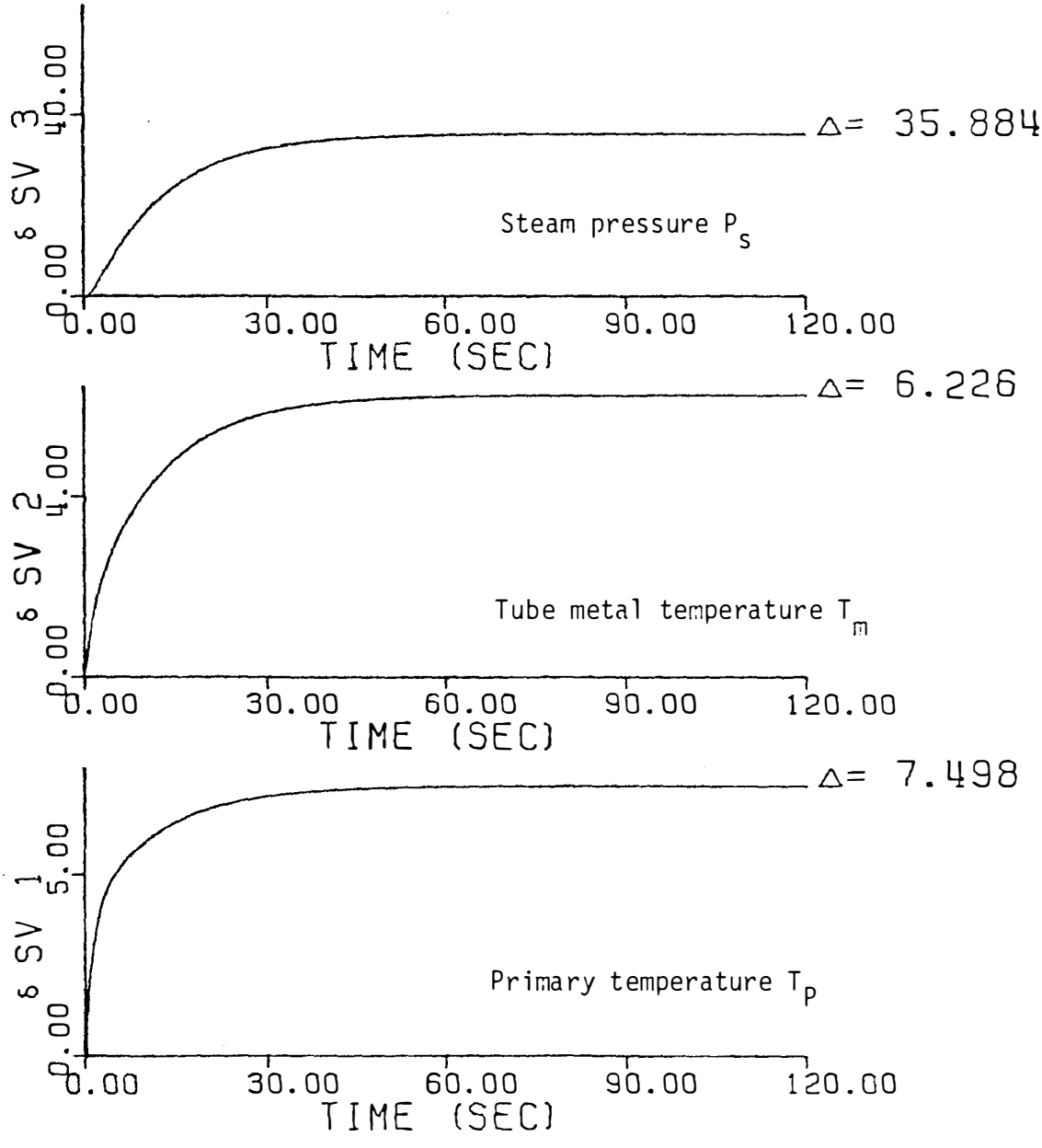

Figure F.1 Step Response for Case A.1.

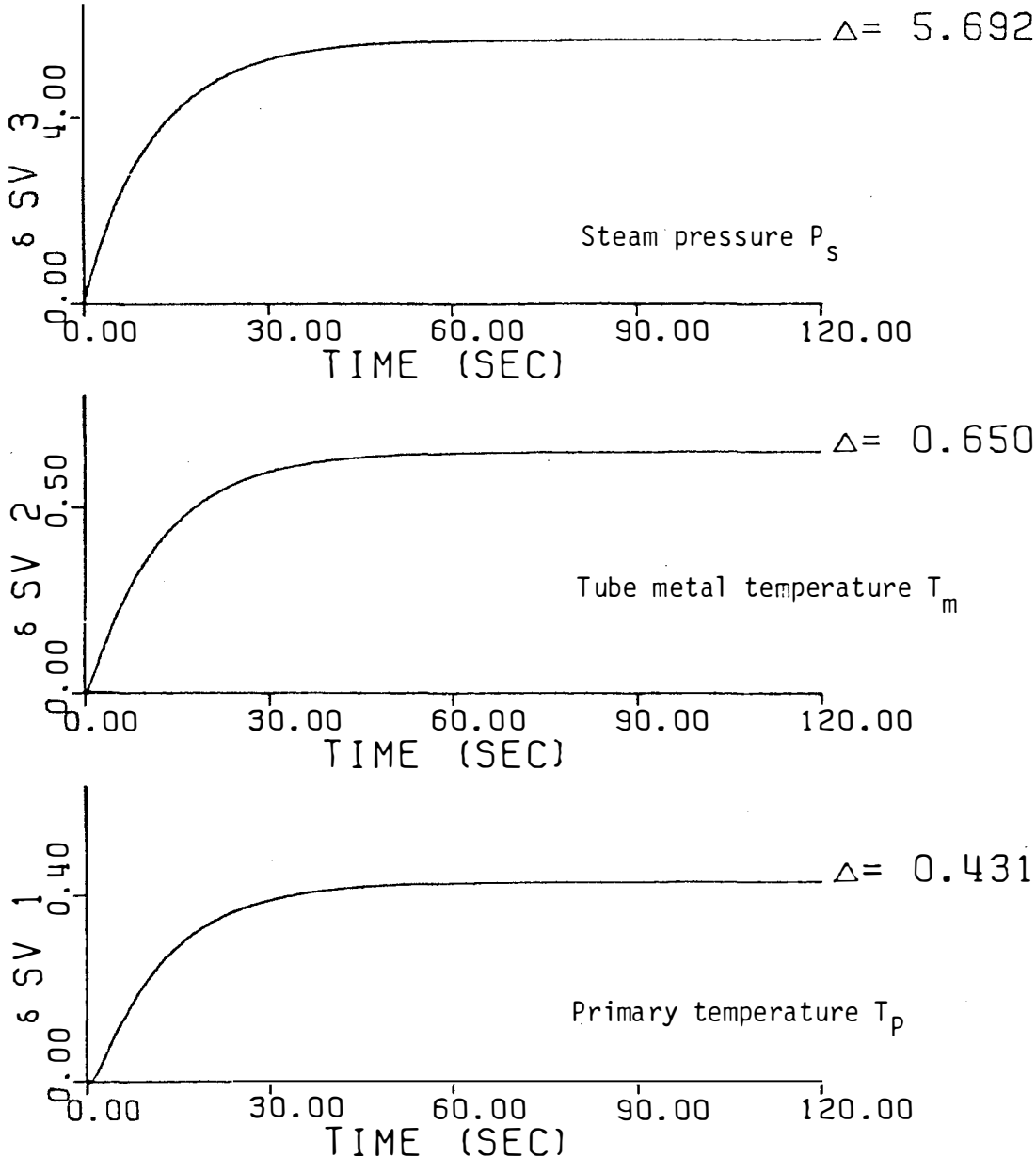

Figure F.2 Step Response for Case A.2.

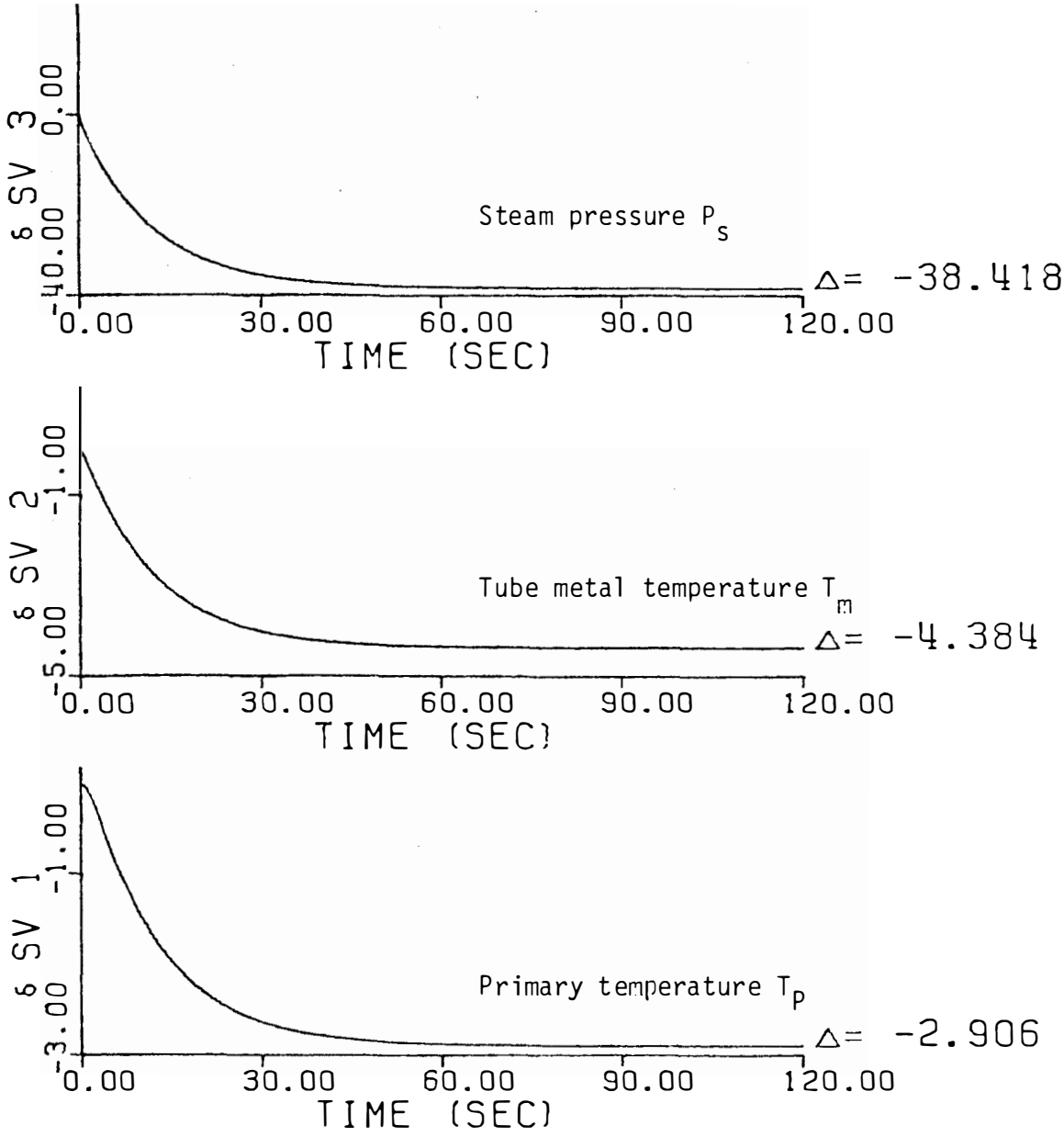

Figure F.3 Step Response for Case A.3.

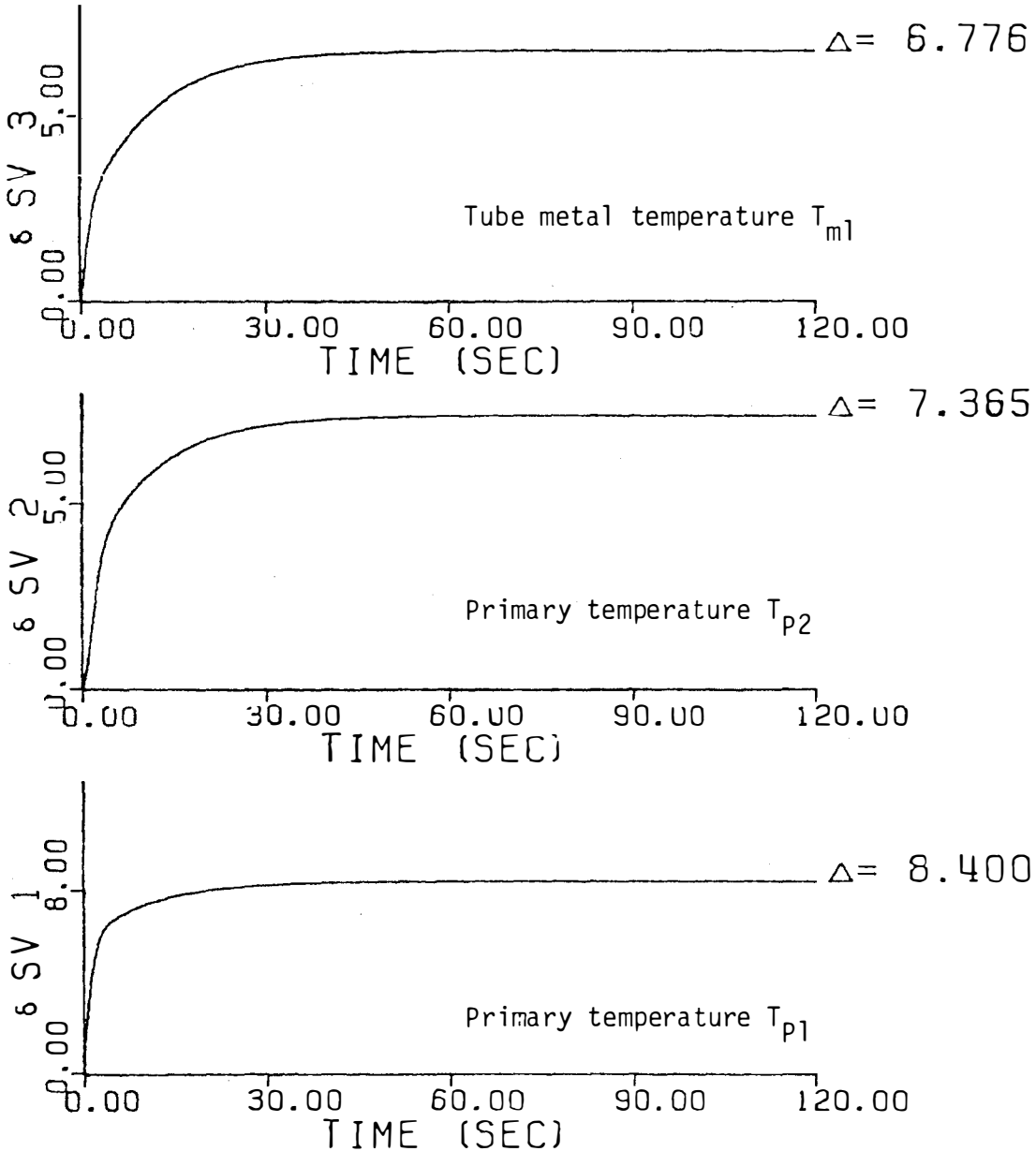

Figure F.4 Step Response for Case B.1.

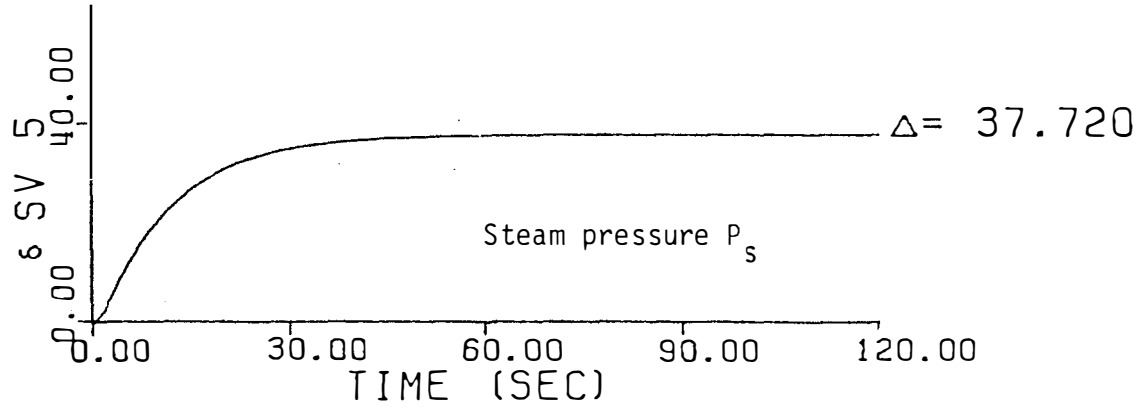

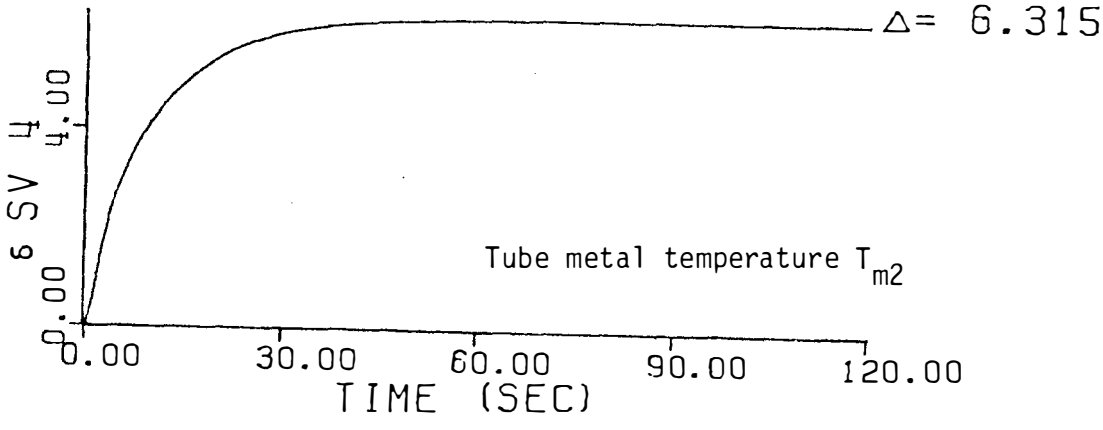

Figure F.4 (Continued).

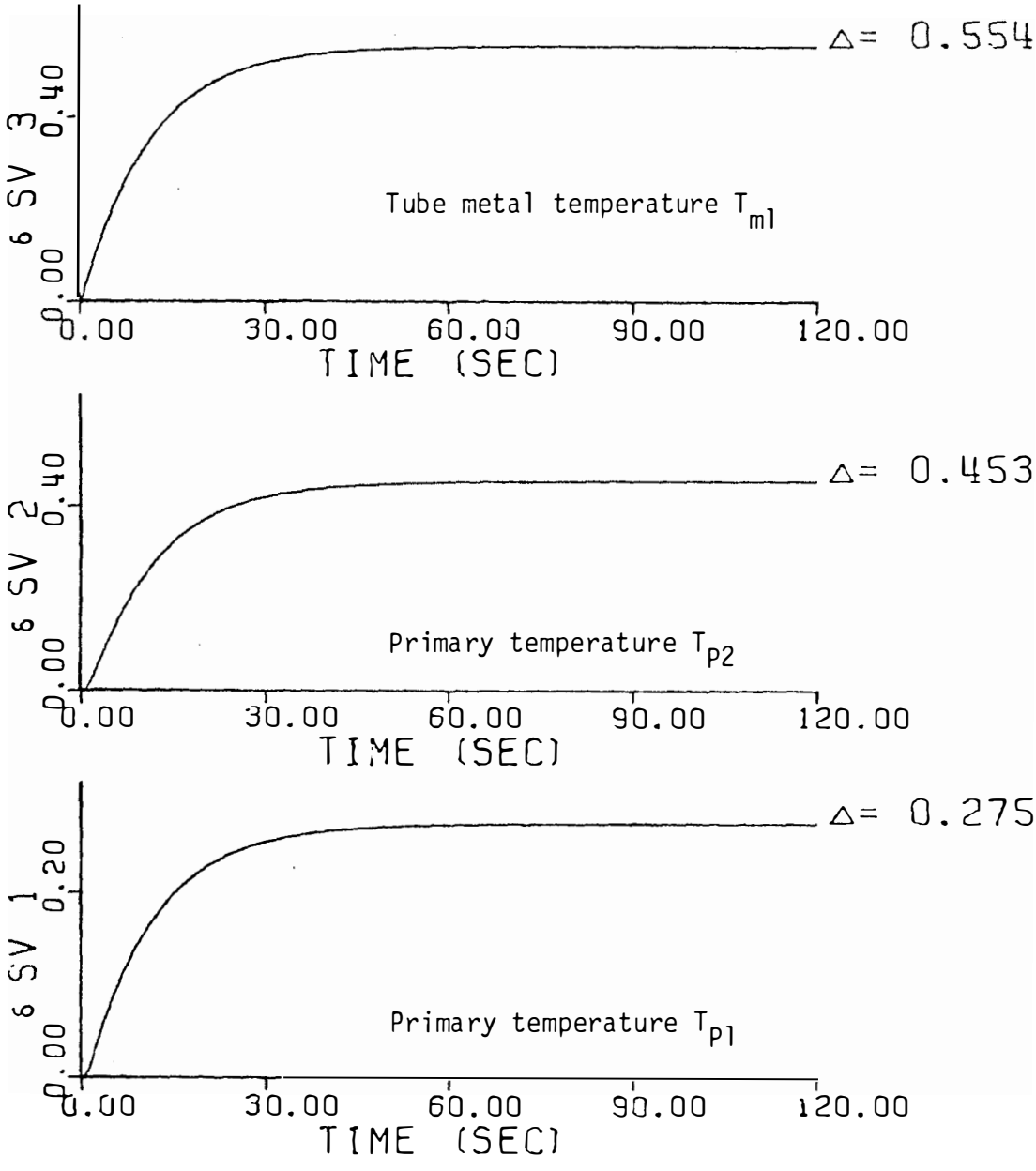

Figure F.5 Step Response for Case B.2.

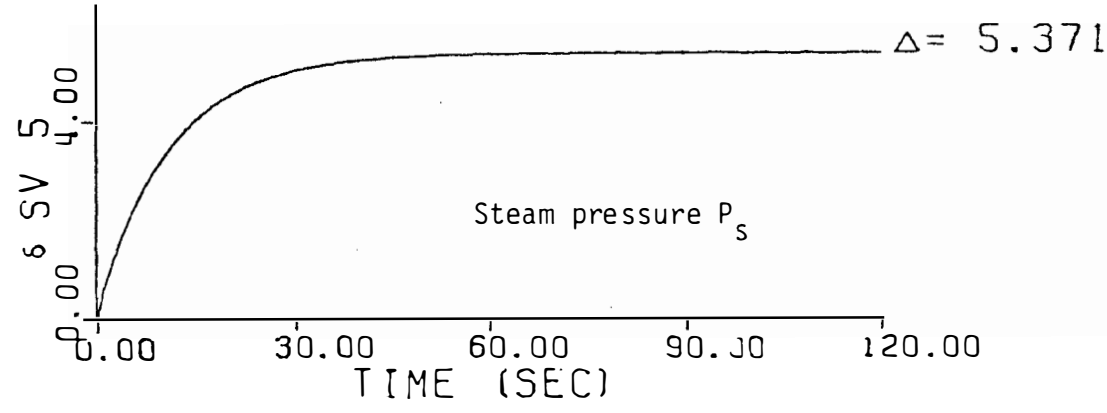

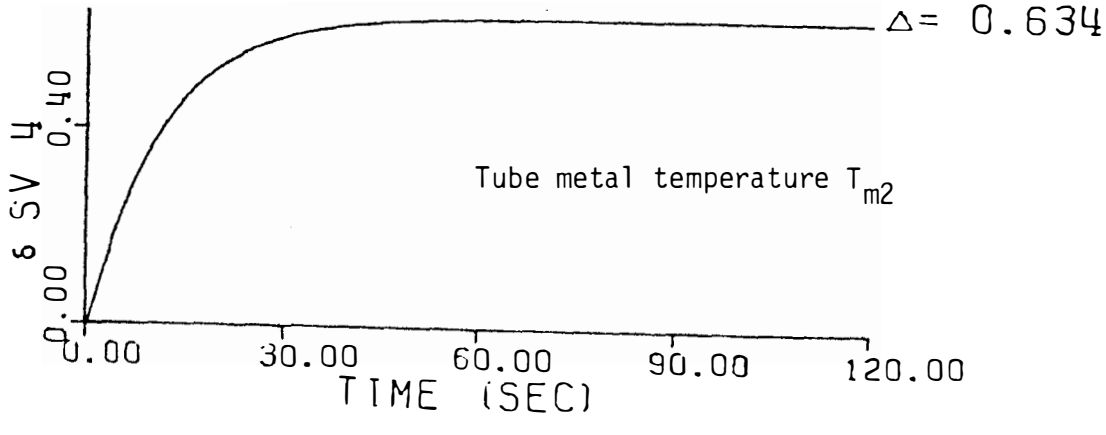

Figure F.5 (Continued).

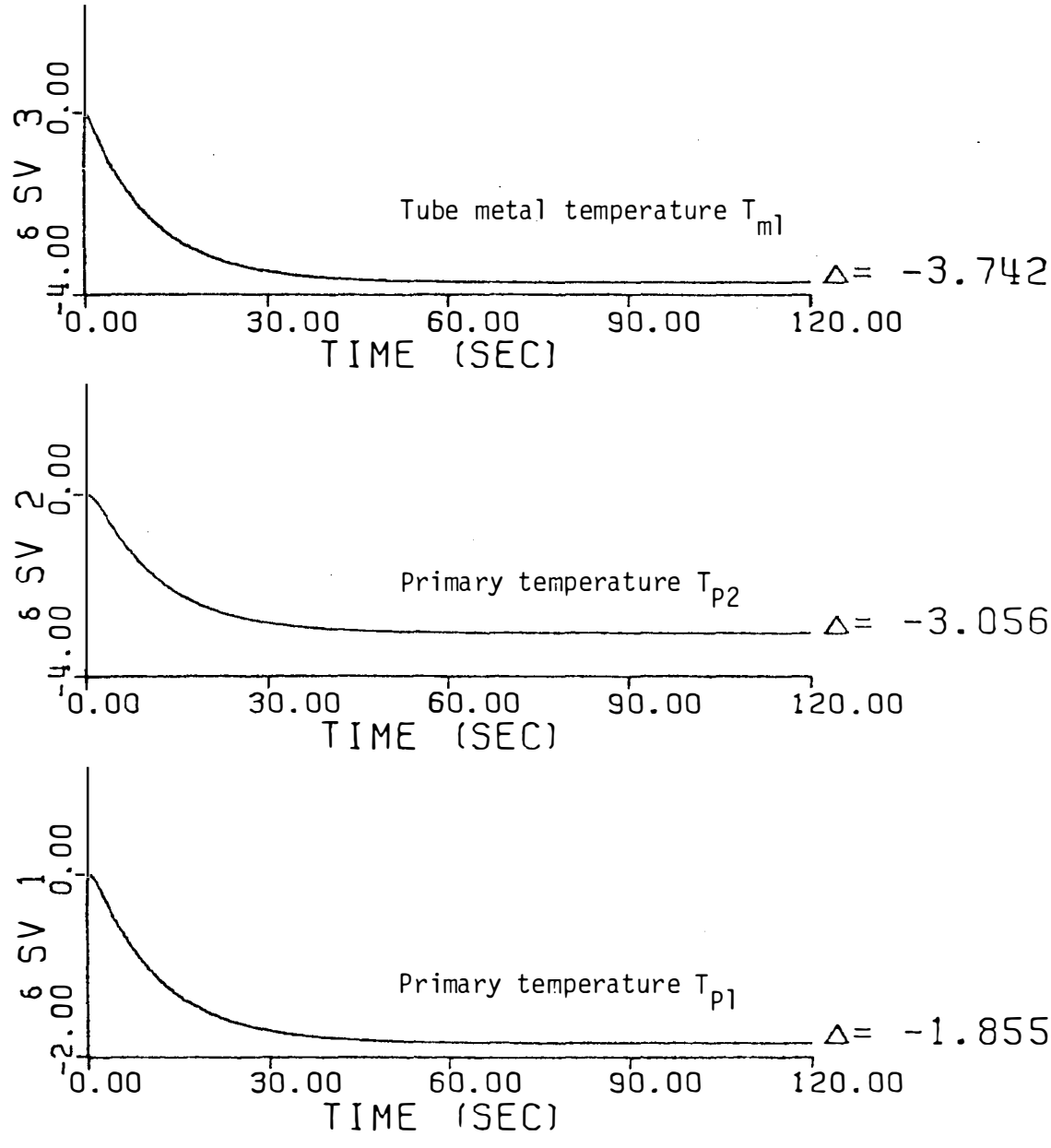

Figure F.6 Step Response for Case B.3.

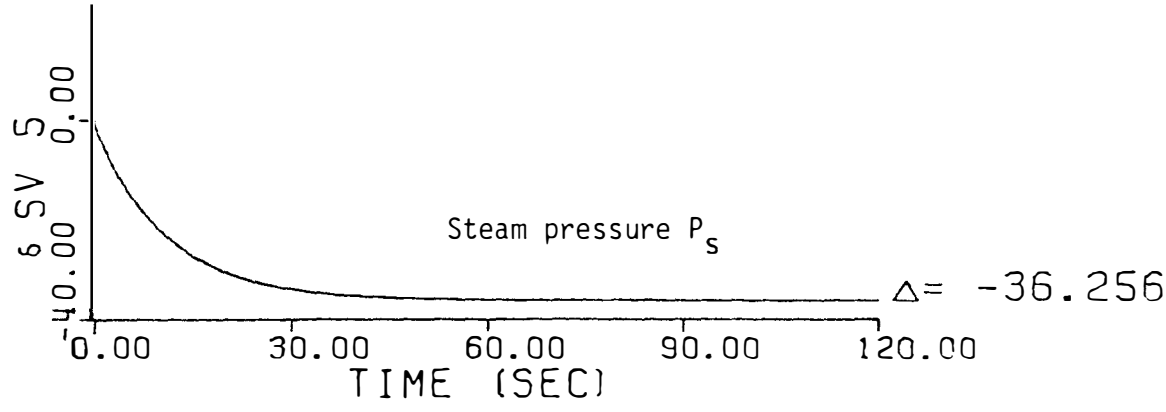

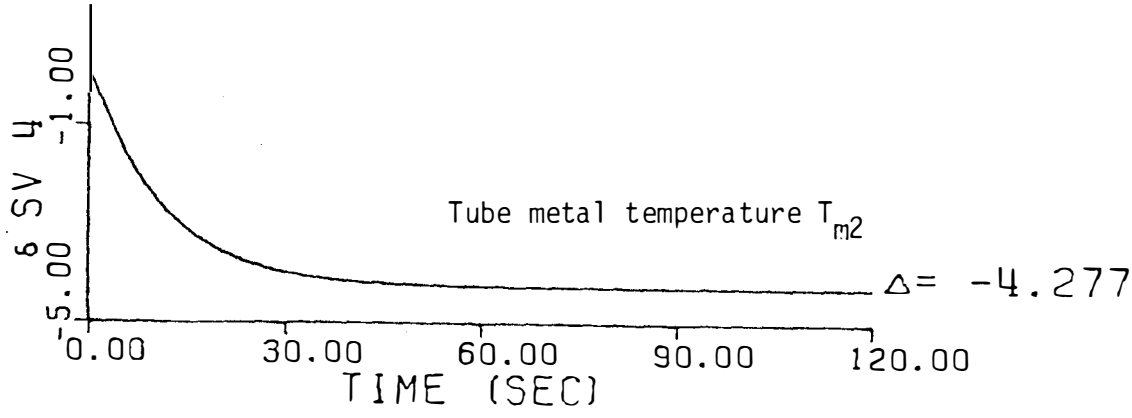

Figure F.6 (Continued).

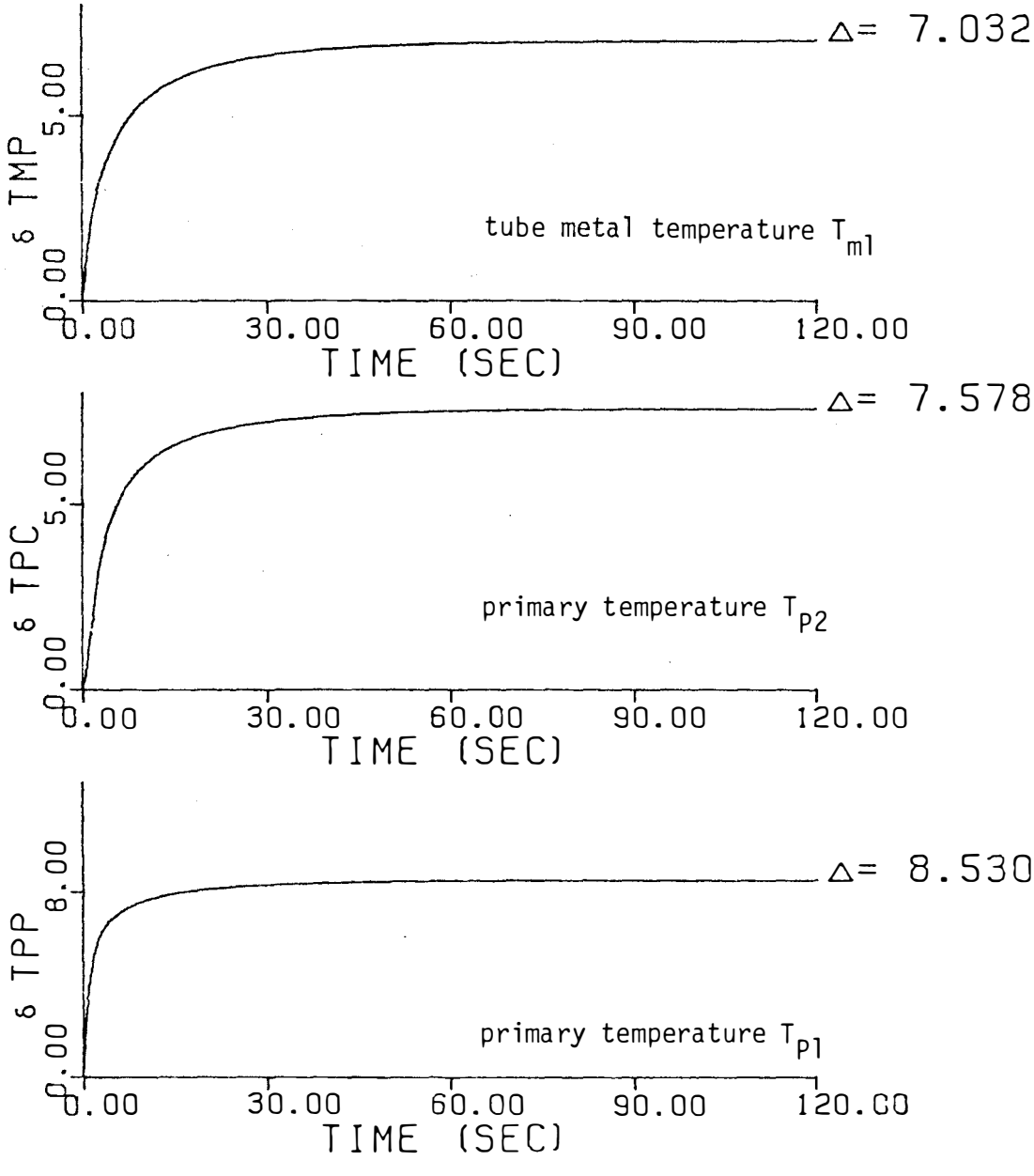

Figure F.7 Step Response for Case C.1.

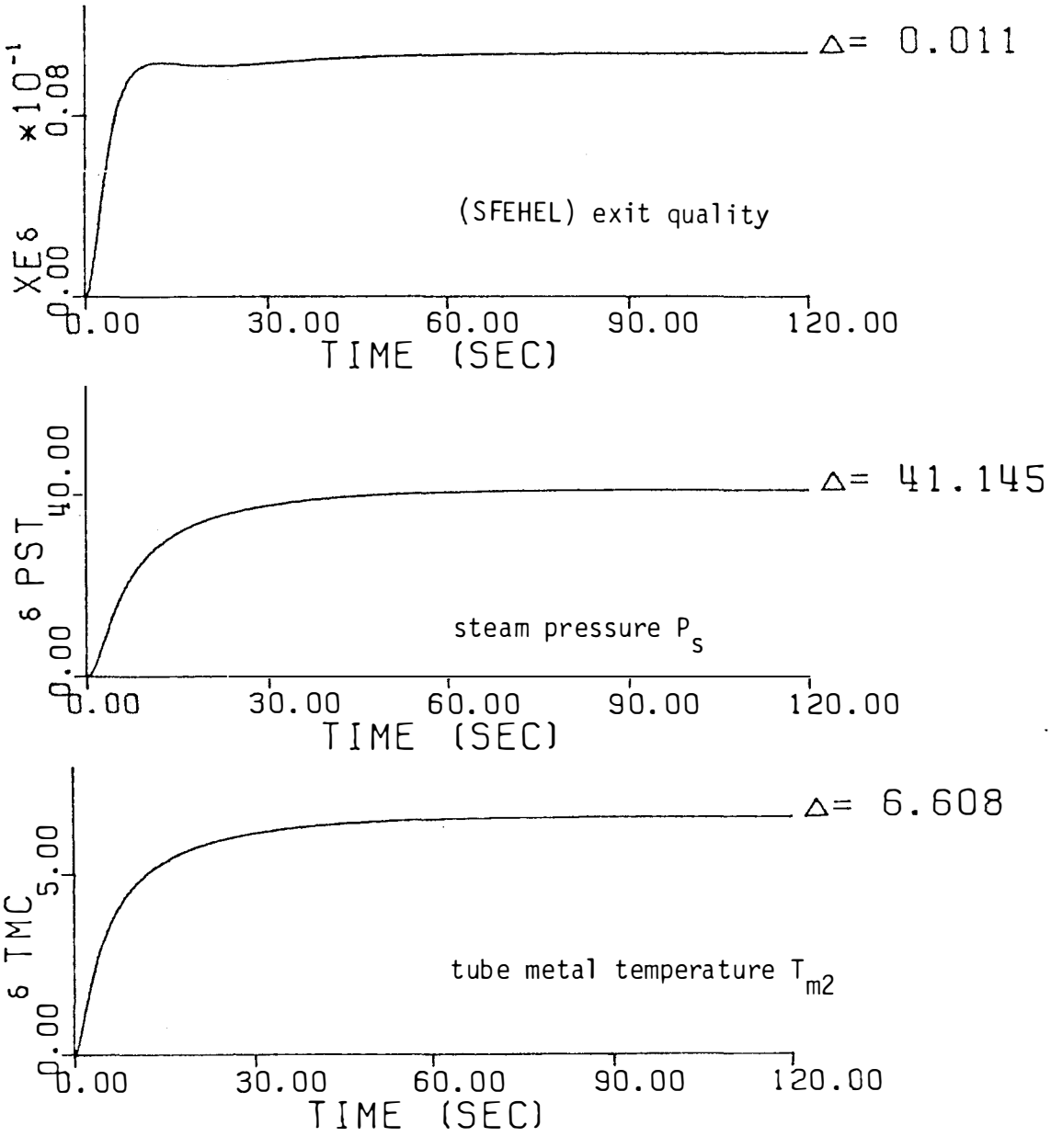

Figure F.7 (Continued).

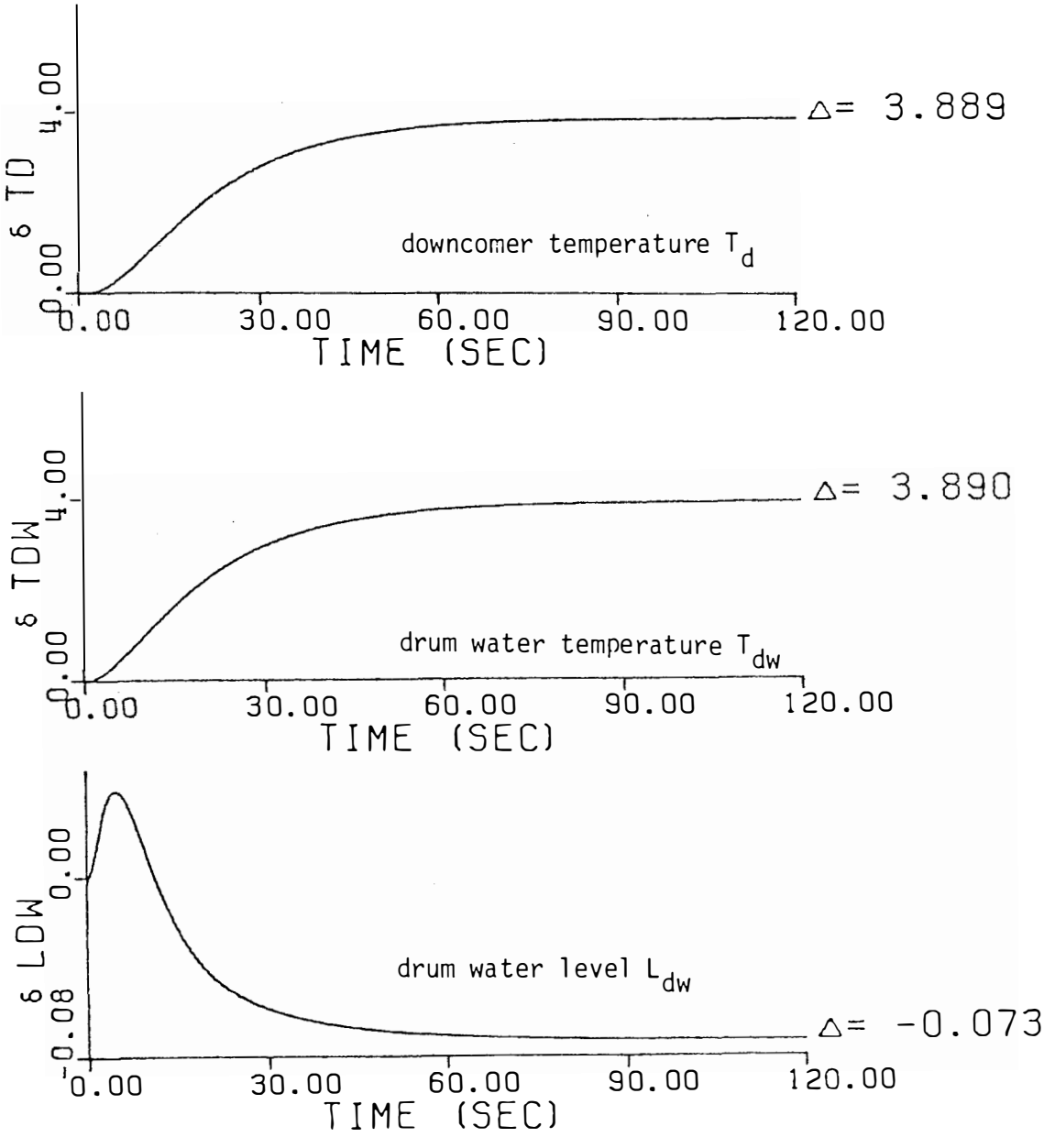

Figure F.7 (Continued).

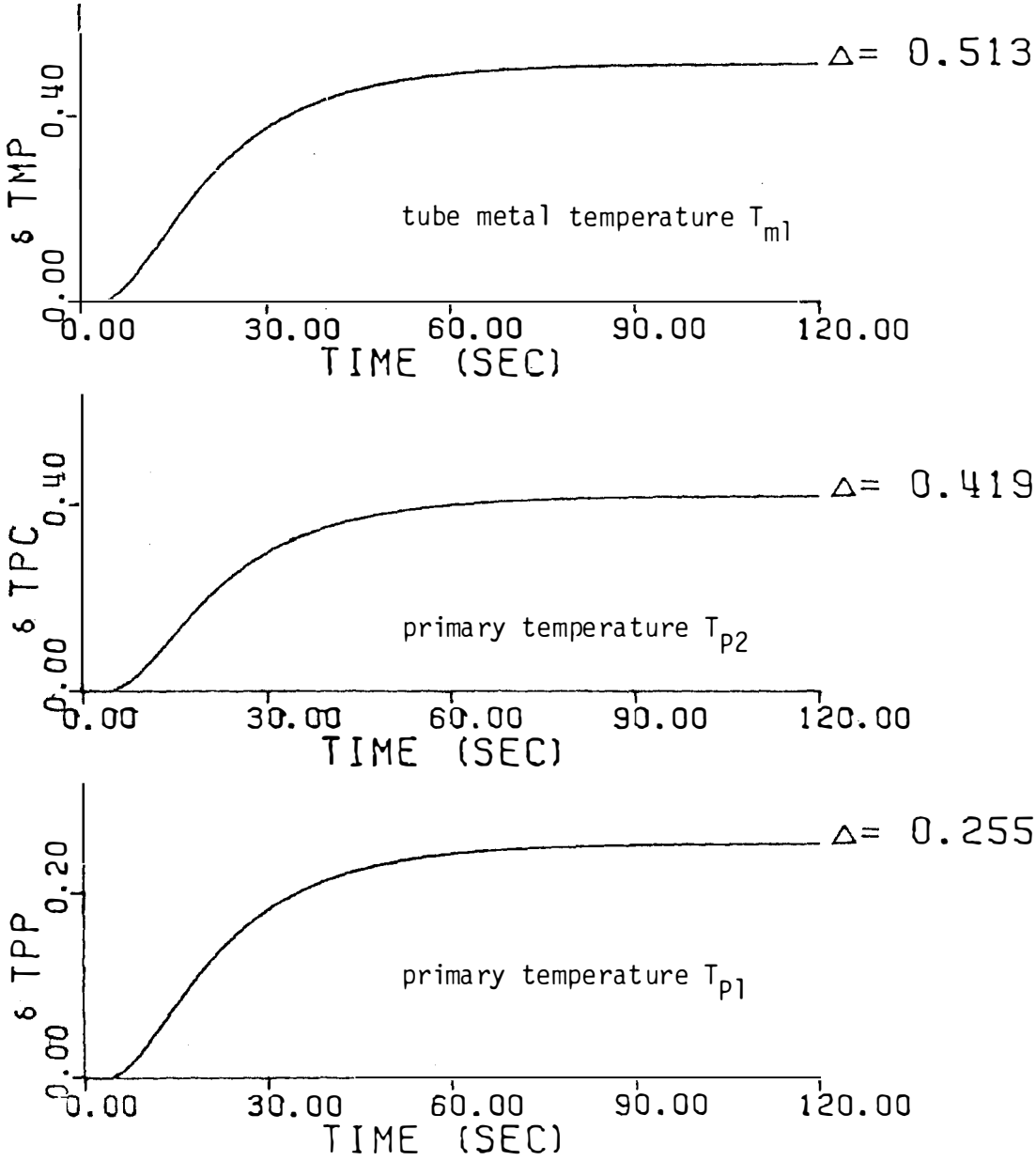

Figure F.8 Step Response for Case C.2.

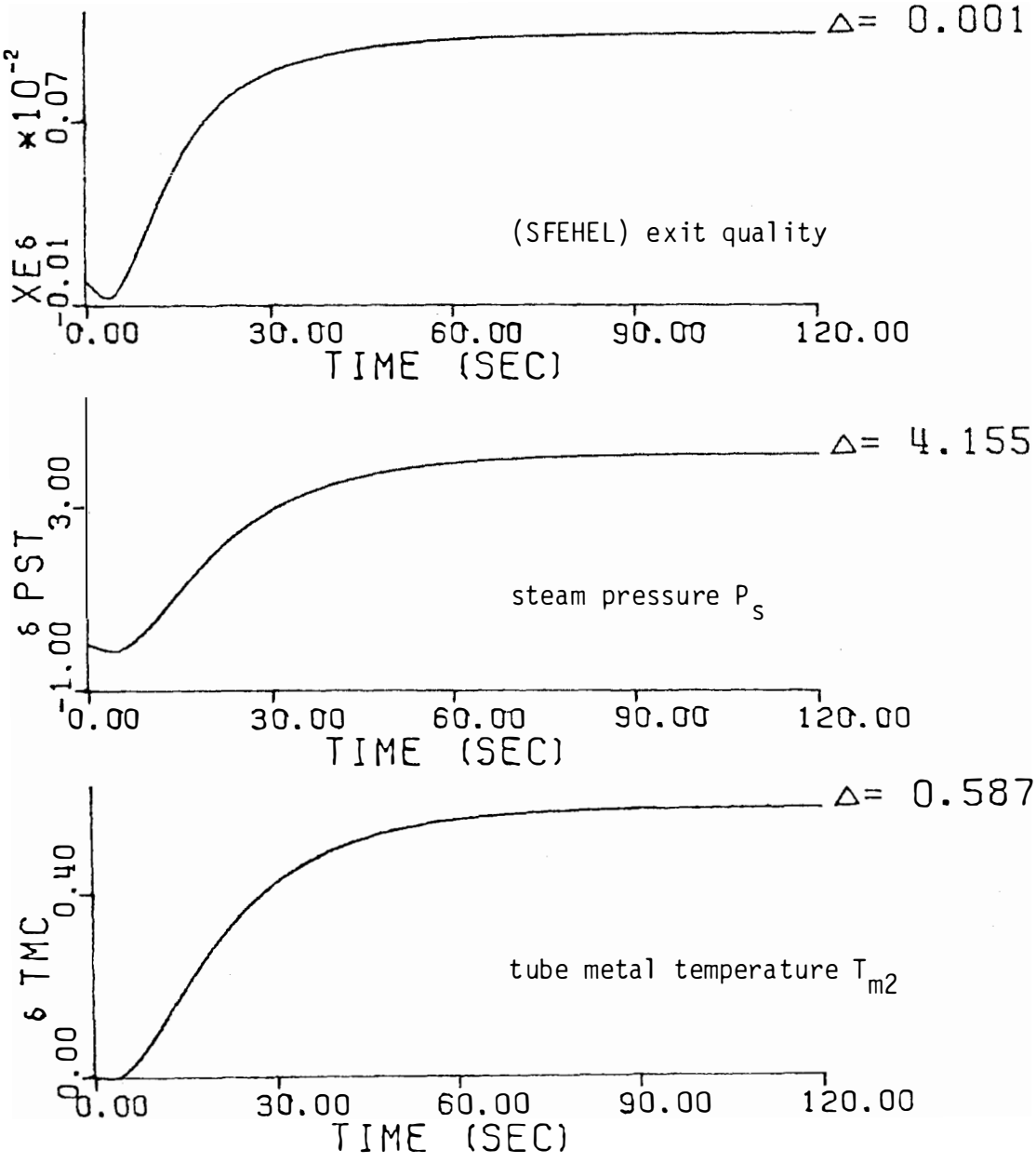

Figure F.8 (Continued).

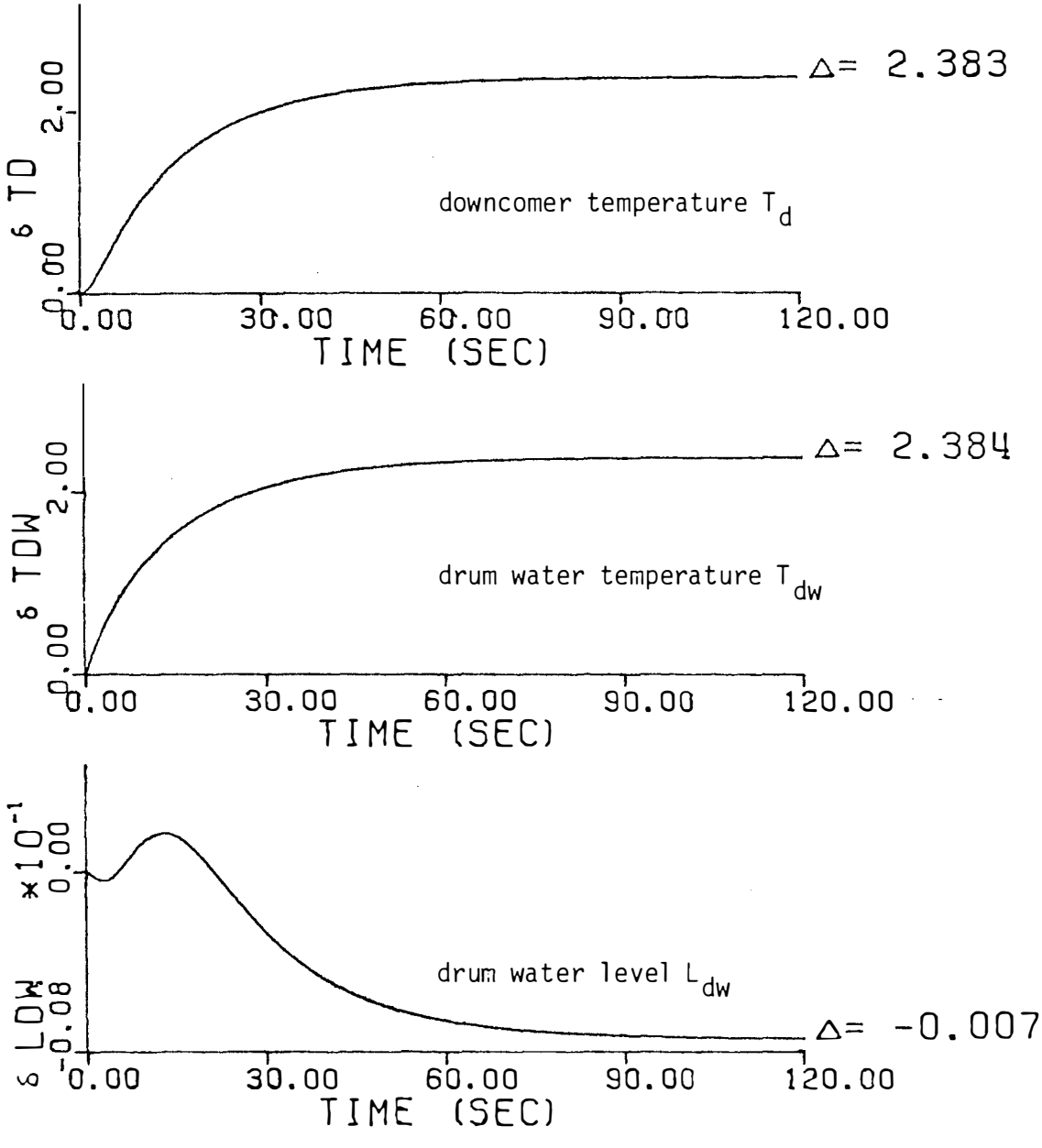

Figure F.8 (Continued).

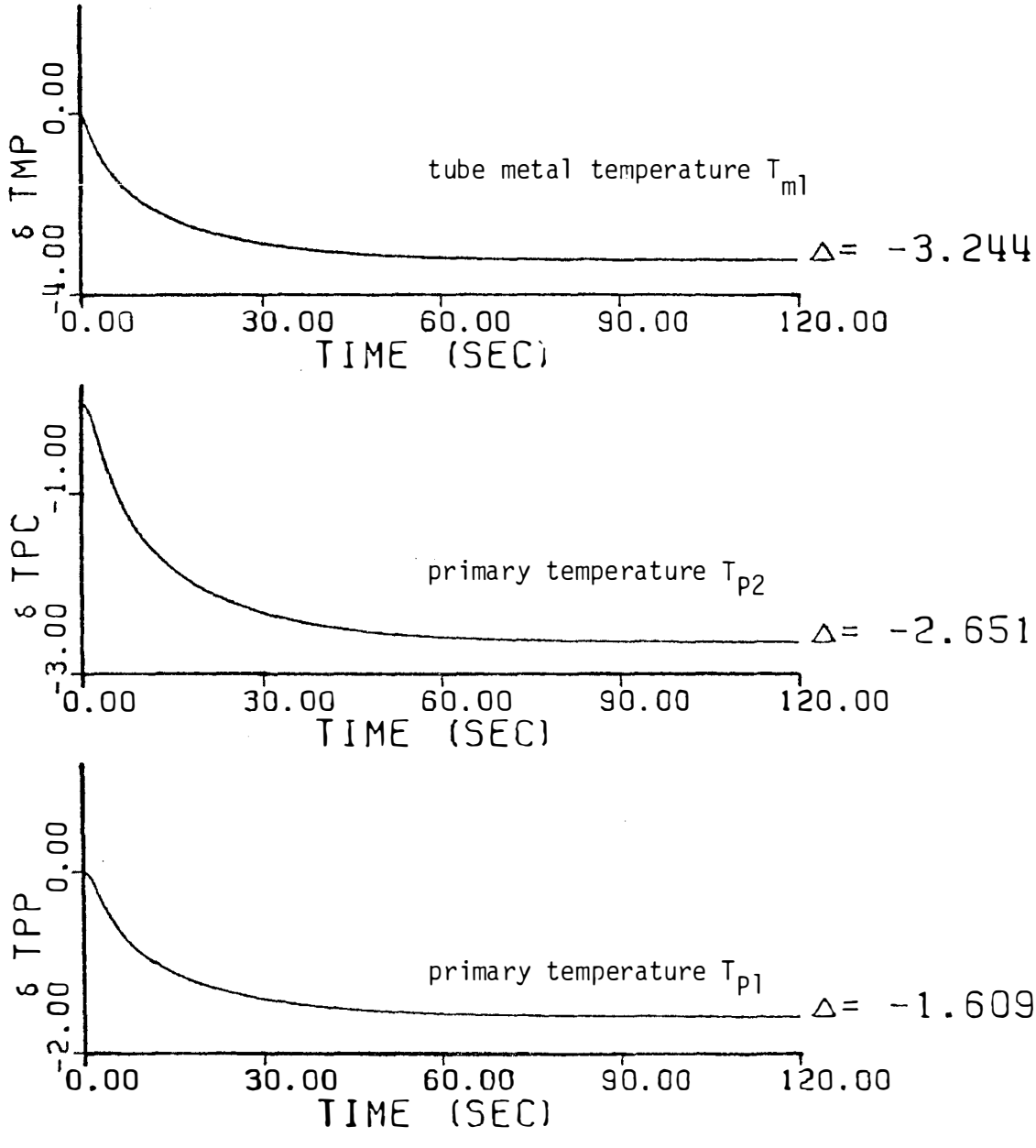

Figure F.9 Step Response for Case C.3.

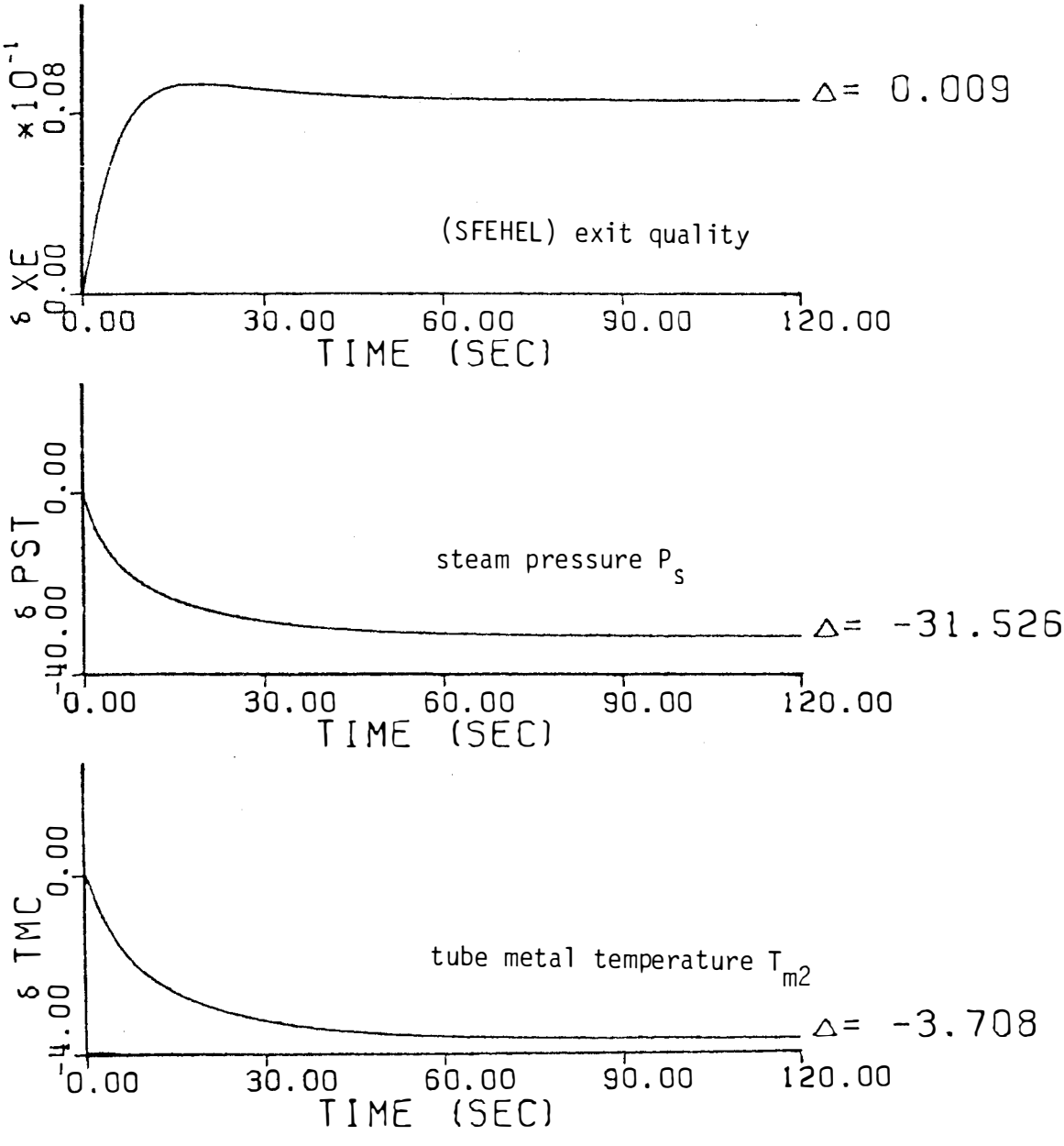

Figure F.9 (Continued).

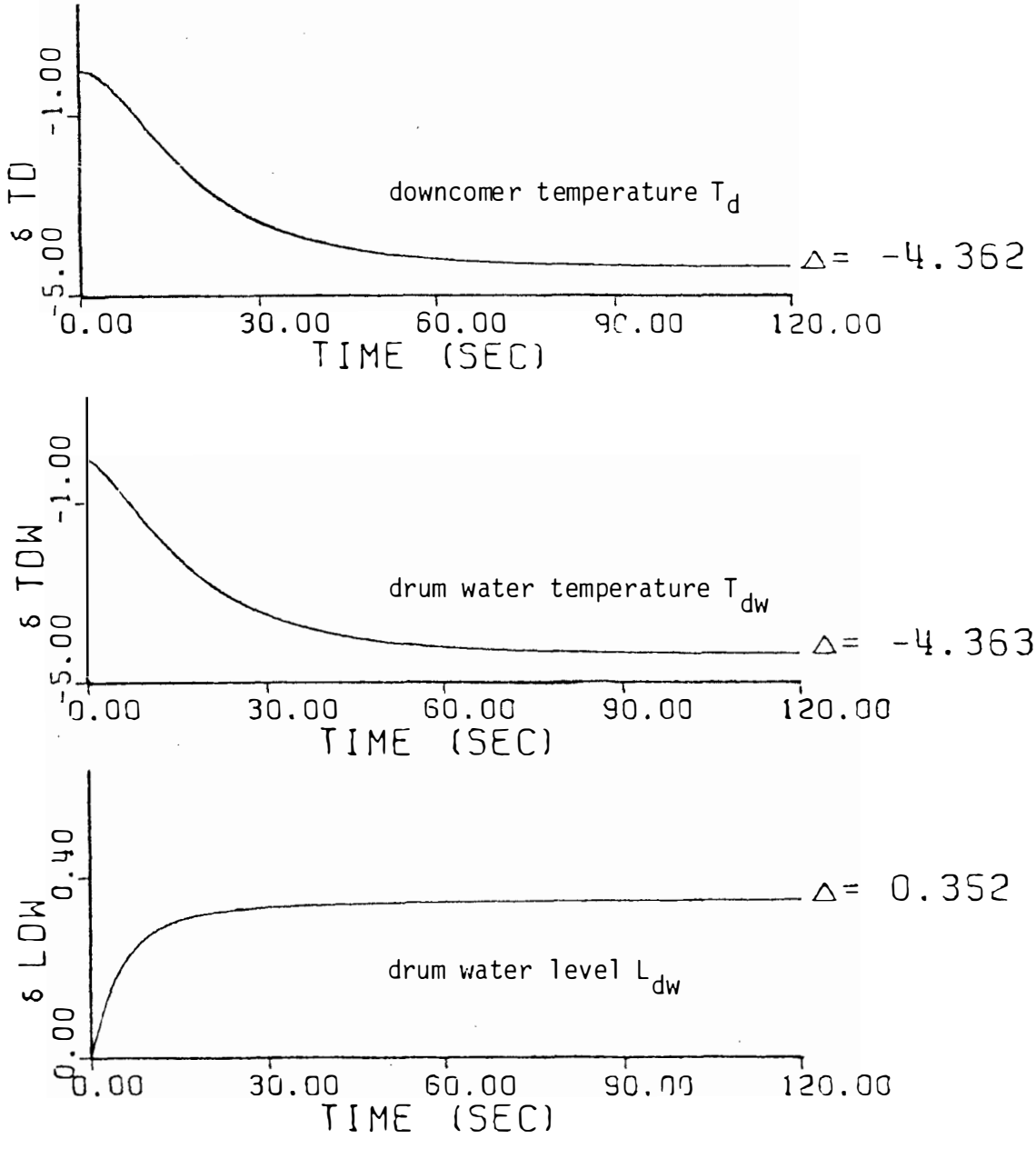

Figure F.9 (Continued).

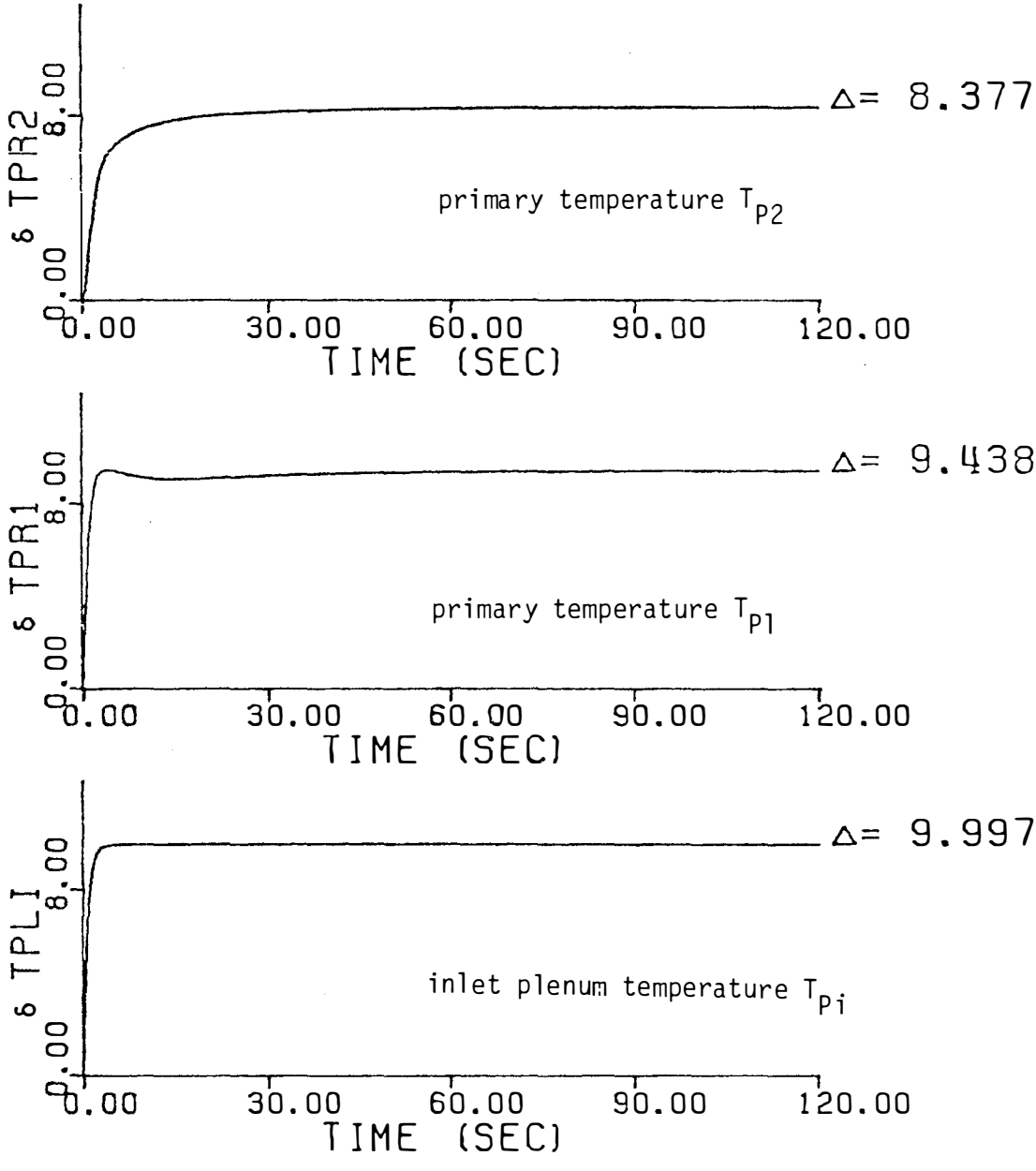

Figure F.10 Step Response for Case D.1.

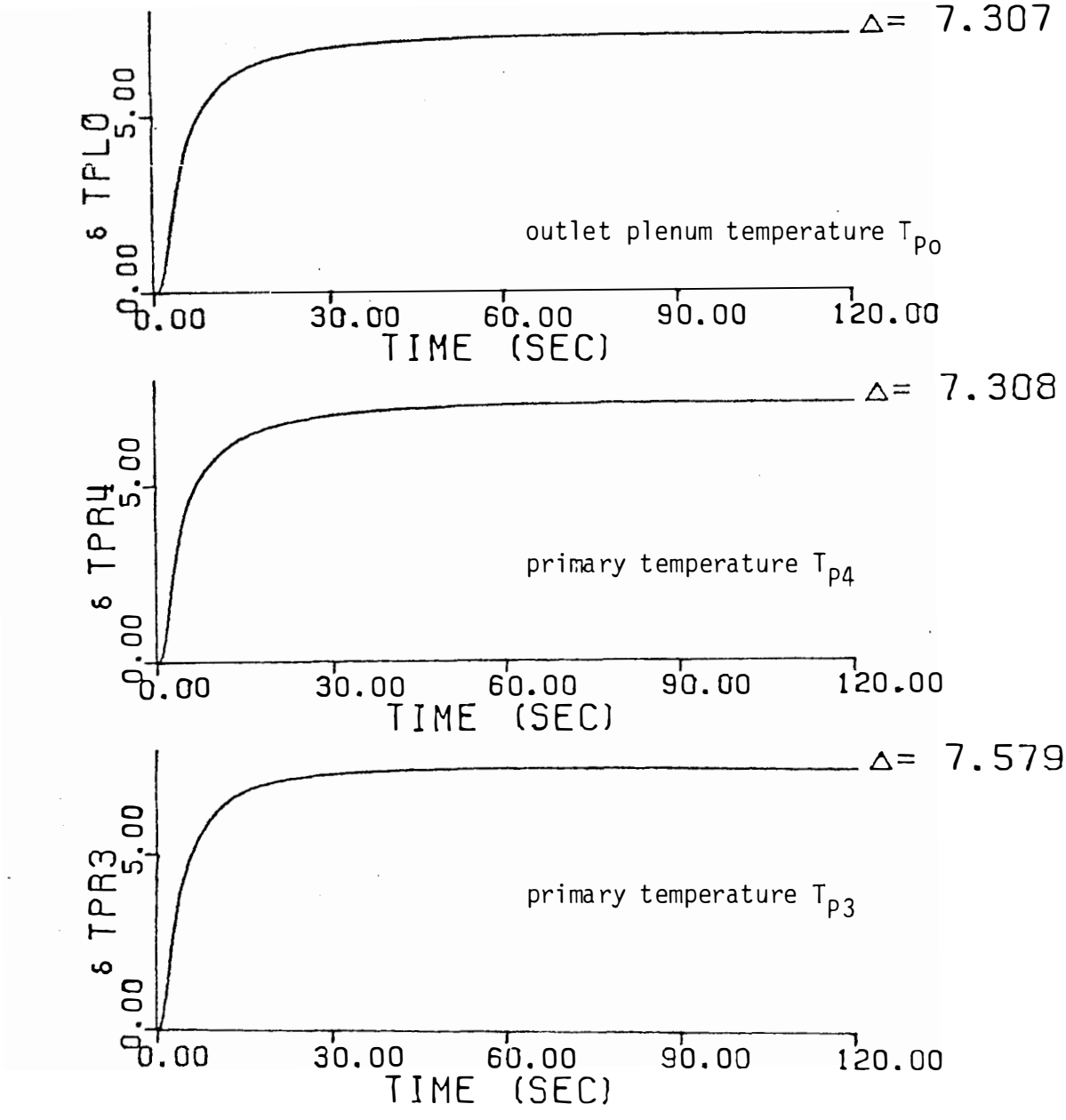

Figure F.10 (Continued).

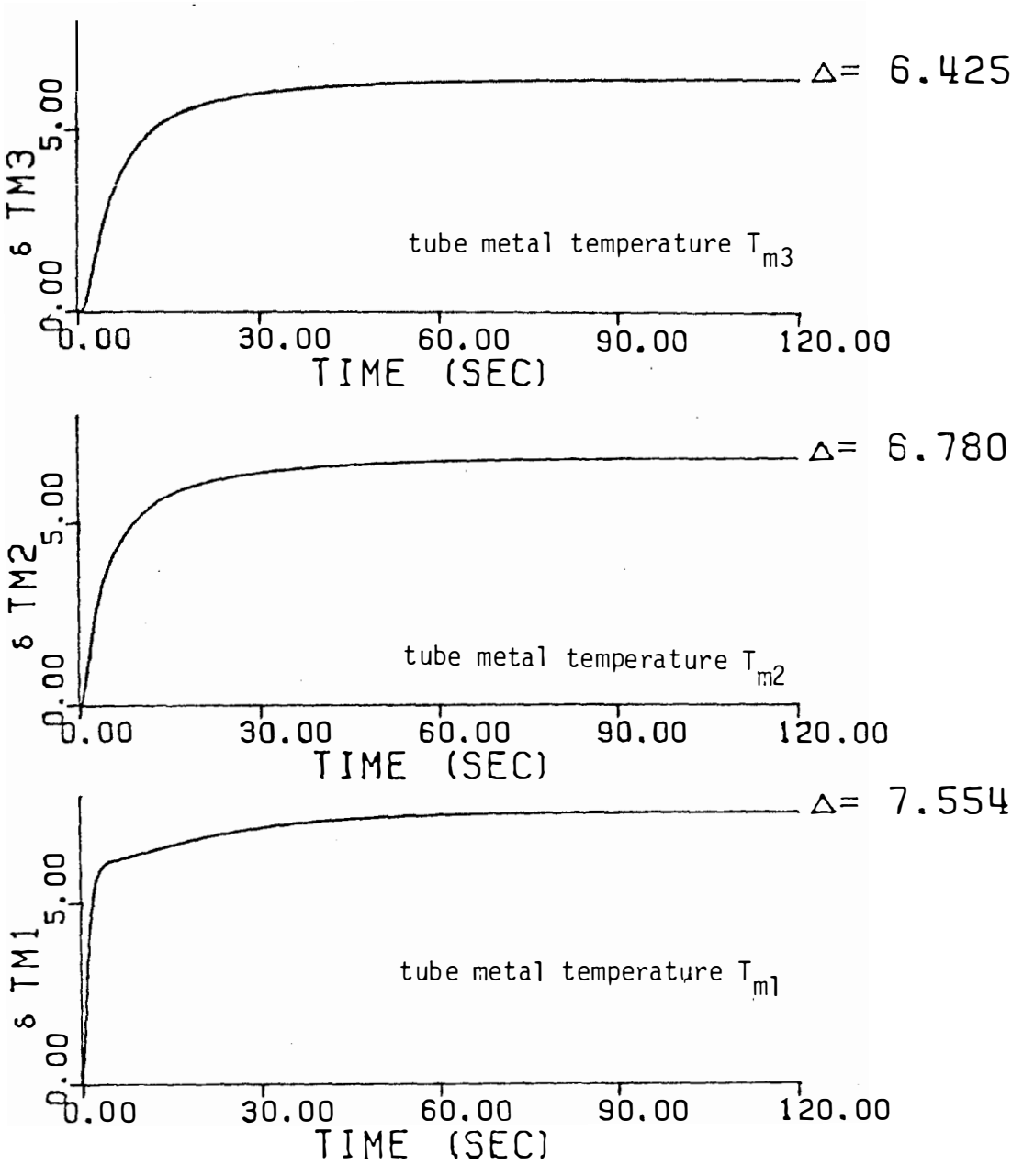

Figure F.10 (Continued).

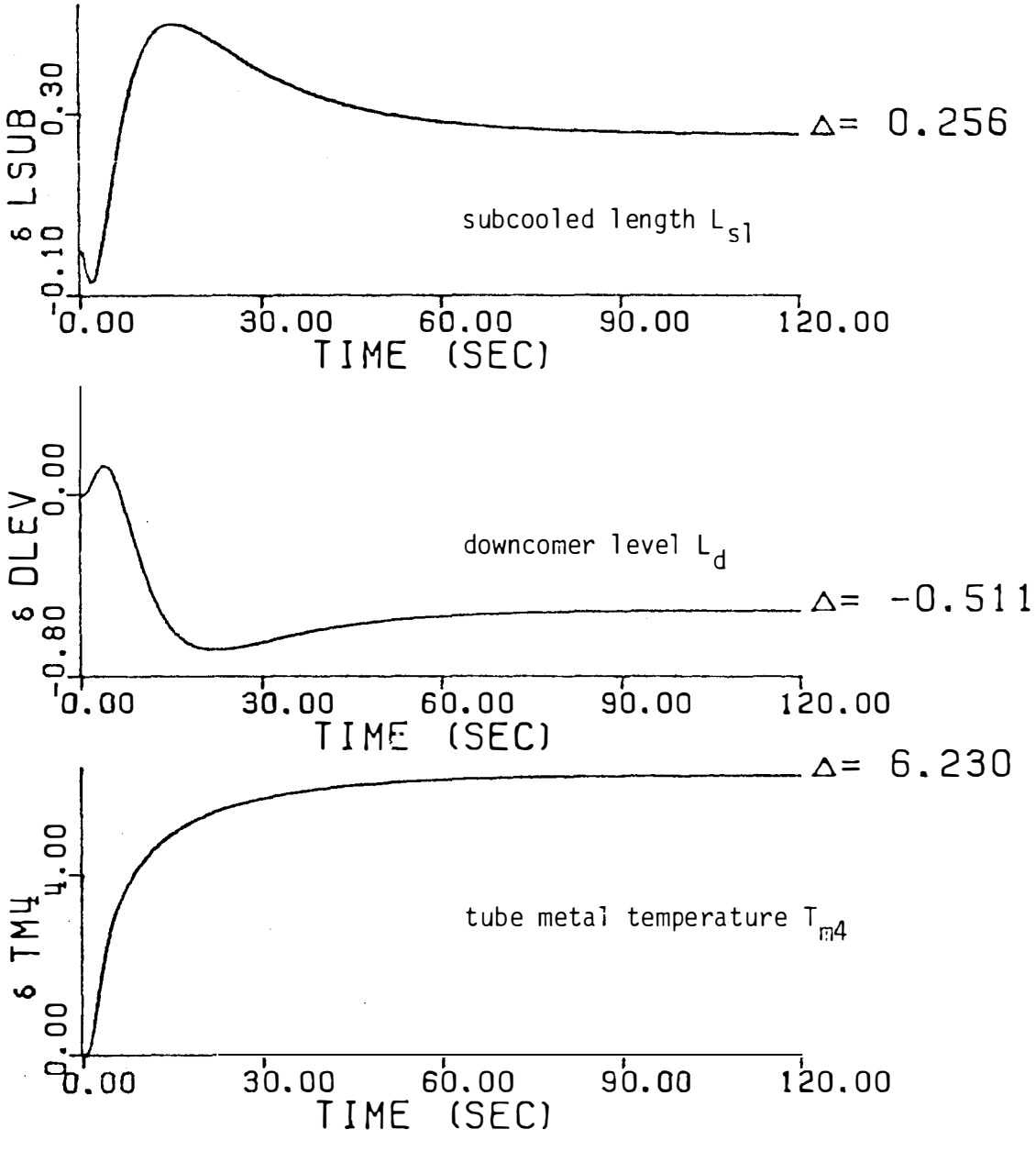

Figure F.10 (Continued).

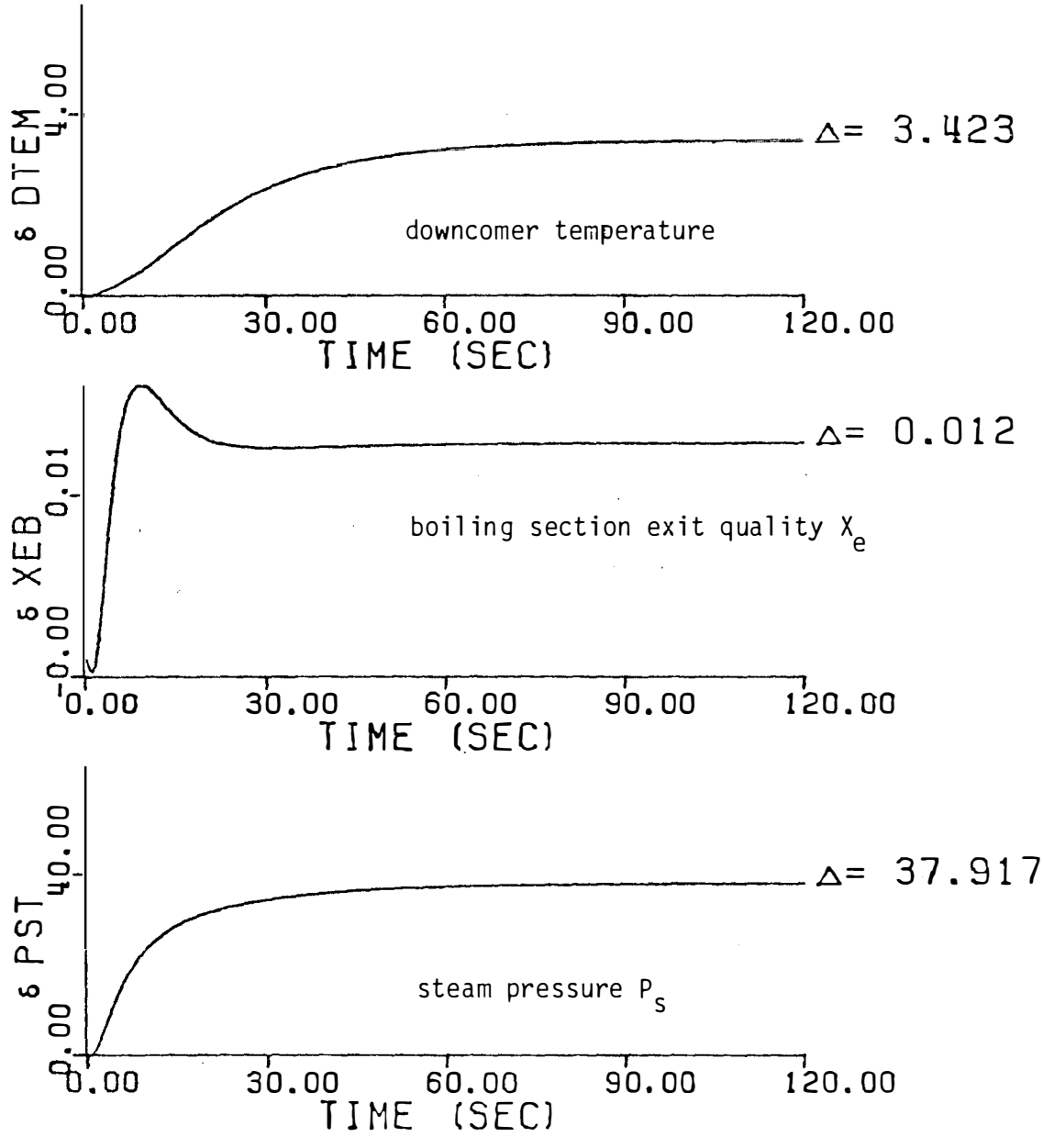

Figure F.10 (Continued).

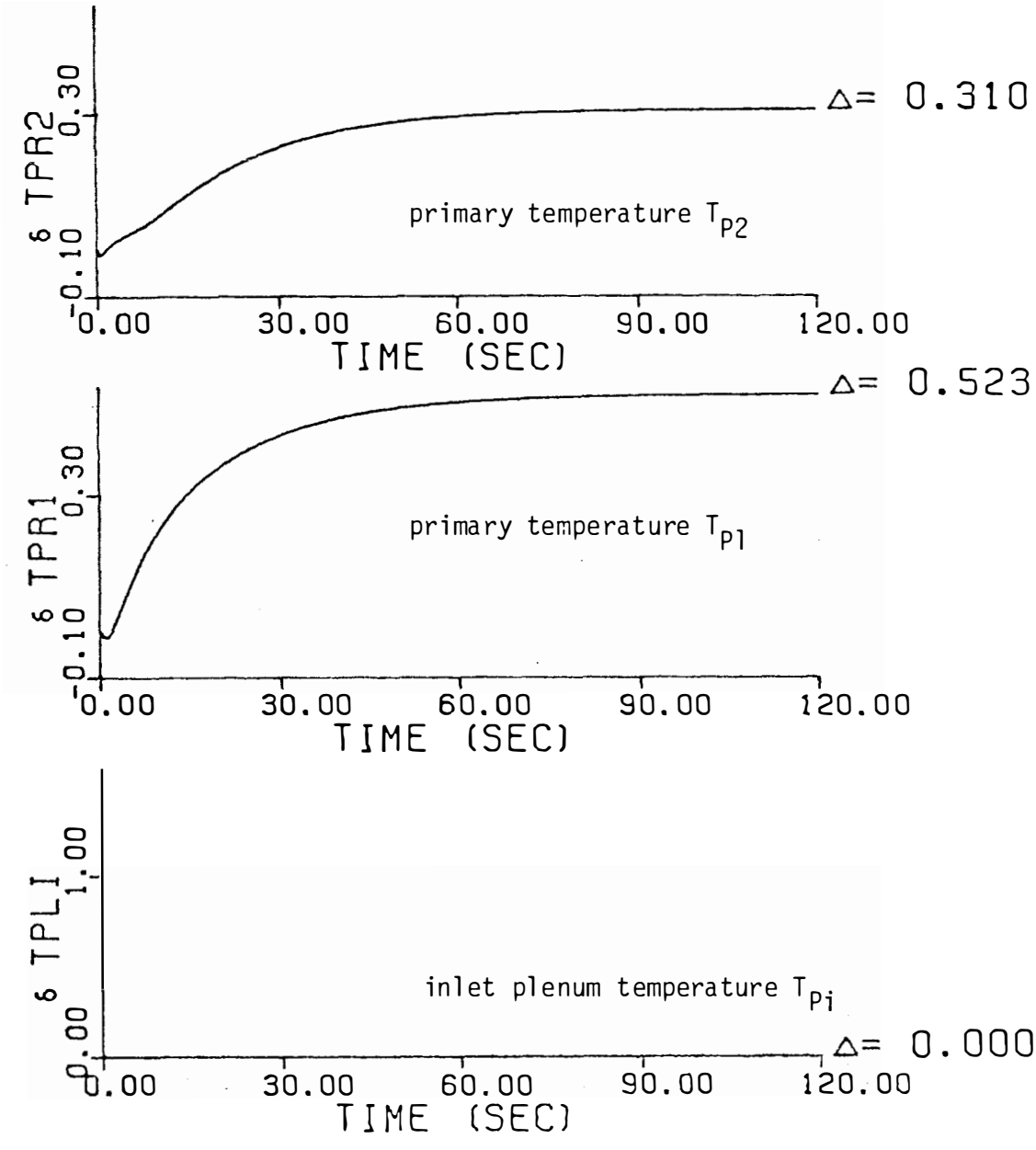

Figure F.11 Step Response for Case D.2.

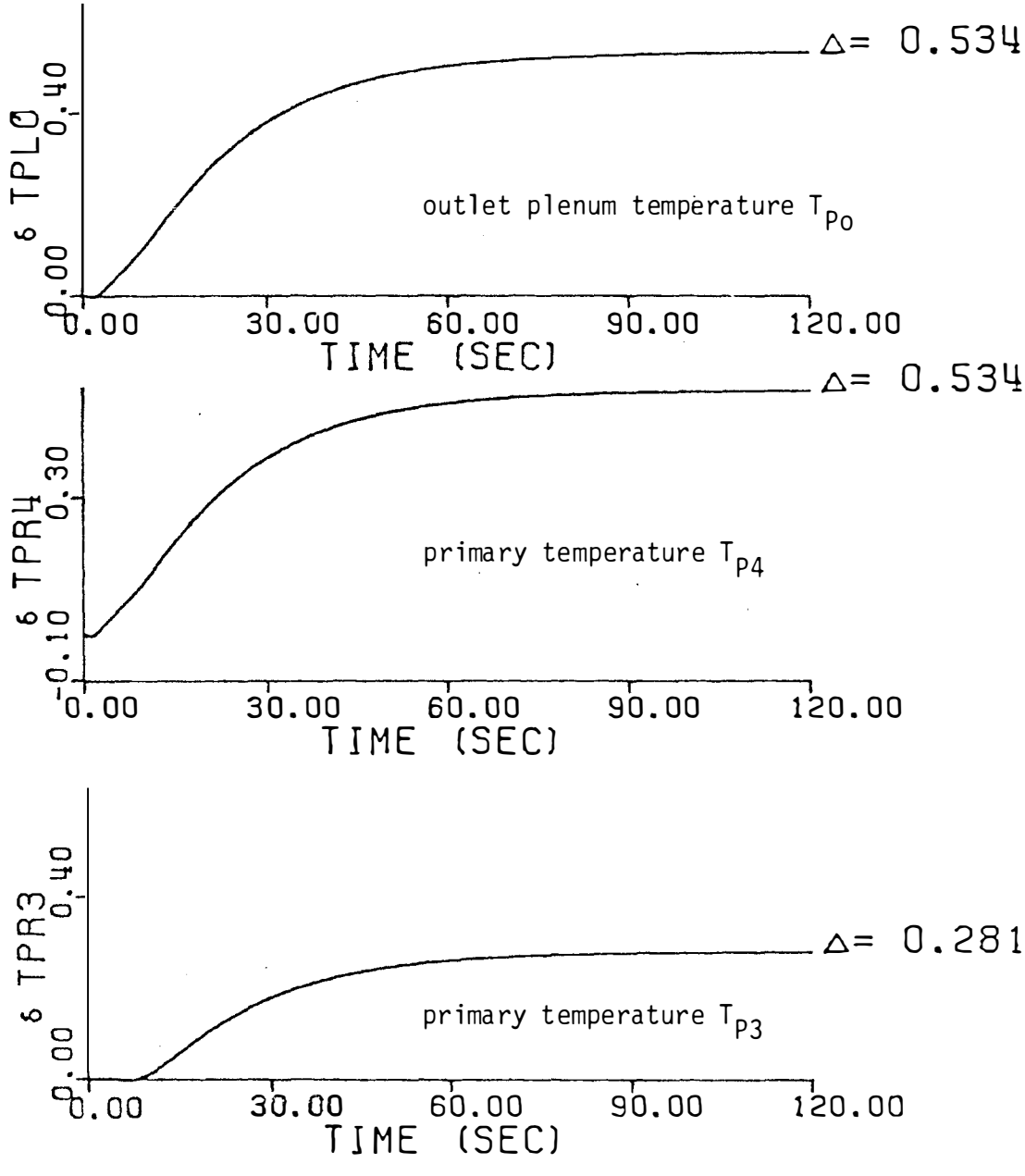

Figure F.11 (Continued).

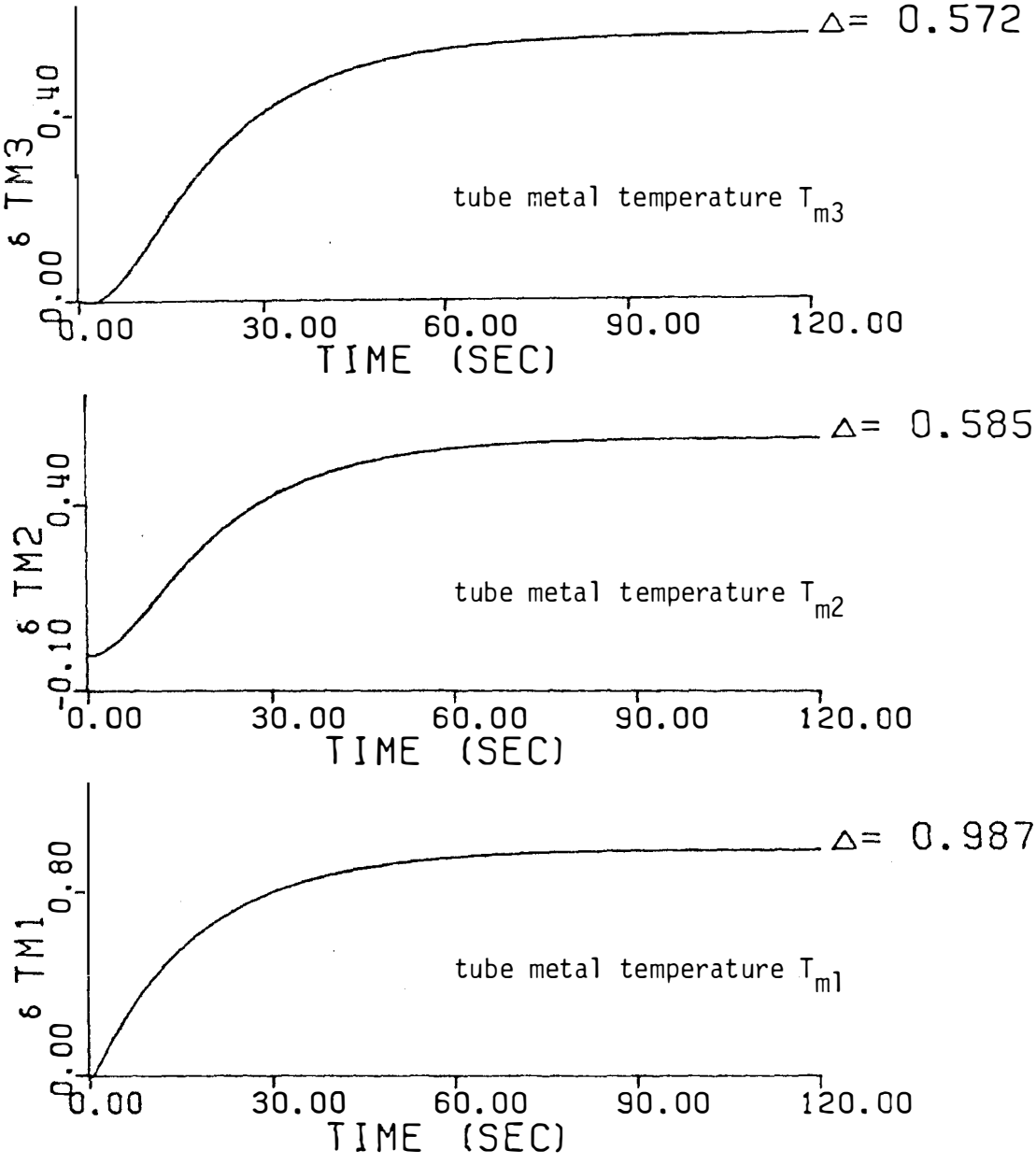

Figure F.11 (Continued).

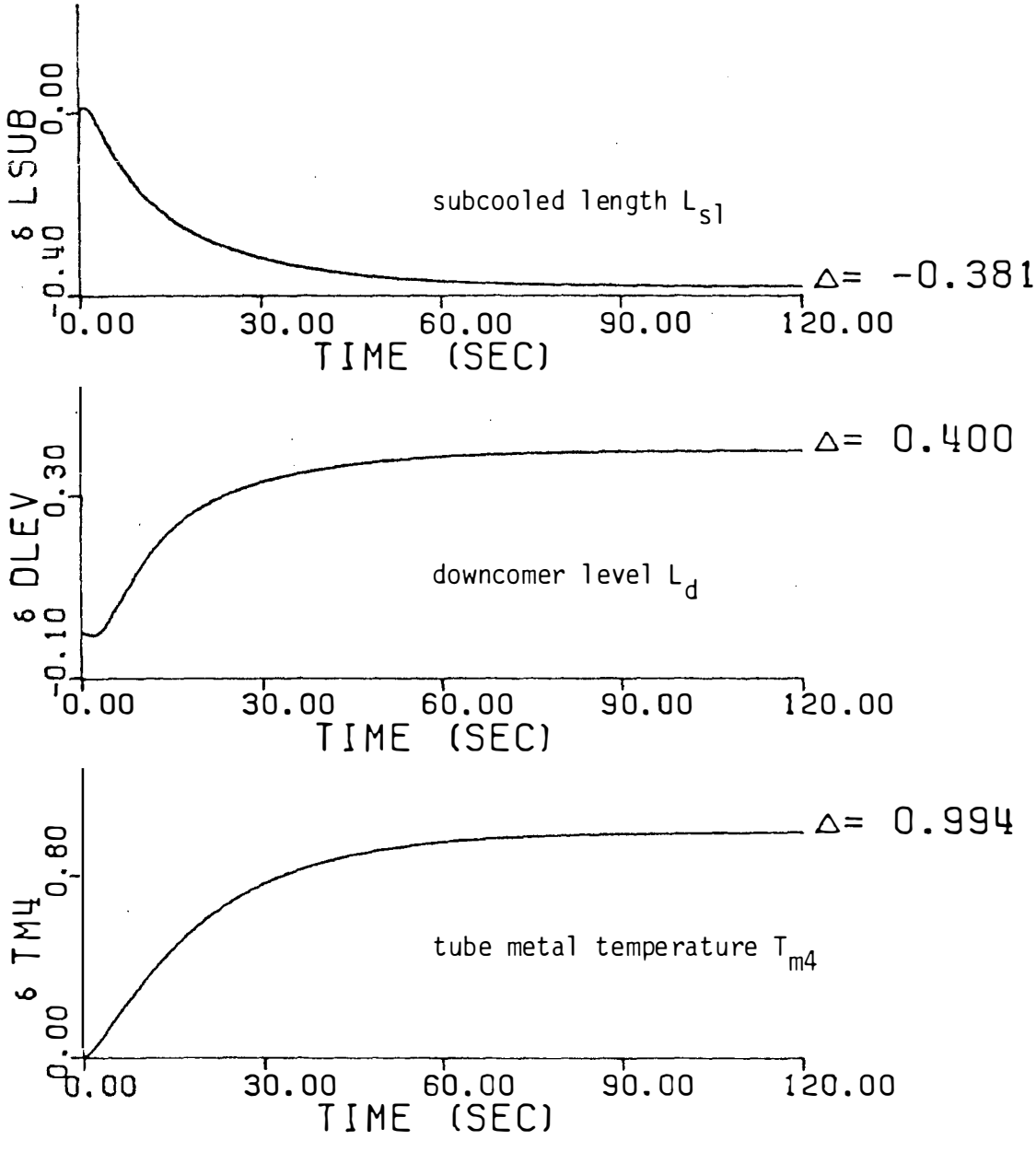

Figure F.11 (Continued).

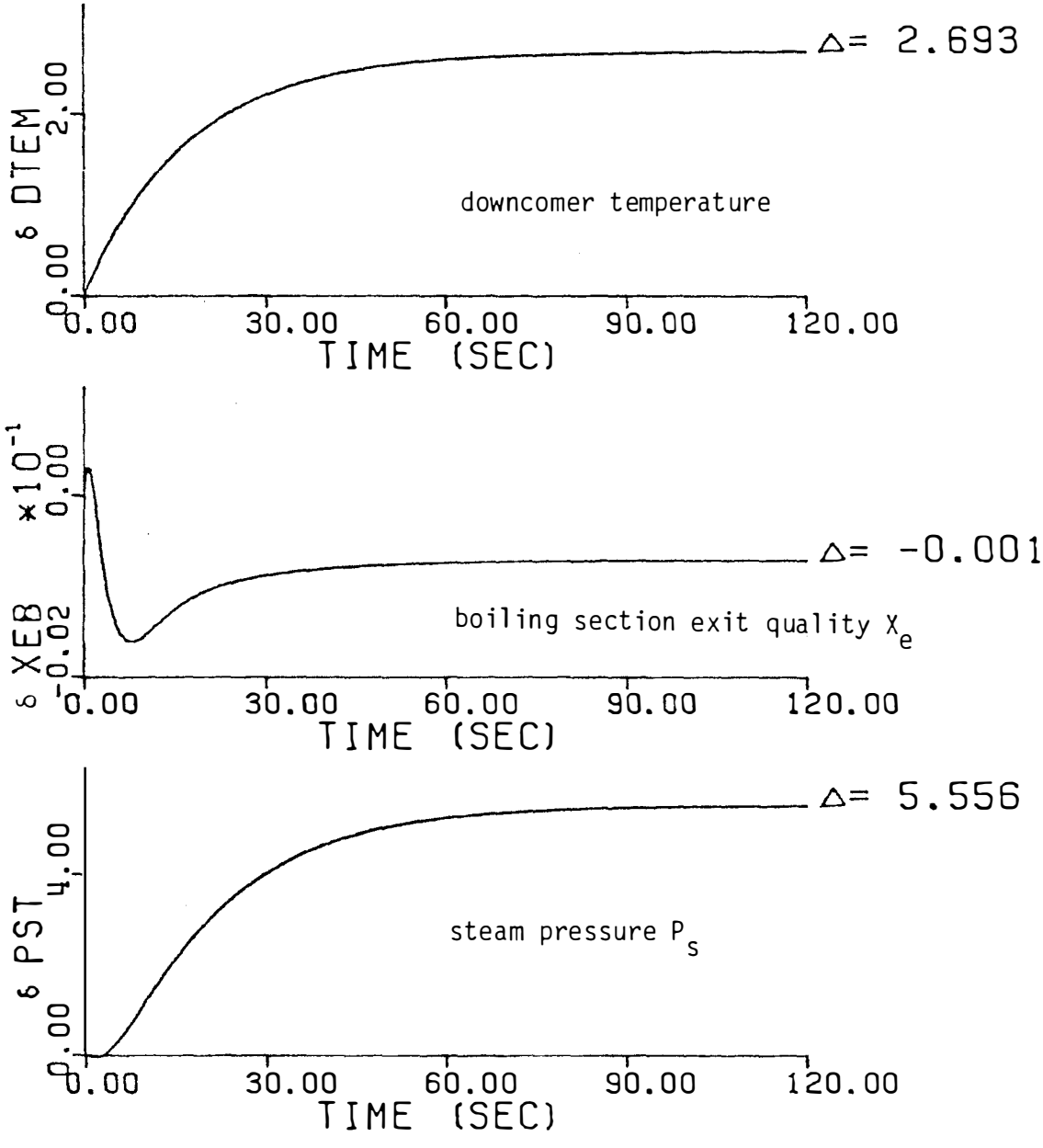

Figure F.11 (Continued).

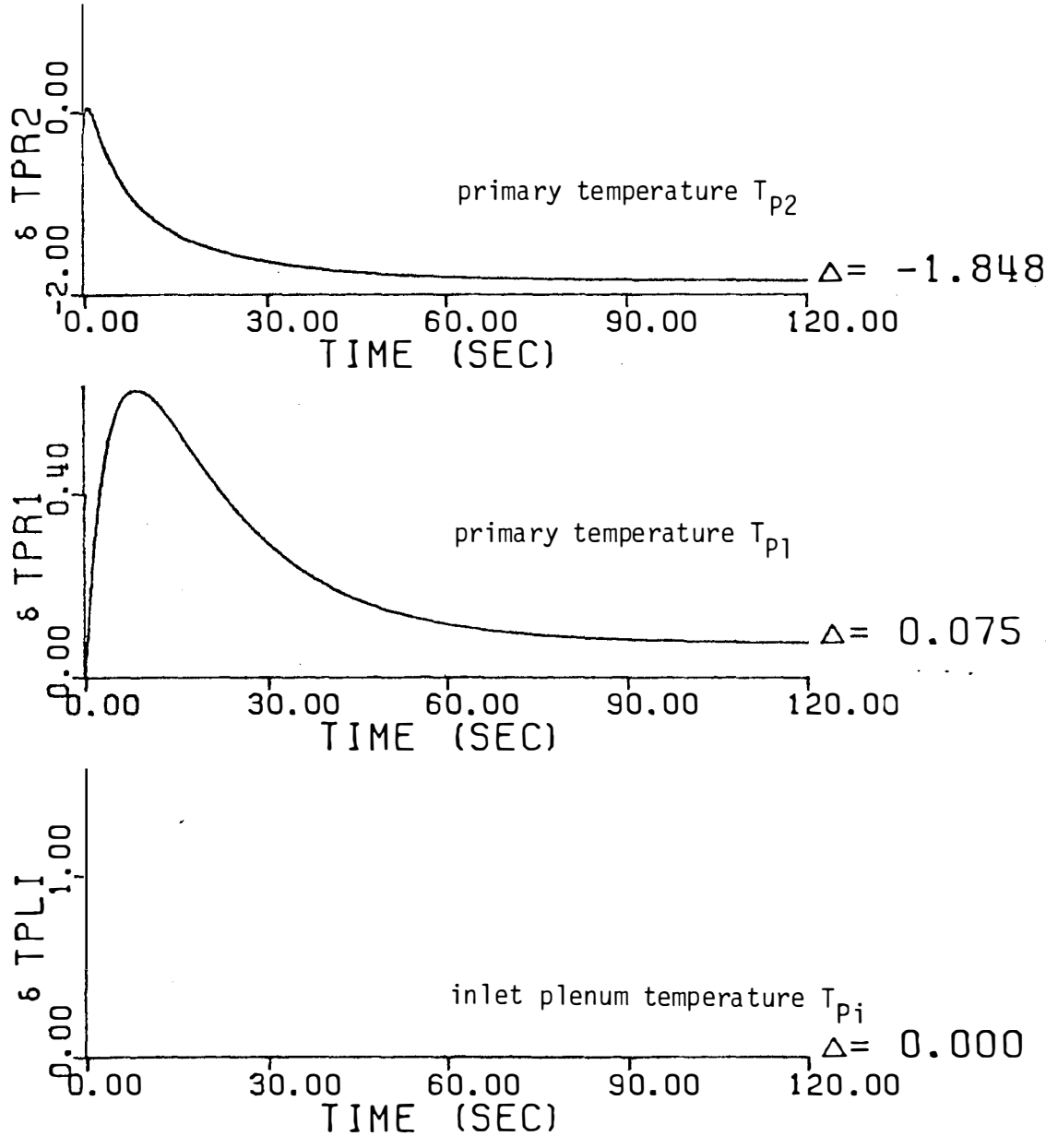

Figure F.12 Step Response for Case D.3.

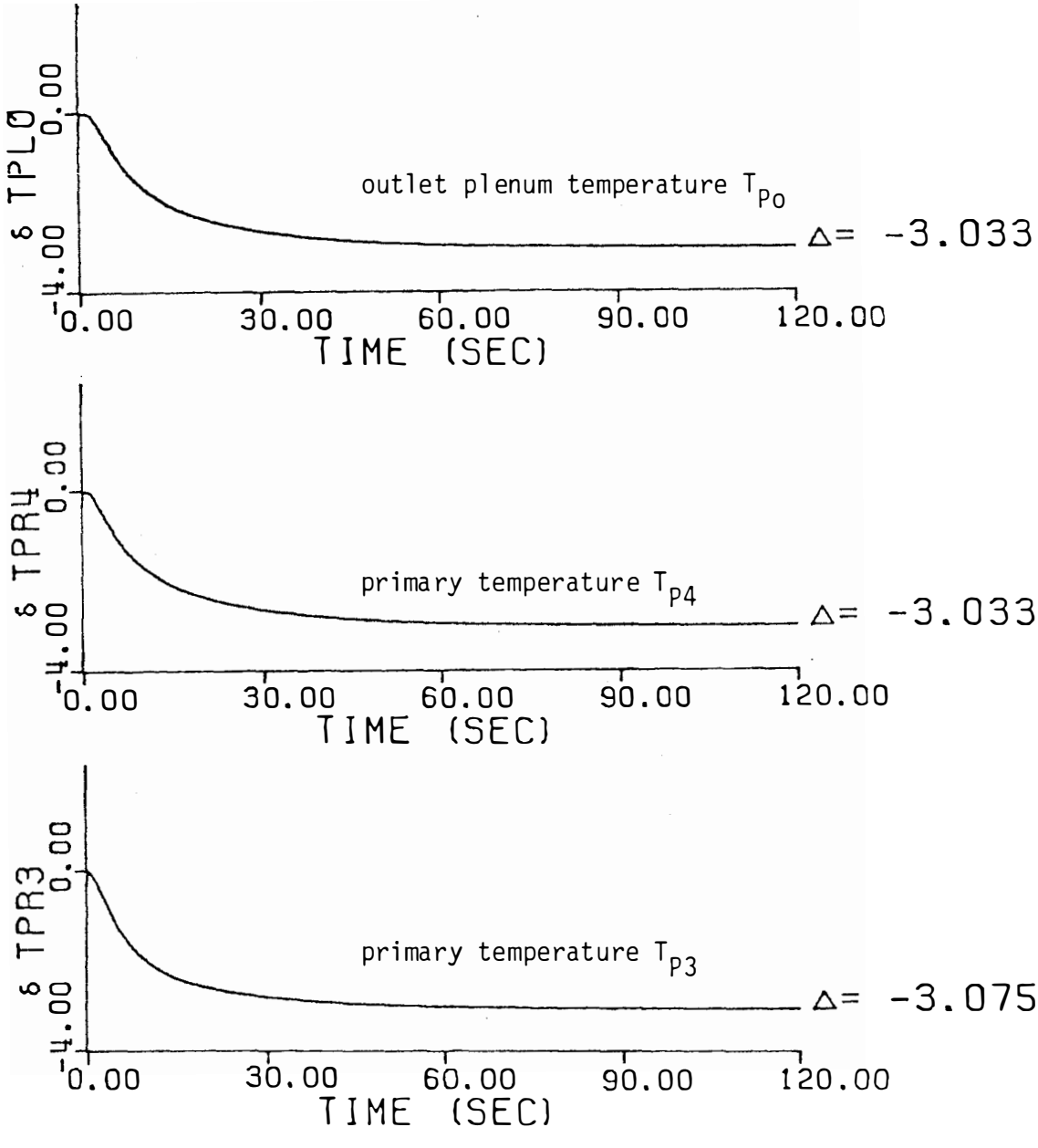

Figure F.12 (Continued).

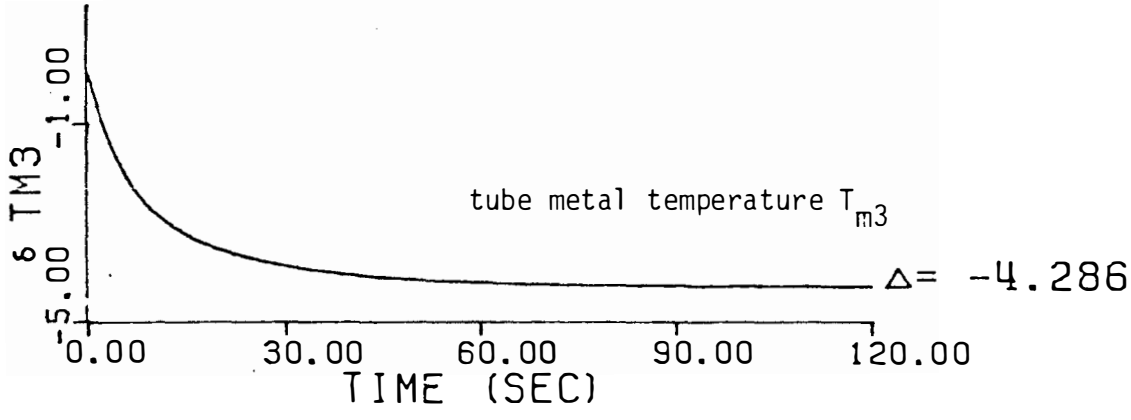

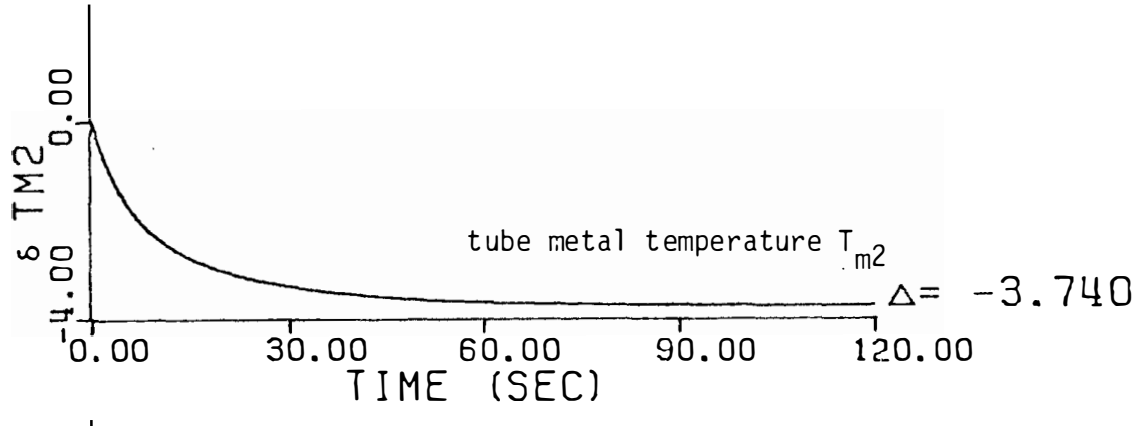

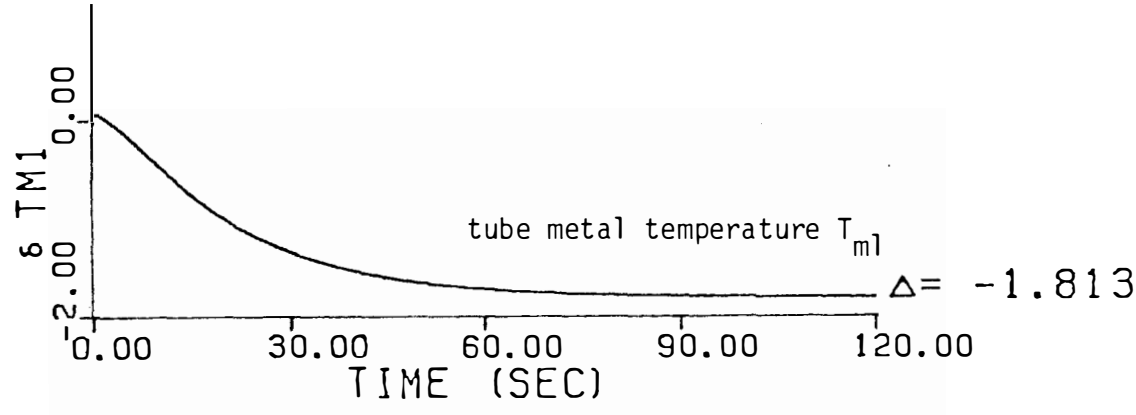

Figure F.12 (Continued).

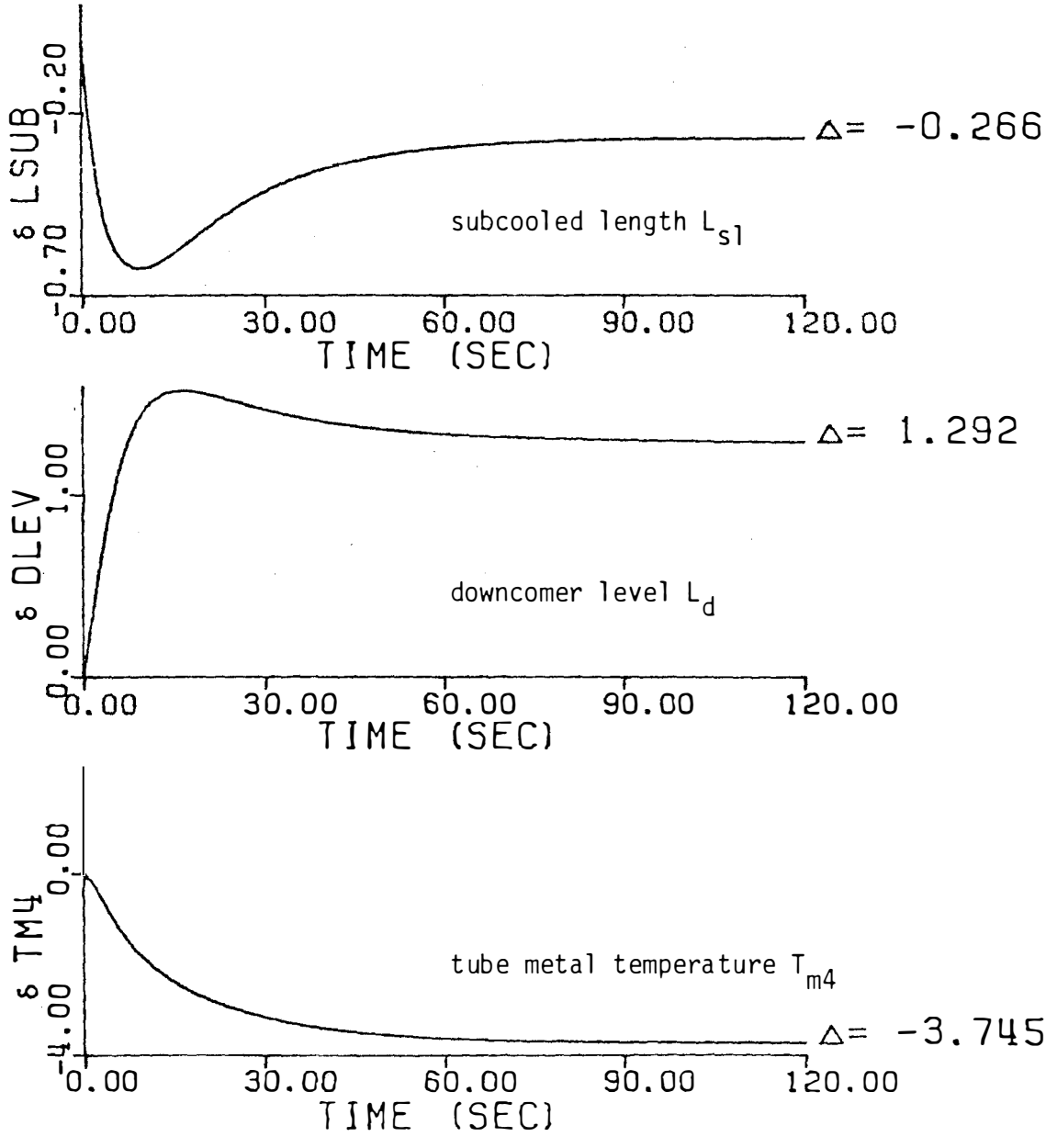

Figure F.12 (Continued).

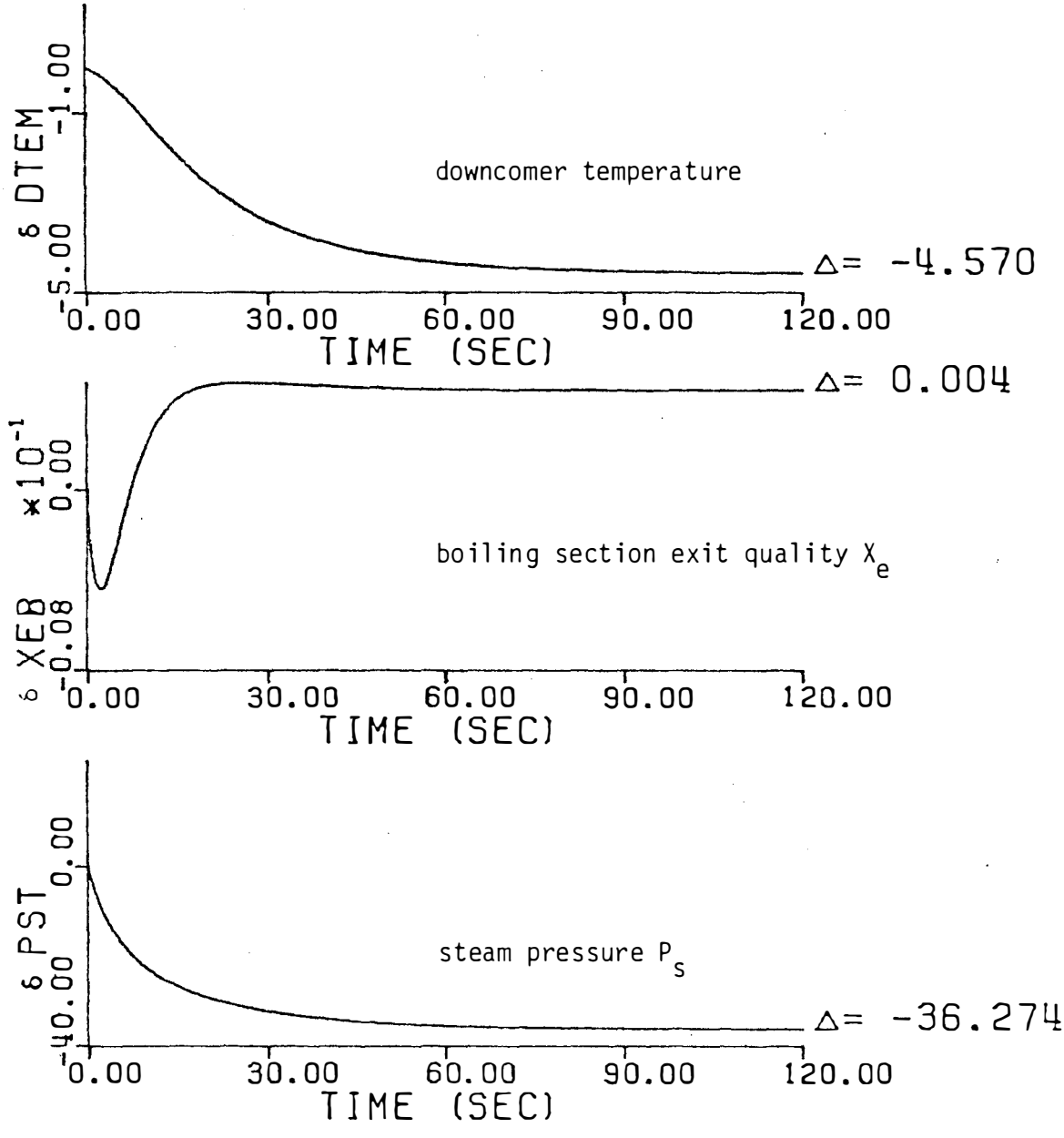

Figure F.12 (Continued).

APPENDIX G

INSTRUCTIONS FOR USING THE DETAILED MODEL DYNAMIC RESPONSE COMPUTER PROGRAM

When Model A or B is used for the dynamic response calculation for a UTSG, the only computer inputs needed are the coefficient matrices and forcing vectors obtained from steam generator design and input data. Once the coefficient matrices are calculated, they can be used to provide the input to the computer codes MATEXP[39] or SFR-3[40] to calculate the time or frequency response respectively.

In case of Models C and D, the calculation procedure is more complicated due to the use of the mixed (differential + algebraic) formulation, the computer program that was prepared to calculate the time response for Model D is outlined and the instructions for using it are given in this appendix.

The computer program is a FORTRAN IV program prepared to be implemented on the IBM 360 Model 65 computer. The program consists of a main routine and several subroutines, the functions of which are described below.

1. The "MAIN" routines read in input data and calculate the parameters needed for the steady state calculation. There are some built-in data that can be collected in data statements for improving the readability of the program.

2. The subroutine "STDYST" is called from "MAIN" to calculate the temperatures and mass quality profiles along the heat transfer path in the effective heat exchange region (core). The subcooled length and boundary temperatures are passed from "STDYST" to "MAIN" so that it can be used to calculate the coefficient matrices AONE and ATWO.
3. After AONE and ATWO are calculated, the program proceeds by reading in the control input data used for subroutine "PART" which handles the partitioning of AONE and ATWO to reduce the system of algebraic plus differential equations into a set of pure differential equations. After that, the forcing vector for "PUREDIFF" is read in.
4. After the pure differential system is obtained, subroutine "MATEXP" is called to calculate and plot the time response using the reduced A matrix and forcing vector.
5. The same procedure can be used to calculate the frequency response by calling the "SFR-3" program instead of "MATEXP".

G.1 Input Data and Format

The following are the input data contained in each data card together with the reading format used.

Card No. 1 (Geometrical parameter)

Column	1-5	6-15	16-25	26-35	36-45	46-55	56-65	66-75
Format	I5	7(E10.4)						
Input	NT	TOD	TMT	USHD	USHT	LSHD	LSHT	OUHT

NT = number of U-tubes

TOD = tube outside diameter (inches)

TMT = tube metal thickness (inches)

USHD = steam generator upper shell diameter (inches)

USHT = steam generator upper shell thickness (inches)

LSHD = steam generator lower shell diameter (inches)

LSHT = steam generator lower shell thickness (inches)

OVHT = steam generator overall height* (ft).

Card No. 2 (Primary side parameters)

Column	1-10	11-20	21-30	31-40	41-50	51-60	61-70	71-80
Format	8(E10.4)							
Input	WP	VP	CPl	TPI	TPO	PP	TOP	PHC

WP = primary water (reactor coolant) mass flow rate into the steam generator (lb/hr)

VP = steam generator primary water volume (including inlet and outlet plenums) (ft^3)

CPl = specific heat at constant pressure of the primary water (Btu/lb°F)

---

*This input is redundant. It was read in because it may be used in the future to calculate water and steam volumes.

TPI = primary water inlet temperature (°F)

TPO = primary water outlet temperature (°F)

PP = primary loop average pressure (psia)

ROP = average density of primary water (lb/ft^3)

PHC = primary side heat content* (Btu).

Card No. 3 (Secondary side parameters)

Column	1-10	11-20	21-30	31-40	41-50	51-60	61-70	71-80
Format	← 8(E10.4) →							
Input	W_{SO}	P_{STG}	T_{SAT}	T_{FWI}	V_{SW}	V_{SS}	R_{OS1}	CP_2

W_{SO} = steam flow rate (lb/hr)

P_{STG} = steam generator pressure (psig)

T_{SAT} = saturation temperature at P_{STG} (°F)

T_{FWI} = feedwater inlet temperature (°F)

V_{SW} = volume of secondary water (ft^3) in the steam generator (including downcomer)

V_{SS} = volume of secondary steam in the drum steam volume (ft^3)

R_{OS1} = subcooled secondary water average density (lb/ft^3)

CP_2 = specific heat of secondary side subcooled water (Btu/lb°F)

Card No. 4 (Heat transfer coefficients)

Column	1-10	11-20	21-30	31-40	41-50
Format	← 5(E10.4) →				
Input	HTA	HP	UM	HS_1	HS_2

*This input is redundant. It can be replaced by 0.0 without affecting the results; it was included for possible future use.

HTA = overall heat transfer area of the steam generator U-tubes (ft^2)

HP = primary side film heat transfer coefficient (Btu/hr ft^2°F)

UM = tube metal conductance (Btu/hr ft^2°F)

HS_1 = subcooled secondary film heat transfer coefficient (Btu/hr ft^2°F)

HS_2 = boiling secondary film heat transfer coefficient (Btu/hr ft^2°F).

Card No. 5 (Steady state thermodynamic properties)

Column	1-10	11-20	21-30	31-40	41-50	51-60
Format	6(E10.4)					
Input	HF	HFG	HG	VF	VFG	VG

HF = enthalpy of saturated water (Btu/lb)

HFG = latent heat of vaporization (Btu/lbm)

HG = enthalpy of saturated steam (Btu/lb)

VF = specific heat of saturated water (ft^3/lb)

VFG = difference between specific volumes for saturated steam and water (ft^3/lb)

VG = specific heat of saturated steam (ft^3/lb)

Card No. 6 (Thermodynamic property gradients)

Column	1-10	11-20	21-30	31-40	41-50	51-60	61-70	71-80
Format	8(E10.4)							
Input	DTSAT	DHF	DHFT	DHG	DVF	DVFG	DVG	DROG

$DT_{SAT} = \partial T_{sat}/\partial P$ (°F/psia)

$DHF = \partial h_f/\partial P$ (Btu/lb/psia)

$DHFG = \partial h_{fg}/\partial P$ (Btu/lb/psia)

DHG = $\partial h_g / \partial P$ (Btu/lb/psia)

DVF = $\partial v_f / \partial P$ (ft^3/lb/psia)

DVFG = $\partial v_{fg} / \partial P$ (ft^3/lb/psia)

DVG = $\partial v_g / \partial P$ (ft^3/lb/psia)

DROG = $\partial \rho_g / \partial P$ (lb/ft^3/psia)

(ρ_g = density of saturated steam).

Cards 7 through 11 (5 title cards)

Format (18 A.4) each.

Card No. 12

Column	1-5	6-10
Format	I5	I5
Input	NRED	NALG

Use the following input values:

NRED = 15 = order of reduced (pure differential system)

NALG = 3 = number of algebraic variables in the mixed mode formulation.

Card No. 13

Column	1-5	6-10	11-15
Format	I5	I5	I5
Input	LALG(1)	LALG(2)	LALG(3)

LALG(I), I = 1, 2, . . ., NALG is the list of NALG algebraic variables.

The algebraic variables in the current program are 16, 17, and 18.

Card No. 14 (Nonzero forcing function elements)

Column	1-5	6-15	Repeat 4 per card
Format	I5	E10-4	
Input	IU(J)	UX(J)	

IU(J) = row number of each nonzero component of the forcing function vector

UX(J) = value of each nonzero component of the forcing function vector.*

Card No. 15

Blank card to end the input of the nonzero forcing function elements.

Card No. 16 (MATEXP control parameters)

Column	1-2		6-7		11-20	21-30	31-40	41-50	51-60	61-62
Format	I2	3X	I2	3X	F10.0	F10.0	F10.0	F10.0	F10.0	I2
Input	NE		LL		P	TZERO	T	TMAX	PLTINC	MATYES

MATEXP control parameters (continued)

Column	63-64	65-66	67-69	70	71-72	73-74	75-80
Format	I2	I2	I3	I1	I2	I2	F6.0
Input	ICSS	JFLAG	ITMAX	LASTCC	IIZ	ICONTR	VAR

NE = number of equations = 15

LL = coefficient matrix tag number, use LL = 1

P = precision of C and HP - recommend 10^{-6} or less

TZERO = zero time (usually 0.0)

---

*See Section III.7.5, page 105, for the calculation of the forcing vector elements.

T = computation time interval

TMAX = maximum time

PLTINC = printing time interval

MATYES = coefficient matrix (A) control flag

1 = use precious A and T

2 = read new coefficients to alter A

3 = read entire new A (nonzero values)

4 = DISTRB to calculate entire new A,

(Use MATYES = 3 for this application)

ICSS = initial condition vector (XIC) flag

1 = read in all new nonzero values

2 = read new values to alter previous vector

3 = use previous vector

4 = vector = 0

5 = use last value of X vector from previous run

(Current program uses ICSS = 4.)

JFLAG = forcing function (Z) flag

1 thru 4 = same as for ICSS for constant Z

5 = call DISTRB at each time step for variable

(Current program uses JFLAG = 3.)

ITMAX = maximum number of terms in series approximation of exp (AT)

(recommend ITMAX = 10)

LASTCC = nonzero for last case

I1Z = row of Z if only one nonzero, otherwise = 0

ICONTR = for internal control options

0 = read new control card for next case

1 = go to 212 call DISTRB for new A or T

-1 = go to 215 call DISTRB for new initial conditions

(Current program uses ICONTR = 0.)

VAR = maximum allowable value of largest coefficient matrix element

*T (Recommend VAR = 1.0).

Card No. 17

Blank card to end the input data.

VITA

Mohamed Rabie Ahmed Ali was born in Matai, El-Minya, Egypt on May 9, 1940. After receiving the Bachelor of Science degree in Electrical Engineering (Power Section) in 1962, he worked in teaching Electrical Engineering and special technology of electrical power equipment at the Abbassia Electric and Electronic Technical Training Center in Cairo, Egypt from November 1962 to February 1965. Since March, 1965, he has worked for the Egyptian Atomic Energy Commission Nuclear Power Project Department.

In 1965, he matriculated at Cairo University and obtained there the Diploma of Higher Studies (Equivalent to a non-thesis M. S. degree) in Power Stations and Electrical Networks in 1967.

He came to the United States in June 1969 where he worked with the Agro Industrial Complex Study Team at Oak Ridge National Laboratory from June to December of 1969. In January 1970, he started his study at the Graduate School of The University of Tennessee on an IAEA Fellowship sponsored by the U. S. National Academy of Sciences for a period of fifteen months. Starting April 1, 1971, he has been awarded a research assistantship from the Nuclear Engineering Department of The University of Tennessee. In December 1971, he obtained the M. S. degree in Nuclear Engineering. In July 1974, he was employed by the Power Systems Group of Combustion Engineering, Inc. He held the position of a senior NSSS Engineer in the Reactor Dynamics Section until May 1976 when he returned to The University of Tennessee and obtained the Ph. D. degree in Nuclear Engineering in August 1976.

Rabie is married to the former Miss Soheir Mohamed Mostafa Kamel of Cairo, Egypt and has a daughter named Amani and a son named Yaser.